GEOLOGICAL SURVEY OF CANADA
BULLETIN 531

SEDIMENTOLOGY, MICROPALEONTOLOGY, GEOCHEMISTRY, AND HYDROCARBON POTENTIAL OF SHALE FROM THE CRETACEOUS LOWER COLORADO GROUP IN WESTERN CANADA

J.D. Bloch, C.J. Schröder-Adams, D.A. Leckie,
J. Craig, and D.J. McIntyre

1999

Natural Resources Canada Ressources naturelles Canada

Canada

GEOLOGICAL SURVEY OF CANADA
BULLETIN 531

SEDIMENTOLOGY, MICROPALEONTOLOGY, GEOCHEMISTRY, AND HYDROCARBON POTENTIAL OF SHALE FROM THE CRETACEOUS LOWER COLORADO GROUP IN WESTERN CANADA

J.D. Bloch, C.J. Schröder-Adams, D.A. Leckie,
J. Craig, and D.J. McIntyre

1999

Catalogue No. M42-531E
ISBN No. 0-660-17729-3

Available in Canada from
Geological Survey of Canada offices:

601 Booth Street
Ottawa, Ontario K1A 0E8

3303-33rd Street N.W.
Calgary, Alberta T2L 2A7

101-605 Robson Street
Vancouver, B.C. V6B 5J3

A deposit copy of this publicaton is available for
reference in public libraries across Canada

Price subject to change without notice

Cover Illustration
Outcrop of the Upper Cretaceous Colorado Group exposed along the Livingstone River, southern Rocky Mountain Foothills. Sediments of the Sunkay Member (Blackstone Formation) are exposed in the foreground. The Vimy Member (Second White Specks Formation) is exposed in the distance.

Critical reviewers
Hugh Abercrombie
Dave McNeil
Wendy Warters
James White

Authors' addresses
J.D. Bloch
Scealu Modus
2617 Cutler Avenue NE
Albuquerque, NM 87106

C.J. Schröder-Adams
Dept. of Earth Sciences
1125 Colonel By Drive
Ottawa, ON K1S 5B6

D.A. Leckie
Wascana Energy Inc.
635 - 8th Ave. S.W.
Calgary, AB T2P 3Z1

J. Craig
Box 668
Bragg Creek
Alberta T0L 0K0

D.J. McIntyre
3503 Underhill Drive N.W.
Calgary, AB T2N 4E9

Original manuscript submitted: 96.06
Approved for publication: 99.02

PREFACE

The Cretaceous Colorado Group shales of the Western Canada Sedimentary Basin contain proven source rocks and hydrocarbon reserves, yet the details of their origin, composition, distribution, and maturity are largely unknown. This basin-scale, multidisciplinary study refines Cretaceous shale stratigraphy and provides a regional basis for further detailed exploration and exploitation of Colorado Group hydrocarbon and mineral resources.

This study integrates geochemical, biofacies, and sedimentological data to identify discrete shale formations within the previously undifferentiated Colorado Group. Detailed geochemical and facies analyses provide new information on source-rock distribution and maturity. Quantitative mineralogy and Rock-Eval data can be used to improve wireline calibrations and correlations in shale-dominated sequences. Paleoenvironmental reconstructions, including sedimentation rates, and identification of diagenetic processes within these shales will aid in the further refinement of basin evolution models of the Western Canada Sedimentary Basin and further enhance our understanding of this important hydrocarbon province.

M.D. Everell
Assistant Deputy Minister
Earth Sciences Sector

PRÉFACE

Les shales du Crétacé du Groupe de Colorado présents dans le Bassin sédimentaire de l'Ouest du Canada renferment des roches mères et des réserves prouvées d'hydrocarbures. Cependant, on a très peu de données précises sur leur origine, leur composition, leur répartition et leur degré de maturité. La présente étude pluridisciplinaire, effectuée à l'échelle du bassin, permet de préciser davantage la stratigraphie de ces shales et de fournir une base de connaissances régionales destinée aux futurs travaux d'exploration détaillés et à l'exploitation éventuelle des ressources minérales et des hydrocarbures du Groupe de Colorado.

La présente étude intègre des données géochimiques, sédimentologiques et de biofaciès afin de mettre en évidence des formations de shales distinctes à l'intérieur du Groupe de Colorado antérieurement non différencié. Des analyses géochimiques et de faciès détaillées fournissent de nouvelles informations sur la répartition et le degré de maturité des roches mères. L'utilisation de la minéralogie quantitative et des données Rock-Eval permet d'améliorer les étalonnages des diagraphies par câble et les corrélations dans les séquences dominées par les shales. La reconstitution des paléoenvironnements, y compris les taux de sédimentation, et la mise en évidence des processus diagénétiques ayant touché ces shales contribueront à perfectionner les modèles d'évolution du Bassin sédimentaire de l'Ouest du Canada et d'accroître notre compréhension de cette importante province de ressources en hydrocarbures.

M.D. Everell
Sous-ministre adjoint
Secteur des sciences de la Terre

CONTENTS

Figures

Tables

Plates

SEDIMENTOLOGY, MICROPALEONTOLOGY, GEOCHEMISTRY AND HYDROCARBON POTENTIAL OF SHALE FROM THE CRETACEOUS LOWER COLORADO GROUP IN WESTERN CANADA

Abstract

Shale of the Cretaceous lower Colorado Group extends across the subsurface of the Western Canada Sedimentary Basin (WCSB) and along the length of the Rocky Mountain Foothills. Four regionally mappable shale units are recognized by their distinctive geochemical, mineralogical, biofacies and sedimentological characteristics: the Late Albian Westgate, the Early Cenomanian Fish Scales, the Middle to Late Cenomanian Belle Fourche, and the latest Cenomanian to Middle Turonian Second White Specks Formation. These units were deposited in a foreland basin during a period of overall sea-level rise punctuated by periods of tectonically induced, relative sea-level falls.

The Westgate Formation is a progradational siltstone to mudstone having a low total organic carbon (TOC) content (< 2 wt %) of dominantly Type III organic matter (OM). The Westgate was deposited above storm wave-base in the Mowry Sea. The inner to middle neritic foraminiferal assemblage (*Milliammina manitobensis* Zone) and oxygen isotope composition of early diagenetic carbonate concretions indicate a cool, low-salinity water mass of Boreal affinity. Compacted sedimentation rates ranged from 1 to 6 cm/10^3 yrs.

The Fish Scales Formation is a transgressive mudstone to claystone with TOC contents of up to 8 wt % of mixed types II and III OM. The basal conglomeratic layer indicates a drastic environmental change at the end of the Albian. The water column was stratified with widespread anoxic bottom waters, as is indicated by well-laminated sediments and the absence of benthic foraminifera. Compacted sedimentation rates ranged from 1 to 2 cm/10^3 yrs.

The contact between between the Fish Scales and the Belle Fourche formations is gradational, signifying a gradual improvement of benthic conditions. OM changes to Type III and the abundance is generally less than 2 wt%. By this time, the seaway connecting Boreal and Tethyan water masses was established but waters of Boreal affinity were dominant in the WCSB. The northwestern part of the basin was influenced by the progradation of deltaic sediments of the Dunvegan Formation. Compacted sedimentation rates ranged from 0.7 to 5.0 cm/10^3 yrs.

The laminated marlstones to limestones of the Second White Specks Formation were deposited under dominantly anoxic conditions beneath an increased water column that fostered fully marine conditions. Increased water depths allowed Tethyan planktonic foraminifera and nannofossils to migrate into the WCSB. These conditions resulted in increased TOC contents of up to 12 wt% of Type II OM. Bottom currents reworked bioclastic sediments deposited below storm wave-base. Compacted sedimentation rates ranged from 1.3 to 2.5 cm/10^3 yrs.

The early diagenesis of lower Colorado Group shales is dominated by sulfate reduction and methanogenesis. These microbially mediated processes resulted in the formation of pyrite, carbonate concretions and some clay mineral neoformation, primarily kaolinite. Carbonate concretions in the Westgate, Fish Scales and Belle Fourche formations are dominantly siderite, whereas those of the Second White Specks Formaton are calcite. Alteration of volcanic ash and hydrolysis of K-aluminosilicates resulted in smectite, mixed-layer illite/smectite and kaolinite authigenesis.

Rock-Eval pyrolysis data indicate that, west of approximately 114° longitude, the lower Colorado Group shales are mature source rocks. The Second White Specks Formation is an effective source rock and apparently there is active localized hydrocarbon migration from the Fold and Thrust Belt. It is inferred that

hydrocarbon migration and production from the Second White Specks Formation is controlled largely by fractures.

Résumé

Les shales du Crétacé de la partie inférieure du Groupe de Colorado se rencontrent dans la subsurface du Bassin sédimentaire de l'Ouest du Canada et sur toute la longueur des Foothills des Rocheuses. Quatre unités de shales cartographiables à l'échelle régionale sont reconnues d'après leurs caractéristiques géochimiques, minéralogiques et sédimentologiques propres, et leurs biofaciès distinctifs, soit les formations de Westgate de l'Albien tardif, de Fish Scales du Cénomanien précoce, de Belle Fourche du Cénomanien moyen–tardif et de Second White Specks du Cénomanien sommital–Turonien moyen. Ces unités se sont déposées dans un bassin d'avant-pays au cours d'une période de montée générale du niveau marin, laquelle a été ponctuée par des périodes d'abaissement relatif du niveau marin provoqué par des événements tectoniques.

La Formation de Westgate est un dépôt de progradation comportant des siltstones passant à des mudstones, dont la teneur en matière organique, essentiellement de type III, est faible (inférieure à 2 p. 100 en poids). Elle s'est accumulée au-dessus du niveau de base des vagues de tempête dans la mer Mowry. L'association de foraminifères de milieu épinéritique à médio-néritique (Zone à *Milliammina manitobensis*) et la composition des isotopes de l'oxygène des concrétions carbonatées syndiagénétiques attestent la présence d'une masse d'eau froide à faible salinité, d'affinité boréale. Les taux de sédimentation compactée s'échelonnaient de 1 à 6 cm/10^3 ans.

La Formation de Fish Scales est composée de matériau transgressif, allant des mudstones aux claystones dont la teneur en matière organique de types II et III mixtes s'élève à 8 p. 100 en poids. Le conglomérat de base met en évidence une modification radicale de l'environnement à la fin de l'Albien. La colonne d'eau était stratifiée et les eaux de fond anoxiques étaient répandues, comme l'attestent la présence de roches sédimentaires à lamines bien développées et l'absence de foraminifères benthiques. Les taux de sédimentation compactée variaient de 1 à 2 cm/10^3 ans.

Le contact entre la Formation de Fish Scales et celle de Belle Fourche est progressif, indiquant que les conditions benthiques se sont améliorées progressivement. La matière organique est de type III et sa teneur est généralement inférieure à 2 p. 100 en poids. À cette époque, la mer reliant les masses d'eau boréales et téthysiennes était déjà en place, mais les eaux à affinité boréale étaient prédominantes dans le Bassin sédimentaire de l'Ouest du Canada. La partie nord-ouest du bassin subissait les effets de la progradation des sédiments deltaïques de la Formation de Dunvegan. Les taux de sédimentation compactée allaient de 0,7 à 5,0 cm/10^3 ans.

La Formation de Second White Specks comporte des marnes laminaires passant à des calcaires qui se sont déposés dans des conditions essentiellement anoxiques sous une colonne d'eau plus profonde qui a favorisé l'apparition de conditions entièrement marines. Les profondeurs accrues d'eau ont permis la migration de nannofossiles et de foraminifères planctoniques téthysiennes dans le Bassin sédimentaire de l'Ouest du Canada, ce qui a augmenté les teneurs en matière organique de type II jusqu'à 12 p. 100 en poids. Les courants de fond ont remanié les sédiments bioclastiques déposés sous le niveau de base des vagues de tempête. Les taux de sédimentation compactée étaient de l'ordre de 1,3 à 2,5 cm/10^3 ans.

La syndiagenèse des shales de la partie inférieure du Groupe de Colorado est dominée par une sulfatoréduction et une méthanogenèse. Ces processus d'origine microbienne ont entraîné la formation de pyrite et de concrétions carbonatées et la néogenèse de minéraux argileux, essentiellement de la kaolinite. Les concrétions carbonatées dans les formations de Westgate, de Fish Scales et de Belle Fourche sont formées principalement de sidérite, alors que celles de la Formation de Second White Specks se composent surtout de calcite. L'altération des cendres volcaniques et l'hydrolyse des aluminosilicates potassiques ont engendré l'authigenèse de smectites, d'illite-smectite et de kaolinite.

Les données de pyrolyse Rock-Eval indiquent qu'à l'ouest d'environ 114° de longitude ouest, les shales de la partie inférieure du Groupe de Colorado sont des roches mères matures. La Formation de Second White Specks est une bonne roche mère et il se produirait localement une migration des hydrocarbures à partir de la ceinture de plissement et de charriage. On présume que la migration et la production d'hydrocarbures depuis la Formation de Second White Specks sont en grande partie contrôlées par des fractures.

Summary

Four regionally recognizable lithostratigraphic units are defined for the Late Albian to Middle Turonian interval of the Cretaceous Colorado Group within the Western Canada Sedimentary Basin (WCSB). In ascending order, these are the Westgate, Fish Scales, Belle Fourche, and Second White Specks formations. These marine shale units are characterized by their distinctive sedimentology, geochemistry, palynology, and biostratigraphy.

Stratigraphic correlations and relative ages are based on foraminifers, nannofossils and dinoflagellates. The Westgate Formation is Late Albian in age, and is represented by the *Miliammina manitobensis* Zone. The Fish Scales Formation, barren of foraminifers, contains an Early Cenomanian dinoflagellate assemblage. A diminished foraminiferal fauna of the *Verneuilinoides perplexus* Zone indicates a Middle to Late Cenomanian age for the Belle Fourche Formation. Abundant planktic foraminifers of the *Hedbergella loetterlei* Zone and nannofossils indicate that the Second White Specks Formation is latest Cenomanian to Middle Turonian in age.

In the Western Interior Seaway (WIS), foraminiferal and nannofossil assemblages indicate dynamic oceanographic conditions linked to sea-level change and variable mixing of Boreal and Tethyan water masses. These Colorado Group marine shales were deposited during a third-order eustatic rise in sea level with superimposed fourth- and fifth-order, tectonically induced, sea-level fluctuations. The Westgate Formation contains common to abundant agglutinated foraminifers and was deposited during the Mowry Sea transgression under dominantly cool, Boreal waters. The base of the overlying Fish Scales Formation is marked by the disappearance of all benthic foraminifers. A stratified water column resulted in bottom water anoxia throughout the Early Cenomanian.

Benthic conditions improved slightly during Belle Fourche deposition when sea level dropped. Subsequent sea-level rise during the latest Cenomanian resulted in the migration of Tethyan-sourced planktic foraminifers and coccoliths to the northern portion of the seaway where they dominated the faunal and floral assemblages of the Second White Specks Formation.

The Westgate Formation is characterized by multiple coarsening-upward successions, and the grain size of agglutinated foraminferal tests reflect changes in substrate grain size. The Fish Scales and Second White Specks formations may be characterized as condensed sections. The basal bed of the Fish Scales Formation is a bioclastic, coarse grained sandstone to conglomerate layer that disconfomably overlies uppermost Westgate strata. The basal contact of the Second White Specks Formation varies from conformable to disconformable. The local presence of a bioclastic layer, formed by submarine erosion, is associated with an abrupt change from a diminished agglutinated fauna to a pelagic fauna. The degree of erosion varies across the basin, but is greatest in central Saskatchewan. Other localities show a more gradational change from benthic to planktic assemblages. The Fish Scales Formation has a gradational upper contact, whereas assemblages disappear abruptly at the top of the Second White Specks Formation.

The variable and dynamic depositional environments of the WIS are reflected in the variable geochemistry of the described formations. Condensed sections (transgressive shales) which include the Fish Scales and Second White Specks formations, as well as the Santonian First Speckled Shale, are characterized by a high marine organic matter (OM) content (dominantly Type II) and C/S values with low variability. Progradational

shales (regressive) contain dominantly Type III OM and have highly variable C/S values. This is particularly evident in the Belle Fourche Formation, where prodeltaic and marine samples show extreme C/S variablity.

The silicate mineralogy of the studied units is relatively uniform and comprises dominantly quartz, mixed layer I/S, kaolinite, illite, feldspars, muscovite, minor biotite, and chlorite. Pyrite is ubiquitous. Accessory minerals include apatite and anatase. Gypsum is present in the Second White Specks Formation and the First Speckled Shale. Additional sulphates include jarosite and alunite. Siderite, primarily as concretions, occurs in the Westgate, Fish Scales, and Belle Fourche formations but may also be present as a disseminated cement, particularly in well-bioturbated samples. Calcite is present in the Second White Specks Formation and First Speckled Shale as concretions and bioclastic detritus. Some samples in these units contain > 80 wt% calcite. Dolomite may also be present.

Variations in mineralogy are caused primarily by depositional environment and secondarily by diagenesis. Samples from the progradational shales (Westgate and Belle Fourche), particularly from the western margin of the WIS, contain a greater proportion of quartz silt and more detrital illite than samples from transgressive shales (Fish Scales and Second White Specks) or those samples from the basin center. Transgressive shales contain numerous bentonites, and distal samples contain a greater abundance of ash-derived matrix than proximal counterparts.

Isotope data from pyrite, carbonate concretions, and clay minerals indicate that the early diagenesis of these marine shales was dominated by sulphate reduction, methanogenesis and the alteration of volcanic ash to clay minerals. Late diagenetic processes include organic matter maturation, quartz, plagioclase, and feldspar dissolution, and continuing clay mineral authigenesis. Localized fracture formation occurred under near maximum burial conditions and may have facilitated fluid movement through these low-permeability formations.

Colorado Group shales generally are immature source rocks east of approximately 114° longitude. They are mature adjacent to and presumably beneath the Fold and Thrust Belt along the western margin of the WCSB. Transgressive shales are oil prone and progradational shales are gas prone. Rock-Eval data suggest that hydrocarbons are migrating updip from beneath the Fold and Thrust Belt. It is inferred that fracture networks control the migration of hydrocarbons to producing zones along the Fold and Thrust Belt and future recovery efficiency is linked to understanding these fracture systems.

Sommaire

Quatre unités lithostratigraphiques reconnaissables à l'échelle régionale ont été individualisées dans l'intervalle allant de l'Albien tardif au Turonien moyen du Groupe de Colorado du Crétacé dans le Bassin sédimentaire de l'Ouest du Canada. Par ordre ascendant, il s'agit des formations de Westgate, de Fish Scales, de Belle Fourche et de Second White Specks. Ces shales marins se définissent individuellement par des caractéristiques sédimentologiques, géochimiques, palynologiques et biostratigraphiques qui leur sont propres.

Les corrélations stratigraphiques et les âges relatifs sont fondés sur les foraminifères, les nannofossiles et les dinoflagellés. La Formation de Westgate remonte à l'Albien tardif à en juger par la Zone à *Miliammina manitobensis*. La Formation de Fish Scales, caractérisée par l'absence de foraminifères, renferme un assemblage de dinoflagellés du Cénomanien précoce. Une faune de foraminifères appauvrie de la Zone à *Verneuilinoides perplexus* indique que la Formation de Belle Fourche s'échelonne du Cénomanien moyen au Cénomanien tardif. La présence d'abondants foraminifères planctoniques de la Zone à *Hedbergella loetterlei* et de nannofossiles indique que la Formation de Second White Specks s'échelonne du Cénomanien sommital au Turonien moyen.

Dans la mer intérieure de l'Ouest, la présence d'assemblages de foraminifères et de nannofossiles témoigne de conditions océanographiques dynamiques reliées au changement du niveau marin et d'un mélange fluctuant des masses d'eau boréales et téthysiennes. Les shales marins du Groupe de Colorado se sont déposés au cours d'une montée eustatique de troisième ordre accompagnée de fluctuations superposées du niveau de la mer de quatrième et de cinquième ordres, d'origine tectonique. La Formation de Westgate renferme des foraminifères agglutinants fréquents à abondants et s'est déposée au cours de la transgression de la mer Mowry sous des eaux essentiellement froides de la mer Boréale. La base de la Formation de Fish Scales sus-jacente est marquée par la disparition de tous les foraminifères benthiques. La stratification de la colonne d'eau a provoqué l'anoxie de l'eau de fond tout au long du Cénomanien précoce.

Les conditions benthiques se sont légèrement améliorées au cours du dépôt de la Formation de Belle Fourche lorsque le niveau marin a chuté. La montée ultérieure du niveau marin au Cénomanien sommital a entraîné la migration de foraminifères planctoniques et de coccolithes d'origine téthysienne vers la portion septentrionale de la mer, lesquels sont prédominants dans les assemblages fauniques et floristiques de la Formation de Second White Specks.

La Formation de Westgate se distingue par de multiples successions à granulométrie croissante vers le haut; la granulométrie des tests de foraminifères agglutinants reflète les changements de la granulométrie du substrat. Les formations de Fish Scales et de Second White Specks peuvent se définir comme des sections condensées. Le lit de base de la Formation de Fish Scales comporte une couche bioclastique allant d'un grès à grain grossier à un conglomérat qui recouvre en discordance les strates sommitales de la Formation de Westgate. Le contact de base de la Formation de Second White Specks varie de concordant à discordant. La présence, par endroits, d'une couche bioclastique, formée par l'érosion sous-marine, est associée au passage abrupt d'une faune agglutinante appauvrie à une faune pélagique. Le degré d'érosion varie dans l'ensemble du bassin, mais il est particulièrement élevé dans le centre de la Saskatchewan. Dans d'autres régions, il y a passage plus graduel d'associations benthiques à des associations planctoniques. La Formation de Fish Scales présente un contact supérieur progressif alors que les associations disparaissent brusquement au sommet de la Formation de Second White Specks.

Les milieux de sédimentation variables et dynamiques de la mer intérieure de l'Ouest se retrouvent dans la composition géochimique variable des formations décrites. Les sections condensées (shales transgressifs), qui comprennent les formations de Fish Scales et de Second White Specks et le Premier shale à taches blanches du Santonien, sont caractérisés par une haute teneur en matière organique marine, essentiellement de type II, et une faible variabilité des taux de sédimentation compactée. Les shales de progradation (régressifs) recèlent principalement de la matière organique de type III et les taux de sédimentation compactée sont très fluctuants. Ces caractéristiques sont particulièrement évidentes dans la Formation de Belle Fourche où des échantillons prodeltaïques et marins montrent des taux de sédimentation compactée extrêmement variables.

La composition minéralogique des silicates des unités étudiées est relativement uniforme; elle est dominée par du quartz, de l'illite et de smectite, de la kaolinite, de l'illite, des feldspaths, de la muscovite, de la biotite en quantités mineures et de la chlorite. La pyrite est ubiquiste. Les minéraux accessoires sont l'apatite et l'anatase. Du gypse est présent dans la Formation de Second White Specks et dans le Premier shale à taches blanches. On trouve aussi d'autres sulfates comme la jarosite et l'alunite. De la sidérite, principalement sous forme de concrétions, se rencontre dans les formations de Westgate, de Fish Scales et de Belle Fourche, mais elle peut aussi prendre l'aspect d'un ciment disséminé, particulièrement dans les échantillons très bioturbés. De la calcite se rencontre dans la Formation de Second White Specks et dans le Premier shale à taches blanches sous la forme de concrétions et de débris bioclastiques. Certains échantillons de ces unités comptent plus de 80 p. 100 en poids de calcite. On trouve parfois de la dolomite.

Les variations observées dans la composition minéralogique sont attribuables d'abord au milieu de sédimentation, puis à la diagenèse. Les échantillons prélevés dans les shales de progradation (formations de

Westgate et de Belle Fourche), en particulier dans la marge occidentale de la mer intérieure de l'Ouest, contiennent des silts quartzeux et de l'illite détritique en proportions plus élevées que les échantillons provenant des shales transgressifs (formations de Fish Scales et de Second White Specks) ou du centre du bassin. Les shales transgressifs comptent de nombreuses bentonites et les échantillons distaux ont une matrice issue de cendres plus abondante que les échantillons proximaux.

Les données isotopiques tirées de la pyrite, des concrétions carbonatées et des minéraux argileux révèlent que la syndiagenèse de ces shales marins a été dominée par une sulfatoréduction, une méthanogenèse et une altération des cendres volcaniques en minéraux argileux. Les processus épidiagénétiques sont la maturation de la matière organique, la dissolution du quartz, des plagioclases et des feldspaths, et l'authigenèse continue des minéraux argileux. Des fractures se sont formées localement dans des conditions d'enfouissement quasi maximales; il se peut qu'elles aient facilité la circulation des fluides dans ces formations peu perméables.

Les shales du Groupe de Colorado sont en général des roches mères immatures à l'est d'environ 114° de longitude ouest. Elles sont matures à proximité de la ceinture de plissement et de charriage le long de la bordure occidentale du Bassin sédimentaire de l'Ouest du Canada et vraisemblablement sous cette ceinture. Les shales transgressifs sont susceptibles de donner du pétrole et les shales de progradation, du gaz naturel. Selon les données Rock-Eval, les hydrocarbures migreraient vers l'amont-pendage depuis la ceinture de plissement et de charriage. On en déduit que les réseaux de fractures régissent la migration des hydrocarbures vers les zones productrices le long de la ceinture de plissement et de charriage; l'efficacité de la récupération est donc liée à la compréhension de ces systèmes de fractures.

INTRODUCTION

The Colorado Group is the thickest and most regionally extensive succession of Cretaceous rocks in the Western Canada Sedimentary Basin (WCSB). The Colorado Group and equivalent strata form an extensive, eastward-tapering wedge of predominantly marine shales and intercalated sandstones that extend for more than 1300 km from the Rocky Mountains to the Manitoba Escarpment. This succession contains most of the clastic oil- and gas-producing units, primarily sandstones (Fig. 1), in the WCSB (Porter, 1992b). Sandstones of the Colorado Group and equivalent strata include, in ascending order, the Colony Formation, Basal Colorado Member, the Newcastle Sandstone, the Boulder Creek Formation, the Viking/Bow Island formations, the St. Walburg and Barons sandstones, the Dunvegan Formation, the Doe Creek, Pouce Coupe and Howard Creek members of the Kaskapau Formation, the Phillips and Jumping Pound sandstones, and the Cardium, Badheart and Medicine Hat formations. Because of their economic significance, the origin and evolution of these coarser clastic units are, for the most part, well-studied (see Macqueen and Leckie, 1992; and references therein; Mossop and Shetsen, 1994), yet they represent only a small fraction of the Cretaceous depositional history of the WCSB. In contrast, the enclosing shales of the Colorado Group contain a much more complete record of deposition, and thus have the potential to provide a comprehensive picture of Cretaceous paleogeography, paleoenvironments and foreland basin development. Despite this fact, relatively little is known regarding the origin and deposition of these fine grained rocks. Some of the shale units of the Colorado Group have been identified as source rocks, or potential source rocks, for much of the hydrocarbons in Cretaceous strata (Macauley et al., 1985; Creaney and Allan, 1992). Recent advances in horizontal drilling technology allow for direct exploitation of shales as reservoirs. In addition, shales of the Colorado Group host diamond-bearing kimberlites in Central Saskatchewan (Lehnert-Theil et al., 1992; Leckie et al., 1997) and it has been suggested that Cretaceous black shales may be the source of placer gold deposits (Ballantyne and Harris, 1995). This economic potential has generated significant exploration activity focused on Colorado Group shales. The economic potential and the wealth of geological information that these rocks contain, and our relatively meager knowledge of them, are the rationale for this multidisciplinary study.

The Geological Survey of Canada undertook this study to: 1) identify distinct shale units in the studied interval, 2) evaluate the depositional and facies controls on shale composition, and 3) provide quantitative mineralogy and bulk chemical properties that may be used for wireline calibration and source rock and reservoir characterization. Geochemical, biofacies and sedimentological data have been integrated to provide a comprehensive analysis of the studied interval and identify four distinct shale formations that make up the Albian to Turonian portion of the lower Colorado Group in the WCSB (Bloch et al., 1993).

ACKNOWLEDGMENTS

This study was funded by the Panel of Energy and Resource Development (PERD), the Geological Survey of Canada, and the Natural Sciences and Engineering Research Council (NSERC) Visiting Scientist Program. CSA was supported by NSERC research and strategic grants. The authors would like to thank Roger Macqueen for his support of this research and his administrative guidance. We are also indebted to Dave McNeil and John Wall of the Geological Survey of Canada for their assistance, taxonomic advice, and many enlightening conversations during the course of this work. Peter Adams is thanked for constructing the Saskatchewan cross-section. Technical assistance was provided by Bob Davidson, Brenda Davies, Ron Fanjoy, Brad Gorham, Al Heinrich, Ram Kalgutkar, Brian Rutley, Bill Sharman, Ross Stewart, Denise Then, Bernie Walker and Jenny Wong of the Geological Survey. In addition, we would like to thank Jun Resultay of the University of Calgary for preparing the polished mounts for electron microscopy; Peter Jones, Chang Huang and Kathy Langill of the Department of Earth Sciences, Carleton University, for SEM work and other technical assistance. Fred Longstaffe is thanked for his support and access to the Stable Isotope laboratory and insightful discussions regarding the stable isotopic data. Paul Middlestead, Jennifer Mackay and Sharon Forbes at the Stable Isotope Laboratory, Department of Earth Sciences, The University of Western Ontario, are thanked for sample processing and isotopic analyses. We are indebted to the staff of the Core Research Centre of the Alberta Energy and Utilities Board (EUB; formerly the Energy Resources Conservation Board of Alberta) in Calgary, and at the core storage facility of the Saskatchewan Geological Survey, Saskatchewan Energy and Mines, in Regina, for their assistance with sample collection. A special thanks to Mike Staniland of the GSC for his assistance in the field and his resourcefulness in solving a large number of seemingly impossible computer and database problems. We are grateful to editor Jim Dixon and reviewers Hugh Abercrombie, Dave McNeil, Wendy Warters and James White for their constructive comments.

PREVIOUS WORK

Historically, shales have been the focus of biostratigraphic studies. Previous work on the Colorado Group has evaluated various aspects of stratigraphy and biostratigraphy (i.e., Dawson, 1881; Malloch, 1911; Wickenden and Shaw, 1943; McLearn, 1944; Wickenden, 1945; Gleddie, 1949; Stott, 1963, 1967; Wall, 1967; Caldwell, 1975; Caldwell et al.,

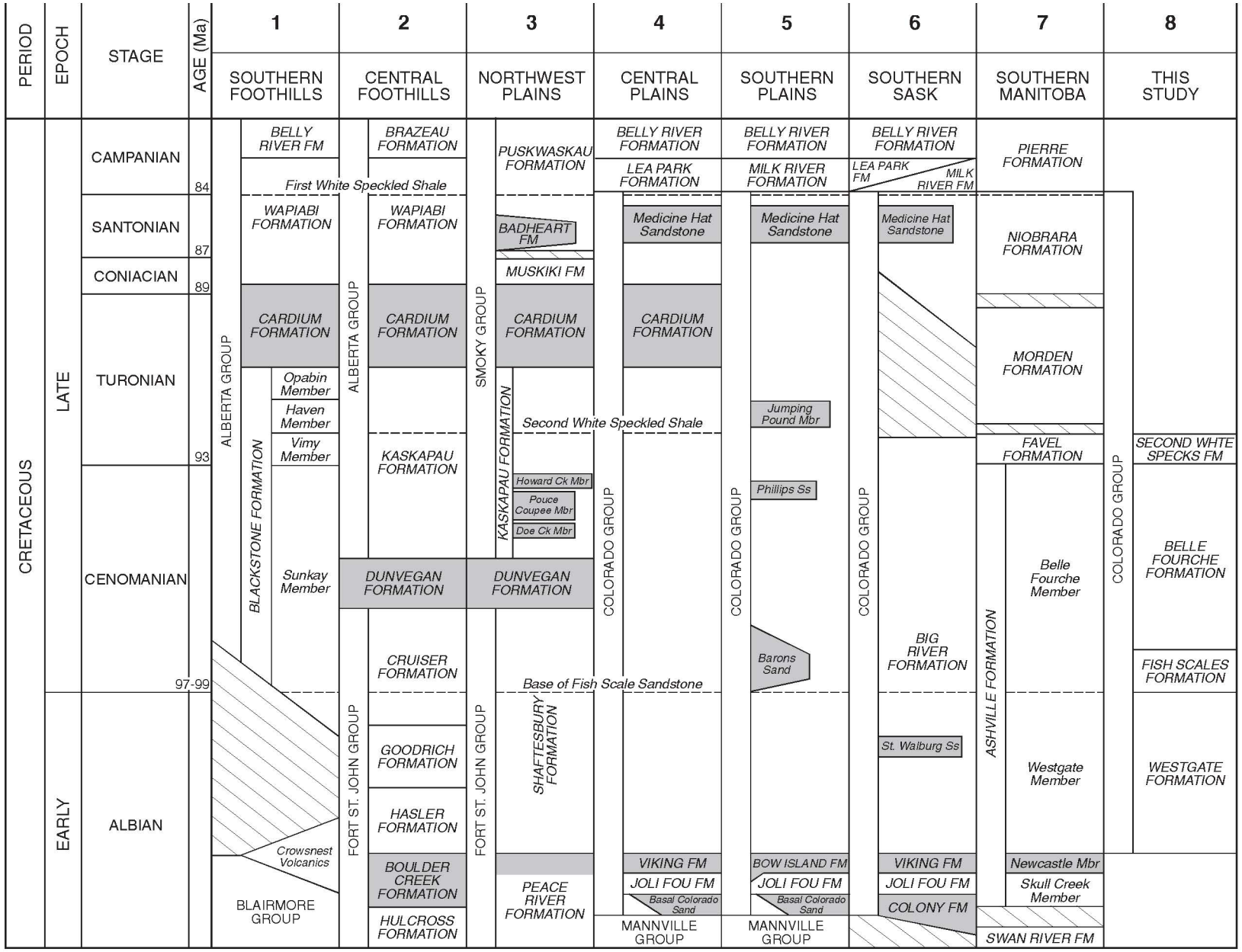

Figure 1. *Stratigraphic nomenclature for the study area (after Leckie et al., 1994). Stippling indicates oil and/or gas producing sandstones of the Colorado Group and equivalent strata. Dashed lines indicate the stratigraphic tops of regionally significant wireline markers.*

1978; Stelck and Armstrong, 1981; Simpson, 1982; Lang and McGugan, 1988; Bloch et al., 1993). The Cretaceous fossil zones of the Western Interior of North America are constructed primarily from shale-derived data (i.e., Cobban and Reeside, 1962; Jeletzky, 1968; Wall, 1967; Caldwell et al., 1978), and Cretaceous paleoenvironmental models of the Western Interior Seaway have been developed primarily from biostratigraphic (e.g., Hattin, 1965; Kauffman, 1969; Schröder-Adams et al., 1996) and geochemical data (Cadrin, 1992). The general architecture of the Colorado Group succession was recently described (Leckie et al., 1994). However, virtually no information regarding the origin or composition of Cretaceous shales of the Western Interior has been extracted from these rocks. Numerous studies have investigated particular aspects of shale geochemistry, such as smectite–illite diagenesis or concretion formation, but have not considered the bulk chemistry or mineralogy of the entire rock. Notable exceptions to this in the Western Interior are the studies of Rubey (1931), Campbell and Oliver (1968), Schultz et al. (1980), Whittaker et al. (1987), and Williams and Bayliss (1988).

The Cretaceous of the WCSB is a major petroleum producer (see Porter, 1992a; for a review) and exploration and exploitation of this resource extends back over two centuries. The first descriptions of Cretaceous coal- and bitumen-bearing strata were made in the late 18th and early 19th centuries (Porter, 1992a, and references therein). Cretaceous shales along the Peace River were first described by Selwyn (1877); and the first documentation of Cretaceous shales in the subsurface of the WCSB occurred in that same year (see Porter, 1992a). Gas production from the Cretaceous Milk River sandstone began in 1883 (Dawson, 1886). Current estimated conventional reserves for Colorado Group and equivalent strata total 3.706 x $10^8 m^3$ of oil and 6.032 x $10^{11} m^3$ of gas (Porter, 1992b). Various aspects of the Colorado Group petroleum system have been described (Macauley, 1984a, b, c; Allan and Creaney, 1988, 1991; Barclay and Smith, 1992; Creaney and Allan, 1990, 1992) that highlight the economic significance of this interval.

REGIONAL STRATIGRAPHY

The Colorado Group was deposited over a period of 25 to 30 m.y., from Albian through Santonian time, when sea level was globally high (Haq et al., 1988; Kauffman, 1977). Specific sea-level maxima occurred during the Late Albian, Early Turonian and middle Santonian (Caldwell and North 1984; Haq et al., 1988). During this part of the Cretaceous, deposition was coincident with a regional tectonic downflexing of the western margin of the North American craton (Lambeck et al., 1987) that resulted in the development of an extensive north–south-trending foreland basin (see summary in Leckie and Smith, 1992).

The Colorado Group unconformably overlies the Mannville Group in the subsurface of central and southern Alberta, the Cantuar and Pense formations in southern Saskatchewan, and the Swan River Formation in southern Manitoba (Fig. 1). The strata are overlain conformably to disconformably by the Milk River and Lea Park formations in the central and southern plains of Alberta and Saskatchewan, and the Pierre Formation in southern Manitoba. In the southern Foothills, Colorado-equivalent Alberta Group strata unconformably overlie the Crowsnest Volcanics and Blairmore Group. In the central Foothills, Colorado Group equivalents include most of the Fort St. John Group, the Dunvegan Formation, and most of the Alberta Group (Fig. 1).

The Colorado Group contains seven shale formations of Late Albian to Santonian age. In ascending order, these are the Joli Fou (Skull Creek), Westgate, Fish Scales, Belle Fourche, Second White Specks (Favel), Morden and Niobrara formations. In southern Manitoba, the Westgate and Belle Fourche formations have member status and comprise the Ashville Formation; the Fish Scales Formation is not recognized as a distinct stratigraphic unit.

Shales of the Colorado Group are intercalated with numerous sandstones that reflect sea-level changes within the WCSB. In ascending order, these are the Basal Colorado Sandstone (Colony Formation), Viking Formation (Peace River and Bow Island formations), St. Walburg, Barons, Phillips and Jumping Pound sandstones, and the Cardium and Medicine Hat (Badheart) formations.

This study focuses primarily on the lower portion of the Colorado Group, which was deposited from Late Albian to Early Turonian time, and includes the Westgate, Fish Scales, Belle Fourche and Second White Specks formations. The rocks of this interval will be referred to informally as the lower Colorado Group. Inclusive in this interval are the regionally extensive Base of Fish Scales and Second White Specks wireline markers. Additional geochemical data from the Joli Fou, Viking and Morden formations and the First White Speckled Shale are also included.

ANALYTICAL METHODS

Prior to this study, most of the Colorado Group in the subsurface of Alberta was undifferentiated and there was little information to guide a sampling program. The EUB well database was searched to provide a list of cores that intersected the Colorado Group. Because of the variable thickness and scarcity of information, it was decided to limit our initial investigation to the interval that extends from the top of the Viking Formation to the Second White Specks wireline marker (Fig. 1). This interval also contains the

boundary between the Lower and Upper Cretaceous, the regionally recognized Fish Scale Marker Bed, Fish Scales Zone, or "Base of Fish Scales" (Gleddie, 1949). Cores that contain a significant thickness (generally more than 10 m), or that encompass major changes in log characteristics, were initially selected to provide stratigraphic control. Additional cores were added at a later time to provide better geographic sample control. The cores used in this study are listed in Table 1 and their distribution within the study area is shown in Figure 2.

Each selected core was examined to provide a description of the macroscopic properties of the sediments including lithology, sedimentary structures, the degree of bioturbation and the presence of observed fossils and ichnofossils. The core logs are provided for reference in Appendix A. Samples of up to 50 g were collected from the cores at regular intervals of one to five metres. Sampling frequency was increased near lithological boundaries to better assess changes at these contacts. Most samples are identified with a six digit number and may be located by matching the first four digits with the Legal Subdivision (LSD) and section numbers of the cores listed in Table 1. The locations of the remaining samples are described in Caritat et al. (1994a), or Bloch and Leckie (1993).

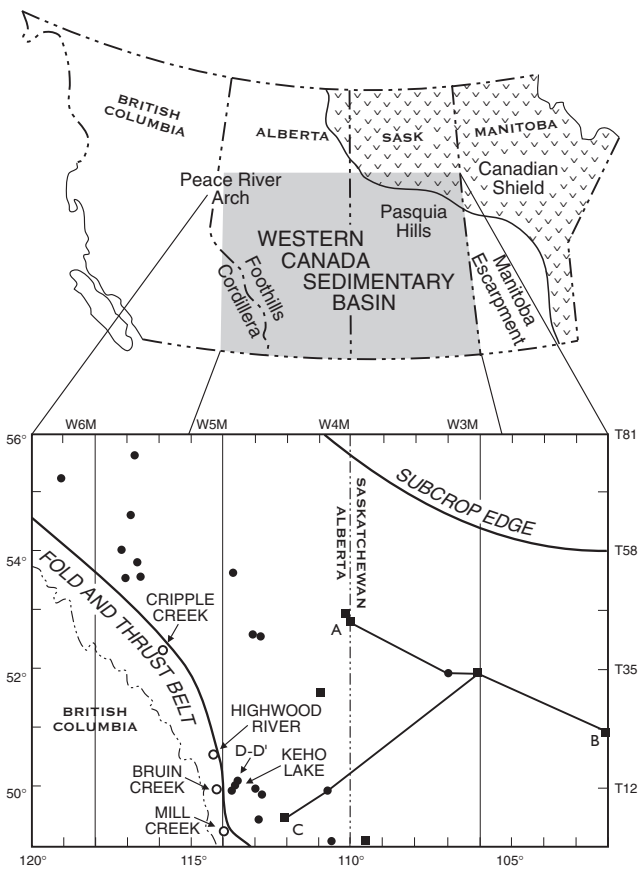

Figure 2. *Study area (stippled) with major physiographic elements and the location of cored wells (see Table 1) from which sample material was selected. Square symbols denote reference sections (see Bloch et al., 1993; and Schröder-Adams et al., 1996). Lettered cross-sections A-B, B-C, and D-D' refer to figures 29, 36, and 37, respectively.*

Selected outcrops of Colorado Group-equivalent strata were also measured and sampled during the course of this study. Rock-Eval and biofacies analyses were done on many of these samples, but other geochemical analyses were not done. Organic-rich, pyritic black shales undergo significant weathering at surface and near-surface conditions. Organic matter is degraded (Leythauser, 1973) and the oxidation of pyrite may enhance mineral alteration. Sulphur is mobilized with groundwater flow and the formation of kaolinite and gypsum perturbs the major element chemistry and mineralogy. For these reasons, extensive geochemical analysis of outcrop samples was not done.

Approximately 20 g of each sample was allotted for geochemical analysis. Figure 3 provides a summary of sample use and indicates the overall analytical procedure. Sample preparation and geochemical analyses were done at the Geological Survey of Canada (Calgary). Additional analyses were done at the the Department of Geology and Geophysics, The University of Calgary. Isotopic analysis was done at the Laboratory for Stable Isotope Studies, Department of Geology, The University of Western Ontario.

Rock-Eval pyrolysis (Espitalié et al., 1977; Peters, 1986) was performed in duplicate on pulverized shale samples, using standard procedures on a DELSI Rock-Eval II/TOC apparatus. Information thus obtained includes the type of organic matter (oxygen and hydrogen indices), its maturity (T_{max}), and the amount of total organic carbon (TOC) contained in the sample. Simple guidelines for interpreting Rock-Eval pyrolysis data are given in Table 2.

X-ray diffraction (XRD) was carried out on disaggregated and gently ground bulk shale and bentonite samples, and on their clay fractions (< 2.0 and < 0.2 µm equivalent spherical diameter) obtained by ultrasonic dispersion in distilled water and centrifugation. XRD results were obtained using a Philips PW1700 automated powder diffraction system with Fe-filtered CoKα radiation generated at 40 kV and 30 mA. Bulk, unoriented samples were scanned from 4 °2θ to 64 °2θ and clay fraction samples were scanned from either 2 or 4 °2θ to 40 °2θ with an increment of 0.05 °2θ at a recording speed of 1 °2θ/cm/50 sec. Clay-fraction diffractograms were obtained under conditions of ambient humidity (~ 45% relative humidity), low humidity (~ 0%), ethylene glycol saturation, and after heat treatment (550°C for 1 hour). Some clay separates were run from 4°2θ to 64°2θ to evaluate 00ℓ peak positions and Bragg behavior of clay minerals in mixtures (see Moore and Reynolds, 1989).

Table 1

Core and outcrop locations with Geological Survey of Canada curation numbers

Location	Name	GSC #
	Core	
05-09-72-08 W6	Imperial Wembley	C-167134
16-01-66-22 W5	Amoco Bigstone	C-167143
05-01-77-20 W5	Imperial Kathleen #1	C-167135
10-25-65-20 W5	Sabine et al. Iosegun	C-167144
10-05-53-20 W5	H.B. Galloway	C-167145
09-09-56-19 W5	HCS et al. Beaver Creek	C-167147
04-13-54-18 W5	Texex Edson	C-167146
14-29-13-29W4	Brascan et al. Oxley	C-205701
10-36-11-29W4	Amtrog Gulf Claresholm	C-205702
06-07-12-28W4	Canadian Superior Oxley	C-190616
14-29-11-28W4	Dome et al. Claresholm	C-205706
06-30-13-27W4	MLC Dekalb Claresholm	C-179967
06-29-13-27W4	Can Hunter et al. Claresholm	C-179966
04-08-13-27W4	Sinclair E. Mathews	C-205704
06-32-13-27W4	Can Hunter et al. Claresholm	C-205708
06-21-55-25 W4	Ajax Morinville	C-167142
08-25-12-24W4	Penn West et al. Barons	C-205707
11-21-12-23 W4	Melaar Barons	C-167150
16-10-12-23W4	Barons Superior #1	C-205703
10-34-42-22 W4	LCD et al. Bashaw	C-167138
06-16-11-22W4	Can Hunter Keho	C-179965
06-34-10-22W4	Can Hunter Kipp	C-205705
06-16-06-22 W4	GULF Mohawk Blood	C-167149
07-12-42-21 W4	LCM et al. Buff Lake North	C-167139
11-12-06-16 W4	Amoco Conrad	C-167148
06-22-11-06 W4	G. Basin Bux Medicine Hat	C-179954
06-34-30-08 W4	Amoco B-1 Youngstown	C-167141
07-14-01-05 W4	Pacific Amoco Sapphire	C-179953
10-35-45-02 W4	Anderson Husky Roros	C-167136
06-18-45-01 W4	Anderson et al. Ribstone	C-167137
10-25-01-27W3	Saskoil Willow Creek	C-179958
11-16-35-08W3	C.M.S. Vanscoy	C-179956
05-22-34-01W3	U.S. Borax & Chemical	C-179955
11-36-22-01W2	S.W.P Bredenbury	C-179957
	Outcrop	
Elk Creek 83B/4 UTM-Zone 11	Cripple Creek 573500-578550	C-190522–C-190614
Kananaskis Lakes 82J UTM-Zone 11	Highwood River 688000-5663000	C-170001–C-170050, C-190451–C-190456
Langford Creek 82J/1 UTM-Zone 11	Bruin Creek 685000-5543500	C-190477–C-190521
Fernie 82/G UTM-Zone 11	Mill Creek 707400-5474300	C-190457–C-190471

Bulk rock chemistry was determined by X-ray fluorescence (XRF) for ten major oxides on crushed shale (Tables 3, 4) and bentonite (Table 5) samples prepared by standard techniques (Baedecker, 1987). Analytical precision on replicate analyses of 1 g samples is less than 0.9 wt% for SiO_2, 0.5 wt% for Na_2O, 0.2 wt% for Al_2O_3 and 0.1 wt% for

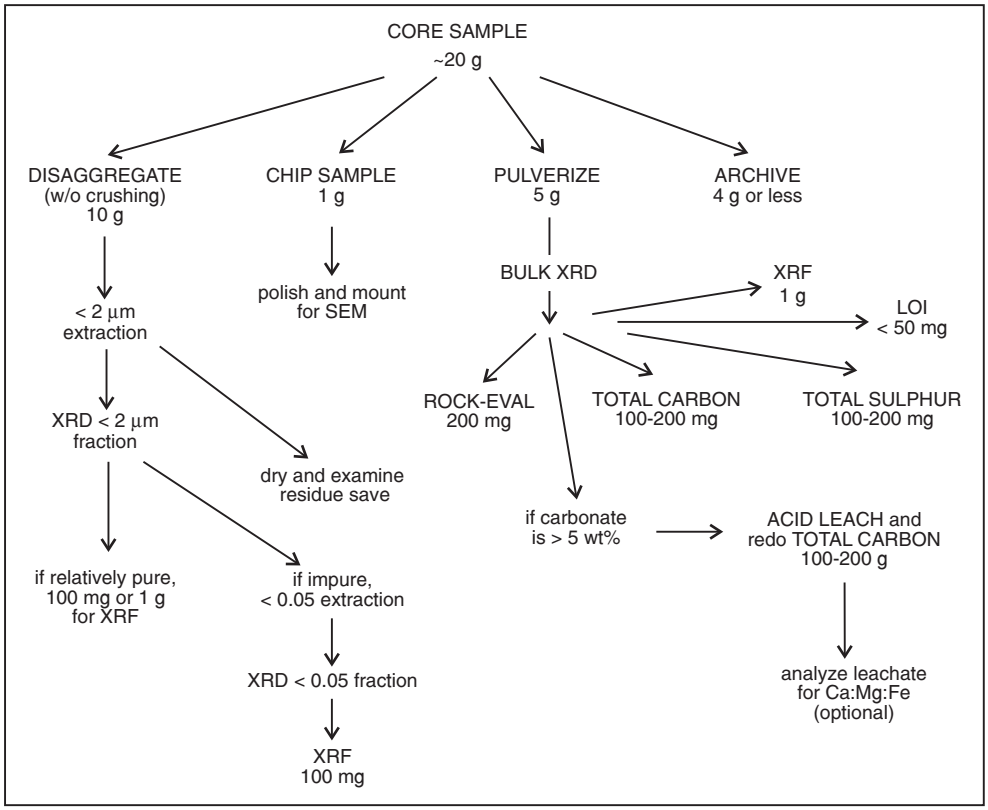

Figure 3. *Flow chart of sample preparation procedures.*

the other elements. Loss on ignition (LOI) was determined by combustion and thermogravimetric analysis, with a precision better than 0.7 wt%. XRF analysis of < 0.2 µm and < 0.1 µm clay fractions, previously characterized by XRD, was undertaken for a subset of samples in order to constrain clay mineral compositions. Because of the small amount of sample available, 100 mg aliquots were used and duplicate samples generally could not be made. Analytical error from replicate analyses of the primary standard (GSP-1), as determined by comparison with published values (see Abbey, 1980), are within 0.4 wt% for all oxides. However, analytical precision for unknowns is significantly higher, especially for Na, because of the reduced sample size. Based on the analysis of one set of duplicate beads (see Table 4; #063419), relative errors for SiO_2, Al_2O_3, Fe_2O_3 and Na_2O are 5, 13, 17 and 79%, respectively.

Total carbon was determined using a LECO WR-12 apparatus. Total sulphur was analyzed on a LECO-32 Sulfur Determinator using standard techniques (see Baedecker, 1987). Carbon and sulphur analyses were run in duplicate and analytical precision is 0.2 wt% and 0.05 wt%, respectively, for carbon and sulphur abundances up to about 8 wt%.

Table 2

Rock-Eval interpretive guidelines

a) Source rock generative potential

Quality	TOC (wt %)	S1 (mg HC/g rock)	S2 (mg HC/g rock)
poor	0.0–0.5	0.0–0.5	0.0–2.5
fair	0.5–1.0	0.5–1.0	2.5–5.0
good	1.0–2.0	1.0–2.0	5.0–10.0
very good	>2.0	>2.0	>10.0

b) Type of hydrocarbon generated

TYPE	HI (mgHC/g TOC)	S2/S3*
gas	0–150	0.0–3.0
gas and oil	150–300	3.0–5.0
oil	>300	>5.0

*assumes Ro = 0.6%

c) Level of thermal maturation

Maturation	PI (S1/(S1+S2))	Tmax °C	Ro (%)
top of oil window	~0.1	430–445*	~0.5
bottom of oil window	~0.4	~465	~1.3

*varies with type of OM

Table 3

Whole rock geochemistry (wt%)

Sample #	SiO_2	Al_2O_3	Fe_2O_3	MgO	CaO	MnO	TiO_2	BaO	Na_2O	K_2O	P_2O_5	LOI[1]	TOTAL	S[2]	TOC[3]
041302	53.48	14.46	6.22	1.72	6.73	0.01	0.66	0.09	0.33	2.64	0.23	9.79	100.00	3.62	4.80
041304	56.47	14.97	6.32	1.49	5.29	0.01	0.85	0.12	0.25	3.28	0.20	8.06	99.95	2.64	3.13
050102	64.47	16.24	5.00	1.50	0.55	0.05	0.76	0.14	0.38	2.65	0.26	7.91	99.99	0.09	1.16
050109	53.86	15.48	6.47	1.41	0.29	0.03	0.70	0.09	0.36	2.42	0.21	15.85	99.91	2.75	2.61
050122	62.24	16.39	5.67	1.28	0.29	0.02	0.83	0.10	0.51	2.20	0.14	9.48	99.98	0.82	2.03
050126	62.60	16.49	6.13	1.31	0.28	0.03	0.89	0.10	0.51	2.37	0.15	8.19	99.96	0.91	1.80
050902	62.24	16.56	6.05	1.68	0.54	0.07	0.80	0.17	0.30	2.94	0.25	8.33	99.99	0.07	1.71
050913	60.41	17.90	5.99	1.68	0.51	0.05	0.82	0.17	0.35	2.87	0.25	8.94	100.00	0.06	2.03
050918	62.82	17.86	4.93	1.54	0.40	0.03	0.82	0.17	0.29	2.83	0.22	8.10	100.11	0.11	1.44
050922	60.64	19.07	5.24	1.51	0.28	0.03	0.78	0.16	0.31	2.80	0.18	7.67	99.91	1.23	1.65
050927	69.51	14.35	3.82	1.15	0.31	0.01	0.80	0.14	0.19	2.58	0.22	6.21	99.97	0.69	1.55
050933	62.80	16.54	6.03	1.43	0.47	0.16	0.86	0.15	0.22	2.73	0.21	8.40	100.61	0.61	1.75
050940	62.66	15.17	5.69	1.33	0.26	0.02	0.78	0.14	0.24	3.00	0.20	7.82	99.88	2.58	2.05
061601	74.76	8.49	3.66	1.70	1.73	0.02	0.45	0.09	0.17	1.95	0.17	5.01	100.00	1.79	2.07
061603	63.28	11.73	6.15	2.19	1.71	0.02	0.56	0.09	0.36	2.65	0.23	7.65	100.00	3.36	5.29
061802	36.82	8.12	4.53	1.29	19.64	0.04	0.38	0.04	0.51	1.92	0.23	19.56	96.56	3.47	12.13
061806	64.38	14.94	5.03	1.12	0.97	0.05	0.88	0.07	0.52	2.16	0.47	8.14	99.99	1.26	1.59
061807	60.98	18.03	4.74	1.16	0.26	0.12	0.81	0.07	0.41	2.14	0.09	11.20	100.53	0.53	1.99
061810	63.12	15.36	4.65	1.43	0.37	0.02	0.67	0.07	0.51	2.38	0.19	10.22	100.01	1.03	2.04
061812	65.41	14.67	4.73	1.37	0.40	0.02	0.73	0.07	0.49	2.46	0.16	8.39	100.00	1.11	1.75
062201	54.50	10.36	3.85	1.98	10.28	0.02	0.46	0.06	0.59	1.77	0.23	14.02	100.00	1.88	2.86
062204	74.04	8.76	3.08	1.72	2.06	0.01	0.51	0.07	0.11	2.09	0.24	5.70	100.00	1.60	1.90
062206	59.83	15.31	6.45	1.37	2.91	0.01	0.79	0.08	0.27	2.61	0.16	7.05	100.00	3.16	2.65
063401	58.32	14.77	5.46	1.76	1.43	0.01	0.73	0.11	0.40	2.98	0.19	9.44	97.77	2.18	5.04
063403	34.58	8.29	3.02	1.67	23.09	0.02	0.43	0.04	0.20	1.99	0.18	24.28	99.40	1.61	5.77
063406	54.58	15.10	7.43	1.79	3.06	0.02	0.86	0.09	0.13	3.43	0.19	9.99	99.97	3.31	5.26
063410	41.27	12.53	9.19	1.08	12.74	0.03	0.67	0.05	0.18	2.50	0.18	15.21	100.03	4.39	8.20
063412	54.67	21.87	5.75	1.10	0.50	0.11	0.87	0.05	0.22	1.64	0.28	10.50	99.97	2.40	1.75
063415	63.81	15.42	4.65	1.52	0.52	0.01	0.73	0.08	0.37	2.58	0.19	9.07	99.98	1.03	2.03
063419	62.95	16.20	5.02	1.30	0.62	0.10	0.84	0.08	0.30	2.56	0.34	9.44	100.00	0.26	1.56
063423	59.10	16.63	7.06	1.42	0.44	0.11	0.95	0.08	0.42	2.83	0.15	10.56	100.00	0.24	1.91
063427	65.48	15.46	4.71	1.30	0.39	0.08	0.78	0.09	0.31	2.60	0.19	8.39	99.99	0.21	1.58
071402	55.03	11.67	2.67	1.80	9.09	0.01	0.56	0.06	0.30	2.82	0.19	15.80	100.86	0.86	4.30
071404	84.32	6.53	2.40	0.67	0.70	0.01	0.39	0.07	0.05	1.49	0.17	3.20	100.83	0.83	0.42
071406	66.38	12.83	5.46	1.18	0.75	0.01	0.79	0.09	0.21	2.57	0.20	7.39	100.00	2.12	1.93
090906	56.83	16.42	6.56	1.82	3.03	0.02	0.82	0.12	0.24	3.36	0.21	7.90	99.93	2.60	2.13
100501	67.34	12.90	5.68	1.37	0.98	0.03	0.68	0.14	0.21	2.61	0.25	4.77	100.00	3.04	3.18
100504	58.14	17.77	7.66	1.60	0.39	0.08	1.00	0.18	0.29	3.61	0.17	8.80	99.99	0.30	1.43
102503	61.82	16.48	5.74	1.55	0.45	0.08	1.01	0.15	0.29	3.61	0.22	8.11	99.99	0.49	1.85
103402	61.86	15.49	4.37	1.68	2.80	0.01	0.78	0.11	0.26	3.10	0.22	7.15	100.00	2.16	2.81
103404	47.18	11.74	3.15	1.52	13.53	0.01	0.52	0.06	0.32	2.27	0.21	17.79	100.00	1.71	5.23
103406	57.49	17.11	5.64	1.37	2.67	0.01	0.79	0.10	0.26	2.98	0.18	8.74	100.00	2.67	3.05
103503	64.02	13.63	4.83	1.99	2.58	0.02	0.58	0.07	0.68	2.18	0.29	5.81	99.96	3.29	4.94
103508	35.73	7.79	4.09	1.22	19.81	0.04	0.33	0.03	0.50	1.66	0.21	25.07	100.02	3.53	10.96
103511	61.92	17.55	4.67	1.36	0.26	0.02	0.87	0.06	0.50	2.14	0.06	10.60	100.74	0.74	1.57
103513	61.40	17.07	4.56	1.25	0.34	0.10	0.76	0.07	0.47	2.23	0.14	11.35	100.00	0.25	1.85
103515	63.15	14.99	4.44	1.32	0.40	0.03	0.65	0.07	0.46	2.28	0.20	10.95	99.99	1.05	1.94
103517	67.28	13.04	5.26	1.20	0.40	0.02	0.62	0.06	0.53	1.85	0.16	8.57	100.00	1.03	1.12
103518	67.25	12.88	4.96	1.20	0.46	0.03	0.70	0.07	0.43	2.33	0.28	8.45	99.99	0.95	1.28
103520	61.84	17.13	4.98	1.43	0.40	0.12	0.81	0.08	0.41	2.81	0.20	9.80	100.30	0.30	1.32
103522	61.16	17.48	4.73	1.35	0.26	0.02	0.76	0.08	0.55	2.75	0.11	10.36	99.99	0.39	1.88
103524	61.10	17.41	5.14	1.33	0.29	0.01	0.82	0.08	0.54	2.73	0.14	10.40	100.52	0.52	1.98
103525	61.19	16.65	5.38	1.29	0.30	0.01	0.84	0.08	0.49	3.09	0.16	9.34	99.98	1.16	2.12
111201	63.59	14.56	5.02	1.61	1.17	0.01	0.73	0.11	0.24	3.04	0.21	7.54	100.00	2.17	3.03
111205	51.91	14.44	6.42	1.90	6.52	0.02	0.67	0.07	0.36	2.86	0.23	10.98	100.10	3.73	6.37
111208	66.37	13.23	5.48	1.16	0.44	0.01	0.80	0.08	0.20	2.54	0.18	7.12	100.00	2.39	2.29
111211	63.79	14.21	5.56	1.20	0.44	0.02	0.74	0.11	0.30	2.77	0.25	8.21	100.00	2.40	3.07
111215	62.24	11.19	5.41	1.71	1.28	0.03	0.56	0.09	0.30	2.56	0.21	11.09	100.01	3.33	7.96
111217	65.89	15.15	4.71	1.54	0.60	0.03	0.78	0.10	0.50	3.09	0.31	6.18	100.00	1.12	4.13
112102	63.82	12.86	5.10	1.80	2.29	0.01	0.68	0.11	0.28	2.92	0.23	4.96	100.00	4.95	2.22

Table 3 (cont.)

Whole rock geochemistry (wt%)

Sample #	SiO_2	Al_2O_3	Fe_2O_3	MgO	CaO	MnO	TiO_2	BaO	Na_2O	K_2O	P_2O_5	LOI[1]	TOTAL	S[2]	TOC[3]
112105	65.57	11.28	4.43	2.26	4.89	0.02	0.58	0.09	0.29	2.57	0.21	5.56	100.00	2.25	3.43
112109	53.94	9.98	3.97	1.91	11.05	0.01	0.49	0.07	0.24	2.34	0.20	13.53	100.01	2.29	4.51
160106	62.39	16.54	6.10	1.74	0.60	0.07	0.83	0.15	0.43	2.88	0.27	8.00	100.07	0.07	1.49
160108	59.43	18.00	6.30	1.80	0.58	0.04	1.03	0.19	0.36	4.00	0.27	7.56	99.99	0.44	1.33
052202A	59.71	17.57	5.59	1.23	0.30	0.01	0.77	0.06	0.57	2.68	0.11	11.40	100.00	1.30	1.63
052208A	61.29	17.49	4.94	1.24	0.34	0.01	0.78	0.06	0.57	2.65	0.14	10.50	100.01	0.95	1.58
052211A	71.36	12.43	3.51	0.90	0.33	0.01	0.76	0.07	0.53	2.55	0.14	7.40	99.99	0.73	1.21
052216A	66.31	14.77	4.40	1.34	0.39	0.03	0.64	0.05	0.59	2.37	0.11	9.00	100.00	0.42	0.55
052224A	61.39	17.19	4.81	1.48	0.41	0.04	0.71	0.04	0.72	2.33	0.08	10.80	100.00	0.52	0.73
052232A	64.55	15.81	4.48	1.49	1.18	0.06	0.75	0.06	0.32	2.48	0.22	8.60	100.00	0.40	0.40
052240A	53.89	14.39	10.81	1.55	1.50	0.54	0.89	0.13	0.39	1.78	0.43	13.70	100.00	0.18	0.69
052244A	37.17	13.08	5.80	1.14	13.73	0.04	0.38	0.07	0.71	2.40	0.29	25.20	100.01	3.85	4.67
052251A	25.90	6.77	3.46	0.78	29.92	0.03	0.25	0.03	0.28	1.36	0.42	30.80	100.00	2.14	4.42
052256A	45.13	13.80	4.48	1.37	8.82	0.02	0.45	0.09	0.49	2.67	0.28	22.40	100.00	2.39	6.67
111601A	67.05	17.59	1.33	0.54	0.16	0.01	1.42	0.07	0.09	2.33	0.10	9.30	99.99	0.09	2.08
111602A	72.55	15.20	0.90	0.45	0.20	0.01	1.05	0.06	0.07	2.01	0.10	7.40	100.00	0.08	1.47
111606A	63.46	17.84	3.54	0.68	0.41	0.03	0.79	0.07	0.19	2.13	0.15	10.70	99.99	1.42	1.21
111610A	60.81	18.72	4.85	1.21	0.31	0.05	0.76	0.05	0.28	2.68	0.09	10.20	100.01	0.81	0.73
111612A	65.50	15.93	4.08	1.20	0.23	0.04	0.66	0.07	0.51	2.37	0.19	9.20	99.98	0.48	0.36
111614A	63.75	16.40	4.39	1.39	0.30	0.03	0.75	0.05	0.51	2.33	0.08	10.00	99.98	0.39	0.78
111616A	69.85	13.23	3.39	0.89	0.34	0.01	0.70	0.08	0.36	2.74	0.20	8.20	99.99	0.85	1.86
111618A	55.18	20.72	5.54	1.43	0.46	0.01	0.56	0.05	0.68	1.98	0.19	13.20	100.00	0.90	0.94
111623A	64.38	15.38	4.67	1.49	0.35	0.02	0.60	0.05	0.55	2.09	0.12	10.30	100.00	0.69	1.08
111628A	64.63	14.21	4.77	1.46	0.52	0.03	0.62	0.06	0.59	2.01	0.21	10.90	100.01	1.06	1.63
111633A	62.40	16.25	4.69	1.17	0.28	0.02	0.74	0.06	0.52	2.00	0.06	11.80	99.99	1.12	1.50
111635A	53.87	17.02	5.50	1.23	0.54	0.03	0.68	0.06	0.52	2.26	0.28	18.00	99.99	2.19	4.58
111637A	61.48	15.27	4.66	1.24	0.25	0.02	0.90	0.06	0.44	2.00	0.07	13.60	99.99	1.41	2.30
111638A	61.15	15.68	4.36	1.28	0.26	0.02	0.89	0.06	0.48	2.14	0.06	13.60	99.98	1.33	2.47
111641A	51.98	14.47	5.44	1.30	4.68	0.03	0.68	0.13	0.41	2.84	0.36	17.70	100.02	2.21	5.94
111646A	37.73	11.40	4.89	1.03	14.95	0.02	0.42	0.07	0.36	2.23	0.30	26.60	100.00	2.58	7.30
113601A	60.21	15.97	5.65	2.05	0.46	0.03	0.69	0.12	0.83	2.66	0.14	11.20	100.01	0.63	1.66
113603A	59.41	17.08	6.00	1.56	0.48	0.03	0.77	0.13	0.59	3.10	0.26	10.60	100.01	1.33	1.64
113606A	30.04	9.15	3.25	0.79	20.92	0.03	0.32	0.04	0.39	1.68	0.29	33.10	100.00	1.97	10.39
113609A	39.22	13.50	3.40	2.09	10.90	0.02	0.39	0.05	0.61	1.42	0.30	28.10	100.00	2.15	7.98
113614A	8.60	2.92	3.27	0.66	48.63	0.06	0.10	0.01	0.08	0.50	0.08	35.10	100.01	2.29	2.87
113616A	38.15	13.56	10.59	0.95	0.62	0.01	0.51	0.09	0.68	2.09	0.25	32.50	100.00	6.51	6.75
113619A	36.90	11.77	12.65	0.87	0.31	0.01	0.40	0.08	0.64	1.75	0.21	34.40	99.99	8.58	6.75
113623A	36.56	12.95	10.33	0.76	1.42	0.01	0.46	0.07	0.55	1.77	1.22	33.90	100.00	6.80	9.14
113628A	21.58	5.23	4.50	0.59	26.71	0.01	0.15	0.10	0.55	1.13	0.24	39.20	99.99	4.15	12.62
113631A	4.18	0.34	0.25	0.33	52.40	0.18	0.02	0.01	0.00	0.05	0.05	42.20	100.01	0.27	1.40
113636A	49.81	14.24	5.40	1.24	3.08	0.01	0.54	0.08	0.40	2.67	0.33	22.20	100.00	3.30	8.99
113640A	52.32	17.69	5.35	1.69	0.57	0.02	0.64	0.06	0.60	2.49	0.16	18.40	99.99	2.07	4.20
113642A	48.28	16.74	8.17	1.75	0.35	0.02	0.55	0.04	0.39	1.66	0.15	21.90	100.00	4.37	2.34
113646A	59.77	14.16	5.67	1.19	0.53	0.02	0.61	0.05	0.70	1.99	0.30	15.00	99.99	2.01	2.64
113650A	71.56	11.27	4.82	1.26	0.60	0.02	0.50	0.05	0.75	1.65	0.20	7.30	99.98	0.51	2.03
113651A	70.39	13.16	3.56	1.20	0.28	0.02	0.61	0.06	0.53	2.19	0.10	7.90	100.00	0.19	1.08
PA02*	63.46	18.35	4.19	1.79	0.44	0.03	0.77	na	0.83	3.56	0.23	5.64	99.27	0.01	0.49
PA05*	62.28	17.85	4.95	1.76	0.51	0.06	0.80	na	0.88	3.53	0.23	6.13	98.95	0.00	0.69
PA08*	62.29	16.30	5.83	1.83	0.81	0.07	0.80	na	0.92	2.69	0.29	8.12	99.94	0.10	0.62
PA10*	52.26	15.56	12.49	2.24	1.43	0.12	0.71	na	0.62	2.75	0.44	11.49	100.11	0.07	1.05
PA11*	63.39	18.16	3.88	1.57	0.44	0.03	0.75	na	0.84	3.03	0.24	6.03	98.34	0.11	0.35
LA01*	64.93	15.82	5.19	1.55	0.47	0.03	0.84	na	0.79	3.09	0.20	6.17	99.07	0.33	0.64
LA02*	68.64	14.98	4.14	1.36	0.28	0.01	0.78	na	0.94	2.89	0.16	5.08	99.25	0.64	0.62
LA05*	59.52	17.63	5.78	2.00	0.58	0.12	0.77	na	0.91	3.79	0.20	8.08	99.36	0.10	2.59
LA07*	63.23	15.52	6.26	1.49	0.38	0.02	0.72	na	0.83	3.22	0.22	7.13	99.02	2.48	1.39
LA10*	62.75	16.72	5.83	1.86	0.58	0.09	0.79	na	0.99	3.40	0.26	6.56	99.82	0.27	0.96
LA11*	70.55	14.27	3.75	1.45	0.43	0.03	0.74	na	1.06	3.02	0.23	4.41	99.93	0.08	0.44
LA13*	67.22	16.17	3.99	1.58	0.40	0.03	0.75	na	1.04	3.11	0.21	4.95	99.45	0.03	0.50
LA17*	64.97	15.70	5.54	1.76	0.43	0.05	0.73	na	1.04	2.99	0.19	6.29	99.68	0.30	0.98
LL01*	70.27	13.87	3.95	1.26	0.29	0.02	0.70	na	0.93	2.63	0.15	4.86	98.91	0.83	0.27

Table 3 (cont.)

Whole rock geochemistry (wt%)

Sample #	SiO_2	Al_2O_3	Fe_2O_3	MgO	CaO	MnO	TiO_2	BaO	Na_2O	K_2O	P_2O_5	LOI[1]	TOTAL	S[2]	TOC[3]
LL04*	66.55	14.74	4.61	1.61	0.52	0.03	0.73	na	0.95	2.80	0.26	5.80	98.59	0.46	1.13
LL07*	60.33	16.62	6.94	1.93	0.73	0.11	0.73	na	0.91	3.16	0.33	6.98	98.77	0.18	0.52
SI01*	63.34	18.25	4.01	1.79	0.39	0.02	0.72	na	0.90	3.48	0.23	5.79	98.91	0.03	0.64
SI03*	61.29	17.49	5.54	2.01	0.60	0.06	0.79	na	0.96	3.33	0.25	6.99	99.30	0.05	1.09
GY02*	65.31	14.97	5.60	1.81	0.85	0.07	0.76	na	1.06	2.82	0.30	6.46	100.00	0.07	0.75
GY04*	62.85	18.41	4.38	1.79	0.33	0.02	0.75	na	1.01	3.42	0.20	6.13	99.29	0.35	0.73
GY06*	64.14	15.65	5.78	1.70	0.49	0.05	0.73	na	1.02	2.90	0.25	6.16	98.88	1.24	0.73
BS01*	64.25	15.85	6.01	1.80	0.63	0.05	0.73	na	1.08	2.94	0.24	6.40	98.99	0.25	0.76
BS04*	65.47	14.23	5.74	1.85	0.96	0.09	0.76	na	1.15	2.50	0.27	6.51	99.52	0.09	0.04
BS05*	60.35	16.01	7.92	1.89	0.83	0.10	0.73	na	0.93	2.89	0.29	7.56	99.49	0.05	0.57
BS09*	59.59	15.91	7.46	1.85	1.33	0.12	0.81	na	0.88	3.12	0.51	8.74	100.31	0.09	1.46
BS10*	57.38	15.42	9.52	2.14	1.27	0.10	0.71	na	0.82	2.91	0.30	9.30	99.85	0.24	0.99

*analyses done at The University of Calgary, Calgary, Alberta. For core locations, see Caritat et al. (1994a)

[1]by thermogravitmetric analysis
[2]by combustion - included in LOI
[3]by pyrolysis - included in LOI

Table 4

Clay separation (<0.2 µm) chemistry (wt%)

Sample #	SiO_2	Al_2O_3	Fe_2O_3	MgO	CaO	MnO	TiO_2	Na_2O	K_2O	P_2O_5	LOI	TOTAL
050102	49.77	22.39	3.92	2.53	0.61	0.00	0.63	4.02	0.15	0.06	15.90	100.00
063415	51.25	21.75	7.15	3.29	0.25	0.00	0.57	-0.05	3.26	0.09	12.40	100.00
063419*	52.30	20.29	5.74	2.57	0.81	0.17	0.76	1.01	3.22	0.15	12.80	100.00
063419D	49.59	23.23	6.27	2.72	0.68	0.11	0.70	0.41	3.22	0.21	12.80	100.00
063427*	50.90	23.14	6.60	2.88	0.26	-0.00	0.74	0.98	3.90	0.09	10.50	100.00
090906	46.11	25.43	3.82	2.88	0.88	0.00	0.33	0.57	5.42	1.11	13.40	100.00
103503	53.90	22.24	1.98	3.74	0.22	-0.00	0.35	1.17	2.53	0.04	13.80	100.00
103515	50.42	19.34	8.48	2.49	0.37	0.01	0.38	3.41	2.75	0.35	12.00	100.00
103518	52.81	19.41	7.49	2.67	0.19	0.03	0.45	3.00	3.27	0.15	10.50	100.00
103522*	52.60	21.46	7.37	2.15	0.19	0.05	0.48	2.25	3.13	0.08	10.20	100.00
061812*	53.76	19.71	3.86	2.77	0.54	0.01	0.58	1.42	2.82	0.07	14.40	99.99
062206*	50.42	24.58	3.85	2.69	0.73	0.00	0.71	0.00	3.93	0.12	12.90	99.99
103511*	52.94	22.26	5.21	2.41	0.39	0.01	0.67	0.97	2.16	0.05	12.90	100.00
061807	49.15	23.27	5.65	2.39	0.44	0.01	0.48	1.11	1.93	0.05	15.50	99.99
061812	49.65	20.86	5.45	3.07	0.61	0.01	0.38	0.95	2.45	0.06	16.50	100.01
062206	47.60	24.16	4.17	2.82	0.91	0.00	0.38	0.46	4.05	0.12	15.30	100.01
103511	50.10	21.69	5.50	2.70	0.42	0.01	0.41	1.71	1.69	0.03	15.70	100.00
103520	49.55	21.96	6.50	2.61	0.65	0.04	0.37	1.79	2.62	0.12	13.80	100.03
103524	50.03	22.07	6.15	2.39	0.45	0.00	0.48	1.51	2.54	0.06	14.30	100.02
111217	49.19	21.24	4.90	2.60	0.67	0.01	0.40	4.08	3.48	0.12	13.30	100.02
052202	49.29	22.61	9.37	2.26	0.39	0.00	0.89	0.96	3.16	0.29	10.80	100.02
052202R	49.67	22.60	9.31	2.21	0.39	0.00	0.89	0.70	3.16	0.27	10.80	100.00
052208	53.32	23.37	3.62	2.64	0.65	0.00	0.79	0.68	2.82	0.06	12.00	99.95
052216	53.09	21.93	5.51	2.75	0.64	0.02	0.62	1.79	2.61	0.05	11.00	100.01
052224	52.28	21.56	6.16	2.72	0.66	0.04	0.78	1.47	2.27	0.05	12.00	99.99
052232*	54.74	23.71	3.59	2.13	0.52	0.01	0.78	0.69	3.16	0.15	10.50	99.98
052244*	59.02	20.43	4.72	2.16	0.88	0.00	0.78	0.20	3.34	0.40	8.00	99.93
052251*	62.83	19.99	3.91	2.07	0.66	0.00	0.84	0.04	3.60	0.27	5.70	99.91
052256*	55.49	21.20	3.82	2.27	0.80	0.00	0.70	1.45	3.33	0.29	10.60	99.95
111610*	55.73	24.29	3.23	1.92	0.56	0.02	0.84	0.27	3.13	0.09	9.90	99.98
111612	51.13	22.12	5.12	2.79	0.70	0.03	0.72	1.43	2.44	0.11	13.40	99.99
111614	51.67	22.16	5.28	2.53	0.51	0.01	0.61	1.47	2.37	0.08	13.30	99.99
111618	51.41	22.75	4.69	2.66	0.61	0.00	0.39	1.66	1.91	0.06	13.90	100.04
111618R	51.43	22.26	4.63	2.41	0.59	0.00	0.40	2.42	1.92	0.08	13.90	100.04
111623	52.16	20.51	5.48	2.75	0.59	0.00	0.35	2.14	2.07	0.06	13.90	100.01

Table 4 (cont.)

Clay separation (<0.2 µm) chemistry (wt%)

Sample #	SiO_2	Al_2O_3	Fe_2O_3	MgO	CaO	MnO	TiO_2	Na_2O	K_2O	P_2O_5	LOI	TOTAL
111633	43.43	20.29	12.53	1.86	0.27	0.01	0.47	4.14	2.28	0.40	14.50	100.18
111635	47.74	22.39	6.63	2.55	0.29	0.01	0.37	1.47	2.09	0.16	16.30	100.00
111641	47.96	23.06	4.86	2.91	1.19	0.01	0.38	0.92	3.56	0.12	15.00	99.97
111646*	60.38	21.36	3.22	1.95	0.93	0.00	0.81	0.23	3.61	0.24	7.20	99.93
113601*	51.08	19.32	6.49	3.26	0.73	0.02	0.54	2.87	2.62	0.06	13.00	99.99
113603	48.38	22.34	5.93	2.92	0.93	0.01	0.52	1.18	3.40	0.16	14.20	99.97
113650	55.62	18.09	6.85	2.73	0.49	0.00	0.27	3.07	1.68	0.03	11.20	100.03
113652	54.30	19.53	6.07	2.73	0.48	0.02	0.60	1.79	2.75	0.04	11.70	100.01
LA01	49.56	24.69	4.50	3.03	0.59	0.02	0.29	2.31	5.31	0.02	9.60	99.92
LA02	48.87	26.94	2.98	3.72	0.50	0.04	0.33	1.45	5.38	0.17	9.50	99.88
LA03	49.52	25.88	5.33	3.66	1.34	0.01	0.70	0.41	4.84	0.12	8.00	99.81
LA05	47.15	23.91	4.81	4.23	0.79	0.10	0.89	2.61	5.16	0.28	9.60	99.53
LA07	49.17	23.77	4.65	3.14	0.54	0.00	0.56	3.13	5.13	0.18	9.60	99.87
LA10	46.00	25.79	5.40	4.19	0.74	0.07	0.40	1.65	5.48	0.27	9.70	99.69
LA13	48.52	26.21	4.76	3.22	0.53	0.00	0.46	2.84	5.33	0.03	8.00	99.90
BS09	44.49	24.63	5.36	3.18	1.07	0.08	0.35	3.79	5.57	0.27	11.00	99.79
BS09R	44.85	24.68	5.35	3.58	1.06	0.07	0.35	3.10	5.55	0.23	11.00	99.82

*< 2.0 µm fraction

D - indicates duplicate bead

R - indicates analysis was repeated on same bead

Table 5

Bentonite chemistry (wt%)

SAMPLE #	SiO_2	Al_2O_3	Fe_2O_3	MgO	CaO	MnO	TiO_2	BaO	Na_2O	K_2O	P_2O_5	LOI	TOTAL	S	TC
050105A	52.56	23.72	3.39	1.96	0.49	0.02	0.56	0.12	0.97	0.15	0.14	15.90	99.97	0.66	0.16
050106A	51.54	21.18	4.88	3.11	0.68	0.03	0.50	0.12	0.75	0.92	0.26	16.00	99.97	0.47	0.13
050108A	56.90	20.57	2.78	2.73	0.96	0.01	0.25	0.08	1.22	0.28	0.12	14.10	99.99	0.42	0.18
050110A	56.67	21.33	3.31	2.48	0.56	0.01	0.15	0.08	1.38	0.41	0.04	16.30	102.69	0.39	0.19
061810A	49.36	18.60	9.52	2.71	0.68	0.15	0.25	0.03	1.95	0.41	0.04	16.30	100.00	0.21	1.21
062101A	57.35	19.76	5.03	2.06	1.37	0.01	0.31	0.09	1.23	0.78	0.11	11.90	100.00	0.01	0.31
063401A	53.05	25.49	2.01	2.45	0.51	0.01	0.22	0.06	0.85	0.20	0.05	15.10	100.00	0.16	0.12
063401B	46.84	24.63	4.83	1.81	0.81	0.01	0.37	0.05	1.41	0.26	0.17	18.80	99.99	2.34	0.11
063403A	49.03	29.71	2.03	1.77	0.40	0.03	0.34	0.05	0.39	0.22	0.12	15.90	99.98	1.18	0.29
063404B	52.69	26.58	1.31	2.17	0.45	0.01	0.26	0.07	0.65	0.35	0.06	15.40	100.00	0.26	0.13
063413A	53.07	20.92	4.99	2.61	1.50	0.04	0.30	0.07	2.01	0.56	0.11	13.80	99.98	0.82	0.47
063413B	55.56	21.59	3.06	2.81	1.70	0.02	0.32	0.05	1.53	0.38	0.27	12.70	100.00	0.42	0.17
063413C	56.18	21.19	3.38	2.71	0.77	0.01	0.14	0.05	1.42	0.41	0.04	13.70	100.00	0.19	0.21
063414A	47.46	18.73	9.97	3.12	1.00	0.13	0.15	0.03	2.25	0.29	0.06	16.80	100.00	0.40	1.56
063424A	25.07	11.66	31.17	3.12	1.33	0.56	0.16	0.27	1.42	0.21	1.24	23.75	99.98	0.09	5.27
103510	56.30	20.59	1.32	4.01	0.61	0.03	0.16	0.04	0.90	0.32	0.04	15.70	100.00	0.66	0.00
103511A	26.41	7.88	16.11	2.34	18.67	0.70	0.34	0.14	0.55	0.98	10.13	15.70	99.97	0.27	3.27
103514C	29.72	5.10	4.81	0.60	30.14	0.41	0.20	0.23	0.46	0.60	18.52	8.80	99.60	2.24	0.95
103516A	47.17	17.57	11.69	2.76	0.94	0.16	0.21	0.03	2.04	0.47	0.06	16.90	100.00	0.31	1.57
142909A	50.43	27.33	1.27	3.60	0.89	0.00	0.26	nr	1.27	4.75	0.05	10.00	99.85	nm	nm
SR01*	56.31	19.12	5.32	2.16	0.49	0.01	0.17	0.04	0.01	0.55	0.03	15.80	100.02	0.95	0.30

*outcrop sample - see Leckie et al. (1992) for location

nr - not reported

nm - not measured

Bulk XRD indicates that some samples contain a significant amount of calcite and dolomite. The amount of a carbonate mineral is determined from the total inorganic carbon (TIC) in the rock. TIC is calculated by subtracting TOC from the total carbon value. If the amount of carbonate is small (< 5 wt%), the error involved in this estimation of TIC is small. However, when carbonate minerals are a significant component, or there is more than one carbonate

mineral present in the sample, then it is necessary to determine the Ca:Mg:Fe values of the carbonate component and mass balance these against TIC to determine individual carbonate mineral compositions. For samples with these characteristics, an additional aliquot of crushed material (~ 5g) was treated with 40 ml of hot HCl (~ 100°C). The leachate was filtered (Whatman #40), extended to 100 ml and analyzed by atomic absorption for Ca, Mg and Fe concentrations. A portion of the residue was dried and analyzed for total carbon as above.

Mineral matrix effects can affect the accuracy of Rock-Eval parameters (Peters, 1986), particularly the presence of carbonate minerals. To assess the accuracy of TOC values determined by Rock-Eval, a subset of carbonate-bearing samples were acid-leached and the total carbon determined by combustion, as above. These results were compared with Rock-Eval TOC values as determined from untreated samples.

Polished sections were prepared from epoxy-impregnated core samples. Back-scattered electron microscopy (BSEM), using a Cambridge Stereoscan 150 electron microscope equipped with an 8 kV threshold annular back scatter detector, provided petrographic information. This was supplemented by energy-dispersive X-ray (EDX) analysis for qualitative mineral identification.

A linear programming method was used to determine the mineralogy of the shales and bentonites from their bulk chemical composition, and to estimate clay mineral compositions from the < 0.2 µm XRF analysis results (Table 6). Linear programming distributes the analyzed oxides according to a set of (linear) equations, which are solved simultaneously using the mathematical method known as linear optimization. The development and use of this method is fully described in Caritat et al. (1994b).

Samples for carbon and oxygen isotopic analysis were selected from hand samples of concretions and core slabs with fracture-fill carbonate cement. The hand samples were subsampled by milling small amounts of material with a dental drill and analyzed by XRD for sample purity. All samples (calcite, dolomite and siderite) were reacted with anhydrous phosphoric acid using standard techniques and fractionation factors appropriate for each mineral at the given reaction temperature (Friedman and O'Neil, 1977; Rosenbaum and Sheppard, 1986). The evolved CO_2 was analyzed on a VG-Optima mass spectrometer at the Laboratory for Stable Isotope Studies at The University of Western Ontario. Analytical results are given in standard delta (δ) notation relative to the Pee Dee Belemnite (PDB) standard for carbon and Vienna Standard Mean Ocean Water (SMOW) for oxygen (Table 7). NBS -19 values of 1.92‰ PDB for carbon and 29.07‰ SMOW for oxygen are obtained routinely. Replicate (n = 8) analyses of samples (unknowns) indicate a standard deviation (2σ) for carbon and oxygen of less than 0.005‰ for calcite and 0.05 and 0.09‰, respectively, for siderite.

Samples for sulphur isotopic analysis were selected from a number of cores to construct vertical profiles across the basin (Table 8). Reduced sulphur was extracted from whole rock powders using a modified chromate reduction technique (Canfield et al., 1986; Tuttle et al., 1986). This method is reduced-sulphur specific and extracts only S^0 and mono- and di-sulphide sulphur as H_2S, which is subsequently trapped as Ag_2S. Sulphide sulphur is then oxidized to SO_2 for analysis (Ueda and Krouse, 1986). Sulphur isotopic analysis was done on a VG - 602 mass spectrometer at the Laboratory for Stable Isotope Studies at The University of Western Ontario. Results are reported relative to the Canyon Diablo Troilite (CDT) standard in standard δ notation. Replicate analyses (n = 9) of an internal laboratory pyrite standard, processed identically to the unknowns, indicate a precision of ±0.3‰ CDT. Standard NBS-123 routinely gives values of 17.4 ± 0.4‰.

Samples from seven reference wells and two outcrop sections were prepared for foraminiferal analysis utilizing the method of Then and Dougherty (1983) and washed over a 63 µm sieve. Individual specimens were handpicked for identification. The foraminiferal listings (Appendix B) reflect the total number of specimens per sample where sample volumes vary slightly. Poorly preserved specimens, which are not unequivocally identifiable, are not included in the total counts. Abundance estimates of bivalve shell prisms, algal cysts and fish remains in the sand-sized fraction, which are important for environmental interpretation, are listed under 'Miscellaneous components'.

Permanent slides of nannofossils were examined under a light-microscope. Slide preparation techniques were modified from those of Edwards (1963), Stover (1966), Gartner (1968), and Smith (1981). Counting techniques varied with the abundance of coccoliths noted during preliminary scans. If coccoliths were abundant, a half-slide scan was performed; otherwise a full slide scan was used. Total numbers of coccoliths per sample are listed in Appendix C.

Palynology samples were prepared from the 10-35-45-2W4 well. Standard acid-processing techniques (Barss and Williams, 1973) were used followed by heavy liquid flotation and sieving to concentrate dinoflagellates in the > 45µm and the 20µm–45µm fractions. Dinoflagellate plates appear in Appendix D.

Table 6

Calculated shale, mixed-layer I/S and bentonite–smectite compositions from XRF data

	Clay Compositions								Structural Formulae									
									Tetrahedral		Octahedral				Interlayer			
Sample #[2]	SiO_2	Al_20_3	Fe_2O_3	MgO	Na_2O	CaO	K_2O	Total	Si	Al	Al	Fe**	Mg	Sum	Na	K	Ca	Mg*
SECOND WHITE SPECKS FORMATION																		
103503.02a	53.56	19.70	2.12	4.01	1.25	0.25	2.71	83.60	3.84	0.16	1.50	0.11	0.39	2.01	0.17	0.25	0.02	0.04
063401A	56.42	20.41	2.47	2.45	0.47	0.00	0.00	82.22	3.98	0.02	1.68	0.13	0.19	2.00	0.06	0.00	0.00	0.07
063401B	52.00	22.93	0.08	3.80	0.00	0.25	0.00	79.06	3.80	0.20	1.77	0.00	0.22	2.00	0.00	0.00	0.02	0.19
063403A	51.48	21.86	0.84	2.87	0.44	0.00	0.00	77.49	3.85	0.15	1.77	0.05	0.18	2.00	0.06	0.00	0.00	0.14
063404B	56.51	22.00	0.02	2.65	0.48	0.54	0.50	82.70	3.95	0.05	1.77	0.00	0.24	2.01	0.07	0.04	0.04	0.04
103510A	53.36	22.88	0.50	3.45	0.45	0.69	0.00	81.33	3.81	0.19	1.74	0.03	0.24	2.00	0.06	0.00	0.05	0.13
103510B	56.36	22.04	0.00	3.39	0.20	0.51	0.00	82.50	3.94	0.06	1.75	0.00	0.25	2.00	0.03	0.00	0.04	0.10
BELLE FOURCHE FORMATION																		
050102.02a(1)	53.19	15.77	6.23	3.96	6.45	0.98	0.24	86.82	3.78	0.22	1.11	0.33	0.49	1.93	0.89	0.02	0.00	0.00
050105A	50.34	26.48	2.15	2.22	0.95	0.00	0.00	82.14	3.59	0.41	1.82	0.12	0.07	2.00	0.13	0.00	0.00	0.17
050106A	51.18	23.79	1.19	4.17	0.82	0.00	0.00	81.15	3.69	0.31	1.70	0.06	0.23	2.00	0.11	0.00	0.00	0.22
050108A	51.45	24.26	0.89	3.32	0.33	0.22	0.23	80.70	3.71	0.29	1.78	0.05	0.18	2.00	0.05	0.02	0.02	0.18
061807.02b	51.43	11.36	8.02	4.62	2.17	0.86	3.77	82.23	3.92	0.08	0.94	0.46	0.52	1.93	0.32	0.37	0.07	0.00
062206.02a	49.84	16.66	7.00	4.73	0.77	1.53	6.80	87.33	3.64	0.36	1.07	0.38	0.51	1.97	0.11	0.63	0.12	0.00
063413A	52.34	22.06	0.37	2.95	0.83	0.72	0.02	79.29	3.84	0.16	1.74	0.02	0.24	2.00	0.12	0.00	0.06	0.08
063413B	56.09	21.88	0.58	2.17	0.48	0.78	0.13	82.11	3.95	0.05	1.77	0.03	0.23	2.03	0.07	0.01	0.06	0.00
063413C	56.34	22.43	1.26	1.83	0.87	0.83	0.37	83.93	3.91	0.09	1.75	0.07	0.19	2.00	0.12	0.03	0.06	0.00
090906.02a	46.81	25.87	4.27	3.22	0.64	0.98	6.06	87.85	3.33	0.67	1.50	0.23	0.27	2.00	0.09	0.55	0.07	0.07
103511.02a	50.71	19.43	6.15	3.07	1.98	0.49	1.96	83.79	3.69	0.31	1.36	0.34	0.33	2.03	0.28	0.18	0.04	0.00
103511A	54.98	20.23	0.50	7.43	1.75	0.00	3.11	88.00	3.76	0.24	1.38	0.03	0.59	2.00	0.23	0.27	0.00	0.17
111633	46.27	19.62	11.75	2.26	5.05	0.33	0.87	86.15	3.40	0.60	1.10	0.65	0.25	2.00	0.72	0.08	0.03	0.00
111635	49.32	20.66	6.75	3.02	1.74	0.46	2.48	84.43	3.59	0.41	1.36	0.37	0.23	1.96	0.25	0.23	0.04	0.10
LA01(1)	50.46	23.18	3.93	3.26	2.74	0.67	6.31	90.55	3.50	0.50	1.39	0.21	0.39	1.99	0.37	0.56	0.00	0.00
LA02	49.83	25.93	2.55	4.24	1.75	0.33	6.49	91.12	3.41	0.59	1.50	0.13	0.37	2.00	0.23	0.57	0.02	0.06
LA03	51.15	25.43	3.81	3.68	0.48	1.37	5.62	91.54	3.46	0.54	1.49	0.19	0.32	2.00	0.06	0.49	0.10	0.05
LA05(1)	48.27	23.60	3.06	4.31	3.03	0.49	5.99	88.75	3.42	0.58	1.38	0.16	0.47	2.02	0.42	0.54	0.02	0.00
LA07(1)	50.21	22.94	3.57	3.17	3.58	0.35	5.86	89.68	3.51	0.49	1.40	0.19	0.36	1.95	0.49	0.52	0.00	0.00
LA10	46.88	24.77	4.53	4.52	1.96	0.46	6.50	89.62	3.31	0.69	1.37	0.24	0.44	2.05	0.27	0.58	0.03	0.04
LA13(1)	49.75	25.50	3.90	3.38	3.34	0.58	6.27	92.72	3.38	0.62	1.42	0.20	0.38	2.01	0.44	0.54	0.04	0.00
BS09(1)	45.37	24.02	4.40	3.19	4.27	0.81	6.28	88.34	3.28	0.72	1.33	0.24	0.41	1.98	0.60	0.58	0.00	0.00
FISH SCALES FORMATION																		
063415.02a	49.43	21.71	8.24	3.79	0.23	0.23	3.77	87.40	3.51	0.49	1.32	0.44	0.24	2.00	0.03	0.34	0.02	0.16
050110A	50.34	25.78	1.29	2.72	0.76	0.20	0.27	81.36	3.62	0.38	1.81	0.07	0.12	2.00	0.11	0.02	0.02	0.17
063414A	56.03	23.76	0.06	2.23	2.49	0.00	0.24	84.81	3.85	0.15	1.78	0.00	0.23	2.01	0.33	0.02	0.00	0.00
103514C(1)	55.65	23.50	0.15	1.51	2.65	4.89	3.45	91.80	3.70	0.30	1.55	0.01	0.45	2.00	0.34	0.29	0.05	0.05
SR01	56.30	24.18	1.85	2.69	0.00	0.58	0.34	85.94	3.82	0.18	1.75	0.09	0.16	2.00	0.00	0.03	0.04	0.11

Table 6 (cont.)

Calculated shale, mixed-layer I/S and bentonite–smectite compositions from XRF data

	Clay Compositions								Structural Formulae									
									Tetrahedral		Octahedral			Interlayer				
Sample #[2]	SiO_2	Al_20_3	Fe_2O_3	MgO	Na_2O	CaO	K_2O	Total	Si	Al	Al	Fe**	Mg	Sum	Na	K	Ca	Mg*
WESTGATE FORMATION																		
061810A	54.74	22.66	0.50	1.96	1.93	0.72	0.35	82.86	3.86	0.14	1.75	0.03	0.21	1.98	0.26	0.03	0.05	0.00
061812.02b	50.09	16.45	6.14	2.96	1.64	0.62	3.26	81.17	3.80	0.20	1.27	0.35	0.33	1.96	0.24	0.32	0.05	0.00
062101A	53.24	21.40	2.42	2.40	0.50	1.26	0.98	82.20	3.83	0.17	1.64	0.13	0.26	2.03	0.07	0.09	0.10	0.00
063419.02a	50.70	20.45	6.46	2.89	1.14	0.91	3.62	86.17	3.63	0.37	1.36	0.35	0.31	2.02	0.16	0.33	0.07	0.00
063424A	52.44	19.88	0.25	7.54	3.63	1.51	0.54	85.79	3.67	0.33	1.31	0.01	0.69	2.02	0.49	0.05	0.11	0.10
063427.02a	48.88	19.91	11.08	4.83	1.64	0.44	6.55	93.33	3.38	0.62	1.01	0.58	0.43	2.02	0.22	0.58	0.03	0.07
103515.02a[1]	56.39	12.37	6.33	3.68	5.65	0.63	4.54	89.58	3.97	0.03	0.99	0.34	0.44	1.77	0.77	0.41	0.00	0.00
103516A-1	52.03	23.30	1.06	4.27	2.39	0.95	0.00	84.00	3.67	0.33	1.60	0.06	0.35	2.01	0.33	0.00	0.07	0.10
103516A-2	50.84	23.95	1.18	3.94	1.94	1.35	0.68	83.88	3.61	0.39	1.61	0.06	0.33	2.00	0.27	0.06	0.10	0.09
103518.02a	53.69	16.86	9.32	3.32	3.73	0.23	4.07	91.22	3.71	0.29	1.09	0.48	0.34	1.91	0.50	0.36	0.02	0.00
103520.02a[1]	51.75	9.83	11.78	4.96	3.44	1.25	5.04	88.04	3.81	0.19	0.66	0.65	0.64	1.95	0.49	0.47	0.00	0.00
103522.02a	53.30	16.70	10.18	2.97	3.11	0.28	4.32	90.86	3.71	0.29	1.08	0.53	0.31	1.92	0.42	0.38	0.02	0.00
103524.02a	52.38	12.98	9.51	3.68	2.34	0.70	3.94	85.53	3.86	0.14	0.98	0.53	0.40	1.91	0.33	0.37	0.06	0.00
111217.02a[1]	47.92	22.39	3.62	2.36	4.33	0.71	3.69	85.03	3.51	0.49	1.44	0.20	0.32	1.96	0.61	0.34	0.00	0.00
052202	51.63	21.44	9.99	2.90	1.07	0.50	3.65	91.18	3.53	0.47	1.26	0.51	0.22	2.00	0.14	0.32	0.04	0.08
052208	53.32	19.98	5.12	3.73	0.96	0.81	3.98	87.90	3.72	0.28	1.36	0.27	0.37	2.00	0.13	0.35	0.06	0.02
111614	52.58	19.43	6.32	3.03	1.76	0.48	2.84	86.44	3.73	0.27	1.35	0.34	0.32	2.01	0.24	0.26	0.04	0.00
111618	51.60	21.92	5.06	2.87	1.77	0.57	2.03	85.82	3.65	0.35	1.48	0.27	0.25	1.99	0.24	0.18	0.04	0.05
111623	52.30	19.49	5.91	2.97	2.31	0.55	2.23	85.76	3.73	0.27	1.36	0.32	0.32	1.99	0.32	0.20	0.04	0.00
OTHER FORMATIONS																		
052216	52.38	20.46	6.67	3.33	2.16	0.69	3.16	88.85	3.64	0.36	1.32	0.35	0.35	2.01	0.29	0.28	0.05	0.00
052224	51.16	19.96	7.65	3.38	1.83	0.74	2.82	87.54	3.62	0.38	1.28	0.41	0.32	2.01	0.25	0.25	0.06	0.04
052232	51.05	22.05	5.62	3.30	1.08	0.81	4.94	88.85	3.57	0.43	1.38	0.30	0.32	2.00	0.15	0.44	0.06	0.02
052244	54.63	23.12	4.29	3.10	0.34	1.50	4.77	91.75	3.65	0.35	1.47	0.22	0.31	2.00	0.04	0.41	0.11	0.00
052251[1]	57.31	20.84	6.20	3.55	0.86	1.42	7.76	97.94	3.69	0.31	1.26	0.30	0.44	2.00	0.11	0.64	0.00	0.00
052256	51.98	18.58	5.99	3.56	2.27	1.25	5.21	88.84	3.67	0.33	1.22	0.32	0.46	2.00	0.31	0.47	0.00	0.00
111610	49.45	19.00	7.40	4.40	0.62	1.29	7.20	89.36	3.53	0.47	1.13	0.40	0.47	2.00	0.09	0.66	0.10	0.00
111612	52.26	19.09	6.13	3.34	1.71	0.66	2.92	86.11	3.72	0.28	1.33	0.33	0.35	2.01	0.24	0.27	0.05	0.00
111641[1]	49.67	19.95	6.00	3.60	1.16	1.50	4.47	86.35	3.59	0.41	1.28	0.33	0.39	2.00	0.16	0.41	0.12	-0.00
111646	59.97	20.42	3.79	2.30	0.27	0.58	4.26	91.59	3.94	0.06	1.52	0.19	0.27	1.98	0.03	0.36	0.00	0.00
113601	51.02	18.52	7.09	3.56	3.14	0.71	2.86	86.90	3.65	0.35	1.21	0.38	0.38	1.97	0.44	0.26	0.05	0.00
113603	49.08	21.31	6.45	3.17	1.28	0.78	3.70	85.77	3.55	0.45	1.36	0.35	0.29	2.00	0.18	0.34	0.06	0.05
113650	55.62	18.09	6.85	2.73	3.07	0.49	1.68	88.53	3.83	0.17	1.30	0.36	0.32	1.98	0.41	0.15	0.00	0.00
113652	55.09	18.26	6.63	2.98	1.96	0.48	3.00	88.40	3.82	0.18	1.31	0.35	0.31	1.96	0.26	0.27	0.04	0.00

Fe** as Fe^{3+}

Mg* interlayer Mg is determined by taking excess octahedral Mg (> 2.00 sites) and assigning it to interlayer

[1]low octahedral total Al+Fe+Mg and high interlayer charge - some Ca is assigned to octahedral layer

[2]samples designated A, B or C and SR01 are bentonites

Table 7

Concretion and fracture-fill cement C-O isotopic data

Sample	Formation	Depth (m)	Mineral	$\delta^{13}C$ ‰PDB	$\delta^{18}O$ ‰SMOW
5-1-77-20W5 - Imperial Kathleen #1					
050117A	Westgate	427.0	SID	-9.82	19.87
5-9-72-8W6 - Imperial Wembley					
050904A	Belle Fourche	1261.0	SID	0.22	21.35
050916A	Belle Fourche	1301.0	SID	1.91	22.85
050921A	Belle Fourche	1314.8	SID	-0.98	21.52
6-18-45-1W4 - Anderson et al. Ribstone					
061810A	Westgate	443.0	SID	-4.62	24.04
061813A	Westgate	456.9	SID	-4.21	26.04
061813A-1	Westgate		SID	-3.22	26.95
061813A-2	Westgate		SID	-3.40	26.44
061813A-3	Westgate		SID	-5.53	23.71
061814A	Westgate	460.9	SID	-3.26	26.66
061814A-1	Westgate		SID	-2.51	26.39
duplicate	Westgate		SID	-2.47	26.91
061814A-3	Westgate		SID	-6.72	23.72
6-34-30-8W4 - Amoco B-1 Youngstown					
063404A	Second Specks	708.4	CAL	4.48	24.00
9-9-56-18W5 - HCS et al. Beaver Creek					
090906A	Belle Fourche	2267.0	CAL	-13.12	27.22
090906A-1	Belle Fourche		CAL	-12.54	26.58
090906A-2	Belle Fourche		CAL	-12.92	27.10
090906A-3	Belle Fourche		CAL	-13.38	27.01
10-35-45-2W4 - Anderson Husky Roros					
103519A	Westgate	471.0	SID	-0.63	26.37
103524A	Westgate	494.3	SID	-5.97	25.51
10-25-65-20W5 -Sabine et al. Iosegun					
102502A	Westgate	1324.7	SID	3.70	22.29
102502A-1	Westgate		SID	0.89	20.59
102502A-2	Westgate		SID	4.37	22.30
102502A-3	Westgate		SID	6.06	23.53
102502A-4	Westgate		SID	5.78	23.44
102502A-5	Westgate		SID	5.52	23.58
102502A-6	Westgate		SID	5.49	23.26
102502A-7	Westgate		SID	3.39	21.72
102502A-8	Westgate		SID	0.69	20.79
102502B	Westgate	1325.0	SID	-1.44	20.85
10-25-65-20W5 -Sabine et al. Iosegun (cont.)					
102502B-1	Westgate		SID	0.35	20.40
102502B-2	Westgate		SID	1.16	21.78
102502B-3	Westgate		SID	2.75	21.48
102502B-4	Westgate		SID	4.49	22.78
102502B-5	Westgate		SID	5.30	23.01
102502B-6	Westgate		SID	4.07	22.47
102502B-7	Westgate		SID	1.97	21.54
102502B-8	Westgate		SID	0.39	20.27
10-34-42-22W4 - LCD et al. Bashaw					
103402A	Second Specks	1050.0	CAL	-1.93	23.01
103402A	Second Specks		DOL/ANK	0.81	22.40
103402A-1	Second Specks		CAL	-15.42	27.04
103402A-2	Second Specks		CAL	-15.13	27.09
103402A-3	Second Specks		CAL	-12.37	26.08
103405A	Second Specks	1062.5	CAL	-21.90	28.65
103405A-1	Second Specks		CAL	-22.15	28.70
103405A-2	Second Specks		CAL	-22.34	28.31
103405A-3	Second Specks		CAL	-22.35	28.60
103405A-4	Second Specks		CAL	-4.67	17.72
103405A-4	Second Specks		DOL/ANK	-4.40	17.79
11-16-35-8W3 - C.M.S. Vanscoy					
111613A	Viking	492.8	SID	-12.69	23.49
111616A	Westgate	481.9	SID	-14.73	23.26
111625A	Westgate	438.3	SID	-12.55	22.82
16-01-61-22W5 - Amoco Bigstone					
160103A	Belle Fourche	1882.6	SID	3.04	23.40
160103A-1	Belle Fourche		SID	1.64	23.18
160103A-2	Belle Fourche		SID	2.97	23.36
160103A-3	Belle Fourche		SID	3.09	23.10
Mill Creek Outcrop					
CG911-1	Second Specks	na	CAL	-1.99	15.98
Bruin Creek Outcrop					
CG9141	Second Specks	na	CAL	-16.53	25.94
CG9142	Second Specks		CAL	-16.17	25.95
CG9143	Second Specks		CAL	-16.84	26.11
CG9144	Second Specks		CAL	-10.10	15.82

RESULTS

Rock-Eval pyrolysis

Rock-Eval data for all Colorado Group samples are given in Appendix E. On a pseudo Van Krevelen diagram (Fig. 4), individual formations show distinct populations of organic matter type. The Westgate Formation contains predominantly Type III organic matter with Hydrogen Indices (HI) generally less than 250 mgHC/gOC. The Fish Scales and Belle Fourche formations show a bimodal distribution containing Types II and III with HI values up to about 450 mgHC/gOC. In the Belle Fourche Formation, most of the Type III organic matter is in samples that come from the northwest part of the study area. The Belle Fourche samples are characterized as pro-deltaic (Caritat et al., 1994a) and are the most proximal of depositional environments for the formation. Samples containing dominantly Type II organic matter are generally from the upper part of the Belle Fourche formation – a transition zone to the overlying Second White Specks, which contains predominantly marine (Type II) organic matter with HI values generally greater than 250 mgHC/gOC.

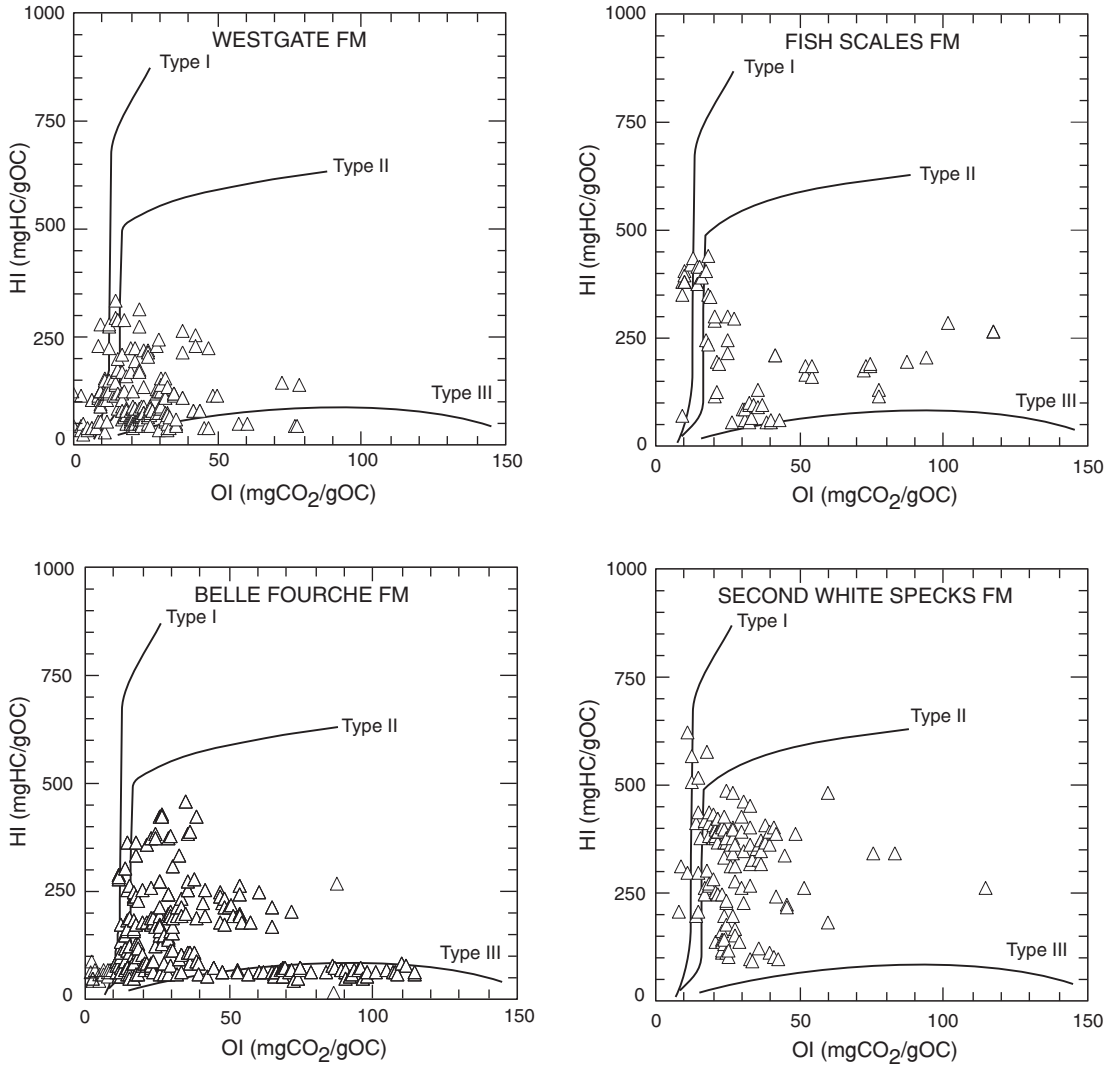

Figure 4. *Pseudo van Krevelen diagram for the Westgate, Fish Scales, Belle Fourche, and the Second White Specks formations.*

Bulk X-ray diffraction

The mineralogy of the Colorado Group dominantly comprises detrital quartz, feldspars and a suite of clay minerals. The clay minerals are mixed-layer illite/smectite (I/S), kaolinite, illite, and minor chlorite. The mineralogy will be discussed in detail in subsequent sections. Other major components include variable amounts of siderite, dolomite, calcite, pyrite, jarosite, gypsum, and apatite. Accessory minerals include biotite, muscovite, glauconite, zeolites, zircon, and oxides of Ti (rutile, anatase, brookite), with trace amounts of sphene, ilmenite and leucoxene.

Whole rock geochemistry - XRF

The results of geochemical analysis by XRF on whole-rock shale, clay separates and bentonites are given in Tables 3, 4, and 5, respectively. Samples designated with a two letter prefix were analyzed at the Department of Geology and Geophysics, The University of Calgary. The results and interpretation of these samples (Caritat et al., 1994a) are included herein as part of a complete presentation of the Colorado Group geochemical data.

The chemical composition of Colorado Group shales is variable and reflects the variable depositional environments and the mineralogy of the different formations (Bloch et al., 1993; Schröder-Adams et al., 1996), particularly the calcareous Second White Specks Formation. An examination of some indicator oxide cross-plots highlights these differences. Figure 5a indicates that most samples contain between 50 and 75 wt% SiO_2 and 13 to 18 wt% Al_2O_3 showing trends towards 100% and 0% SiO_2. These trends reflect the mixing of quartz silt and carbonate, respectively, with a clay-mineral matrix. As indicated by XRD, this matrix is composed of I/S, kaolinite, and a 10Å mineral, probably illite, with minor chlorite. K_2O varies

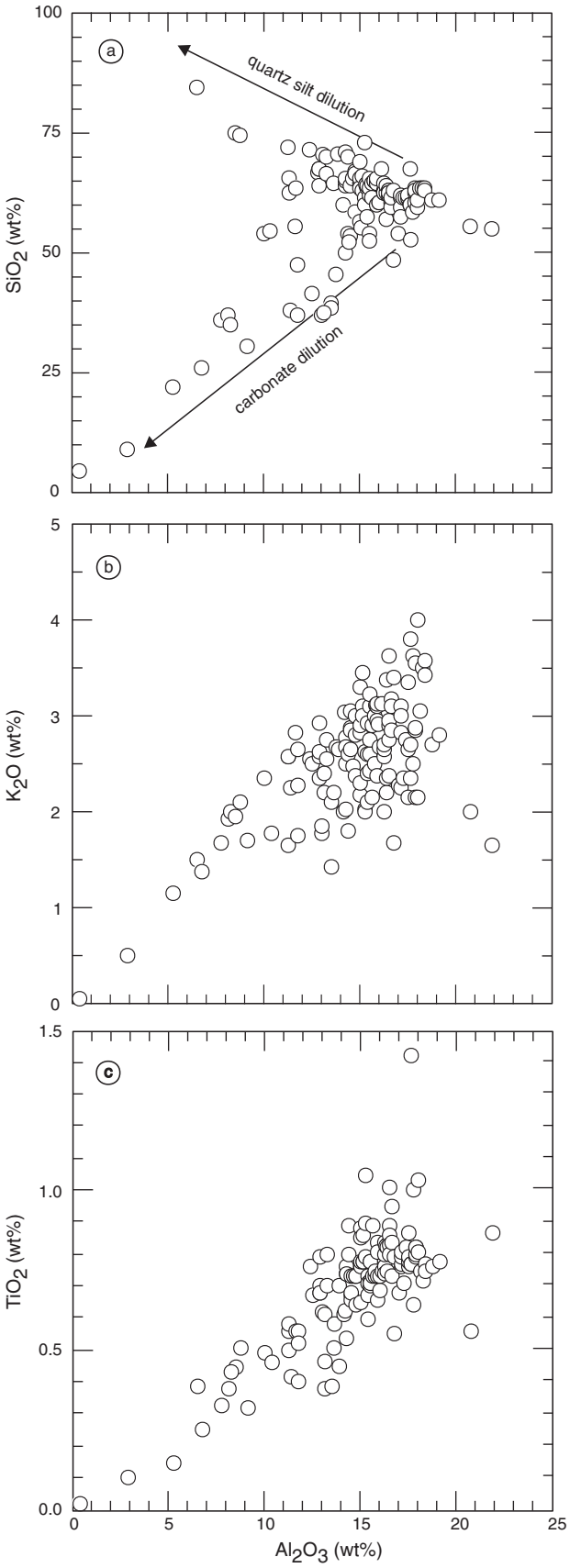

Figure 5. *Bulk-chemical element crossplots for all units. See text for discussion.*

from ~ 0 to > 4.0 wt% (Fig. 5b) with most samples containing between 2 and 4 wt%. TiO_2 ranges from ~ 0 to ~ 1.5 wt% with most samples between 0.5 and 1.0 wt% (Fig. 5c). Samples with low K_2O (< 1.5 wt%) and TiO_2 values (~ < 0.4 wt%) generally correspond to those diluted with quartz silt or carbonate.

Total organic carbon and sulphur

The results of TOC and total sulphur analyses on whole rock samples are included in Table 3. The accuracy of TOC values as determined by Rock-Eval is assessed by comparing TOC values determined by Leco combustion on acid-leached samples with those from Rock-Eval. The results are shown in Figure 6. The correlation coefficient is 0.95 but the slope is less than one and there is a positive y- (acid treated) intercept. Rock-Eval TOC values are affected by absorption on clay minerals of the volatized organics (Peters, 1986). At low TOC values (~ 0.5 wt%), the significance of this effect is reflected in the positive y-intercept of Figure 6. These results suggest that at these low TOC values (< 0.5 wt %), Rock-Eval TOC values may significantly overestimate the organic carbon content. The magnitude of this error within the context of bulk chemistry, however, is small.

More significant is the slope of the regression in Figure 6. A slope of m < 1 indicates that with increasing TOC (> 6 wt%) in carbonate-rich samples, Rock-Eval pyrolysis may significantly overestimate TOC with 10–15% relative error at TOC values of ~ 7 wt%. These data indicate that

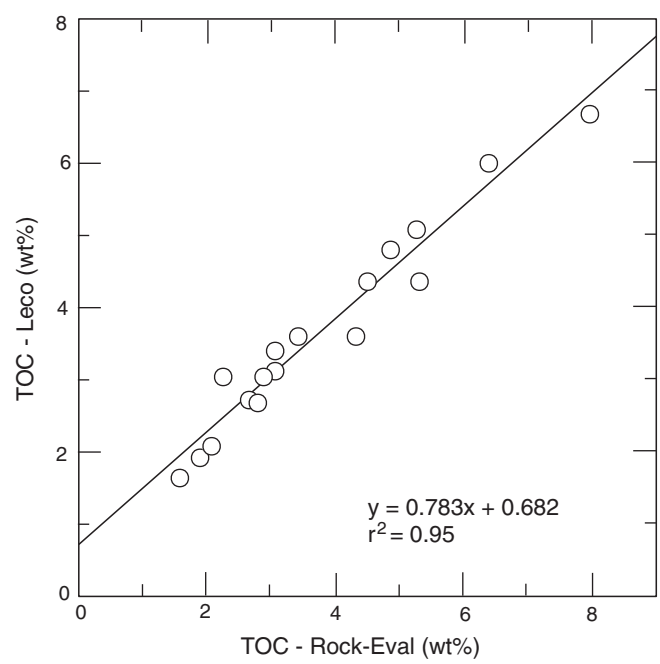

Figure 6. *TOC measured by Leco combustion on acid-treated samples versus TOC measured by Rock-Eval pyrolysis.*

carbonate-bearing, TOC-rich samples should be acid-treated and reanalyzed by combustion after initial Rock-Eval screening.

TOC and sulphur (S) data are shown in Figure 7. Two groups of shales are identified. Group I (Joli Fou, Viking, Westgate, and Belle Fourche formations) are characterized by low S (< 1.5 wt%) and TOC (< 2.0 wt%) values, whereas Group II (Fish Scales, Second White Specks, Morden formations and First Speckled Shale have high S (> 2.0 wt%) and TOC (> 2.0 wt%) values. This correlates with the Rock-Eval data (Fig. 4) that indicate dominantly Type III organic matter in Group I and Type II in Group II. An Fe–S cross-plot (Fig. 8) shows a similar grouping of the shale units. Group I contains more Fe and plots well away from the stoichiometric pyrite line. Group II contains less Fe and more S and plots close to the pyrite line. The Morden Formation shows a distinct enrichment in both Fe and S.

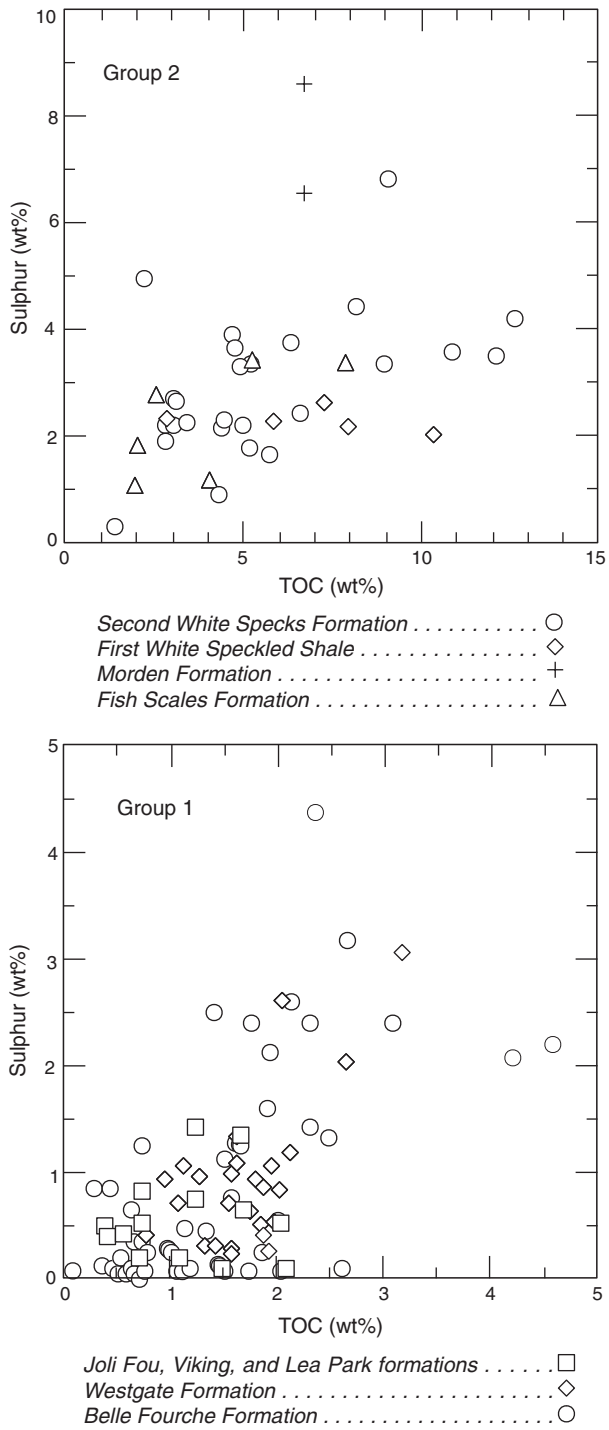

Figure 7. *Carbon and sulphur systematics for shales identified as transgressive (Group 2) and progradational (Group 1). Note different scales for axes.*

Sulphide and sulphate

The dominant sulphur-bearing mineral in the Colorado Group is pyrite, which is typically the only detectable sulphur-bearing mineral. In some samples, however, sulphate minerals are detected by XRD. For these samples, speciation of sulphur is necessary to accurately determine mineral modes. The quantitative determination of sulphide, SO and sulphate is a laborious and time-consuming task (Tuttle et al., 1986) and not suited to the processing of a large number of samples that are involved with a regional study. To circumvent this problem, a calibration method was used to estimate the amount of sulphide and sulphate in samples with multiple sulphur-bearing species. The amount of pyrite in a sample is calculated by converting the S content to stoichiometric pyrite (S (wt%)/ 0.5345). This value is plotted against the 0.270 nm intensity as determined by XRD. As shown in Figure 9a, samples that contain only pyrite show a very good correlation with the 0.270 nm diffraction intensity. This set of samples is then used to determine an equation by linear regression for calculating the pyrite abundance from the 0.270 nm intensity (Fig. 9b). The resulting abundances are used in subsequent calculations (see below). Graphical assessment of the error associated with this kind of calibration suggests it could be as high as 50% (shaded area, Fig. 9b) when pyrite abundances are 4 wt% or less. A small positive x-intercept results from this regression, suggesting a slight excess of sulphur assigned to pyrite. This occurs because of the presence of undetected sulphur-bearing species and/or organic sulphur. It should be noted that the presence of apatite, which has a peak at 0.271 nm, invalidates this correction method. If detectable amounts of apatite are present or the peak at 0.270 nm is not sharp and distinct, an alternative pyrite peak should be used.

Ca-Mg-Fe in carbonate

Twelve samples with variable amounts of total carbonate and generally more than one carbonate mineral were treated with HCl and the leachate analyzed for Ca, Mg, and Fe. The concentrations were converted to oxide wt% and assigned to

$CaCO_3$, $MgCO_3$, and $FeCO_3$. These end-member components were then used to determine the abundance of ideal calcite ($CaCO_3$), dolomite ($CaMgCO_3$), and siderite ($FeCO_3$) by assigning CO_2, as determined from the carbon analysis. Calcite and dolomite are the dominant carbonate minerals present in the calcareous Second White Specks Formation and the calculated abundances are plotted against the characteristic peak intensity (Fig. 10). These results indicate that for calcite, the method works reasonably well (Fig. 10a). However, for dolomite, the correlation is poor

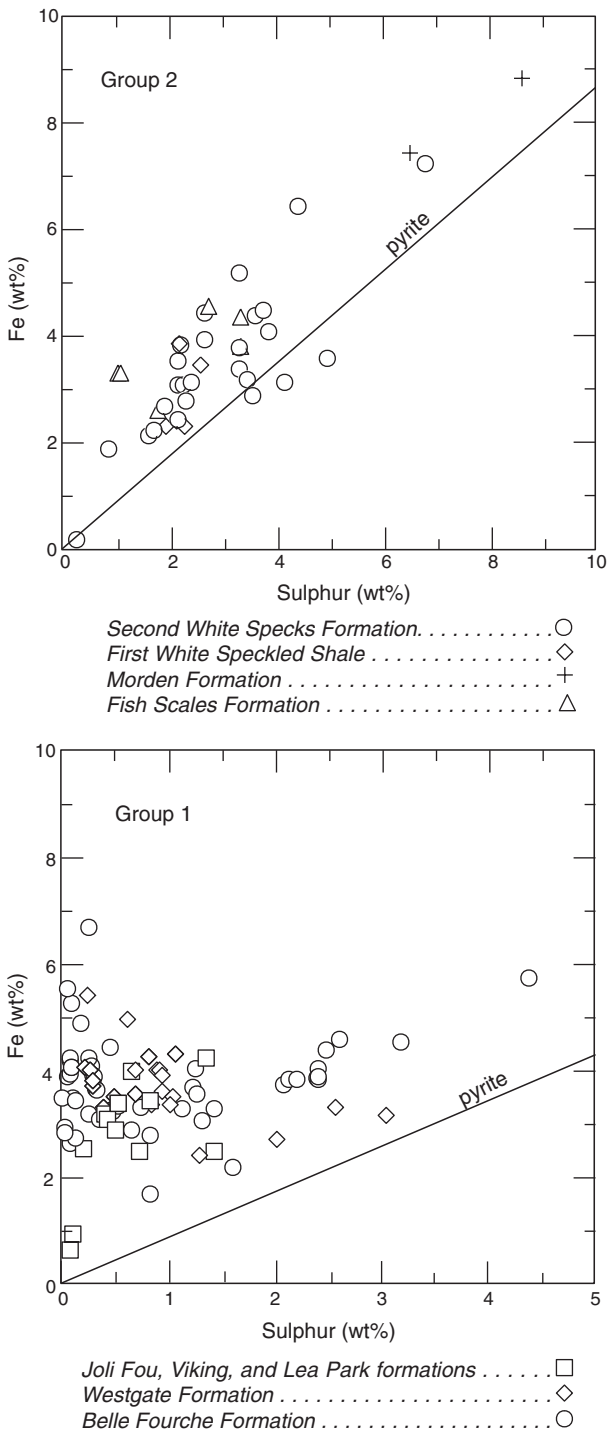

Figure 8. *Sulphur and iron systematics for transgressive (Group 2) and progradational (Group 1) shales. Pyrite line is composition of stoichiometric pyrite. Note scale difference for the x-axis.*

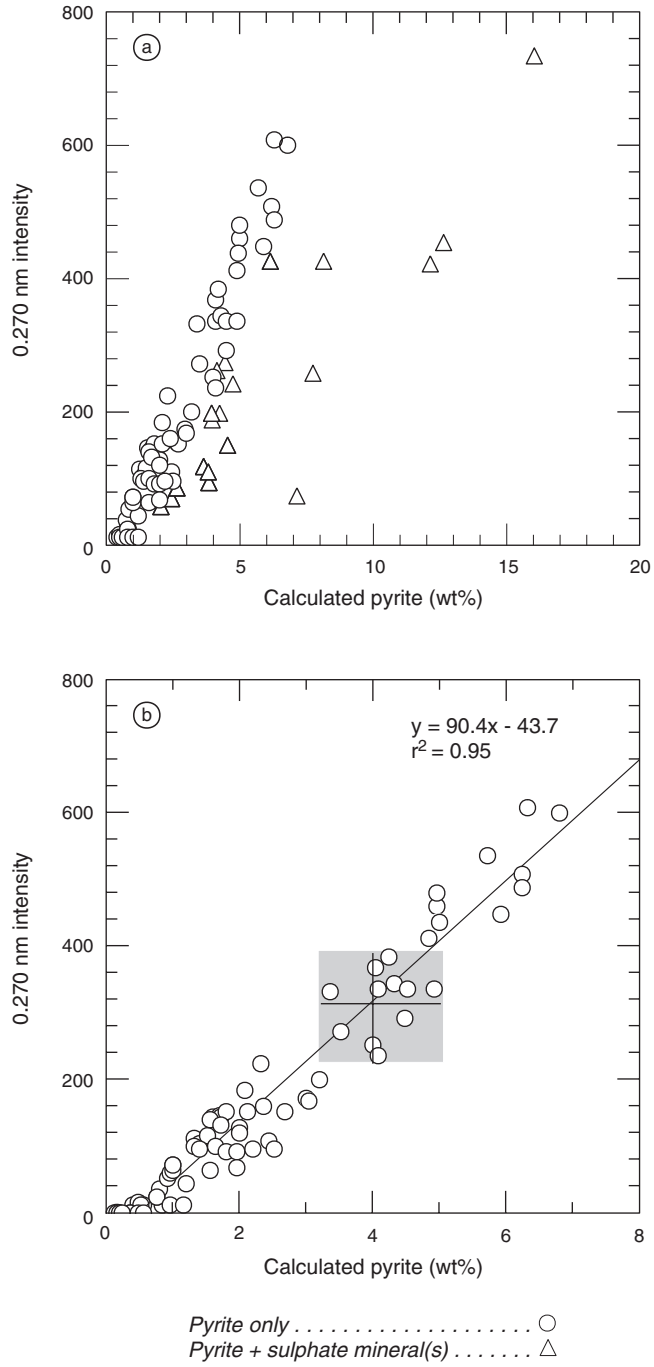

Figure 9. *Characteristic peak XRD intensity versus the calculated abundance of pyrite. The presence of sulphate minerals (a) distorts the regression (b) if sulphate sulphur is assigned to pyrite. The regression in (b) is used to calculate pyrite abundances where no sulphur analyses are available.*

(Fig. 10b). This is due to either the presence of small amounts of chlorite in the sample or a variable dolomite composition that includes some ankerite. Chlorite, particularly clinochlore, is susceptible to acid treatment and Mg contribution to the leachate from this clay mineral is probable. The oxide abundances must be balanced with the TIC and therefore carbonate totals should be accurate. However, in samples with multiple carbonate species and chlorite, the calculated composition of individual species may be significantly in error.

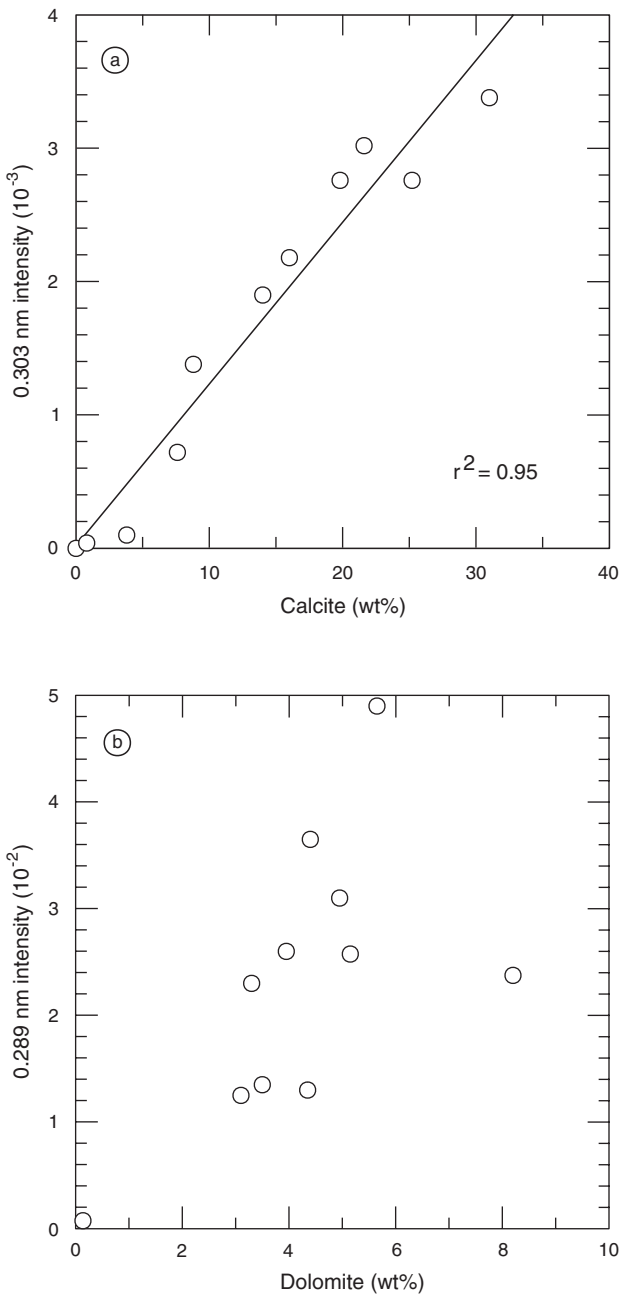

Figure 10. *Characteristic XRD peak intensity versus the calculated abundances of calcite and dolomite. Calcite abundances (a) may be estimated from the 0.303 nm intensity whereas the characteristic dolomite peak (b; 0.289 nm) is unreliable.*

Clay mineralogy

Standard XRD treatments of these samples (Fig. 11) indicate that this fraction is composed largely of I/S, kaolinite, quartz, and minor chlorite. In some samples, a sharp, symmetrical peak at ~ 10Å suggests the presence of well-crystallized illite or muscovite, which is confirmed by SEM (see below). Discrete illite is determined to be present by the occurrence of a series of peaks that show no change with EG-solvation and that exhibit "ideal" Bragg behavior (Fig. 12), as defined by Bailey (1982). The expandable component in the I/S is highly variable (Fig. 11, 13). Using the methods of Srodon (1980) and Moore and Reynolds (1989), estimates of the proportion of expandable component (smectite) range from < 10 to > 90 per cent, with most samples in the 70 to 90 per cent range. Estimates of expandability are hampered by the presence of detrital illite (Srodon, 1980) and comparison of the results from different methods is poor. Ordering of the I/S is predominantly random (R0). Only two samples exhibit a peak between 11 and 13Å with EG saturation, suggesting the presence of a superlattice peak and R1 or greater ordering (Moore and Reynolds, 1989).

Even the smallest size fractions (< 0.2 to 0.05 µm) are not monomineralic and the separation of detrital illite and the I/S is not complete (Fig. 13). In order to constrain the composition of an "end-member" smectite, bentonites from the Colorado Group were analyzed by XRF. XRD of these samples indicates that the clay component is virtually pure smectite with variable amounts of kaolinite (Fig. 14). The compositions of matrix I/S and smectite from bentonites were calculated from the XRF analyses by linear programming. The results are given in Table 6.

Mixed-layer clay compositions are commonly plotted on ternary diagrams (Fig. 15) with vertices represented by the minerals celadonite, muscovite and pyrophyllite (CMP diagram). The rationale for this comes from the observation that variable cation substitutions in tetrahedral and octahedral positions are the primary replacement mechanism in micas (Yoder and Eugster, 1955) and a major control on resulting 2:1 clay mineral (and mica) compositions (Ross and Hendricks, 1945). Increasing cation substitution for Si in the tetrahedral layer results in an increased tetrahedral layer charge. Divalent cation substitution for Al in the octahedral layer results in an octahedral layer charge and it is the variable layer charges that result in the attraction of different interlayer cations and the formation of 2:1 dioctahedral clay minerals. Pyrophyllite ($Al_2Si_4O_{10}(OH)_2$) has no layer charge; muscovite ($KAl_3Si_3O_{10}(OH)_2$) has only a tetrahedral layer charge; and celadonite ($K(Al,Fe,Mg)_{2-3}Si_4O_{10}(OH)_2$) has only an octahedral charge. The range of

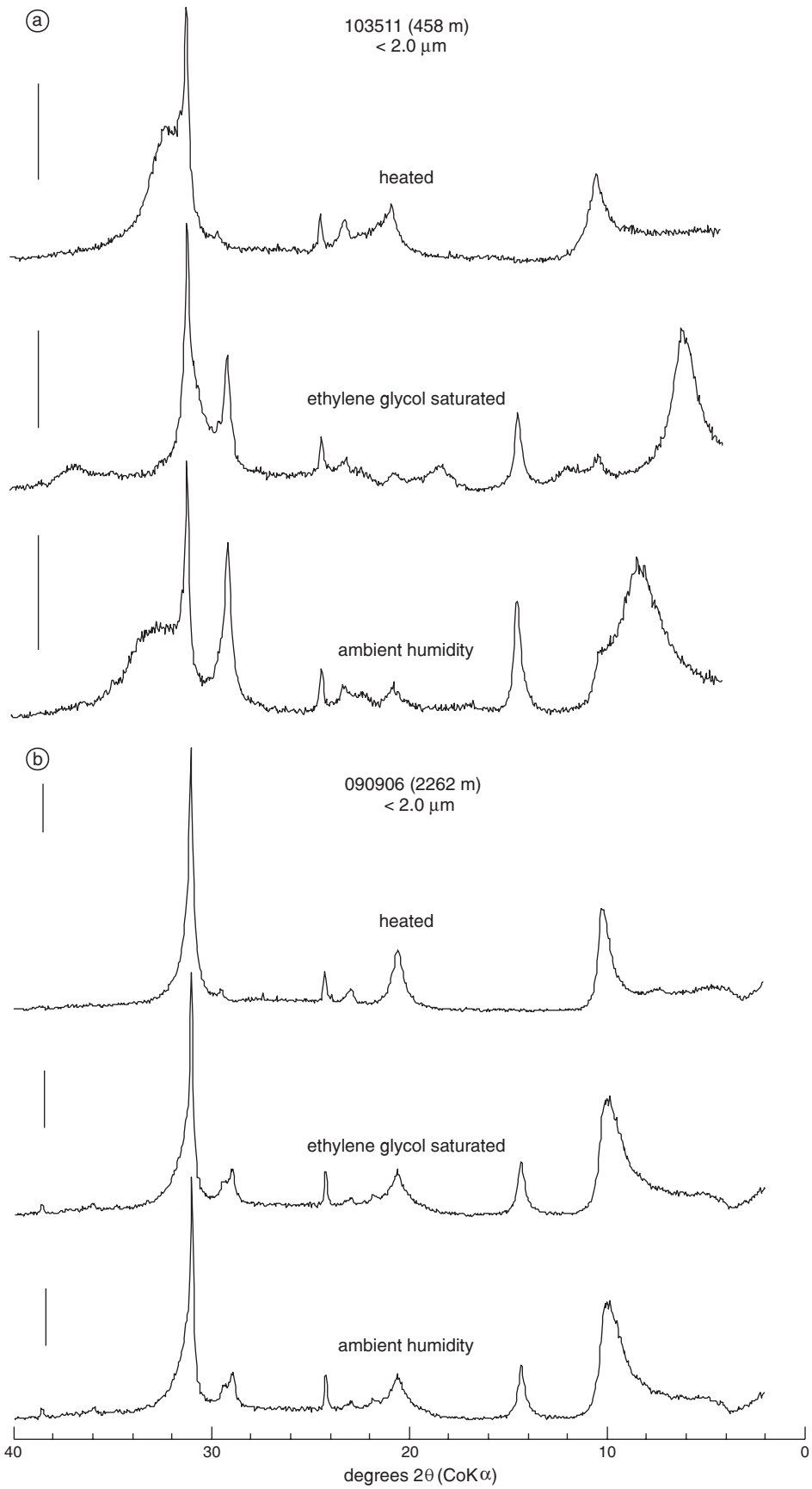

Figure 11. *XRD patterns of < 2 μm separates after standard treatments - a) sample 103511, b) sample 090906. Scale bars = 1000 cps.*

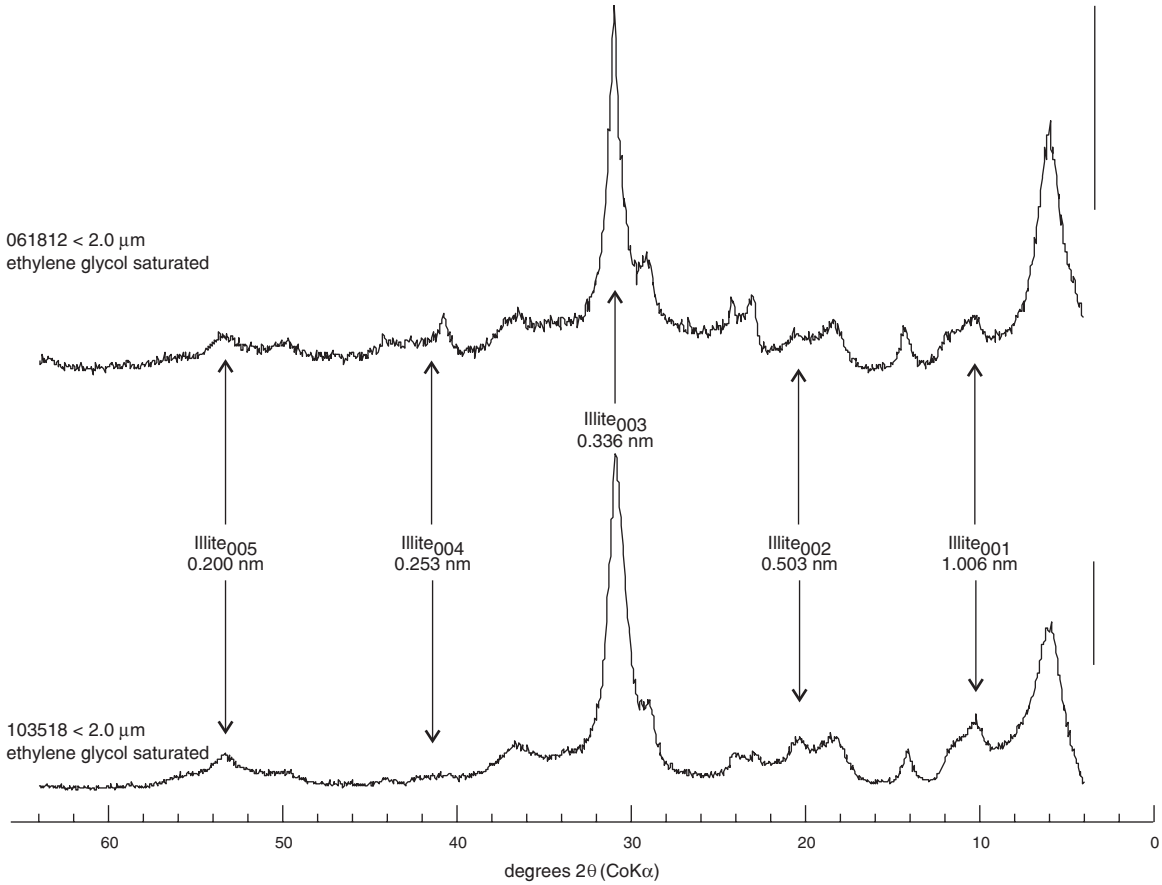

Figure 12. *Ethylene glycol saturated < 2 µm samples showing the presence of discrete illite as determined by well-characterized Bragg behavior (see text). Scale bars = 1000 cps.*

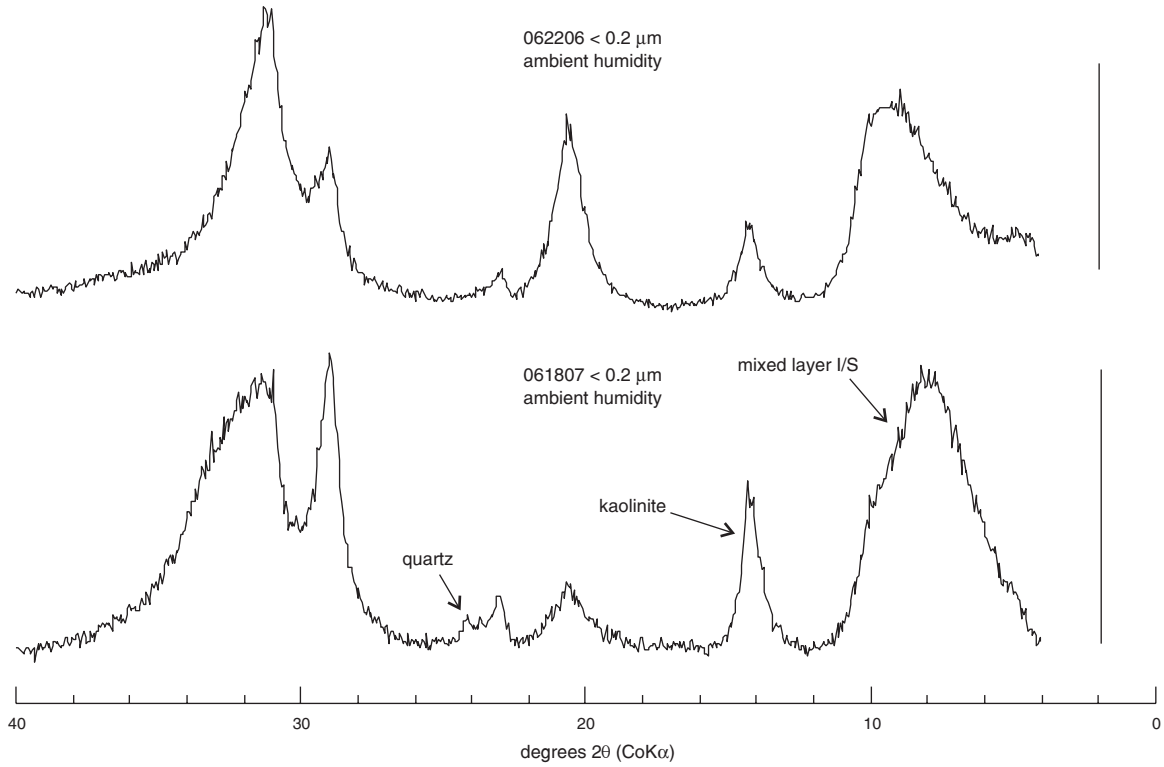

Figure 13. *Fine fraction (< 0.2 µm) mixtures of kaolinite and I/S. Scale bars = 1000 cps.*

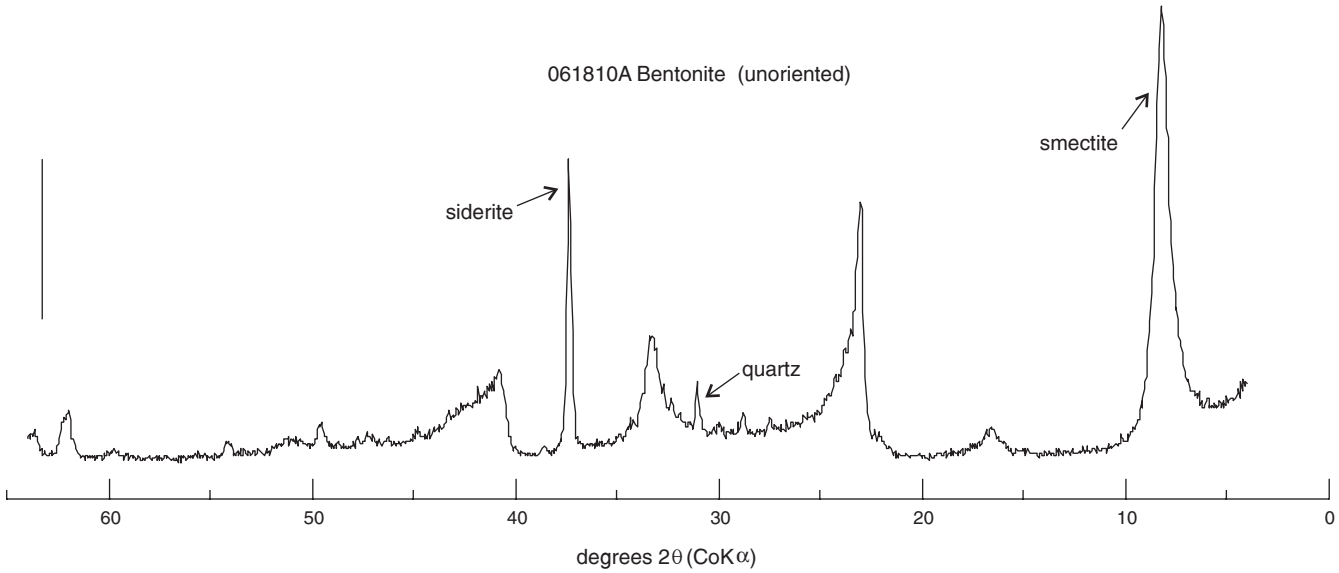

Figure 14. *XRD pattern of a whole-rock bentonite. Scale bar = 1000 cps.*

chemical compositions of 2:1 dioctahedral clay minerals, including smectite, illite and mixed layer I/S, can be represented in this compositional space (Hower and Mowatt, 1966).

The compositions of Colorado Group I/S and bentonites are plotted on a CMP ternary (Fig. 15) and an element ratio plot (Fig. 16). Most smectites from bentonites show little tetrahedral substitution (Fig. 15) and therefore plot closer to the pyrophyllite end-member. There are exceptions. One smectite from each of the Westgate, Fish Scales and Belle Fourche formations falls above the 40% celadonite value indicating enrichment in Fe and/or Mg. In the case of the Westgate smectite, XRD indicates that this bentonite contains a considerable amount of siderite. The high celadonite component may reflect the Fe-rich bulk chemistry or may result from contamination by adsorbed Fe-oxides. Fe-oxides may be produced from the oxidation of reduced Fe by meteoric water or Fe oxidation during sample preparation.

In the case of the Fish Scales, the bentonite in question contains a large amount of apatite and the smectite composition is Ca-rich. The substitution of octahedral Mg or Fe^{2+} by Ca would have the effect of increasing the celadonite component on this type of diagram. The sample from the Belle Fourche Formation contains a significant amount of both apatite and siderite.

The shale matrix I/S contains a greater proportion of the muscovite component, indicating a more illitic composition compared to the bentonites. In the Westgate Formation, there appears to be a significant increase in the celadonite component. In the Belle Fourche, a large number of samples have virtually no pyrophyllite component. Most of these Belle Fourche samples are from proximal prodeltaic deposits (Caritat et al., 1994a) in the northwest part of the study area and are also the most deeply buried. The I/S in these samples is illite-rich (Fig. 11b) and two of these samples (#062206, 540 m and #090906, 2262 m) show R1 or greater ordering.

Another way to examine the clay compositions is on a cross-plot of diagnostic element ratios (Fig. 16). This type of plot has the advantage of examining the chemical data directly without introducing the artifact of normalization to a structural formula of 22 charges, as is done on the muscovite–celadonite–pyrophyllite ternary. In addition, on an element ratio diagram, minerals plot as points and the bulk chemistry can be interpreted in terms of individual phases. The Si/Al–K/Al plot is used because: 1) Si and Al are the primary building blocks of phyllosilicates, 2) Si and K are essentially a coupled substitution in I/S, and 3) if Al is conserved in the system, mineralogical trends should be evident as the ratio of Si to K changes (Pearce, 1967).

Figure 16 indicates the low K and high Si content of the bentonite smectite. Westgate Formation matrix I/S shows higher Si whereas the Belle Fourche Formation shows lower Si with no discernible difference in K content. In the Fish Scales and Second White Specks formations, an increase in K content distinguishes the matrix I/S from the bentonite smectite. This type of diagram will be used in subsequent sections to evaluate bulk chemical compositions and diagenetic processes.

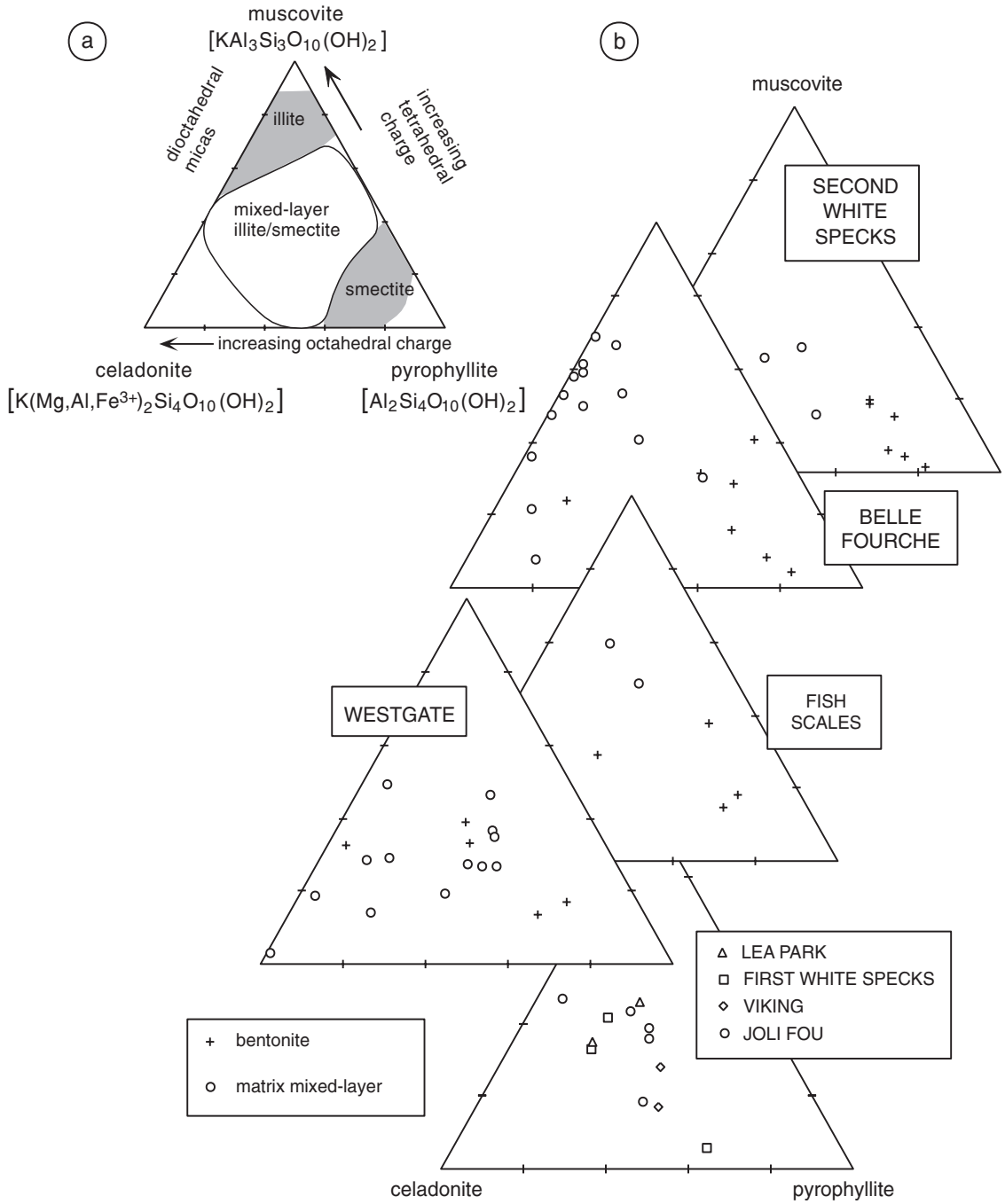

Figure 15. *a) Schematic celadonite–muscovite–pyrophyllite (CMP) ternary diagram illustrating the relationship between layer charge and the compositions of illite, smectite, and mixed-layer clays (after Hower and Mowatt, 1966). b) Colorado Group shale I/S and bentonite smectite compositions for each formation on a CMP ternary.*

Carbonate isotopic compositions

Carbonate isotopic data are summarized in Table 7. Three concretion types are present in Colorado Group shales: calcite, zoned siderite and unzoned siderite concretions. Calcite concretions, which occur only in the calcareous upper Belle Fourche and the Second White Specks formations, are depleted in ^{13}C and relatively enriched in ^{18}O and show little or no isotopic zoning (Fig. 17). Isotopically zoned and unzoned siderite concretions occur in the lower Belle Fourche (noncalcareous) and the Westgate formations (Table 7 and Fig. 17).

The $\delta^{18}O$ values for the calcite concretions suggest formation from basinal fluids of nearly marine oxygen isotopic composition at low temperatures. The very depleted

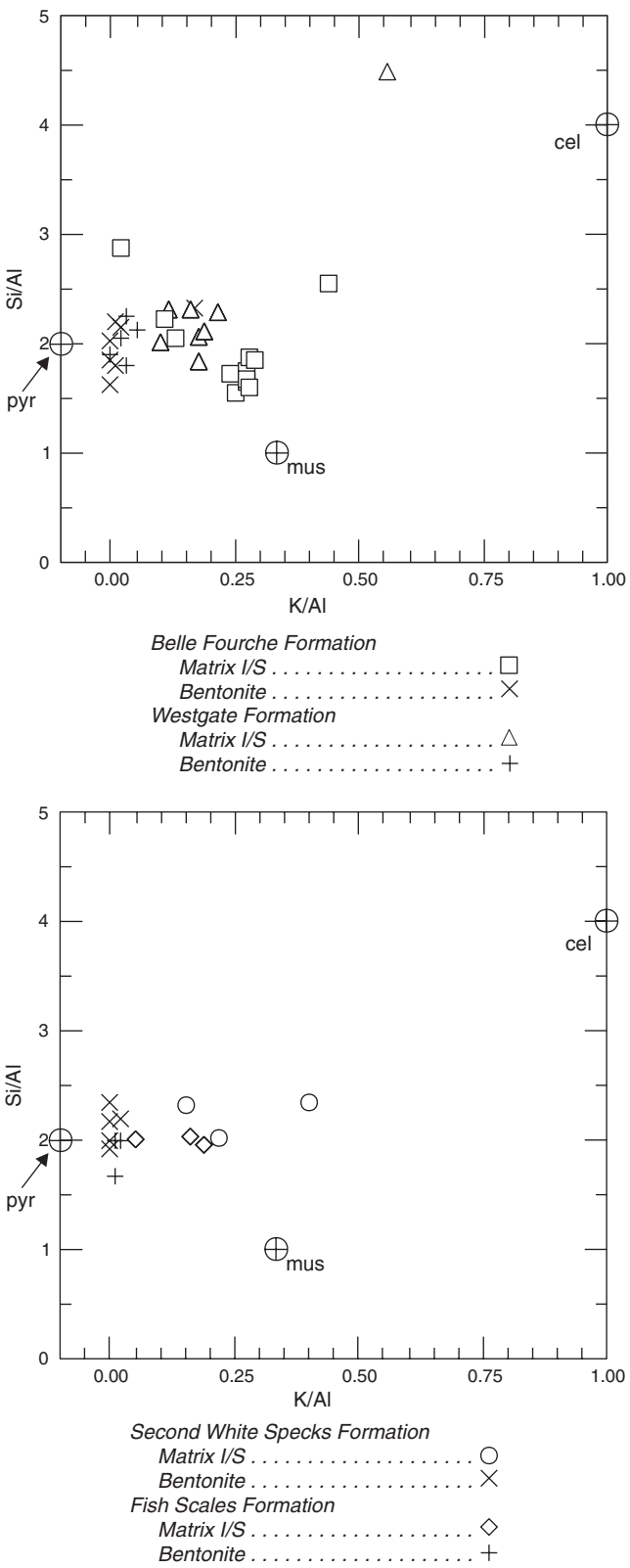

Figure 16. *Shale I/S and bentonite–smectite compositions on an element ratio plot. See text for discussion.*

$\delta^{13}C$ values reflect OM oxidation, and the carbon isotopic signature suggests most carbon is sourced from OM. The mechanism of OM oxidation is most likely sulphate reduction (see below). In contrast, fracture-fill calcite (Fig. 17) is enriched in $\delta^{13}C$ and depleted in $\delta^{18}O$. Paired concretion and fracture-fill calcite show a consistent difference in $\delta^{18}O$ of approximately 10.2‰.

Unzoned siderite concretions in the Belle Fourche Formation have $\delta^{13}C$ values near 0‰ PDB and $\delta^{18}O$ values between ~21 and 24‰ SMOW. Unzoned concretions in the Westgate have similar oxygen isotopic compositions but are depleted in ^{13}C (Fig. 17). Isotopically zoned concretions from the Westgate Formation show about a 3‰ depletion in $\delta^{18}O$ from the concretion center to the margin. $\delta^{13}C$ values similarly decrease, albeit more variably, from core to margin (Fig. 17). The oxygen isotopic compositions of both the zoned and unzoned siderite concretions could result from one, or a combination, of processes that include: 1) variable mixing of meteoric and marine pore waters, 2) formation from marine pore waters that have been altered isotopically by clay mineral authigenesis, and 3) formation at temperatures greater than surface temperature. Negative $\delta^{13}C$ values reflect the mixing of dissolved HCO_3- derived from the oxidation of organic matter with marine HCO_3-. Positive $\delta^{13}C$ values, which range up to ~ 7‰ PDB, indicate CO_2 from methanogenesis incorporated into concretion carbonate minerals. The nature of concretion formation is discussed further in the diagenesis section.

Sulphide sulphur isotopic composition

Sulphur isotopic data are summarized in Table 8. The extreme range of ^{34}S values is characteristic of sedimentary sulphide and the predominance of very depleted ^{34}S values indicates that bacterial sulphate reduction is the primary mechanism of sulphur incorporation into Colorado Group shales (Thode et al., 1951). A detailed discussion of the sulphur isotopic data is deferred to the section on diagenesis.

FORMATION DESCRIPTIONS

The integration of lithological, geochemical and biostratigraphic data results in the differentiation of four regionally mappable lithostratigraphic shale units that comprise the lower Colorado Group. Biostratigraphic analysis relies primarily on foraminiferal, dinoflagellate and coccolith assemblages. In addition, there are local accumulations of sandstone that interfinger conformably or disconformably with the shales. Shale descriptions and the stratigraphic nomenclature used herein were originally presented in Bloch et al. (1993) and Schröder-Adams et al.

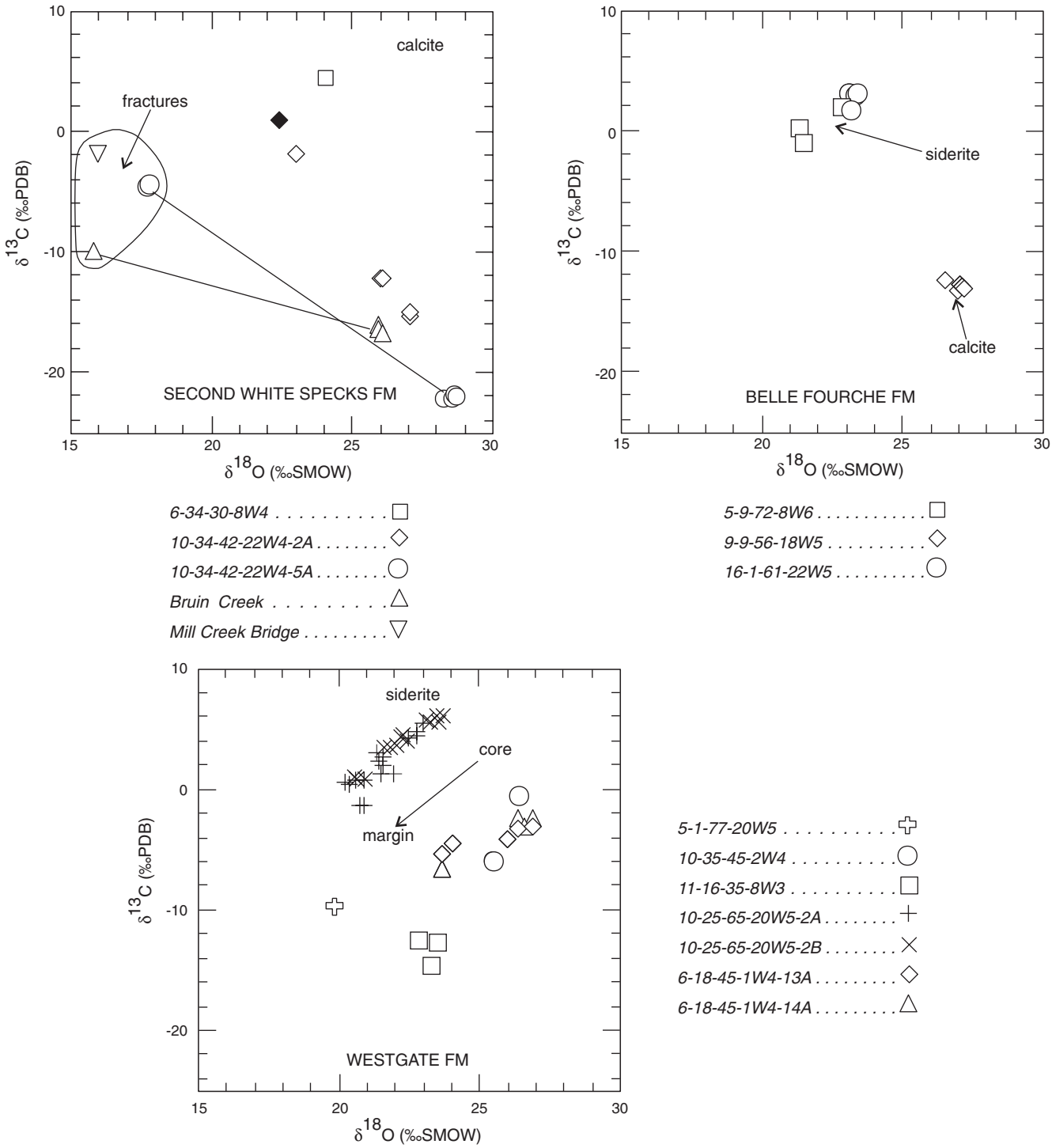

Figure 17. *Carbon and oxygen isotopic composition of calcite and siderite concretions for the Second White Specks, Belle Fourche, and Westgate formations. Second White Specks Formation fracture-fill cements are circled. Lines connect fracture cements with concretion matrix of the same sample. Filled diamond is dolomite. See Table 1 and Figure 1 for outcrop locations.*

(1996) and much of that data is reiterated below. Additional data on the shales (Tables 9, 10) are included in this report to provide a comprehensive description of the lower Colorado Group succession.

Westgate Formation

The Westgate Formation is a wedge of noncalcareous mudstone to siltstone that thickens from approximately 20 m

Table 8

TOC, S, Fe abundance and S isotopic data by borehole (east to west)*

Sample #	Formation	Depth (m)	TOC (wt%)	HI mgHC/gOC	OI mg CO_2/gOC	Fe_2O_3	S (wt %)	$\delta^{34}S$ ‰
11-36-22-1W2	S.W.P. BREDENBURY							
113601	Lea Park	195.40	1.59	49	43	5.65	0.63	-37.8
113603	Lea Park	205.50	1.64	57	34	6.00	1.33	-27.6
113605	1st Specks	215.50	8.02	367	41			-35.3
113607	1st Specks	225.65	7.50	359	37			-38.5
113609	1st Specks	235.65	7.98	497	41	3.40	2.15	-33.6
113611	1st Specks	242.65	5.51	323	63			-31.0
113613	1st Specks	246.65	12.17	370	34			-33.4
113615	1st Specks	247.49	9.11	316	40			-33.4
113617	Morden	250.80	5.15	70	54			-33.7
113618	Morden	252.40	6.21	73	53			-33.1
113621	Morden	256.30	6.91	120	56			-34.7
113622	Morden	258.30	6.46	274	24			-32.3
113625	2nd Specks	264.90	4.65	374	40			-30.3
113630	2nd Specks	273.70	0.82	255	113			-17.4
113634	2nd Specks	281.30	4.88	415	36			-33.7
113636	Belle Fourche	285.10	8.99	419	27	5.40	3.30	-29.1
113638	Belle Fourche	288.90	5.51	401	38			-22.3
113639	Belle Fourche	290.80	4.95	181	30			-18.9
113640	Fish Scales	291.70	4.20	191	30	5.35	2.07	-13.6
113641	Westgate	296.70	3.91	147	29			-17.4
113643	Westgate	311.80	5.09	204	26			-28.6
113645	Westgate	321.80	1.69	67	25			-6.8
113647	Westgate	332.60	1.71	44	60			-5.7
11-16-35-8W3	C.M.S. VANSCOY							
111648	1st Specks	376.30	7.34	416	27			-34.5
111644	1st Specks	396.30	5.60	367	27			-34.3
111642	1st Specks	398.40	5.60	400	25			-24.6
111640	1st Specks	400.25	4.62	303	30			-15.2
111639	2nd Specks	401.00	8.67	379	26			-21.3
111638	Belle Fourche	401.70	2.47	163	28	4.36	1.33	5.4
111634	Belle Fourche	405.20	1.28	78	25			12.6
111631	Fish Scales	408.20	1.26	57	9			11.4
111630	Westgate	413.20	1.20	59	14			-14
111626	Westgate	435.80	1.56	47	13			-22.8
111624	Westgate	445.80	1.62	52	16			-40.7
111622	Westgate	455.80	1.17	40	3			-31.5
111620	Westgate	465.80	1.22	61	8			-22.9
111616	Westgate	484.30	1.86	117	21	3.39	0.85	-6.6
111610	Joli Fou	510.00	0.73	47	29	4.85	0.81	-32.1
111606	Joli Fou	516.90	1.21	54	24	3.54	1.42	3.6
111602	Joli Fou	520.90	1.47	187	20	0.90	0.08	-1.7
10-35-45-2 W4	ANDERSON HUSKY ROROS							
103511B	Belle Fourche	429.00	fracture-fill pyrite					15.1
103512A	Belle Fourche	433.00	fracture-fill pyrite					10.0
06-34-30-08 W4	AMOCO B-1 YOUNGSTOWN							
063401	2nd Specks	693.00	5.04	258	23	5.46	2.18	-25.3
063403	2nd Specks	703.00	6.19	322	20	3.02	1.61	-28.6
063406	2nd Specks	718.00	5.26	286	22	7.43	3.31	-29.3
063408	2nd Specks	728.00	8.11	316	22			-32.4
063410	2nd Specks	738.00	8.21	335	21	9.19	4.39	-30.5
063411	2nd Specks	743.00	8.73	408	20			-30.6
063412	Belle Fourche	748.00	1.75	100	35	5.75	2.40	2.2
063413	Belle Fourche	753.00	1.88	108	31			6.0
063414	Fish Scales	765.00	5.57	229	25			-21.7
063415	Fish Scales	770.00	2.03	93	35	4.65	1.03	-7.7
063416	Westgate	775.00	1.71	80	28			5.3

Table 8 (cont.)

TOC, S, Fe abundance and S isotopic data by borehole (east to west)*

Sample #	Formation	Depth (m)	TOC (wt%)	HI mgHC/gOC	OI mg CO_2/gOC	Fe_2O_3	S (wt %)	$\delta^{34}S$ ‰
063419	Westgate	790.00	1.56	110	50	5.02	0.26	5.5
063427	Westgate	829.00	1.57	136	76	4.71	0.21	6.2
11-12-06-16 W4 AMOCO CONRAD								
111201	2nd Specks	549.00	3.03	196	13	5.02	2.17	-28.3
111203	2nd Specks	559.00	2.37	154	22			-27.1
111205	2nd Specks	569.00	6.37	427	16	6.42	3.73	-29.2
111208	Belle Fourche	584.00	2.29	106	16	5.48	2.39	-25.6
111211	Belle Fourche	599.00	3.07	157	15	5.56	2.40	-29.5
111214	Belle Fourche	615.00	2.09	197	25			-30.2
111215	Fish Scales	620.00	7.96	415	13	5.41	3.33	-28.3
111216	Fish Scales	625.00	3.39	294	20			-26.0
111217	Westgate	630.00	1.57	77	21	4.71	1.12	4.3
06-07-12-28W4 CANADIAN SUPERIOR OXLEY								
060704	2nd Specks	2575.00	2.81	403	23			-29.5
060707	2nd Specks	2578.00	1.51	365	47	2.63	1.42	-23.8
060711	2nd Specks	2582.00	2.77	399	20	4.88	2.09	-25.1
060717	2nd Specks	2588.00	3.00	300	26	8.16	4.53	-22.9
060719	2nd Specks	2590.00	2.33	366	32	6.33	3.06	-22.4
060721	Belle Fourche	2592.00	0.74	241	58			-14.8
060725	Belle Fourche	2595.50	0.56	222	50			-19.8
060729	Belle Fourche	2599.00	0.39	188	64			-25.2
060733	Belle Fourche	2603.00	0.80	315	32			-25.0
4-13-54-18W5 TEXEX EDSON								
041302	2nd Specks	2104.00	4.83	296	10	6.22	3.62	-26.2
041304	2nd Specks	2114.00	3.13	265	17	6.32	2.64	-22.5
05-01-77-20 W5 IMPERIAL KATHLEEN #1								
050109	Fish Scales	405.38	2.61	59	42	6.47	2.75	-31.8
050111	Fish Scales	411.48	3.19	89	35			-28.3
050114	Fish Scales	419.40	2.04	56	29			-15.1
050116	Westgate	423.98	2.15	55	25			-13
050122	Westgate	441.96	2.03	75	21	5.67	0.82	11.5
050126	Westgate	451.00	1.50	44	24	6.13	0.91	-4.8
16-01-66-22 W5 AMOCO BIGSTONE								
160106	Belle Fourche	1893.00	1.49			6.10	0.07	-1.6
160108	Belle Fourche	1903.00	1.34			6.30	0.44	39.9

*TOC, HI abd OI by pyrolysis; Fe_2O_3 by XRF; S by combustion

on the Saskatchewan–Manitoba boundary to 120 m in northwestern Alberta. In southwestern Alberta, the Westgate Formation is less than 20 m thick and pinches out by onlap west of the 5th Meridian.

The basal contact with the underlying Viking Formation is characterized by the disappearance of sandstone and/or a noticeable decrease in siltstone and sandstone content. The wireline signature of the basal contact with the underlying Viking Formation is best expressed by a marked increase in resistivity and sonic transit time.

The Westgate Formation is characteristically heterolithic, typically comprising finely interbedded siltstone and claystone laminae. Siltstone beds are 1 to 5 cm thick, sharp-based and locally graded. The basal Westgate Formation is commonly finely laminated with minimal bioturbation. Bioturbation increases upsection, becoming moderate to intense near the top of the formation. Identifiable trace fossils include *Planolites*, *Chondrites*, *Terebellina*, and *Helminthopsis*. Resistivity, density, and gamma-ray responses as well as composition of the Westgate Formation are relatively uniform throughout (see Bloch et al., 1993, fig. 8; Table 9).

Detrital grains are primarily silt-sized quartz and K-feldspar (Plates 1c, 3e, 4d-f) with subordinate, plagioclase feldspar (Plates 1d, 2a), muscovite (Plate 3f), biotite (Plate 1b, d), apatite – primarily as bioclasts (Plate 4c), oxides of Ti (Plate 5f), and chamosite (Plate 1f). Other

Table 9

Colorado Group mineralogy calculated from XRF data

Sample #	Pyr	Jar	Alu	Cal	Sid	Dol	Gyp	Apa	Ana	Qtz	I/S[1]	Kao	Ksp	Plg	Chl	TOC	Total
Lea Park Formation																	
113601A	1.18							0.33	0.69	22	58	11	6		tr	1.66	100.86
113603A	1.55						2.70	0.61	0.77	24	50	13	7			1.64	101.27
mean	1.37							0.47	0.73	23	54	12	7			1.65	
First Speckled Shale																	
052244A	4.86			19.88			6.73	0.68	0.38	11	34	12	5		tr	4.67	98.45
052251A	2.53			49.95			4.23	0.99	0.25	12	15	8		2		4.42	99.37
052256A	4.47			11.96		6.98		0.66	0.45	19	28	18	6			6.67	102.19
111641A	4.13			7.71	0.43			0.85	0.68	19	57	7		2	tr	5.94	104.74
111646A	4.83			24.98	2.92			0.71	0.42	14	29	12		6	tr	7.3	102.16
113606A	1.74			31.83			5.59	0.68	0.32	10	26	9	3			10.39	98.55
113609A	4.02			22.79				0.71	0.39	12	28	18	6			7.98	99.89
113614A	4.28			81.92				0.19	0.10	3	10					2.87	102.36
mean	3.86			31.38				0.68	0.37	12	28	12	5			6.28	
Morden Formation																	
113616A*	5.13	15.55	11.07				0.36	0.59	0.51	20	23	12				6.75	94.96
113619A*	8.55	20.60	8.88				0.00	0.50	0.40	20	23	10				6.75	98.68
mean	6.84	18.08	9.98				0.18	0.55	0.46	20	23	11				6.75	
Second White Specks Formation																	
041302	6.77			8.79	1.08	4.41		0.56	0.66	37	13	22	1			4.80	100.08
041304	4.94			7.48		3.28		0.47	0.85	35	21	16	5		tr	3.05	97.07
061802	3.04			25.16		3.47	9.93	0.54	0.38	25	14	1	4	3		10.92	100.44
062201	3.52			16.13		1.84		0.56	0.46	34	30	6	4	tr		2.86	99.37
063401	4.08			0.50				0.45	0.73	24	48	13	4	tr	tr	4.75	99.51
063403	3.01			30.88		5.16		0.43	0.43	17	18	10	5	tr		6.80	96.71
063406	6.19			1.32		5.46		0.45	0.86	32	30	14	tr	tr	tr	5.01	95.30
063410	5.59			19.80			7.49	0.44	0.67	26	16	14	1	tr	tr	8.55	99.53
071402	1.61			12.80	1.22	4.94		0.45	0.56	37	19	14	5		tr	3.58	100.15
103402	4.04			1.84		4.85		0.54	0.78	41	24	14	5		tr	2.81	98.86
103404	3.20			20.71	0.79	3.95		0.50	0.52	31	13	19	4		tr	5.23	101.90
103406	5.00			4.27				0.44	0.79	32	28	24	3		tr	3.05	100.54
103503	4.27	2.15	4.16	3.67		4.38		0.69	0.58	52	20	2	2	tr		4.94	100.83
103508	3.46			24.00		4.00	9.00	0.50	0.33	23	22	2	1	tr		10.96	100.26
111201	4.06			0.69	1.00	1.49		0.50	0.73	42	24	21	2		tr	3.03	100.50
111205	6.98	2.35		2.29			12.98	0.55	0.67	31	16	25	4		tr	6.37	101.21
112102	4.94	4.54				6.33		0.56	0.68	48	21	9	3		tr	2.22	100.27
112105	4.21			4.90		6.08		0.50	0.58	52	23	3	3		tr	3.43	100.71
112109	4.28			15.99		5.66		0.48	0.49	40	14	12	4		tr	4.36	101.27
113623A*	5.45	11.47	11.37				3.56	2.88	0.46	20	21	11				9.14	96.33
113628A**	3.32			27.25			12.76	0.57	0.15	10	17					12.62	83.67
113631A	0.00			87.92			1.45	0.12	0.02	2	5					1.40	97.91
mean	4.18			15.82		4.35		0.60	0.56	31	21	13	3			5.45	
Belle Fourche Formation																	
050102	0.17				1.74			0.62	0.76	38	25	23	6		tr	1.12	96.40
050902	0.13				2.41			0.60	0.80	35	28	22	7			1.61	97.55
050913	0.11				2.22			0.61	0.82	32	29	25	6		tr	1.62	97.38
050918	0.21				1.25			0.52	0.82	34	40	20	1		tr	1.44	99.24
050922	2.30				4.05			0.42	0.78	32	19	33	7			1.19	99.75
061806	2.36				2.99			1.13	0.88	41	30	19	1			1.29	99.65
061807	0.99				0.00			0.21	0.81	26	43	22	5			1.83	99.84
062204	2.99					5.75		0.57	0.51	59	14	11	4		tr	1.90	99.72
062206	5.91			1.60		5.53		0.39	0.79	38	21	19	4		tr	2.65	98.87
063412	4.49				0.58			0.68	0.87	25	20	43	2			1.07	97.69
071404	1.55					1.54		0.40	0.39	73	11	8	3		tr	0.42	99.31
071406	3.97			0.86	4.17			0.48	0.79	46	22	14	5		tr	1.93	99.20
090906	4.86					8.18		0.51	0.82	33	24	22	5		tr	2.33	100.71
103511	1.38				1.06			0.14	0.87	31	40	22	3			1.57	101.02
103513	0.47				0.39			0.33	0.76	27	45	19	4		tr	1.85	98.79

Table 9 (cont.)

Colorado Group mineralogy calculated from XRF data

Sample #	Pyr	Jar	Alu	Cal	Sid	Dol	Gyp	Apa	Ana	Qtz	I/S[1]	Kao	Ksp	Plg	Chl	TOC	Total
111208	4.47			0.35	3.39			0.44	0.80	48	27	13	tr		tr	2.29	99.74
111211	4.49			0.23	3.79			0.61	0.74	42	16	23	4		tr	3.07	97.93
111633A	1.09	4.20		0.33				0.15	0.74	34	29	23	5	3	tr	1.50	102.01
111635A	2.10	8.34						0.66	0.68	25	29	26		4		4.58	100.36
111637A	1.38	5.25			1.74			0.17	0.90	35	24	24		5		2.30	99.74
111638A	1.21	5.34			1.93			0.14	0.89	34	27	23		6		2.47	101.98
113636A	6.17			5.75				0.78	0.54	19	35	15	9			8.99	100.23
160106	0.13				3.38			0.64	0.83	33	34	23	3		tr	1.49	99.47
160108	0.82				4.44			0.65	1.03	28	42	18	4			1.30	100.23
mean	2.24				2.32			0.49	0.78	36	29	21	5			2.16	
Fish Scales Formation																	
050109	1.30	12.65	2.23					0.50	0.70	34	28	12	1		tr	2.35	94.73
063415	1.93							0.45	0.73	34	40	14	5			2.10	98.21
111215	6.23					2.30		0.51	0.56	42	26	10	5		tr	6.65	99.25
111217	2.10				1.21	0.60		0.74	0.78	38	26	24	6		tr	1.57	100.99
113640A	1.48	6.58	2.82		2.40			0.38	0.64	24	33	22	3			4.20	100.50
061601	3.35					4.99		0.40	0.45	63	26		tr		tr	2.07	100.26
061603	6.29					4.64		0.55	0.56	46	23	15	tr		tr	4.34	100.38
mean	3.24							0.50	0.63	40	29	14	3			3.33	
Westgate Formation																	
050122	1.53							0.34	0.83	30	45	17	3		tr	1.97	99.67
050126	1.70							0.35	0.89	31	41	20	5		tr	1.80	101.74
050927	1.29				1.93			0.52	0.80	46	29	15	4			1.43	99.97
050933	1.14				4.44			0.50	0.86	38	18	25	5		4	1.75	98.69
050940	4.83				1.93			0.48	0.78	37	26	22	5			2.88	100.89
052202A	1.66	3.22						0.26	0.77	26	43	19		5		1.63	100.54
052208A	1.78				0.77			0.33	0.78	27	34	24		8	tr	1.58	98.24
061810	1.93				1.64			0.46	0.67	31	38	20	4			2.04	99.74
061812	2.08				0.77			0.39	0.73	35	35	19	5			1.87	99.84
063419	0.49				2.03			0.81	0.84	31	42	21	tr			1.72	99.88
063423	0.45				0.96			0.36	0.95	24	44	20	4		tr	1.94	96.66
063427	0.39				1.06			0.46	0.78	37	31	22	5			1.80	99.49
100501	5.69				2.11	2.10		0.59	0.68	52	12	20	1		tr	3.18	99.35
100504	0.56				6.46			0.40	1.00	28	32	28	3		tr	1.49	100.91
102503	0.62				2.22			0.54	1.01	30	39	22	1		tr	1.83	98.21
103515	1.96							0.48	0.65	34	47	12	2			1.94	100.04
103517	1.93				3.18			0.37	0.62	45	24	19	2			1.12	97.22
103518	1.78							0.67	0.70	38	36	14	5			1.10	97.25
103520	0.56							0.47	0.81	25	43	23	4		tr	1.28	98.12
103522	0.73							0.27	0.76	25	41	24	4			1.88	97.63
103524	0.97							0.33	0.82	25	43	24	5			1.88	101.00
103525	2.17				0.87			0.38	0.84	27	38	24	5			2.12	100.38
111616A	1.59				0.96			0.47	0.70	40	31	13	6	5	tr	1.86	100.58
111618A	1.68				3.38			0.45	0.56	15	51	22		6	tr	0.94	101.01
111623A	1.29				0.19			0.28	0.60	29	51	11		6	tr	1.08	100.44
111628A	1.98							0.50	0.62	31	50	9		5	tr	1.63	99.73
113642A	5.17	9.18	2.79		3.46			0.35	0.55	17	43	20	1			2.34	104.34
113646A	1.61	8.58	0.33		1.61			0.71	0.61	34	36	11		1		2.64	97.69
mean	1.77				2.10			0.45	0.76	32	37	19	4	5		1.81	
Viking Formation																	
052211A	1.37				0.87			0.33	0.76	45	25	15	9		tr	1.21	98.54
111612A	0.90				1.54			0.45	0.66	33	37	19	5	3		0.36	100.91
111614A	0.73				1.06			0.19	0.75	30	36	21		8		0.78	98.51
113650A	0.95							0.47	0.50	40	48	4		5		2.03	100.95
mean	0.99				1.16			0.36	0.67	37	37	15	7	5		1.10	
Joli Fou Formation																	
052216A	0.79				1.45			0.26	0.64	35	41	13		6		0.55	98.69
052224A	0.97				1.16			0.19	0.71	26	45	18		6	tr	0.73	98.76

Table 9 (cont.)

Colorado Group mineralogy calculated from XRF data

Sample #	Pyr	Jar	Alu	Cal	Sid	Dol	Gyp	Apa	Ana	Qtz	I/S[1]	Kao	Ksp	Plg	Chl	TOC	Total
052232A	0.75				4.19	3.34		0.52	0.75	37	24	23	7	1		0.4	101.95
111606A	2.15	2.12			0.77			0.35	0.79	26	16	35	6			1.21	90.39
111610A	1.52				2.70			0.21	0.76	30	28	32	4			0.73	99.92
113651A	0.36							0.23	0.61	39	41	12	3	3		1.08	100.28
mean	1.09				2.05			0.29	0.71	32	33	22	5	4		0.78	
Mannville Group																	
111601A	0.17				1.93			0.24	1.42	39	18	33	6			2.08	101.84
111602A	0.15				0.96			0.24	1.05	48	18	28	5			1.47	102.87
052240A	0.34				18.13	3.61			0.89	30	24	22	4				102.97
mean	0.16				1.45			0.24	1.24	44	18	31	6			1.78	

Abbreviations: Pyr = pyrite, Jar = jarosite, Alu = alunite, Cal = calcite, Sid = siderite, Dol = dolomite, Gyp = gypsum, Apa = apatite, Ana = anatase, Qtz = quartz, I/S = mixed-layer illite/smectite, Kao = kaolinite, Ksp = K-feldspar, Plg = plagioclase feldspar, TOC = total organic carbon (from Rock-Eval)

Low totals indicate presence of some amorphous material, primarily iron oxides and hydroxides, but may also result from errors associated with clay mineral compositions, particularly I/S

[1]I/S includes trace amounts of muscovite, as determined by BSEM, and discrete illite, as determined from XRD characteristics

*contains Ca- zeolite, most likely heulandite or mordenite

**contains 15–20 wt% heulandite, not reflected in total

detrital clasts include argillaceous rock fragments (Plate 1e) and volcanic clasts (Plate 2a–c). Rare detrital grains are medium sand-sized (Plate 1d). The rock fabric is characterized as matrix supported (Plate 1b), but silt laminae may be framework supported (Plate 1c). Calculated mineral abundances are shown in Table 9.

Authigenic silicate minerals include quartz (Plate 2e), I/S (Plate 3a, b), kaolinite (Plate 3d–f), and glauconite (Plate 4a, b). Authigenic framboidal pyrite is ubiquitous (Plate 5a–f) but heterogeneously distributed (Plate 5a, b). The highest concentrations of pyrite are associated with organic-rich laminae. Pyrite occurs as framboids, zoned aggregates, and as pseudomorphs of feldspars, micas (Plate 5c), and bioclastic debris (Plate 5e). Siderite occurs dominantly as concretions up to 1 m thick. In bioturbated samples, authigenic siderite is abundant in the matrix (Plate 6a–f) and the fabric of the rock is noticeably homogeneous (Plate 2e). Minor authigenic calcite is also present (Plate 6d).

Feldspar dissolution is a common texture (Plates 2d, 6a) and much of the kaolinite occurs as pseudomorphic replacement of K-feldspar or plagioclase (Plate 3c–e). Plagioclase feldspar appears more susceptible to dissolution than K-feldspar (Plate 2d). Biotite and muscovite are also replaced by kaolinite (Plates 1b, 4b).

The total organic carbon (TOC) content averages 1.8 wt% (range 1.1–3.3 wt%) and is mainly terrestrially derived Type III OM (Fig. 4). The sulphur content averages about 0.9 wt% (range 0.2–3.0 wt%). The carbon/sulphur values vary from < 0.5 to ~8.5 with a mean of 2.7 (Table 3, Fig. 7). High TOC (3.0 wt%), sulphur abundances (3.0 wt%), and HI values (> 200 mgHC/gOC) occur near the base of the Westgate Formation in some cores (e.g., 10-25-65-20W5, 10-5-53-20W5).

Fish Scales Formation

The Fish Scales Formation is a finely laminated, non-calcareous claystone to mudstone, generally less than 20 m thick. In the central Foothills of Alberta the Fish Scales Formation contains a thin sandstone up to 3.5 m thick (Fish Scales Sandstone; Wall and Germundson, 1963) and capped with chert pebbles. In central Saskatchewan, the Fish Scales Formation is difficult to distinguish but may be recognized by the occurrence of a thin (< 5 cm), coarse grained sandstone or pebble layer, overlain by organic-rich shale. This coarse grained, basal layer contains bioclastic debris composed largely of phosphatic skeletal vertebrate remains, belemnites, and other phosphatized bioclastic debris. The base of this unit is typically sharp and may be overlain by parallel-laminated or ripple crosslaminated sandstone (Leckie et al., 1992). In southwestern Alberta, the Barons sandstone unconformably overlies the Fish Scales Formation and locally may remove Fish Scales shales westward toward outcrop in the Rocky Mountain Foothills. South of Township 25 and west of the 5th Meridian, the Fish Scales Formation, like the Westgate Formation, is not present.

The wireline expression of the contact between the Westgate Formation and the Fish Scales Formation (commonly referred to as the "Base of Fish Scales") is a sharp increase in the gamma-ray and resistivity responses and an abrupt, but lower magnitude decrease in sonic transit

Table 10

Bentonite mineralogy calculated from bulk XRF data

Sample	Depth (m)	Smc	Kao	Alb	Ano	Ksp	Qtz	Ill	Chl	Ann	Phg	Bte	Anl	Ana	Apa	Pyr	Jar	Sid	Cal	Total
063401A	693.7	55	23	4	2		2			2		tr		0.22	0.12	0.30		1		90
063401B	695.6	26	38	11	tr		4		4					0.37	0.40	3.30	3		1	91
063403A	705.9	29	53	2	1		3				2			0.34	0.28	2.21		1		94
063404B	711.2	47	31	3	2		4			tr		3		0.26	0.14	0.49				91
071401B	582.5	55	10	13			5					3		0.18	0.09	1.00		tr	2	89
103510	417.0	69		7	3		6				1	2		0.16	0.09	1.00				89
142909A*	2764.0	7	22	7	4		tr	52		3	tr			0.26	0.12					95
111203C	562.9	39	23	10	9		4					6		0.55	0.28	1.00				93
111204A	567.0	41	29	7	4		tr					7		0.32	0.13	3.00				91
112105B	1213.8	32	26	18	8		1					6		0.58	0.21	2.00				94
113632B	279.2	53		17	6		4					5		0.19	0.11	1.00				86
113633A	279.7	54		8	5		6					5	6	0.17	0.09	2.00				86
050105A	394.0	71	5	2	2	1	3		3					0.56	0.33	1.23		2		91
050106A	397.0	59	9	2	1		6					9		0.50	0.49	0.88		1		89
050108A	403.0	66		6	3	1	10					1		0.25	0.23	0.79		2		90
063413A	754.2	56		13	7		5			2	2			0.30	0.26	1.53		5		92
063413B	755.2	61		9	7		7		1	2	2			0.32	0.64	0.79		2		92
063413C	756.2	66		7	3		8		4		tr			0.14	0.09	0.36		2	tr	90
103511A	431.0	17	5				10				3	6		0.34	24.00	0.51		21	10	97
111210A	569.4	12	56		2		10			5		7		0.61	0.52					93
111213A	610.0	46	24	6	5		6			3				0.08	0.05					90
111213D	612.9	32	22	15		3	8					7		0.25	0.26	1.00		1	5	95
050110A	409.0	72	tr		2		11					1		0.15	0.09	0.73		2		89
063414A	767.0	57		10		2	4		1					0.15	0.14	0.75		13	2	90
103514C	446.0	18					19							0.20	43.69	4.19		3	5	93
SR01	na	54			2	3	20							0.17			6	3	3	88
061601A	974.3	45	3	15	3	5	8					10		0.21	0.19					89
112115A	1279.0	32	20	13	7	8	8					3		0.10	0.05			3		94
061810A	443.0	58		5	3	tr	7			3	1	1		0.25	0.09	0.39		12		89
062101A	863.0	49	4	1	6	5	18		6					0.31	0.26	tr		3		93
063424A#	816.0	26	9	3		1	3			0						0.17		49		91
103516A+	453.0	50		1	4	3	13		5					0.21	0.14	0.58		15		92

Smc = smectite, Kao = kaolinite, Alb = albite, Ano = anorthite, Ksp = K-feldspar, Qtz = quartz, Ill = illite, Chl = chlorite, Ann = annite, Phg = phlogopite, Bte = biotite, Anl = analcime, Ana = anatase, Apa = apatite, Pyr = pyrite, Jar = jarosite, Sid = siderite, Cal = calcite

*illite composition is $K_{.71}Mg_{.61}\ Al_{2.01}\ Si_{3.51}$ per 10 oxygens
#siderite composition is $Fe_{.87}Mg_{.12}Mn_{.01}\ CO_3$
+siderite composition is $Fe_{.85}Mg_{.13}Mn_{.02}CO_3$

time and formation density. Within the Fish Scales Formation, log responses are variable, reflecting a heterogeneous lithology that includes numerous bentonites, the presence of well developed Barons Sandstone lenses in southwestern Alberta, and variable organic-matter content.

Fish remains and algal cysts dominated by *Lanceolatta lancetopsis* are abundant. Bioturbation is sparse to nonexistent. Bentonites are common, range in thickness from < 1 to about 30 cm, and increase in abundance to the southwest. Some bentonites are graded and contain biotite and feldspar (sanidine?) crystals. Buff to black phosphatic beds up to 5 cm thick also may be present.

The silicate mineralogy of the Fish Scales Formation is similar to that of the Westgate Formation (Table 9) but the silt fraction is noticeably finer grained (Plate 7a–d). Silt grains larger than 20 µm are rare. The detrital silt-sized material is dominantly quartz with K-feldspar (Plate 7d), plagioclase feldspar (Plate 7c), micas and a suite of accessory minerals similar to that of the Westgate Formation. The silt- and sand-sized fractions are made up of quartz (29–60 wt%) and potassium feldspar (7–13 wt%). Clay minerals include I/S (8–20 wt %), kaolinite (4–20 wt%), and illite (4–12 wt %), with minor chlorite. Pyrite is more abundant than in the Westgate Formation (up to 6.2 wt%) and is dominantly framboidal in habit (Plate 7 e, f). Dolomite is common in abundances less than 5 wt%. Siderite is rare but, where present, contains detectable amounts of Mn (Plate 7c).

TOC values within the Fish Scales Formation average 3.2 wt% (range, 1.8–8.0 wt%) with HI values from approximately 50 to 440 mgHC/gOC. Low TOC and HI values (Fig. 4, 7) are generally restricted to the northwest (e.g., 5-1-77-20W5) but locally bioturbated zones also show lower HI values. The mean sulphur content is 2.2 wt% (range,1.0–3.4 wt%). Carbon/sulphur values vary from 0.8 to 2.0 with a mean of 1.5 (Fig. 7).

Belle Fourche Formation

The Belle Fourche Formation is a westward-thickening wedge of noncalcareous to slightly calcareous mudstone and siltstone. The minimum thickness is about 20 m in eastern Saskatchewan, and increases to over 150 m in the Foothills of northwestern Alberta. In southwestern Alberta, the Belle Fourche Formation is tabular, about 50 m thick, and contains intervals up to 10 m thick of well-developed, sharp-based lenses of Barons Sandstone. Near the 5th Meridian, south of Township 25, the Barons Sandstone unconformably overlies the Fish Scales Formation and in some places the Westgate Formation, indicating that the lowermost strata of the Belle Fourche Formation in this area may be erosionally truncated.

Where the Fish Scales Formation is present, its contact with the Belle Fourche is transitional and commonly contains numerous thin bentonites. The transition is indicated by the first occurrence of calcareous sediment, the presence of Inoceramids, or a noticeable increase in bioturbation. In some cases, no change in sediment composition or texture is observed and the basal Belle Fourche may only be differentiated from the underlying Fish Scales Formation by a change in organic matter type and abundance, or the occurrence of rare, agglutinated foraminifera (see below).

The wireline expression of this contact is manifested as an abrupt increase in sonic transit time and formation density. Resistivity and gamma-ray signatures are variable and may mimic those of the Fish Scales Formation. Within the Belle Fourche, the gamma-ray response generally declines upsection, and is accompanied by an increase in sonic velocity and formation density (see Bloch et al., 1993, fig. 8).

Bioturbation in most of the Belle Fourche is sparse to moderate, with *Planolites* and *Chondrites* the only observed traces. Siltstone beds are sharp based, erosive and may be graded. Parallel laminae and combined-flow ripples are common.

In the western Interior Plains (e.g., 5-9-72-8W6), coarsening-upward cycles up to 20 m thick, comprising coarse silt to medium sand, are present in the middle and upper sections of the Belle Fourche Formation. These cycles thicken to the west-northwest and contain abundant sideritic concretionary horizons. Bioturbation within these cycles varies from moderate to intense, and *Gordia*, *Helminthopsis*, *Teichichnus*, *Planolites*, and *Chondrites* are present. In comparison, to the south and east, the equivalent of this cyclic interval consists of thin (< 5 cm), erosive and sharp-based sand or silt beds. Beds composed of bioclastic macrofossil debris also are present.

The mineralogy of the Belle Fourche Formation is similar to that of the Westgate Formation (Table 9) but minor amounts of dolomite may be present, particularly in the upper part of the section. Quartz (28–74 wt%) and potassium feldspar (1–11 wt%) are the major silt-sized mineral constituents and the silt fraction is noticeably coarser than that of the underlying Fish Scales Formation (Plate 8a, b, d, e). The clay minerals are dominantly kaolinite (7–40 wt%) and I/S (3-17 wt%). Siderite averages 2.4 wt% (range 0–4.5 wt%). Pyrite occurs as framboids and aggregates in abundances from < 0.1 to 5.9 wt%. Calcareous bioclasts are more common in the upper Belle Fourche (Plate 8c, f). Large, detrital micas are locally common (Plate 8a, b, d, e). Authigenic minerals include pyrite, siderite, and kaolinite (Plate 8c, e).

Belle Fourche TOC abundances average 1.7 wt% (range, 0.4–2.7 wt%) with relatively low HI values (m=104 mgHC/gOC). The sulphur content is from < 0.1 to 3.2 wt%, averaging 1.2 wt%; carbon/sulphur values are variable (~1–27; mean = 5.5) and poorly correlated (Fig. 7). This reflects the wide range of mixing of Types II and III OM and the extremely variable sulfur content (expressed as pyrite and sulfate minerals in Table 9) within the Belle Fourche Formation (Fig. 4).

Second White Specks Formation

The Second White Specks Formation is a limestone to marlstone in Saskatchewan, a calcareous claystone to siltstone in eastern and southern Alberta, and grades to a calcareous siltstone in northwest Alberta. This unit thickens from about 25 m at the Saskatchewan–Manitoba boundary (Williams and Bayliss, 1988) to over 90 m in the Peace River Arch area of northwestern Alberta (Stelck and Wall, 1954). The thickness of the Second White Specks Formation (SWS) is generally less than 20 m in southern Alberta, but reaches up to 55 m in southeast Alberta. The base of the Second White Specks is generally distinct and defined by an abrupt change to a very calcareous matrix. This change in lithology is typically marked by a bed of coarse bioclastic, calcareous debris 1 to 5 cm thick (Plate 9e). A bentonite bed up to 20 cm thick is typically associated with this basal bioclastic bed over much of Alberta. A calcite concretionary layer up to 30 cm thick commonly occurs in association with the bentonite.

On wireline logs, the contact between the Belle Fourche and the Second White Specks formations is expressed by an increase in resistivity and radioactivity. The gamma ray response is more variable compared to that of the Belle Fourche Formation, reflecting the greater number of bentonites. The upper contact of the Second White Specks Formation is characterized by a decrease in resistivity and sonic velocity. The overlying, noncalcareous shale also has a more uniform gamma-ray response.

Bioturbation is absent to sparse and sediments are well laminated. In the west and northwest of the study area, siltstone beds contain parallel laminae and rare, current or combined-flow ripples. The Second White Specks Formation is distinctively fissile in core and weathers to a blocky, silvery grey in outcrop. Calcite concretions up to 20 cm thick are common and generally disk shaped. The speckled nature of this unit is due to the abundance of millimetre- (or smaller) sized fecal pellets composed of calcareous coccolithic debris (Plate 9c). Other bioclasts include benthic and planktonic foraminifers (Plate 9b), pelecypod fragments, fish scales and bones (Plate 9d), ammonites, whole shells, shell fragments, Inoceramid prisms (Plate 9d, e), and algal cysts. Inoceramid debris is particularly abundant in the Second White Specks Formation. The calcareous nature of this formation is due mainly to the abundance of this bioclastic material.

The mineralogy of the Second White Specks Formation is markedly different than that of the underlying shales (Table 9) because of the variable, dominantly bioclastic, carbonate content (0–88 wt%). In addition, dolomite (1.5–6.3 wt%) and framboidal pyrite (0.0–7.0 wt%) are relatively abundant. Pyrite occurs almost exclusively as disseminated framboids (Plate 9a, b). Siderite is rare. The silicate mineralogy includes quartz (2–52 wt%), I/S (5–48 wt%), kaolinite (2–25 wt%), potassium feldspar (0–5 wt%), and plagioclase (< 3 wt%), with minor to trace amounts of biotite, muscovite, and chlorite (Plate 9f, Table 6). Clay-sized quartz is abundant (Plate 9f). Authigenic kaolinite fills foraminiferal tests (Plate 9b) and trace amounts of glauconite may be present. Authigenic jarosite, gypsum, and anhydrite occur as cement in horizontal microfractures (Plate 9a), locally constituting up to about 13 wt%.

The mean TOC content is 5.1 wt% (range, 2–12 wt%) with HI values generally greater than 200 mgHC/gOC (Fig. 3, 10). Second White Specks Formation samples with low TOC and HI values (2–4 wt% TOC and HI < 300 mgHC/gOC) are commonly found in northwestern Alberta. The sulphur content averages 2.7 wt% (range, 0.8–4.5 wt%) and shows a crude correlation with TOC content (Fig. 7). Carbon/sulphur values vary from ~0.5 to 2.2 with a mean of 2.2.

STRATIGRAPHY AND AGE

Stratigraphic correlations and the relative ages of the studied formations are determined primarily by foraminiferal assemblages (Fig. 18, 19, Appendix B). Dinoflagellate assemblages are also utilized, particularly where sediments are barren of foraminifers. In latest Cenomanian- to Turonian-aged formations, coccoliths may also provide useful stratigraphic information. As previously indicated, foraminiferal biostratigraphy is well developed for the Cretaceous of the WCSB and the studied interval contains three foraminiferal zones. The Upper Albian *Miliammina manitobensis* Zone is present in the Westgate Formation. A detailed biostratigraphic correlation of this zone is provided by Stelck (1975). The Fish Scales Formation is barren of foraminifers and the determination of a Cenomanian age for this formation relies on the dinoflagellate assemblage (Singh 1983; Bloch et al., 1993) and its stratigraphic position (Leckie et al., 1992).

The *Verneuilinoides perplexus* Zone, of middle to Late Cenomanian age, is present in the Belle Fourche Formation. The *Hedbergella loetterlei* Zone occurs in the Second White Specks Formation, deposited during latest Cenomanian to

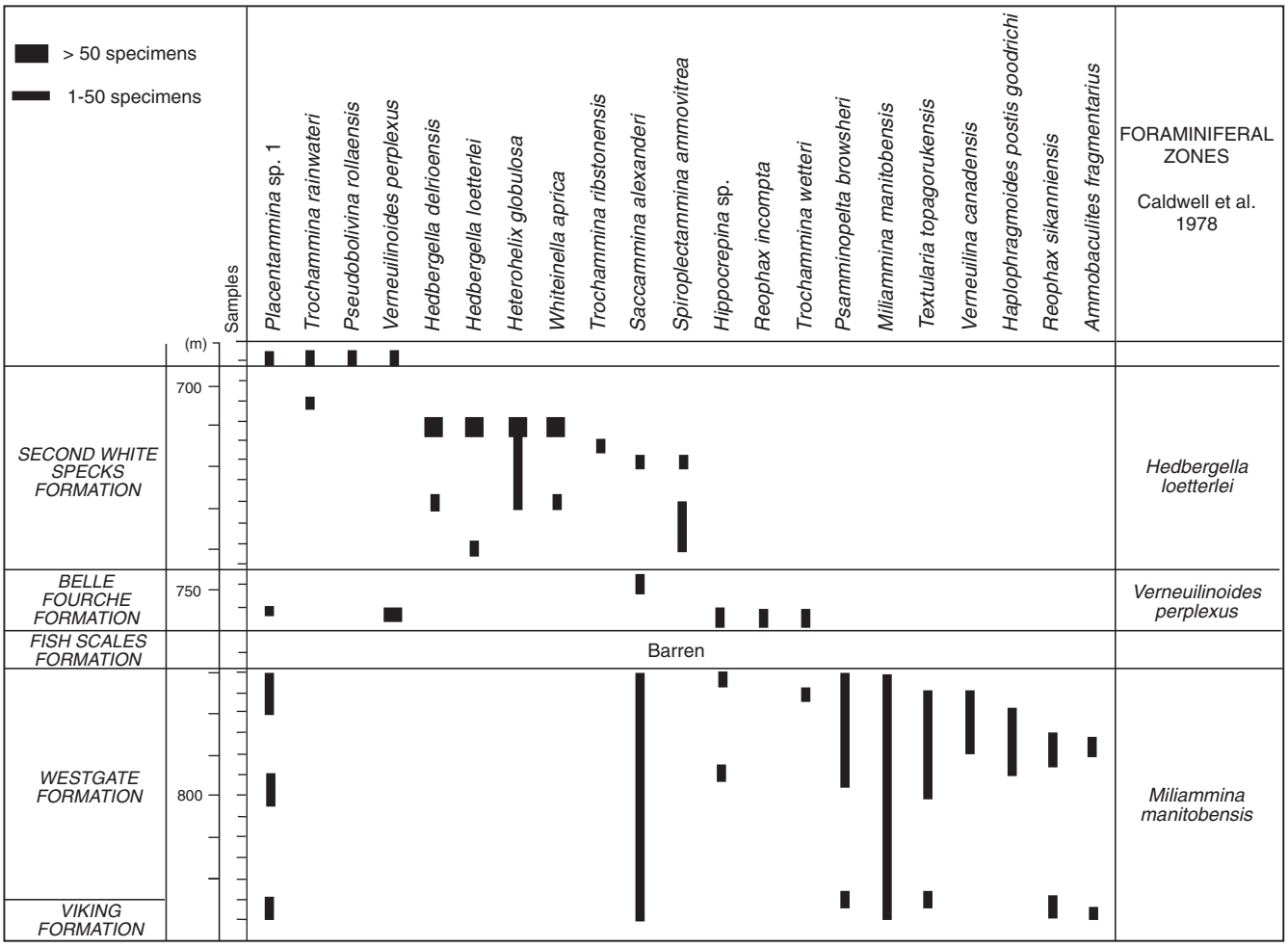

Figure 18. *Biostratigraphic ranges of foraminiferal species with common occurrences at 6-34-30-8W4 in southeastern Alberta. Primitive agglutinated taxa such as* ***Placentammina*** *sp. 1 and* ***Saccammina alexanderi*** *range through several formations, but disappear in the Fish Scales Formation. The assemblage contains numerous rare species not shown in this figure (see Appendix B).*

Middle Turonian time. In eastern Saskatchewan, this zone is divided into the *Clavihedbergella simplex* and *Whiteinella aprica* subzones. The base of the *C. simplex* Subzone is placed in the Upper Cenomanian, based on bivalve occurrences (McNeil and Caldwell, 1981), whereas Caldwell et al. (1978) originally had placed it in the Lower Turonian.

Absolute ages for the formations are derived from radiometric age data, primarily sanidine Ar^{40}/Ar^{39} ages, of Obradovich (1991), Cobban et al. (1994) and Kowallis et al. (1995) (Fig. 20). These data have been used to calibrate the macrofossil zones of the Western Interior (Cobban and Reeside, 1962) and provide a direct correlation to the foraminiferal zonations of Western Canada (Caldwell et al., 1978). The presence of *Collignoniceras woollgari* (Mantell) at 14-29-11-28W4 (2508.8m) supports a Middle Turonian age for upper Second White Specks Formation (R. Hall, pers. comm.). Sanidine (K-feldspar) is noticeably absent from sampled bentonites in lower Colorado group shales (Table 10). This fact has to date prevented accurate age determinations from these shales.

The status of the Albian–Cenomanian boundary is confused. Recently, the *Neogastroplites* fauna has been moved from the latest Albian to the earliest Cenomanian (Cobban and Kennedy, 1989; Obradovich, 1993; Cobban et al., 1994) which makes the age of the boundary considerably older (Fig. 20). However, in Canada near Fort St. John, the entire *Neogastroplites* fauna, with the exception of the uppermost ammonite zone *N. maclearni*, is found in sediments that contain the assemblages of the *Milliammina manitobensis* zone (Wall, 1967; Warren and Stelck, 1969), long recognized as latest Albian in age. At the same location, the Albian–Cenomanian boundary, which has been defined as the base of the Fish Scales Formation, falls between occurrences of *N. maclearni* (Reeside and Cobban) and *N. americanus* (Reeside and Weymouth) (Stelck and

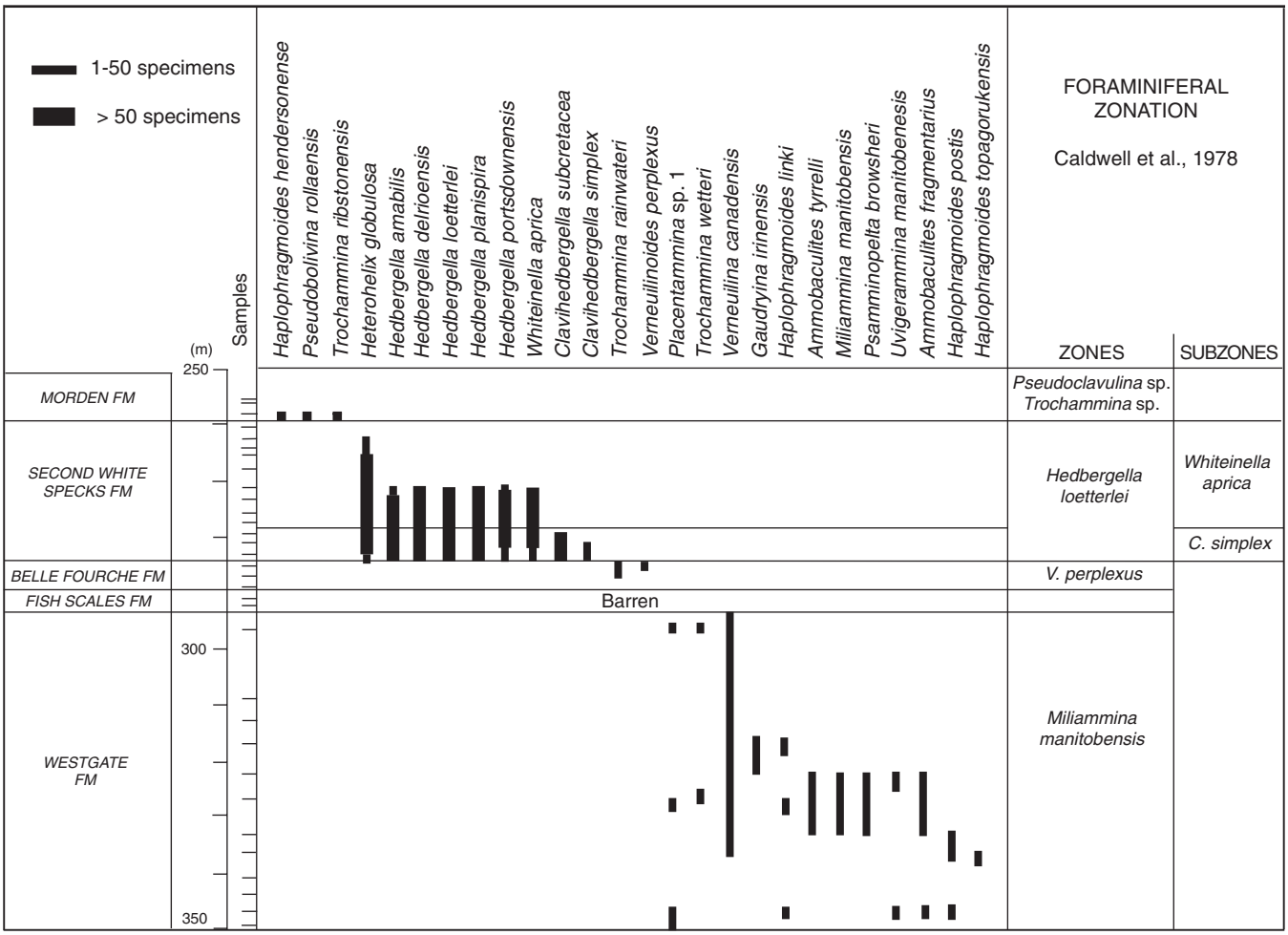

Figure 19. *Biostratigraphic ranges of foraminiferal species with common occurrences at 11-36-22-1W2 in eastern Saskatchewan. All species of the Upper Albian Westgate Formation disappear at the contact with the Fish Scales Formation. All planktic species except* ***Heterohelix globulosa*** *disappear in the middle of the Second White Specks Formation, showing that the biofacies boundary is not coincident with the lithofacies boundary. This is the only location where the* ***Clavihedbergella simplex*** *Subzone could be recognized. The assemblage contains numerous rare species not shown in this figure (see Appendix B).*

Armstrong, 1981). Herein, we consider the position of *N. maclearni* to be of earliest Cenomanian age, which leaves the remaining Neogastroplites species in the latest Albian (see also discussion by Leckie et al., 1992).

Westgate Formation

The foraminiferal assemblage of the Westgate Formation consists of agglutinated taxa (Fig. 18, 19). Total abundance of specimens and species diversity vary significantly throughout the formation and between wells (Fig. 21, Appendix B). Faunal preservation is moderate, and includes a high percentage of severely deformed specimens, which allows, in many cases, identification only on a generic level. The assemblage contains common species such as *Bathysiphon brosgei* Tappan, *Saccammina alexanderi* (Loeblich and Tappan), *Placentammina* sp., *Miliammina manitobensis* Wickenden, *Psamminopelta bowsheri* Tappan, *Reophax tundraensis* Chamney, *Reophax minuta* Tappan, *Reophax sikanniensis* Stelck, *Haplophragmoides postis goodrichi* Sutherland and Stelck, *Haplophragmoides gilberti* Eicher, *Haplophragmoides linki* Nauss, *Haplophragmoides hendersonense* Stelck and Wall, *Ammobaculites fragmentarius* Cushman, *Verneuilina canadensis* Cushman, *Verneuilinoides borealis* Tappan, *Gaudryina irenensis* Stelck and Wall, *Textularia topagorukensis* Tappan, *Trochammina rutherfordi* Stelck and Wall, and *Trochammina* spp. (Plate 10). This species composition is typical for the *Miliammina manitobensis* Zone of Late Albian age (Caldwell et al., 1978). In the Rocky Mountain Foothills of northeastern British Columbia, this zone is divided into three subzones of which only the lowest, the *Verneuilina canadensis* Subzone, can be recognized

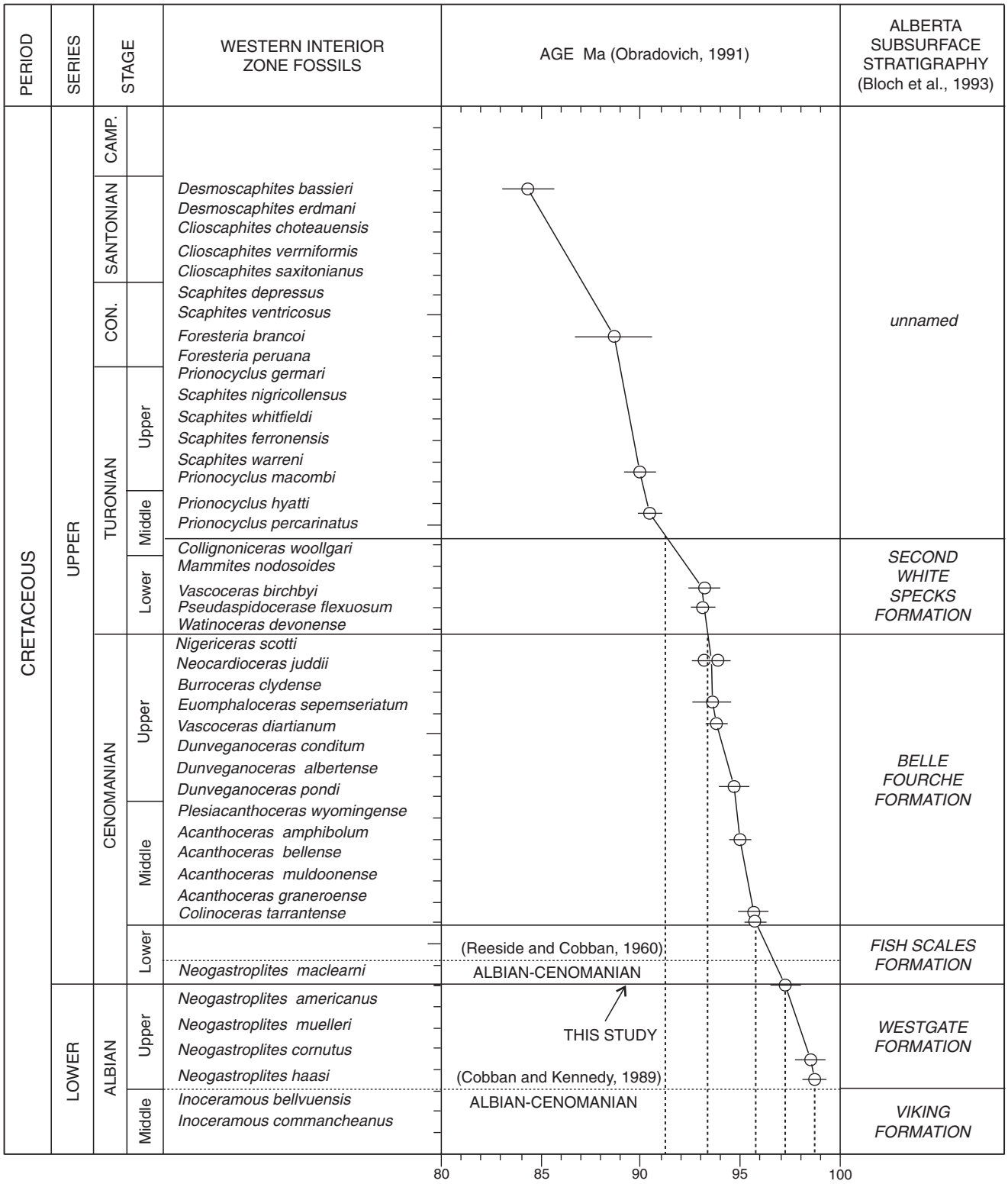

Figure 20. *Macrofossil zones of the Western Interior and $^{40}Ar/^{39}Ar$ ages (modified from Obradovich, 1991) showing the estimated ages of the lower Colorado Group formations. Estimated ages for the Cenomanian-Turonian boundary range from 93.3±0.2 (Obradovich, 1993) to 93.1±0.3 Ma (Kowallis et al., 1995). Refer to text for the assignment of the Albian-Cenomanian boundary.*

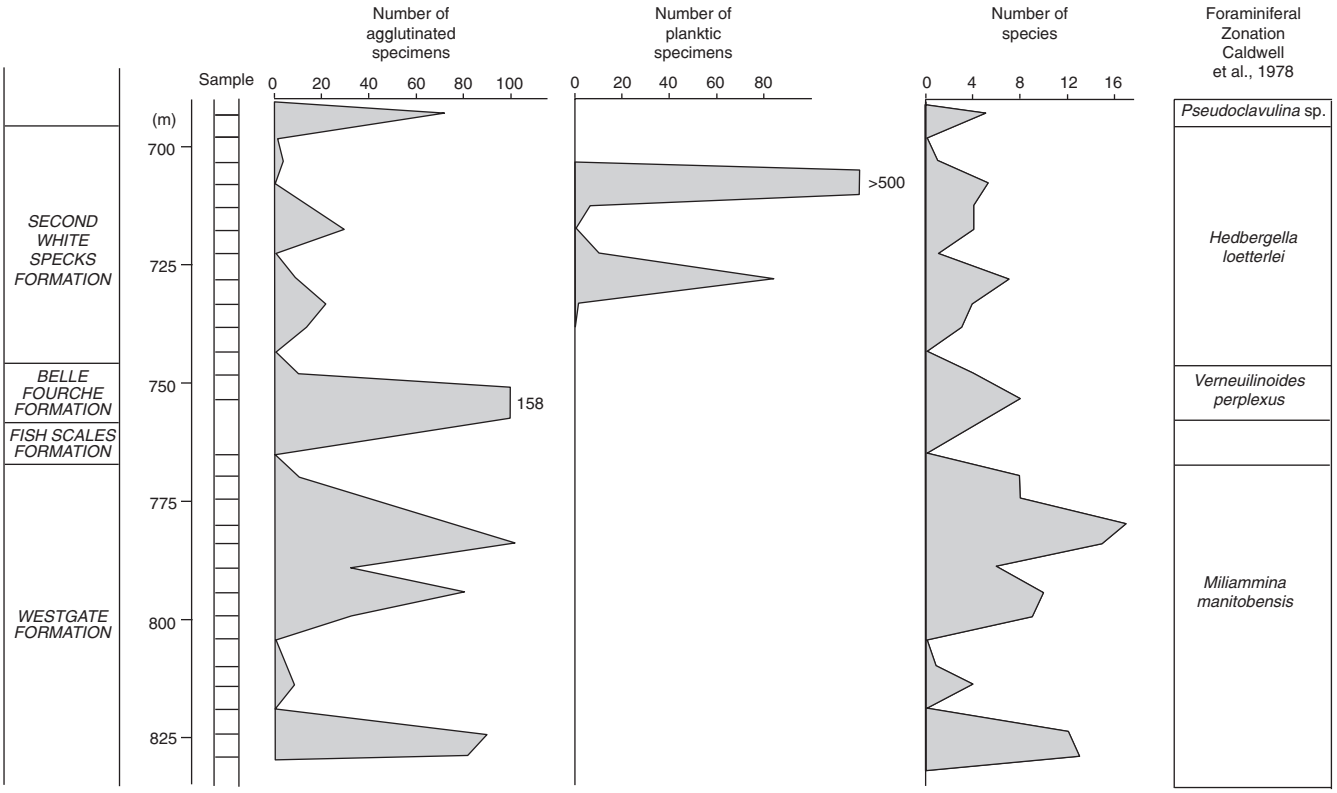

Figure 21. *Total number of agglutinated and planktic foraminiferal specimens and number of species per sample at 6-34-30-8W4. Note that agglutinated foraminifera persist throughout the Second White Specks Formation at this locality.*

across the plains of Alberta and Saskatchewan (Caldwell et al., 1978). In the studied sections of the Westgate Formation, no distinct faunal change is observed that would imply a regionally valid subzonation. All foraminifers disappear at the top of the Westgate Formation.

Dinoflagellate assemblages of the Westgate Formation are similar to those described by Brideaux (1971) and Singh (1971) from the correlative lower Shaftesbury Formation. Although assemblages of dinoflagellates are typically rich and varied in the Westgate, the abundance of species and specimens varies considerably. Preservation is excellent in eastern Alberta but is poor to the west, especially in Foothills sections, where increased thermal alteration causes problems in identification. Species that occur commonly in the Late Albian Westgate Formation are *Luxadinium propatulum* Brideaux and McIntyre, *Chichaouadinium vestitum* (Brideaux) Bujak and Davies, *Ovoidinium verrucosum* (Cookson and Hughes) Davey, *Cribroperidinium intricatum* Davey, *Oligosphaeridium totum* Brideaux, *Pseudoceratium expolitum* Brideaux, *Florentinia cooksoniae* (Singh) Duxbury, *Fromea fragilis* (Cookson and Eisenack) Stover and Evitt, and *Palaeoperidinium cretaceum* Pocock emend Davey (Fig. 22, 23). The above species also occur in the Cenomanian. *Luxadinium propatulum* and *Ovoidinium verrucosum* first appear in the Late Albian whereas the others have earlier first appearances. Other species in the Westgate Formation having Late Albian first appearances are *Catastomocystis spinosa* Singh, *Ascostomocystis gigantea* Singh, *Florentinia verdieri* Singh, *Bourkidinium psilatum* Singh and *Ginginodinium evittii* Singh. The following species last appear in the Westgate: *Discorsia nanna* (Davey) Duxbury, *Microdinium opacum* Brideaux, *Protoellipsodinium spinocristatum* Davey and Verdier, *Senoniasphaera microreticulata* Brideaux and McIntyre, *Wigginsiella grandstandica* Lucas-Clark (Fig. 22). At present, a zonal scheme for dinoflagellates within the Westgate Formation cannot be determined because of the absence of distinct floral changes.

Fish Scales Formation

The Fish Scales Formation and equivalent strata are barren of foraminifers (Fig. 18, 19). Stratigraphic correlations and age must rely on dinoflagellate assemblages and stratigraphic position. No new dinoflagellate species typify the Fish Scales Formation in the study area since most species range from the Late Albian into the Cenomanian. The Fish Scales Formation assemblage is diverse, but is strongly dominated by *Ovoidinium verrucosum*, *Pseudoceratium expolitum*, *Cribroperidinium intricatum*, and *Cyclonephelium vannophorum*.

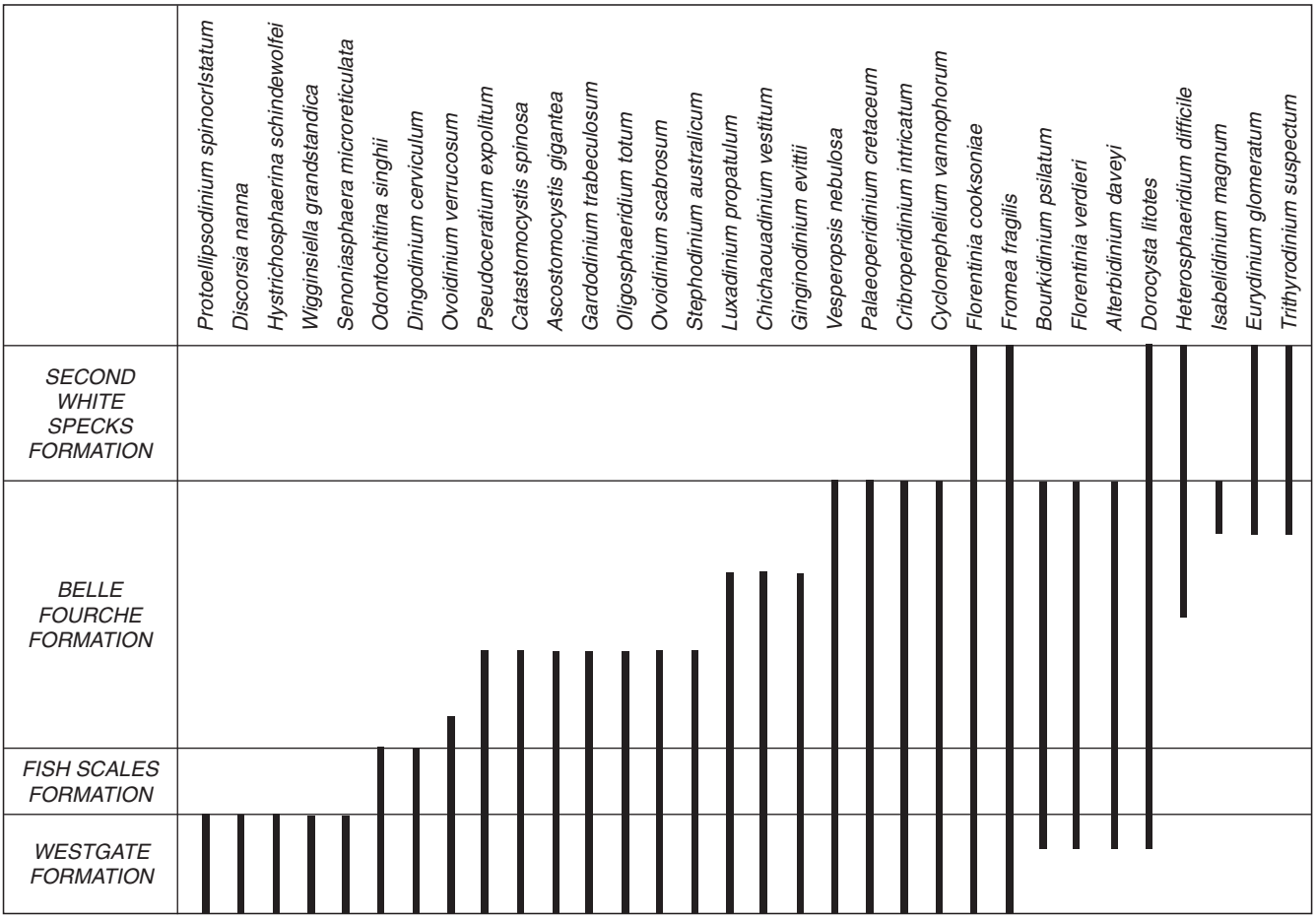

Figure 22. *Dinoflagellate ranges in southwestern Alberta.*

The Early Cenomanian age of the Fish Scales Formation is based on dinoflagellates from assemblages in northern Alberta, where a distinct floral change is observed between the Westgate and Fish Scales formations (Singh, 1983; Leckie et al., 1992). The transition to the overlying Belle Fourche Formation is gradational and is marked by the appearance of rare, agglutinated foraminifers of Late Cenomanian affinity.

Belle Fourche Formation

Rare to common agglutinated foraminiferal species of low diversity mark the Belle Fourche Formation. In central Alberta and Saskatchewan, Cenomanian foraminiferal assemblages are poorly developed (Fig. 18, 19). The zonal marker species, *Verneuilinoides perplexus* (Loeblich) (Plate 11), is dominant and relates the Belle Fourche Formation to the *V. perplexus* Zone of Middle Cenomanian age (McNeil and Caldwell, 1981). Taxa such as *Trochammina rainwateri* Cushman and Applin, *Haplophragmoides* Cushman, *Reophax* de Montfort, *Placentammina* Thalmann, *Uvigerammina* Majzon, *Verneuilina* d'Orbigny, *Saccammina* Sars, and *Hippocrepina* Parker complement the assemblage.

The dinoflagellate floras of the lower part of the Belle Fourche Formation are generally similar to those of the Fish Scales and Westgate formations. A few species are abundant in this interval, and assemblage compositions are similar. Species which may last appear in the Belle Fourche Formation (Fig. 22, 23) are *Luxadinium propatulum*, *Chichaouadinium vestitum*, *Ginginodinium evittii*, *Cribroperidinium intricatum*, *Pseudoceratium expolitum*, *Dingodinium cerviculum* Cookson and Eisenack, *Gardodinium trabeculosum* (Gocht) Alberti, *Oligosphaeridium totum*, and *Odontochitina singhii*. However, in section 10-35-45-2W4, some of these species last appear in the Westgate Formation (Fig. 23). Species which range up through the Belle Fourche are *Fromea fragilis*, *Cyclonephelium vannophorum*, *Palaeoperidinium cretaceum*, and *Florentinia cooksoniae*. The upper limit of the range of *Ovoidinium verrucosum* is apparently near the base of the Belle Fourche in some sections but in others its last occurrence is in the Fish Scales Formation. *Ovoidinium scabrosum* (Cookson and Hughes) Davey also has its last

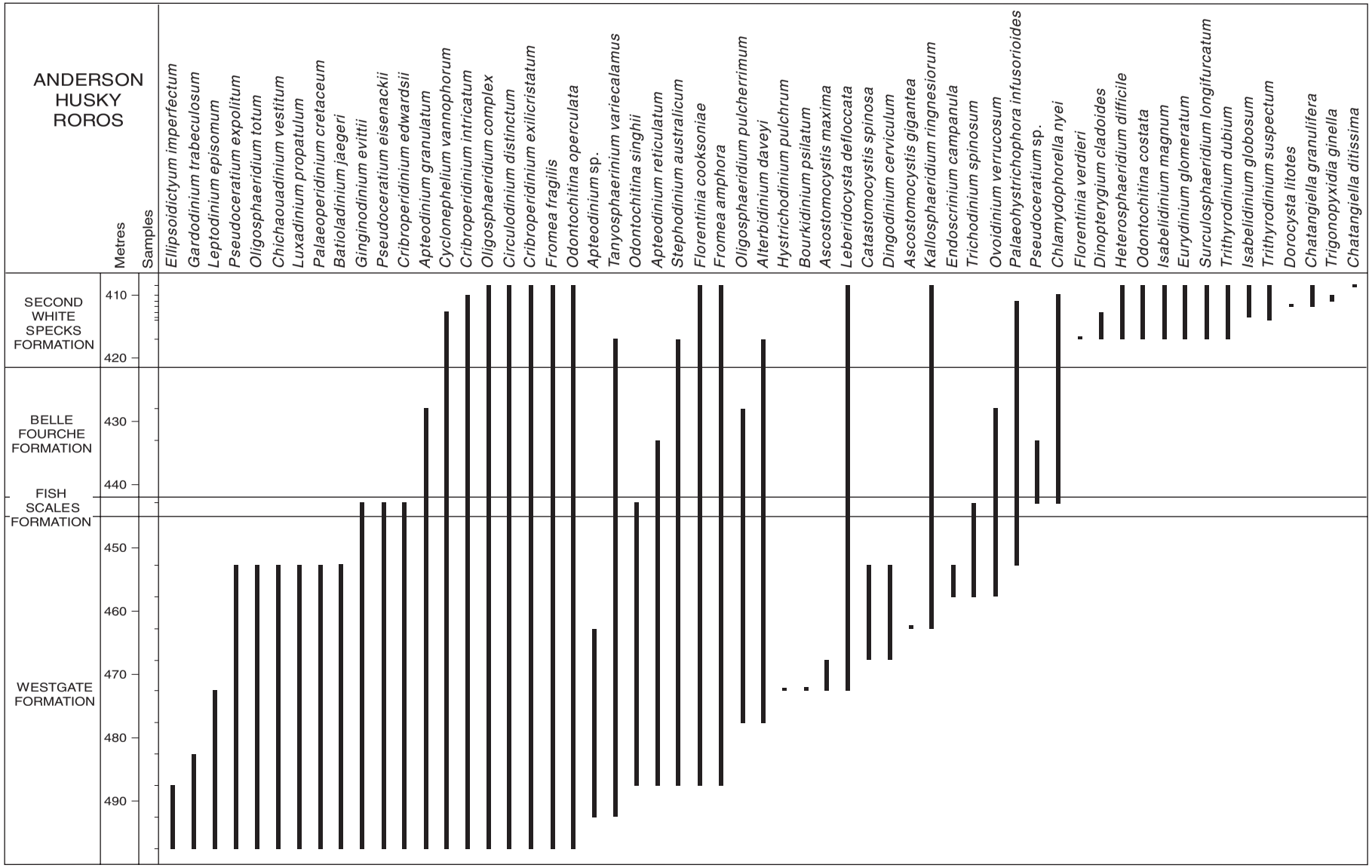

Figure 23. *Dinoflagellate ranges determined from well 10-35-45-2W4, Anderson Husky Roros.*

occurrence in the Belle Fourche. Other species present in the Belle Fourche, and which first appear in the upper part of the Westgate Formation, are *Ascostomocystis gigantea*, *Catastomocystis spinosa*, *Bourkidinium psilatum*, *Florentinia verdieri*, *Stephodinium australicum* Cookson and Eisenack, and *Alterbidinium daveyi* (Stover and Evitt) Lentin and Williams.

The dinoflagellate assemblages are similar to those described by Singh (1983) and indicate an Early Cenomanian age for the lower part of the Belle Fourche Formation. The diversity of assemblages varies considerably between samples and some contain very few species and specimens. The upper part of the Belle Fourche Formation is marked by the first appearance of *Isabelidinium magnum* (Davey) Stover and Evitt and *Eurydinium glomeratum* (Davey) Stover and Evitt, which are commonly abundant in the interval. Upper Cretaceous species with their first occurrence in the upper Belle Fourche include *Trithyrodinium suspectum* (Manum and Cookson) Davey and *Heterosphaeridium difficile* (Manum and Cookson) Ioannides. However, these species are rare. The assemblage in the upper part of the Belle Fourche indicates a Late Cenomanian age.

Second White Specks Formation

The foraminiferal fauna of the Second White Specks is characterized by the appearance of planktonic species. Compositional differences are observed between locations. At 6-34-30-8W4 (Fig. 21) the assemblage is entirely pelagic in nature, containing abundant planktonic foraminifers (over 1000 specimens/sample) of low diversity. At this location, however, faunal changes at the boundary between the Belle Fourche and Second White Specks formations cannot be recorded because of missing core. Typical species such as *Hedbergella loetterlei* Nauss, *Hedbergella amabilis* Loeblich and Tappan, *Hedbergella delrioensis* (Carsey), *Hedbergella portsdownensis* (Williams-Mitchell), *Whiteinella aprica* (Loeblich and Tappan), and *Heterohelix globulosa* (Ehrenberg) are constituents of the *Whiteinella aprica* Subzone which forms the upper part of the *H. loetterlei* Zone (Plate 12). Caldwell et al. (1978) have assigned an Early Turonian age to the *W. aprica* Subzone, whereas McNeil and Caldwell (1981) extend the age to early Middle Turonian.

At 6-18-45-1W4 (Fig. 24) the faunal assemblage of Second White Specks Formation is characterized by a two-fold subdivision. The lower interval contains a mixed

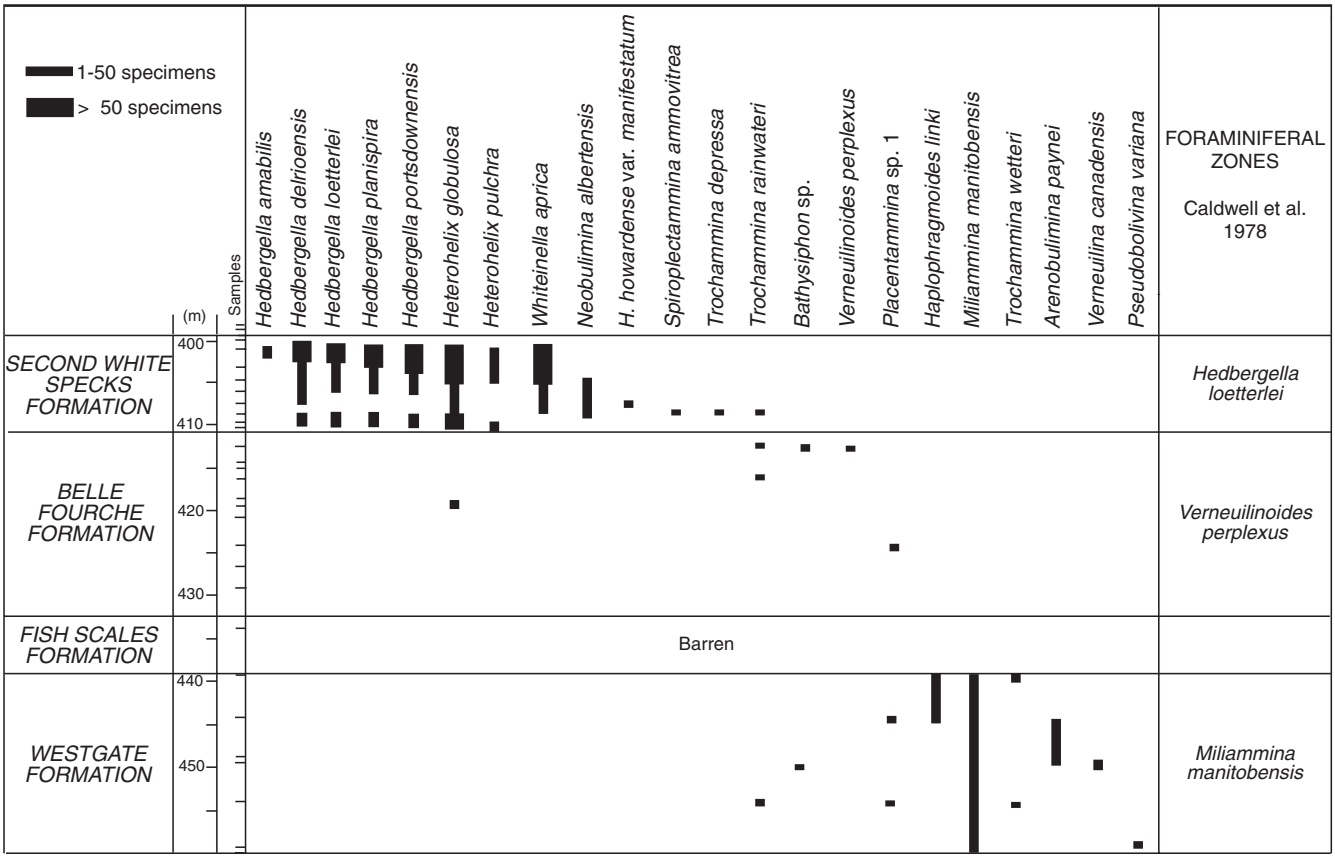

Figure 24. *Biostratigraphic ranges of selected foraminiferal species at 6-18-45-1W4 in eastern Alberta. A transitional zone in the lower Second White Specks Formation is indicated by the occurrence of the calcareous species* ***Neobulimina albertensis*** *and short ranges of several agglutinated species.*

assemblage of agglutinated and calcareous benthic and planktonic taxa and forms a transition to the fully pelagic *W. aprica* Subzone. Subzonal marker species such as *Clavihedbergella simplex* (Morrow) typical for Saskatchewan (North and Caldwell, 1975) and Manitoba (McNeil and Caldwell, 1981), or *Haplophragmoides spiritense* Stelck and Wall, characteristic for the Peace River District (Stelck and Wall, 1954), do not occur. However, the mixed nature of the assemblage and the occurrence of *Neobulimina albertensis* (Stelck and Wall) suggest a time equivalent interval in southeast Alberta of Late Cenomanian/ Early Turonian age. This subzone cannot be identified at 10-35-45-2W4 because of missing core. The upper pelagic assemblage belongs to the *W. aprica* Subzone.

At 6-34-30-8W4 (Fig. 18) the transition between the agglutinated fauna and the pelagic fauna is gradual, as at 6-18-45-1W4. Agglutinated specimens are poorly preserved and are assigned to *Spiroplectammina phauloides*, *Ammomarginulina*, *Ammobaculites*, *Textularia*, and other ataxophragmiids. No calcareous benthic species were found. Planktonic foraminifera are not as abundant as at the other locations (Fig. 25), but suggest the presence of the *W. aprica* Subzone. In this anomalously thick section of the Second White Specks Formation, a two-fold foraminiferal zonation connected with a more definitive time frame cannot be identified. Therefore, the Cenomanian/Turonian boundary is drawn at the first occurrence of planktonic foraminifers and coccoliths (see below). Certain faunal characteristics may have been obscured or missed completely because of the larger sample interval at this location.

The dinoflagellate assemblages of the Second White Specks Formation have many similarities to those of the underlying Belle Fourche Formation (Fig. 22, 23), including a dominance of *Eurydinium glomeratum* and *Isabelidinium magnum*. In the Second White Specks Formation, *Trithyrodinium suspectum* and *Heterosphaeridium difficile*, which are rare in the Belle Fourche, locally become abundant. Other species that continue into the Second White Specks from the Belle Fourche are *Cyconephelium vannophorum*, *Fromea fragilis*, *Florentinia cooksoniae*, *Palaeohystrichophora infusorioides* Deflandre, and *Catastomocystis spinosa*.

Some important Upper Cretaceous species make their first appearances in the Second White Specks Formation. These include *Chatangiella granulifera* (Manum) Lentin and Williams, *Chatangiella ditissima* (McIntyre) Lentin and Williams, *Isabelidinium cooksoniae* (Alberti) Lentin and Williams, and *Isabelidinium globosum* (Davey) Lentin and Williams. The dinoflagellate assemblages indicate a

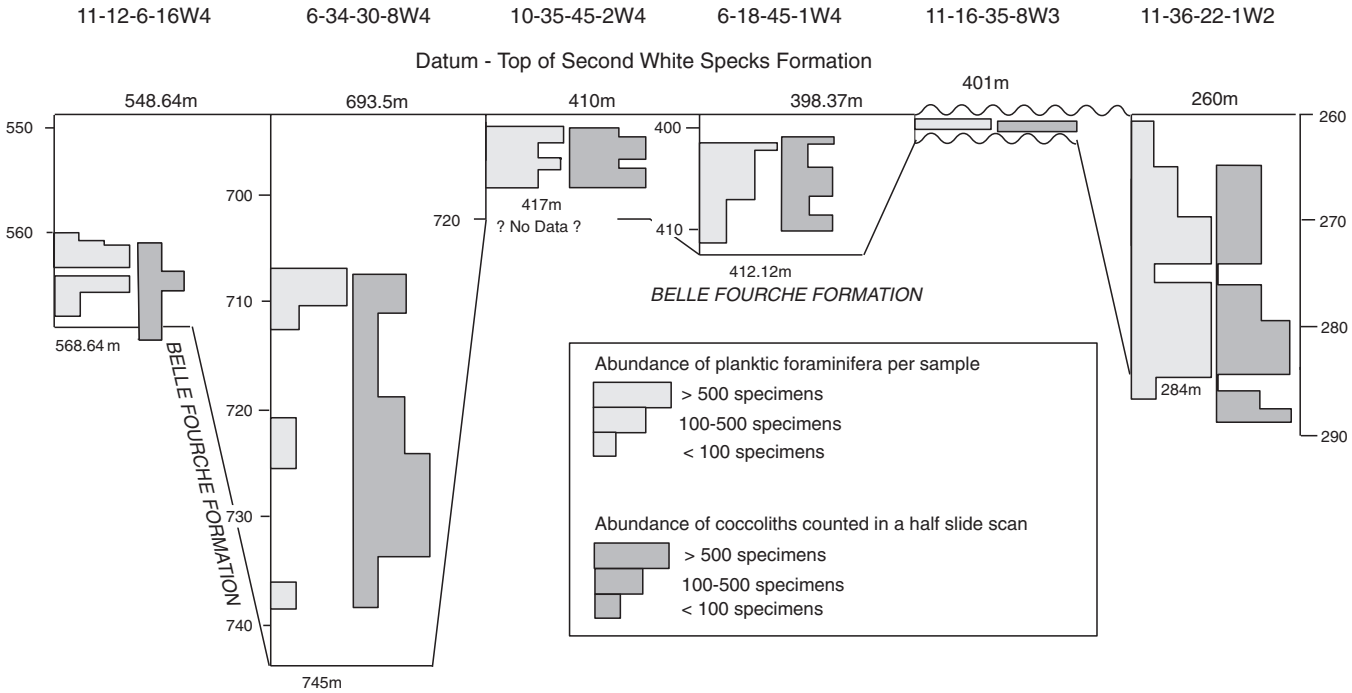

Figure 25. *Relative abundance of planktic foraminifera and coccoliths in the Second White Specks Formation in a SW/E profile. At 11-12-6-16W4 and 11-36-22-1W2 coccoliths migrated into the region before planktic foraminifers. In central Saskatchewan, at 11-16-35-8W3, the Second White Specks Formation is represented by a thin interval because of unconformities at the top and at the base. It is directly overlain by the Santonian First Speckled Shale and underlain by the Belle Fourche Formation. The* ***Whiteinella aprica*** *Subzone is present whereas the* ***Clavihedbergella simplex*** *Subzone is missing.*

Turonian age for the Second White Specks Formation. Abundant amorphous organic detritus, presumably of algal origin, is also present.

Generally, nannofossils first appear in the Second White Specks Formation (Dawson, 1874). Exceptions to this have been observed in eastern Saskatchewan (11-36-22-1W2) and south-central Alberta (11-12-6-16W4; see Fig. 25). Coccoliths occur as individual clasts or more commonly as aggregates in the remains of copepod fecal pellets (McNeil, 1984; Houghton, 1991) and give the Second White Specks its characteristic feature – calcareous white "specks" that are visually striking in comparison to the adjacent noncalcareous shales. Coccolith preservation is moderate to good. The assemblage (see Plate 13 and Appendix C) is dominanted by long-ranging forms such as *Arkhangelskiella cymbiformis Vekshina*, *Ahmuellerella octoradiata* (Gorka), *Biscutum constans* (Gorka), *Broinsonia bevieri* Bukry, *Cretarhabdus conicus* Bramlette and Martini, *Cretarhabdus surirellus* (Deflandre), *Cribrosphaerella ehrenbergii* (Arkhangelsky), *Eiffellithus eximus* (Stover), *Eiffellithus turriseiffeli* (Deflandre), *Predicosphaera cretacea* (Arkhangelsky), *Predicosphaera spinosa* (Bramlette and Martini), *Staurolithites crux* (Deflandre and Fert), *Stephanolithion laffittei* Noel, *Vagalapilla matalosa* (Stover), *Watznaueria barnesae* (Black), *Zygodiscus acanthus* (Reinhardt), *Zygodiscus diplogrammus* (Deflandre in Deflandre and Fert), and *Zygodiscus elegans* Gartner (Thierstein, 1976; Smith, 1981, and references therein).

The assemblage also includes *Corollithion exiguum* Stradner, *Cylindralithus coronatus* Bukry, *Kamptnerius punctatus* Stradner, *Lithastrinus grilli* Stradner, *Microrhabdulus decoratus* Deflandre, *Micula decussata* Vekshina, *Micula staurophora* (Gardet), and *Zygodiscus compactus* Bukry, which have their first appearance in the Turonian. No nannofossil zonal scheme is proposed at this time for the WCSB and therefore stratigraphic correlations must rely on foraminiferal assemblages.

Sedimentation rates

Minimum and maximum compacted sedimentation rates, based on observed thicknesses and radiometric dates (Obradovich, 1991), are shown in Table 11. These rates are generalized and do not take into account periods of either nondeposition or erosion. Reconnaissance observations suggest tectonic thickening in the Rocky Mountain Foothills and the maximum observed thicknesses are likely exaggerated. Sedimentation rates are generally low, with maximum rates ranging from 2 to 6 cm/10^3y. The highest sedimentation rates occur in the Westgate (1–6 cm/10^3 yr) and Belle Fourche (0.7–5 cm/10^3 yr) formations (Table 10). The lowest rates occur in the Fish Scales (1-2 cm/10^3 yr) and Second White Specks formations (1.25–2.5 cm/10^3 yr).

Isopachs through four slices of the lower Colorado Group in Alberta are shown in Figure 26. The isopachs indicate how basement subsidence and Cordilleran tectonics affected sedimentation. The isopach of the Westgate-equivalent interval (top of the Viking to Base of Fish Scales) shows maximum thickness of up to 400 m in northeastern British Columbia, with thinning toward the southeast. The isopach from the base of the Fish Scales Formation to the base of the Dunvegan Formation (Fish Scales and lowest Belle Fourche formations) shows a similar southeastward thinning, with maximum thicknesses over the Peace River Arch in northeastern British Columbia and northwestern Alberta.

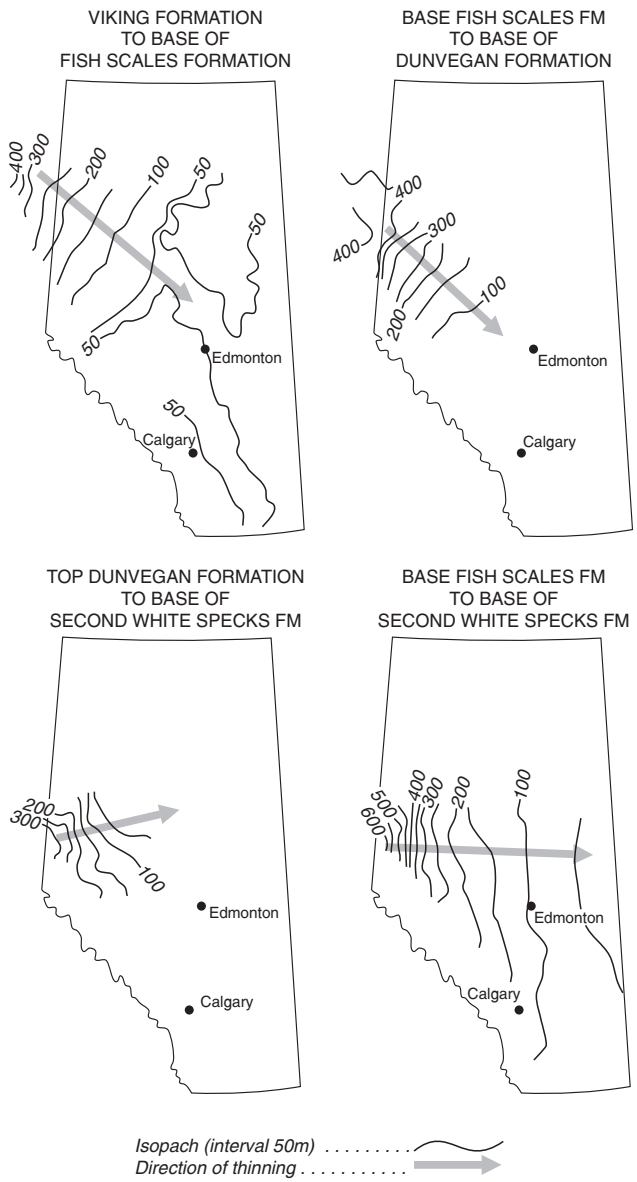

Figure 26. *Isopach maps of four time slices within the Upper Albian Viking Formation to uppermost Cenomanian base of Second White Specks Formation. (Modified from Leckie et al., 1994).*

Table 11

Sedimentation rates for lower Colorado Group formations (after Schröder-Adams et al., 1996)

Formation	Age* Ma	Thickness (m)		Compacted sedimentation rate (cm/1000 yr.)
		min	max	
Westgate	99-97	20	120	6
Fish Scales	97-96	10	20	2.5
Belle Fourche	96-93	20	150	5
Second White Specks	93-91	25	50	2.75

*from Obradovich (1991)

The isopach from Dunvegan to Second White Specks Formation (most of the Belle Fourche Formation) shows a thick area on the Peace River Arch, but the thinning trend has shifted and is northeastward. The isopachs of Fish Scales and Belle Fourche formations show a general eastward thinning. Isopach maps from above the Second White Specks Formation (Leckie et al., 1994) show a general southward shift of the depocentre and basin, with thinning toward the northeast.

PALEOENVIRONMENTS

Regional paleoenvironmental conditions for the Late Albian to Middle Turonian period in the WCSB are reconstructed from the synthesis of regional lithostratigraphy, sedimentology, biofacies data, and geochronology. Paleoenvironmental changes are discussed in Schröder-Adams et al. (1996). New maps (Fig. 27) are presented to incorporate this data and also incorporate palinspastic reconstructions of McMechan and Thompson (1993). Our maps include data from maps presented for the southern portion of the Western Interior by Cobban et al. (1994) and make significant modifications to those presented by Sageman and Arthur (1994).

Westgate Formation

The major transgressive phase, which begins at the base of the Westgate Formation, follows the Viking sea-level lowstand (Leckie 1986; Beaumont 1984; Stelck and Koke 1987; Leckie and Reinson, 1993). During Late Albian time, this sea-level rise culminated in the expansion of the Mowry Sea, which extended from Colorado to the Arctic and from the Rocky Mountain Foothills to eastern Manitoba (Stelck 1975; Williams and Stelck 1975). The southern extent of this seaway is illustrated by Cobban et al. (1994, fig. 3), purportedly for the Early Cenomanian Mowry Sea (*Neogastroplites americanus*). However, it is our contention that the Mowry Sea is of Late Albian age, which is consistent with the foraminiferal data of McNeil and Caldwell (1981) and Caldwell et al. (1993). McNeil and Caldwell (1981, fig. 9) demonstrate the correlation of the Westgate Formation in the Manitoba Escarpment with the Mowry Shale in the northern United States.

The distribution of sediments deposited in the Late Albian Mowry Sea is shown in Figure 27. Essentially, most of the preserved part of the basin comprises marine shale containing fauna of Boreal affinity. The Mowry Sea (*Neogastroplites americanus* time) was closed to the south in the north-central United States (Williams and Stelck, 1975; Cobban et al., 1994). The sea may have had a narrow opening or been partly restricted north of 60° (Williams and Stelck, 1975). There are no Westgate Formation sediments exposed in the Foothills of southwestern Alberta, where material was either not deposited or was eroded. In the subsurface of southern Alberta, the Westgate Formation onlaps nonmarine Mannville Group rocks. The effect of kimberlite emplacement in central Saskatchewan on Westgate sediments (Leckie et al., in press) is still poorly understood.

The abundance of benthic foraminifers, the degree of bioturbation and the presence of horizontal trace fossils such as *Planolites*, *Terebellina*, *Helminthopsis*, and *Muensteria* indicate that moderately to well-oxygenated bottom-waters were present (Ekdale et al., 1984). A diverse foraminiferal assemblage that represents numerous benthic foraminiferal feeding strategies in intervals of high bioturbation also suggests the presence of a well-oxygenated benthic environment (Koutsoukos et al., 1990; Jones and Charnock, 1985). Foraminiferal composition, including taxa of *Miliammina* Heron-Allen and Earland, *Trochammina* Parker and Jones, *Ammobaculites*, and numerous ataxophragmiids, as well as wave rippled and hummocky cross stratified, fine grained sandstone, suggest a shallow, wave-influenced sea of inner neritic to possibly middle neritic water depth. The formation is characterized by low TOC values (< 2wt%) and dominantly Type III organic matter (Fig. 4, 7); the latter indicates a terrestrial origin as the primary sediment source. Vertical variations in grain size, indicated by changes from mudstone to siltstone (coarsening- or fining-upward cycles), may be linked to fluctuations in relative sea level or changes in sediment source and/or supply. Changes in grain size, based on gamma-ray log signatures and visual core descriptions, are detected in the texture of agglutinated foraminiferal tests, which reflect the grain size of the substrate (Fig. 28). In some wells, two coarsening-upward cycles correspond to a concomitant change in grain size of agglutinated foraminiferal tests. Toward the top of the formation, a relative shallowing of the basin is indicated by a widespread coarsening-upward trend, an increase in foraminiferal species with coarse grained, robust tests and an increase in bioturbation. Evidence that waves affected the sea floor include hummocky cross-stratification, wave-

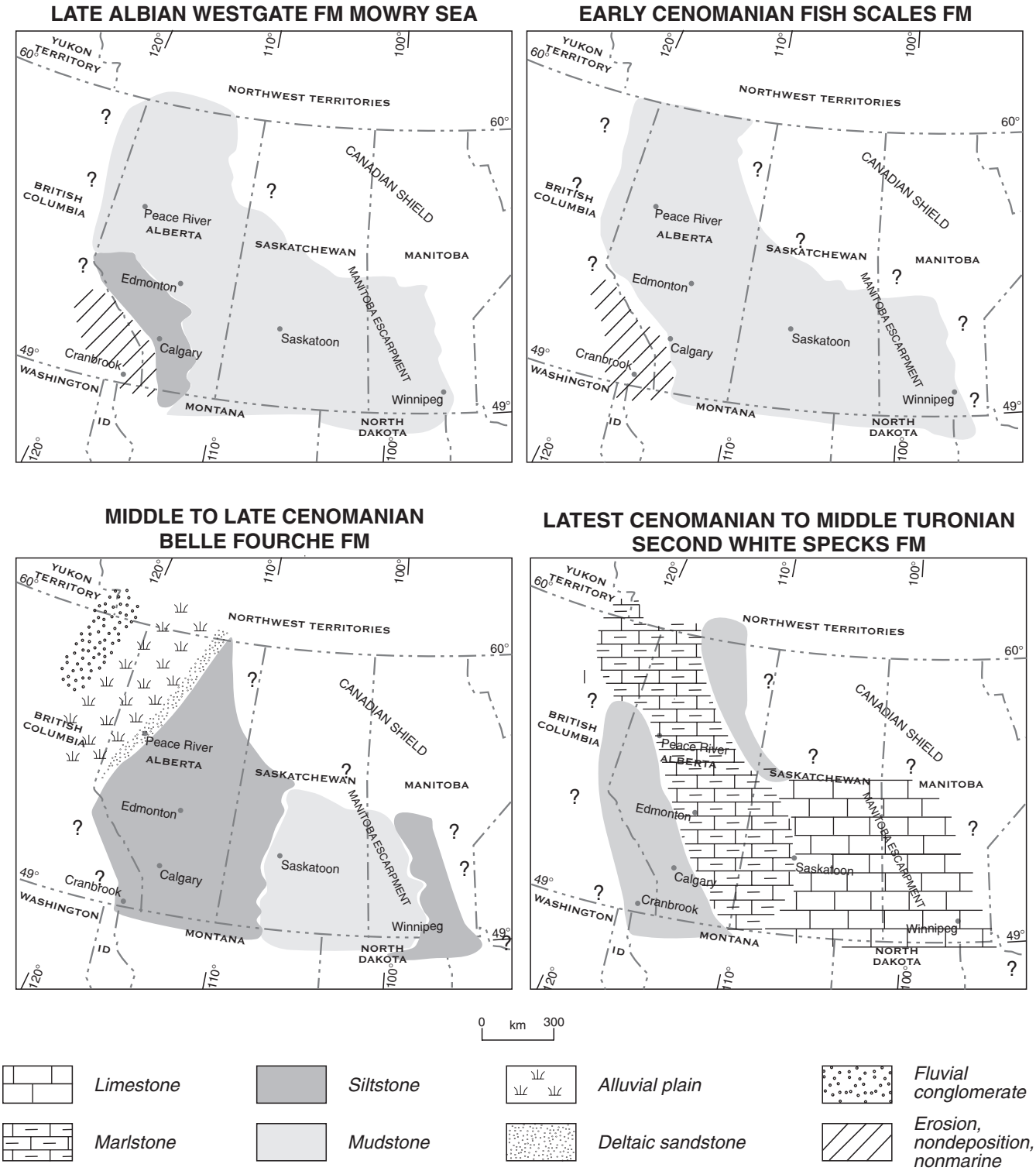

Figure 27. *Paleoenvironment maps for the four formations of the lower Colorado Group.*

ripples, and combined-flow ripples in thin sandstone beds. Sharp-based, graded siltstone beds in this interval may be the result of distal or low-intensity storm events.

The foraminiferal species composition shows an affinity to Arctic agglutinated assemblages of the Albian Tuktu and Grandstand formations of northern Alaska, described by Tappan (1962), Bergquist (1966), and Sliter (1979). Taxa such as *Verneuilinoides borealis* Tappan, *Textularia*

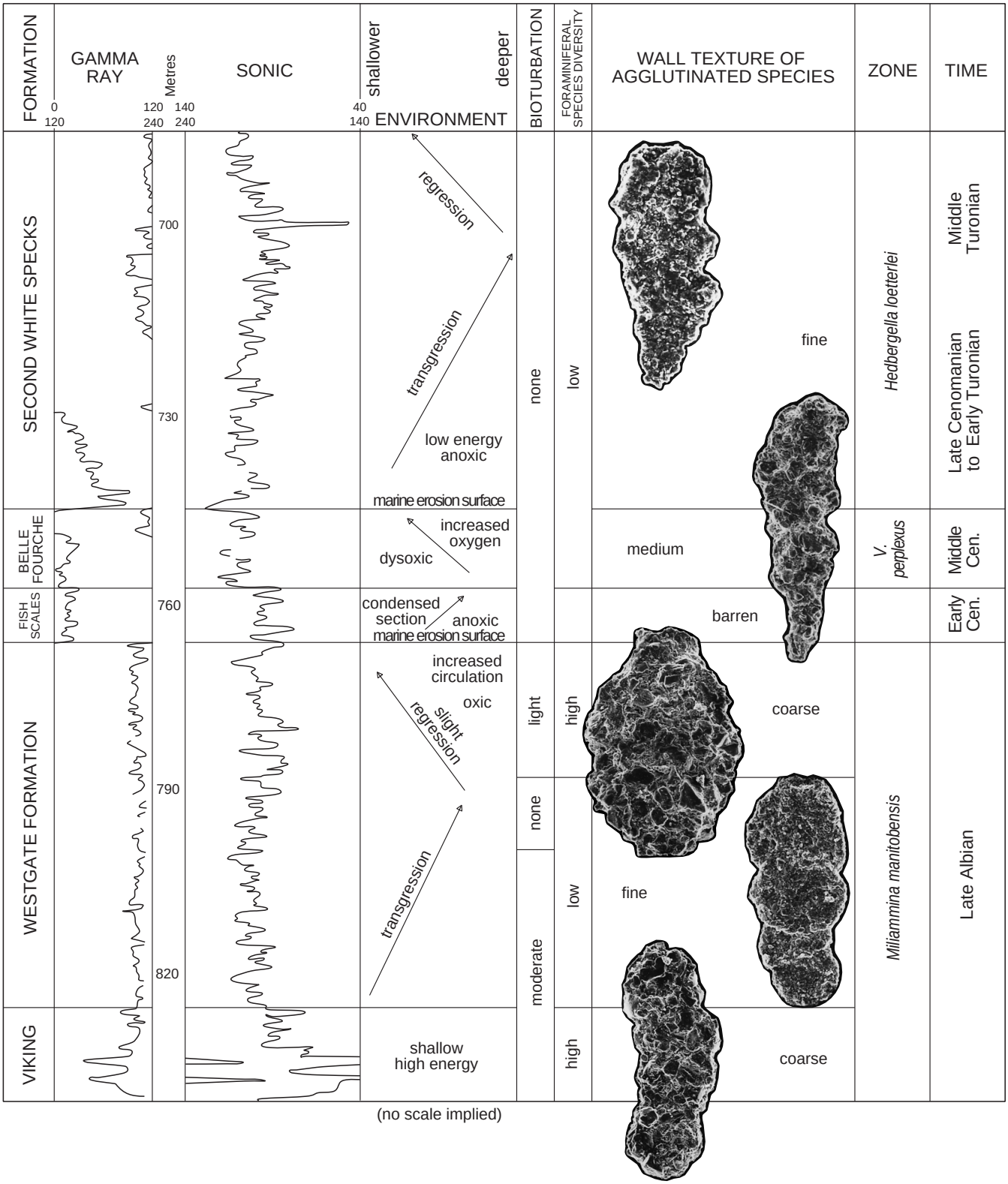

Figure 28. *Summary of environmental changes in the Colorado Group at 6-34-30-8W4 in southeastern Alberta. Sandy (Viking) to silty (Westgate) substrates show increased bioturbation and contain relatively more diverse coarse grained foraminiferal assemblages, whereas fine substrates have a diminished fine grained fauna or are barren of benthic taxa. Belle Fourche and Second White Specks assemblages signal dysoxic to anoxic bottom water conditions. During the major third-order Late Albian to Turonian transgression, several smaller sea-level oscillations took place (modified after Schröder-Adams et al., in press).*

topagorukensis, *Psamminopelta browsheri*, *Ammobaculites fragmentarius*, *Miliammina manitobensis*, and *Haplophragmoides topagorukensis* Tappan in both areas indicate a path of faunal exchange. Dinoflagellate assemblages also suggest the migration of plankton between the Boreal and interior Mowry seas. Among the numerous species in common are *Batioladinium jaegeri* (Alberti) Brideaux, *Chichaouadinium vestitum*, *Ellipsoidictyum imperfectum*, *Florentinia cooksoniae*, *Gardodinium trabeculosum*, *Luxadinium propatulum*, *Odontochitina singhii*, *Oligosphaeridium totum*, *Ovoidinium verrucosum*, *Palaeoperidinium cretaceum*, and *Pseudoceratium expolitum* (Doerenkamp et al., 1976; Brideaux and McIntyre, 1975; Dixon et al., 1989; May, 1979; May and Stein, 1979).

The exclusively agglutinated foraminiferal assemblage over such a wide, shallow basin is unique and lacks modern analogs. During the latest Albian, the Mowry Sea had no connection with the Tethys to the south and therefore probably had a cool, low-salinity water mass of Boreal affinity (Stelck, 1975). Brackish water conditions, inferred from oxygen isotope data from Westgate Formation concretions (Fig. 17), may have limited foraminiferal populations.

Fish Scales Formation

In Canada, at the Albian–Cenomanian boundary, drastic environmental changes occurred that resulted in the loss of benthic foraminiferal assemblages (Fig. 18, 19), increased organic-matter content (Fig. 7), a change in organic matter type (Fig. 4), and widespread bottom-water anoxia. Cobban et al. (1994) considered that the Mowry Sea was Early Cenomanian, based on ammonite occurrences. This, however, is not consistent with our foraminiferal and dinoflagellate zonations.

During the Early Cenomanian transgression associated with the Fish Scales Formation, most of the basin was inundated by marine waters, except in southwestern Alberta, where the sediments were either not deposited or were eroded (Fig. 27). Coarse grained clastic sediment of the Barons and Fish Scales sandstones along the Rocky Mountain Foothills and adjacent subsurface indicate a Middle Cenomanian drop in relative sea level and subsequent reworking during the Late Cenomanian to Turonian transgression.

The boundary between the Westgate and Fish Scales formations is a sharp lithological contact, typically expressed as a thin, parallel- or crosslaminated sandstone or pebble layer with abundant disarticulated fish and other vertebrate remains overlying shale. Leckie et al. (1992) suggested three possible mechanisms to explain deposition of the coarse grained basal sediment within the Fish Scales Formation at the Judah outcrop in northern Alberta. The first is that a sharp drop in sea level at the end of the Albian resulted in submarine erosion and the formation of a lag deposit. In the Peace River area, Stelck et al. (1958) described the *Textularia alcesensis* Zone from the uppermost Albian to Lower Cenomanian. The absence of this zone over the broad area of the WCSB (Caldwell et al., 1978; Caldwell and North, 1984; Bloch et al., 1993) may be explained by a disconformity, suggesting that the basal deposit of the Fish Scales Formation is a lag. This faunal assemblage is reported only in northwestern Alberta and northeast British Columbia, and the limited distribution of the *T. alcesensis* Zone may also reflect localized facies development.

The second proposed mechanism is that the Fish Scales Formation was deposited during continued transgression. Minor changes in the dinoflagellate assemblage at this boundary (Fig. 22) indicate no significant change in surface waters. Sea-level rise resulted in the deposition of a condensed interval comprising concentrated fish debris (Leckie et al., 1992; Leckie and Smith, 1992). The Fish Scales Formation exhibits numerous features of a condensed section, as described by Loutit et al. (1988). It is relatively thin; contains considerable bioclastic debris indicating low sedimentation rates; has a high Type II organic matter content, and contains numerous bentonite layers.

A third mechanism, which is also based on continued sea-level rise, suggests that the bioclastic debris was winnowed from the substrate by vigorous bottom currents (Leckie et al., 1992). These currents may have been generated when two separate water masses (Tethyan and Boreal) joined to form the Western Interior Seaway (WIS), sometime in the Early Cenomanian (Hay,1989; Hay et al., 1993). The submarine erosion caused by these currents may also have removed sediments of the *T. alcesensis* Zone. The presence of warm Tethyan waters in the northern region of the seaway, however, is problematic because Tethyan nannofossils and planktic foraminifera, such as *Hedbergella* Brönnimann and Brown, and *Heterohelix* Ehrenberg, are not found. Both genera are known to be the hardiest planktic foraminifers to make their first appearance in the WIS during the Greenhorn transgression (Leckie et al., 1991) and rare occurrences of these taxa are reported from Lower Cenomanian sections only as far north as Colorado (Eicher and Diner, 1985; Caldwell et al., 1993).

Regardless of the causal mechanism(s), the sharp basal lithological contact, the occurrence of bioclastic conglomerate and the abrupt disappearance of agglutinated species suggest a period of marine erosion at the Albian–Cenomanian boundary. This boundary in the WCSB coincides with an unconformity in Arctic Canada that is associated with sea floor spreading in the Amerasia Basin

(Embry and Dixon, 1990; Dixon, 1993). It also approximately coincides with, or just postdates, an episode of kimberlite emplacement in central Saskatchewan (Gent, 1992). A possible link between these events invites further investigation.

Belle Fourche Formation

The contact between the Fish Scales and Belle Fourche formations is conformable. A slight and gradual improvement of conditions for benthic organisms during Belle Fourche deposition is indicated by a return of agglutinated foraminifers (Fig. 18, 19). Low abundance and low species diversity might have resulted from stressed benthic conditions. Cold and low-salinity waters of Boreal origin continued to dominate the WIS (Cadrin, 1992; Eicher and Diner, 1985; Caldwell et al., 1993). A remnant connection to the south (Tethys) and the wide extension of the Boreal water mass are implied by distributions of the same agglutinated taxa over the entire WIS (e.g., Eicher, 1967; Eicher and Worstell, 1970; Loeblich, 1946). South of the Canada/U.S. border, marine conditions continued to support rare occurrences of planktic foraminifera in the partially time-equivalent Graneros Shale in Colorado (Eicher and Diner, 1985, 1989), South Dakota and Wyoming (Eicher and Worstell, 1970). In Canada, the prevalence of Boreal waters prevented planktic foraminifers and coccoliths from colonizing northern regions during most of the time of Belle Fourche deposition.

In northeast British Columbia a major clastic wedge prograded southeastward, depositing the deltaic sediments of the Dunvegan Formation (Stott, 1982; Bhattacharya and Walker, 1991). Much of the finely interbedded sandstone, siltstone and shale of the Belle Fourche Formation is related to Dunvegan sedimentation. The abundance of finely interbedded sandstones and siltstones in southwest Alberta indicates a probable deltaic source to the west. Palinspastic reconstructions (McMechan and Thompson, 1993) reposition Belle Fourche sediments, now in the Rocky Mountain Foothills, to a position 70 to 160 km to the southwest. An easterly to northeasterly sediment source, from the craton, is indicated by an increased abundance of detrital illite near the Saskatchewan–Manitoba boundary (Caritat et al., 1994a). Sediments are finer grained seaward, toward the centre of the basin. The distribution of Middle to Late Cenomanian Belle Fourche sediments is shown in Figure 27.

Bottom-oxygen levels changed from anoxic during Fish Scales deposition to dysoxic during Belle Fourche deposition, which allowed a few opportunistic agglutinated foraminiferal species to colonize the substrate. Unstable environmental conditions are reflected by abrupt fluctuations in total numbers of one or two dinoflagellate (Leckie et al., 1992) and foraminiferal species (Appendix B). A similar pattern was observed in the Belle Fourche Member of the Ashville Formation in the Manitoba Escarpment (McNeil and Caldwell, 1981) and in Cenomanian sediments of Wyoming and Montana (Eicher, 1967). Numerical modeling of paleoceanic circulation in the WIS suggests that circulation was generally storm-dominated with currents affecting the sea floor down to 200 m (Ericksen and Slingerland, 1990). Brief increases in oxygen levels at the sediment/water interface can be achieved by the breakdown of water mass stratification during storms. Storm-related oxygenation events have been invoked as the mechanism of colonization by macrofaunal communities in the Cenomanian Hartland Shale Member (Greenhorn Formation; Sageman, 1989).

In northwestern Alberta, progradation of the Dunvegan Delta is attributed to a Middle Cenomanian sea-level lowstand (Bhattacharya and Walker, 1991). A lowering of sea level may destabilize a stratified water column by reducing water depth, itensifying storm-related oxygenation or changing circulation patterns. A relatively rapid sea-level rise after the Middle Cenomanian lowstand is indicated by nannofossil and planktic foraminiferal occurrences in the uppermost Belle Fourche at 11-12-6-16W4 and at 11-36-22-1W2. These occurrences signal the first presence of Tethyan-sourced waters in the Canadian part of the WIS.

Second White Specks Formation

During the latest Cenomanian to Early Turonian, sea level in the WIS reached a maximum (Kauffman, 1977, 1984; Haq et al., 1988; Kauffman et al., 1993; Caldwell et al., 1993) and the Second White Specks Formation was deposited at this time. Warm Tethyan waters of normal salinity entered the northern parts of the basin and fostered the northern migration of planktic foraminifera and coccoliths (Fig. 18, 19, 21, 25). Dinoflagellate assemblages also became more diverse near the Cenomanian/Turonian boundary (Fig. 22, 23). Thin, rippled, nannofossil-bearing sand laminae are inferred to be the result of bottom-flowing, unidirectional currents in the seaway. Sedimentary structures do not indicate significant wave activity or influence and this is evidence for deposition in relatively deep water, primarily below storm wave-base. The abundance of pelagic organisms, coupled with widespread bottom water anoxia, resulted in high TOC values (up to 12 wt%) of dominantly Type II organic matter (Fig. 4).

The distribution of Latest Cenomanian to Early Turonian Second White Specks sediments is shown in Figure 27. The southern margins of the seaway in the United States (at *Collignoniceras woollgari* time) are shown by Cobban et al. (1994) and it is inferred that the shoreline shifted markedly to the west in west-central Montana. This is consistent with

our observations from the Rocky Mountain Foothills, which would place the Second White Specks shoreline considerably west of Cranbrook, British Columbia, when Foothills outcrops are palinspastically restored (McMechan and Thompson, 1993). The shoreline trend for western Canada illustrated by Sageman and Arthur (1994) should be placed at least 200 km west of their indicated position. East of the Alberta–Saskatchewan boundary and across Saskatchewan, shales of the Second White Specks Formation grade from marlstone to limestone.

A northward decrease in surface-water temperature is indicated by the progressively smaller number of planktic foraminiferal and coccolith species in the Second White Specks Formation in Canada compared to the Greenhorn Formation of the United States (Eicher, 1969; Eicher and Worstell, 1970; Eicher and Diner, 1985). No keeled planktic foraminifers, with the exception of one questionable specimen of *Praeglobotruncana delrioensis* Loeblich and Tappan in the most southern well at 10-25-1-27W3, are found in the WCSB. The most northern reported occurrence of Late Cenomanian keeled foraminifers are from the Cone Member of the Marias River Formation in northern Montana and southernmost Alberta (Lang and McGugan, 1988). Keeled genera are the deepest-dwelling mid-Cretaceous planktic foraminifers and are regarded as being the most sensitive to environmental change (Leckie, 1987).

Persistent bottom-water anoxia is indicated by a lack of benthic foraminifers at most localities (Appendix B) and the widespread occurrence of well laminated, non-bioturbated sediments. During the latest Cenomanian to Early Turonian sea-level highstand, warm, normal-marine waters from Tethys entered the WCSB and extended to northern Canada and Alaska. Planktic foraminifers in the Turonian Seabee Formation of the Arctic North Slope of Alaska (Tappan, 1962) indicate the northernmost extent of Tethyan waters. The lack of calcareous and agglutinated benthic foraminifers in most cores indicates persistent bottom-water anoxia in the northern part of the sea, in contrast to the south (Arthur et al., 1985; Eicher and Diner, 1985). A Lower Turonian zone, rich in benthic species, was described from the Great Plains (Eicher and Worstell, 1970) and from the Black Mesa Basin in Arizona (Leckie et al., 1991), but was not found in the WCSB. It was implied that increased benthic species diversity was the result of more vigorous circulation between the WIS and the Tethys during peak transgression. However, by the time these waters reached the northern regions, they were oxygen depleted and did not support a diverse benthos. Hay et al. (1993) suggested that the mixing of southern and northern water masses during the Cenomanian produced a dense, oxygen-poor intermediate body of water. The gradual northward incursion of these oxygen-depleted waters into Canada may have resulted in widespread anoxic benthic waters. Outflow either to the north or to the south was balanced by the inflow of northern and southern surface waters, which created major plankton kills during mixing. This introduced large amounts of organic matter into the lower water column, creating an extensive oxygen minimum zone (Hay et al., 1993). The characteristics of the Second White Specks Formation are consistent with this hypothesis. Faunal evidence for an oxygen minimum zone was also found in the Black Mesa Basin and linked to the incursion of warm waters from the south (Leckie et al., 1991).

In contrast to the lack of benthic foraminifers, bivalves, primarily of the genus *Inoceramus* Sowerby, are especially abundant throughout the Second White Specks Formation. Inoceramids were epifaunal suspension feeders that rested above the sediment–water interface, and did not burrow (Hattin, 1982). These organisms evidently survived environmental conditions, including anoxia, that were limiting factors for others (Kauffman, 1988; Sageman, 1989). The number of fragmented calcite prisms in the sand-sized fraction increases significantly at the top of the formation where planktic foraminifers and coccoliths disappear. This suggests that inoceramids continued to thrive during the initial stages of the Turonian regression.

Above the Second White Specks Formation, a basinwide sea-level drop is recorded by the change in organic-matter type (to Type III), the disappearance of planktic foraminifers and coccoliths, and the introduction of coarser grained clastics, culminating in the deposition of Cardium sandstones and conglomerates (Fig. 1).

In central Saskatchewan two unconformities (Fig. 29) are prominent in some cores (e.g., 11-16-35-8W3). A thin interval of the Second White Specks Formation, identified in only one sample, is preserved (Appendix B). This sample contains foraminifers of the *Whiteinella aprica* Subzone of Early Turonian age and overlies directly the *Verneuilinoides perplexus* Zone of Middle to early Late Cenomanian age. The *Clavihedbergella simplex* Subzone of latest Cenomanian to earliest Turonian age (McNeil and Caldwell, 1981) is missing. Also absent is a transitional zone that includes the benthic calcareous taxon *Neobulimina albertensis*, which is present in the section at 6-18-45-1W4. These missing subzones are interpreted as indicating a local unconformity spanning the Cenomanian–Turonian boundary.

The second unconformity is indicated by the occurrence of Santonian sediments of the First White Speckled Shale (Fig. 1, 29) directly overlying the Second White Specks Formation. The Santonian age is determined by the occurrence of the *Globigerinelloides* sp. Zone (Caldwell et al., 1978) and the nannofossil assemblage with common occurrences of *Kamptnerius magnificus* Deflandre and *Marthasterites furcatus* (Deflandre). The unconformities are mapped in a west-to-east cross-section of well logs across Saskatchewan (Fig. 29). To the south at 10-25-1-27W3,

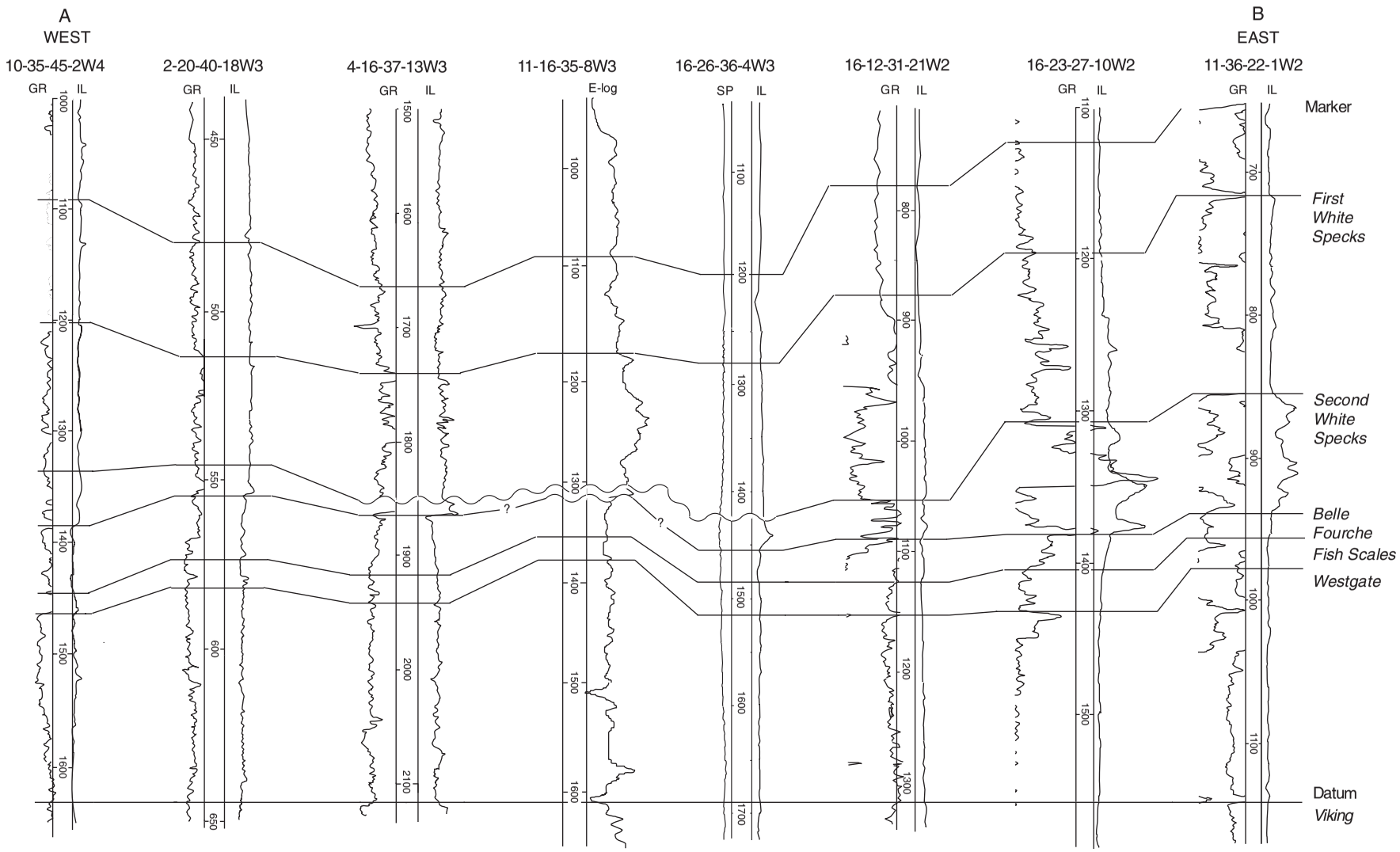

Figure 29. *East–west cross-section across Saskatchewan (see Fig. 2 for location) using the Viking Formation as datum (after Schröder-Adams et al., in press). Note thinning due to erosional unconformities in 11-16-35-8W3.*

Santonian nannofossil assemblages occur in an interval just above the Second White Specks Formation, indicating that the second unconformity may extend to the southwest. At this locality, it cannot be determined if Santonian sediments directly overlie Lower Turonian sediments because of a barren zone (Morden Formation?) of 3 m between the Second White Specks Formation and the First Speckled Shale (Appendices B, C).

The regional cross-section through the Colorado Group in Saskatchewan (Fig. 29) demonstrates the relatively flat, conformable stratigraphy of the lower Colorado Group except for the area in east-central Saskatchewan (11-16-13-8W3) where marked unconformities occur over an apparent structural high.

Bioclastic conglomerate

The Fish Scales and Second White Specks formations contain horizons of bioclastic conglomerate, a few centimetres to a few decimetres thick, which occur discontinuously across the basin (e.g., Leckie et al., 1992; Bloch et al., 1993). Bioclastic conglomerate associated with the Second White Specks Formation consists of fish and shark teeth, fish scales, disarticulated vertebrate remains, angular to subangular clasts of mudstone and a green, chloritic, marine clay. Rare extraformational pebbles (commonly chert or quartz clasts) up to 2 cm in diameter and coalified wood debris may be present locally. Bed thicknesses vary from 2 to 20 cm. The conglomerates are generally massive, although crude subhorizontal bedding occurs locally. On exposed surfaces of the conglomerate, tapered shell or bone bioclasts are aligned, indicating current activity. Alignment in overlying laminae may be in the opposite direction, suggesting the influence of wave action.

A bioclastic conglomerate or coarse grained sandstone, a few centimetres to decimetres thick, commonly occurs at the base of the Fish Scales Formation, in sharp contact with the underlying Westgate Formation (see Leckie et al., 1992; Bloch et al., 1993). This conglomerate is more regionally persistent than that at the base of the Second White Specks Formation. Both conglomerates are largely bioclastic, although with a different composition. The Fish Scales conglomerate may locally contain a larger siliciclastic component comprising chert or quartz, intraformational shale clasts and siderite clasts. Other components include belemnites and phosphatized bioclastic debris.

A horizon of bioclastic conglomerate has been used as a marker for the base of the Second White Specks Formation (Bloch et al., 1993). However, at 11-12-6-16W4 and 6-34-30-8W4, bioclastic conglomerate is overlain by beds containing an agglutinated Belle Fourche microfauna. In central Saskatchewan at 11-16-35-8W3, a bioclastic conglomerate is associated with an unconformity spanning the Cenomanian–Turonian boundary. In contrast, at 6-18-45-1W4 and 11-36-22-1W2, where there is no conglomerate between the Belle Fourche and Second White Specks formations, the microfauna shows a transitional zone that contains the calcareous benthic taxon *Neobulimina albertensis* (6-18-45-1W4) or the *Clavihedbergella simplex* Subzone (11-36-22-1W2) (Fig. 19). In southern Saskatchewan at 10-25-1-27W3, a bioclastic layer occurs at the top of the Second White Specks Formation. At this locality, the bioclastic layer is probably linked to a later unconformity that places the First White Speckled Shale (Santonian) on Turonian Second White Specks Formation. Other occurrences of coarse bioclastic layers in marine shales of the Western Interior Sea are reported from the Central Great Plains and southern Rocky Mountains of the U.S. Extensive skeletal grainstones are described from the basal Lincoln Limestone of Late Cenomanian age (Hattin, 1986).

The origin of these Late Cenomanian conglomerate layers associated with the organic-rich, deeper water marine shales is enigmatic. Locally, missing faunal zones indicate a marine erosion surface; there is no evidence from the WCSB to suggest subaerial exposure. The sporadic distribution of a conglomerate at the base of the Second White Specks Formation most likely reflects varying water depths in the basin. Where the basin was shallower, such as in central Saskatchewan, a drop in base level resulted in winnowing and erosion of older sediments. The occurrence of species of the *V. perplexus* Zone above the bioclastic layers at 11-12-6-16W4 and 6-34-30-8W4 indicates this erosional event occurs at a similar stratigraphic position to that of the erosional event within the Dunvegan Formation (Bhattacharya and Walker, 1991). In the Pasquia Hills of east-central Saskatchewan, vertebrate faunal assemblages from a time-equivalent bioclastic conglomerate suggest reworking of sediment that was initially deposited in a nearshore to possibly estuarine depositional setting (Cumbaa et al., 1992; Cumbaa, 1993). The disarticulated bioclastic layers are interpreted as being evidence of basin shallowing and subsequent winnowing on the sea floor. Alternatively, the conglomerates may be winnowed lags, which result from storms that are able to reach the sea floor at a lower base level. Beds of aligned, tapered bioclasts aligned oppositely in succeeding laminae are evidence for wave reworking. However, wave activity would be expected to form coarse grained ripples (cf., Leckie, 1986) which we have not observed.

DIAGENESIS

The early diagenesis of marine shales is commonly dominated by microbial processes that oxidize organic matter and may result in mineral dissolution or authigenesis

(Gautier and Claypool, 1984; Gautier et al., 1985; Gautier, 1986; Pratt et al., 1992). The heirarchy of microbial redox processes reflects the decreasing availability of oxygen in organic-matter-bearing sediments during burial and the free-energy yields of the specific reactions (Berner, 1980). This reaction heirarchy is commonly described as a series of diagenetic zones characterized by the dominant redox reaction. With increasing depth, these zones include aerobic oxidation, nitrate reduction, manganese and iron reduction, sulfate reduction and methanogenesis (Claypool and Kaplan, 1974). However, studies of modern marine sediments indicate that these processes, particularly methanogenesis and sulphate reduction, may not be mutually exclusive (Oremland and Taylor, 1978).

Petrographic, chemical, mineralogical, and isotopic data indicate that the early diagenesis of lower Colorado Group shales is dominated by two of these reactions: sulfate reduction and methanogenesis. In addition, petrographic, isotopic, and chemical data from clay minerals indicate that clay authigenesis is also an early diagenetic process.

Late diagenesis, that is, mineral reactions that occur in response to a burial induced increase in temperature and pressure, is commonly characterized by dissolution–precipitation reactions involving silicates and carbonates, as well as organic matter maturation. Information regarding the nature of late diagenetic alteration of Colorado Group shales comes from petrographic observations, isotopic data, and XRD characteristics of clay minerals. These data indicate that late diagenesis of Colorado Group shales is dominated by quartz and feldspar dissolution, and Fe-carbonate precipitation. Caritat et al. (1994a) indicate that mixed-layer clay and/or illite authigenesis also occurs within the Belle Fourche Formation.

Sulphate reduction

As previously described, authigenic pyrite is a common constituent in the lower Colorado Group, ranging in abundance from < 0.2 to approximately 8.5 wt % (Plate 5, Table 9). This is the primary evidence for the occurrence of early diagenetic sulphate reduction. Sulphur isotopic data from pyrite also indicate that sulphate reduction is the primary reaction leading to pyrite authigenesis (Table 8).

Organic matter type and abundance, and benthic activity, are primary controls on the extent and rate of sulphate reduction within sediments (Berner, 1970; Goldhaber and Kaplan, 1974). The variablity of the type and abundance of organic matter within the discrete shale units (Fig. 4) suggests that the rate and extent of reaction also will be variable from unit to unit. The shales of this interval can be divided into two groups based on their carbon–sulphur (C–S) and sulphur–iron (S–Fe) systematics (Fig. 7, 8). As previously discussed, Group 1 is characterized by TOC and S values of < 2 wt% and Fe/S values much greater than 1. Group 2 is characterized by high TOC and S values, generally > 2 wt%, and Fe/S values greater than or equal to 1. Group 1 includes the Joli Fou, Westgate, and Belle Fourche formations and the shales of the Viking and Lea Park formations. Group 2 includes the Fish Scales, Second White Specks, and Morden formations as well as the First Speckled Shale.

Group 2 shales were deposited beneath a relatively deep, productive water column during transgressive periods, where bottom water conditions were anoxic to dysoxic. The characteristics of Group 1 shales indicate a less productive, shallower water column, with more oxygenated bottom waters and an increased sediment input. These two depositional conditions are reflected in the isotopic composition of pyrite sulphur (Fig. 30). The $\delta^{34}S$ values of most Group 2 shale samples are consistently depleted with most values < -22‰ CDT. Group 1 values are variable with a range of more than 80‰ (Fig. 30).

Using the simplest approximation of the process of sulphate reduction, the rate at which this process occurs is dependent on the reactivity of organic matter and the availability of sulphate. Under conditions characteristic of condensed sections (low sedimentation rates and high, reactive TOC content), rapid and efficient sulphate reduction results in very large and consistent depletions in ^{34}S in pyrite sulphur, as observed in the Group 2 shales. In progradational shales, where sedimentation rates are higher, and the organic matter is less reactive (contains a higher proportion of Type III OM), sulphate reduction proceeds more slowly. The rate of reduction at or near the sediment–water interface initially is controlled by the reactivity of the organic matter. With increasing burial, however, sulphate availability may become the limiting factor.

A Rayleigh distillation model (Hoefs, 1987) predicts that in a closed system (i.e., buried sediment) where the sulphate reservoir is completely consumed, the initial (sulphate) and final (sulphide) isotopic compositions approach equality. Because of the increasingly extreme ^{34}S enrichment in the residual sulphate reservoir, the instantaneous ^{34}S values of the dissolved HS^- may also show extreme enrichment. The range of sulphide ^{34}S values under conditions that may approach a "closed system", therefore, may be extremely variable, as seen in Group 1 shales (Fig. 30).

Concretion morphologies, attributes, and isotopic composition

Siderite and calcite concretions occur in Colorado Group and stratigraphically equivalent sediments in a variety of morphologies. Carbonate concretions in marine sediments

commonly result from early diagenetic processes (Irwin et al., 1977; Gautier and Claypool, 1984) and their chemistry and isotopic compositions therefore provide information about early diagenetic processes within the host sediments. The fabrics and isotopic compositions of the calcite and siderite concretions of the Colorado Group are distinct and reflect the variable influences of organic matter oxidation, including sulphate reduction, methanogenesis, and water-rock interaction.

Calcite concretions

Calcite concretions occur only within calcareous facies in the upper Belle Fourche and Second White Specks formations and may form stratigraphically continuous horizons or stratabound lenses. Another common morphology is discrete spheroidal or elliptical concretions up to several tens of centimetres (long axis) in size. The calcite habit ranges from micrite to cone-in-cone spar. Septaria are common and may contain multiple generations of anhedral to euhedral calcite spar. Calcite concretions are generally laminated (Plate 14) and divergent laminae are observed adjacent to or within some calcite concretions, indicating very early growth beneath the sediment–water interface (Plate 14). Calcite concretions commonly have pyrite rinds up to 0.5 cm thick. This suggests growth prior to, or coincident with, the onset of vigorous sulphate reduction.

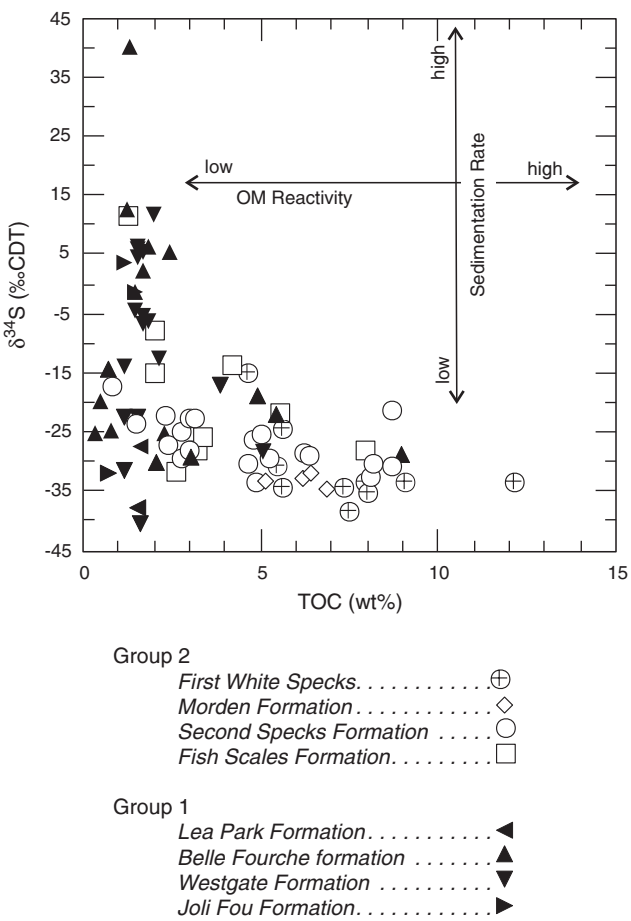

Figure 30. *Total organic carbon (TOC) versus the sulphur isotopic composition (^{34}S) of pyrite from transgressive (Group 2) and progradational (Group 1) shales. Arrows illustrate the general effect of organic matter (OM) reactivity and sedimentation rate on the isotopic composition of pyrite.*

Carbon and oxygen isotopic data (Fig. 17) also are consistent with an early diagenetic origin. Calcite concretions from the Second White Specks and Belle Fourche formations are very depleted in ^{13}C (< -10‰ PDB) and relatively enriched in ^{18}O (> +25‰ SMOW). Depleted carbon values result from the incorporation of dissolved CO_2 derived from the oxidation of organic matter, probably by sulphate reduction, that occurs in the underlying sediment. In calcareous sediments, where the activity of dissolved Ca^{2+} in pore waters is likely to be high, the upward diffusion of dissolved CO_2 may result in calcite precipitation if the pH is buffered to near neutral or greater values. The oxygen isotope values reflect calcite precipitation from pore waters somewhat depleted in ^{18}O when compared to normal marine values (δ^{18}O = 0‰ SMOW).

The oxygen isotopic composition of concretions is determined by the temperature of formation and the isotopic composition of the pore waters from which they form. Cadrin (1992) determined from biogenic calcite and aragonite that bottom waters of the WCSB in the Late Cenomanian and Early Turonian were about -7‰ SMOW. Belle Fourche kaolinite and I/S isotopic values also are consistent with this initial pore-water value (Caritat et al., 1994a). Assuming that an oxygen isotopic value for pore water is -7‰ SMOW, the temperature of calcite concretion formation may be calculated using the calcite–water geothermometer of Friedman and O'Neil (1977):

$$1000 \ln \alpha_{calcite-water} = 2.78 \times 10^{-6}/T^2 - 2.89 \qquad (1)$$

where T is in °K, and the relationship between α and δ,

$$\alpha_{calcite-water} = (\delta_{calcite} + 1000)/(\delta_{water} + 1000) \qquad (2)$$

Using an average $\delta^{18}O_{calcite}$ = 27‰ (see Table 7) and a $\delta^{18}O_{water}$ = -7‰, the calculated temperature of formation for calcite concretions is ~3°C. This low bottom-water temperature suggests that cool, Boreal waters that dominated the WCSB in the Albian (Schröder-Adams et al., 1996) persisted into the Turonian. This is consistent with a wealth of data (Kauffman, 1977; Pratt, 1984; Cadrin, 1992) that

indicates that the WIS was a stratified water body throughout the early Late Cretaceous.

One calcite and one dolomite sample (10-34-42-22W4-2A) show normal marine values for $\delta^{13}C$ and lower $\delta^{18}O$ values. The calcite sample is from a bioclastic-rich layer at the margin of concretion 10-34-42-22W4 (Plate 14) and the isotopic composition is interpreted as reflecting biogenic marine carbonate with some recrystallization during diagenesis, which results in the lower $\delta^{18}O$ value (22.4‰ SMOW, see below). Similarly, the dolomite sample reflects dolomitization of bioclastic carbonate during early diagenesis.

Siderite concretions

Siderite concretions occur in the Westgate, Fish Scales, and Belle Fourche formations and exhibit a range of morphologies similar to calcite concretions. In addition, large (up to 1 m in diameter) siderite kettle concretions are observed in outcrops of the Sunkay Member of the Blackstone Formation (Belle Fourche equivalent). The siderite is cryptocrystalline and concretions commonly show evidence of extensive burrowing by a variety of benthic organisms (Plates 15, 16). Disseminated siderite also occurs in well bioturbated sediments of the Westgate (Plate 6A) and Belle Fourche formations.

Siderite concretions show a range of isotopic compositions and complex textural relationships that highlight variable, but generally early, growth conditions. Siderite concretions are either isotopically zoned or unzoned.

The sediment in which isotopically zoned concretions of the Westgate Formation (Plates 15, 16) have formed shows evidence of extensive bioturbation, and individual trace fossils are well preserved, indicating relatively early siderite formation. In concretion 10-25-65-20W5-2A (Plate 16), numerous small burrows that appear as "starbursts" have circular centers and are filled with dolomite. The circular shape indicates that cementation occurred prior to any significant burial. In contrast, a large burrow preserved near the center of the concretion shows some flattening. This indicates that siderite formation occurred after loading by additional sediment.

In concretion 10-25-65-20W5-2B (Plate 15), botryoidal pyrite fills circular burrows indicating early pyritization of these structures. Burrows are commonly sites of preferential pyritization because they are organic rich and allow irrigation of the sediment by sulphate-bearing fluids (Pratt, 1984).

In the zoned concretions from the Westgate Formation, the isotopic compositions are more enriched in ^{13}C and ^{18}O in the concretion centers and $\delta^{13}C$ and $\delta^{18}O$ values decrease toward the margins (Plates 15, 16). In the unzoned siderite concretion from the Belle Fourche Formation, the $\delta^{18}O$ values are similar to those at the centres of the zoned concretions. The $\delta^{13}C$ values are positive, but not as high as the $\delta^{13}C$ values of the zoned concretions (see Table 7). The similarity of these isotopic values is interpreted as indicating that the precipitation of siderite in both zoned and unzoned concretions began under similar conditions. The growth of unzoned concretions most likely terminated early, whereas the growth of zoned concretions continued under evolving burial conditions.

The initial pore water isotopic composition for Westgate (Late Albian) concretions can be determined as above, using the siderite–water geothermometer of Carothers et al. (1988),

$$1000 \ln \alpha_{siderite-water} = 3.31 \times 10^{-6}/T^2 - 3.50 \qquad (3)$$

and assuming a bottom temperature similar to that of calcite concretion formation. At 3°C, and utilizing an initial $\delta^{18}O_{siderite}$ = 23.5‰ (see Table 7) the calculated $\delta^{18}O_{pore\ water}$ = -14.5‰ SMOW. This calculation suggests that Late Albian basinal waters in the northwest part of the study area were much more depleted in ^{18}O than those of the Late Cenomanian to Early Turonian WIS in more distal portions of the basin.

Within the zoned concretions, the decrease in the $\delta^{18}O$ values of siderite to ~ 20.5‰ may reflect the increasing temperature of siderite precipitation during burial or a change in pore-water isotopic composition to lower $\delta^{18}O$ values. A decrease in pore-water isotopic values could result from either: 1) the incursion of meteoric waters into sediments during subsequent regression or, 2) the neoformation of clay minerals under relatively closed system conditions.

Using Equation #3, the calculated $\delta^{18}O_{pore\ water}$ = -14.5‰ SMOW, and a concretion margin siderite $\delta^{18}O$ value of -20.5‰, the temperature of formation for the outer portions of the zoned concretions would be ~ 16°C. This suggests growth of the zoned concretions over ~ 13°C temperature increase or about 500 m of burial, assuming a 25°C/km geothermal gradient. Using the maximum sedimentation rate for the Westgate Formation (Table 10) of 6 cm/k.y., concretion growth is estimated to take up to 8 m.y.

Changes in pore water isotopic composition are difficult to constrain. The incursion of meteoric waters into basin sediments several hundred kilometres from the inferred

shoreline has been invoked as a mechanism of change in pore water isotopic composition (i.e., Machemer and Hutcheon, 1988). The zoned concretions are from the proximal northwest part of the study area, but the location of the shoreline in the Late Albian is unknown (Fig. 27). Additional study of coeval concretions to determine the geographic variability of isotopic compositions, as well as a better understanding of Albian paleogeography, is necessary to test the meteoric incursion hypothesis.

There is evidence indicating that clay mineral authigenesis occurred during early diagenesis and therefore, clay mineral authigenesis may be a viable mechanism for reducing pore water $\delta^{18}O$ values.

Early diagenetic clay mineral authigenesis

Early diagenetic authigenesis for some clay minerals is indicated primarily from petrographic data. Minor to trace amounts of a Fe- and K-rich, fibrous aluminosilicate are observed as well-rounded clots, perhaps psuedomorphs of fecal material (Plate 4a). This peloidal habit, with a Fe-rich composition, is commonly interpreted as glauconite but may also be celadonite, chlorite, nontronite, corrensite, or mixtures of these Fe-rich clay minerals. Discrete green clay minerals or mixtures of green marine clays are commonly identified petrographically as "glauconite" and the term used herein is so defined. The presence of "glauconite" in Colorado Group sediments is associated with bioturbation and/or high bioclastic input. Some textures suggest replacement of Fe-rich argillaceous clasts (Plate 4b). "Glauconite" formation has been shown to occur at or near the sediment–water interface under dysoxic conditions (Taylor and Curtis, 1995) and the textures observed in Colorado Group shales are consistent with this mode of formation, but are not unequivocal.

Early diagenetic kaolinite authigenesis (Plates 8c, 9b) is inferred from observed kaolinite habits. It has been suggested that kaolinite formation is favored under acid conditions in carbonate-poor sediments by the hydrolysis of K-aluminosilicates (Pollastro, 1981; Huggett, 1994), where:

$$2KAl_3Si_3O_{10}(OH)_2+3H_2O+2H^+ \rightarrow 3Al_2Si_2O_5(OH)_4+2K^+ \quad (4)$$

and/or

$$2KAlSi_3O_8+H_2O+2H^+ \rightarrow Al_2Si_2O_5(OH)_4+4SiO_2+2K^+ \quad (5)$$

However, Abercrombie (1988) has shown that pore water pH may be rock-buffered by hydrolysis reactions to near neutral values, even when water/rock ratios are higher than those characteristic of diagenetic conditions. Mildly acidic conditions may develop in organic-rich sediments where organic matter oxidation occurs more rapidly than buffering reactions such as hydrolysis. An alternative condition in which kaolinite may form is when pore waters are dilute. While the specific conditions of kaolinite formation in Colorado Group shales remain unknown, petrographic observations indicate some early kaolinite neoformation.

Petrographic observations also indicate smectite and/or mixed-layer clay authigenesis occurs during early diagenesis by neoformation (Plate 3a, b) or devitrification (by hydrolysis or halmyrolysis) of volcanic ash. Caritat et al. (1994a) demonstrated a genetic relationship between the clay fraction (< 0.2 µm) composition and bentonite smectite, which suggests a tephra precursor for much of the I/S, and possibly kaolinite, in immature samples of the Belle Fourche Formation.

A compositional relationship between the shale clay fraction and bentonite is evaluated by plotting the molar compositions of each group on an element ratio diagram that widely separates both groups. This separation is achieved by plotting Si/K (y-axis) versus Al/K (x-axis) as the K content of bentonites is very low (see Table 5). A regression through the clay fraction (< 0.2 µm) compositions of two formations, the Westgate and Second White Specks (shown in Fig. 31), intersects the field of bentonite compositions, suggesting a compositional relationship. The Fish Scales Formation samples are plotted on Figure 31 but no regression is calculated because of the small number of data points.

Published clay-mineral oxygen isotope data may also be interpreted as indicating neoformation of clay minerals from a precursor volcanic ash (Caritat et al., 1994a) at low temperatures. In summary, several lines of evidence indicate that the formation of matrix clay minerals of the Colorado Group shales results, in part, from the early diagenetic alteration of volcanic ash. A similar conclusion was reached by Nadeau and Reynolds (1981) based on the composition of I/S and K/Ar data from matrix clays and bentonites of the Late Cretaceous Mancos Shale.

Clay mineral neoformation will affect the pore water $\delta^{18}O$ composition only under relatively "closed-system" conditions, where pore water exchange with the overlying basinal waters is restricted. Pore water $\delta^{18}O$ values will decrease as a result of clay mineral authigenesis because of the large fractionation factor at low temperatures (see Longstaffe, 1987). Studies of modern ocean sediments indicate a decrease of up to ~4‰ SMOW in pore water $\delta^{18}O$ values over depths of several hundred metres (Savin and Yeh, 1981). The difference in oxygen isotopic values from zoned siderite concretion suggests a decrease in pore water values of about 3‰ in Westgate sediments.

Late diagenetic processes

Late, or burial-induced diagenetic effects are difficult to discern in Colorado Group shales. Some recent studies of

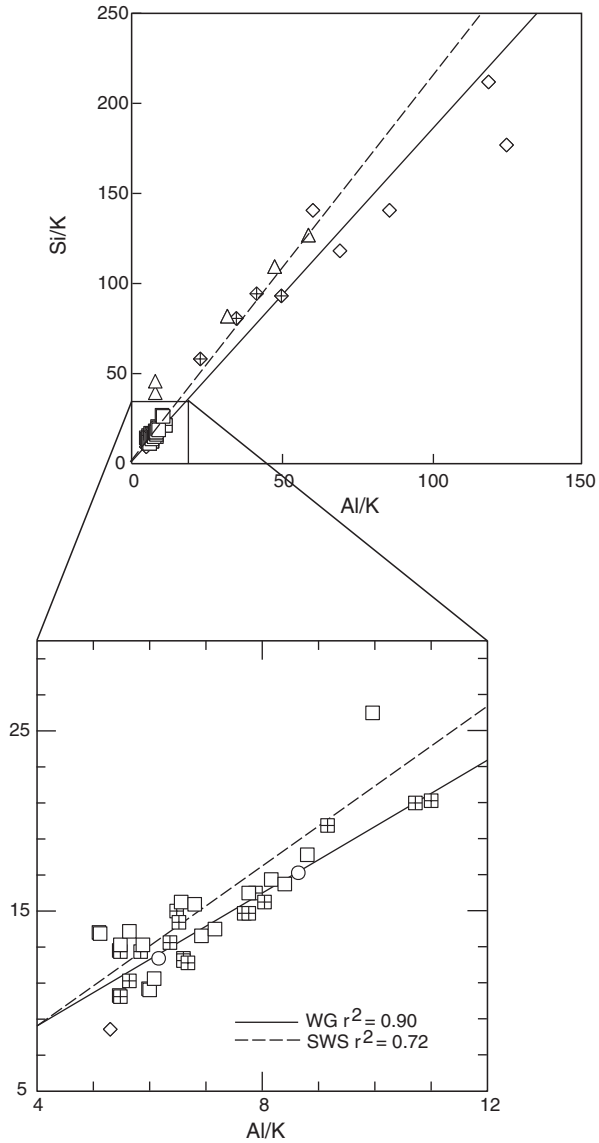

Bentonite
- *Second White Specks Fm* . . . ◇
- *Fish Scales Formation* . . . . . △
- *Westgate Formation* . . . . . ⌖

Clay Fraction
- *Second White Specks Fm* . . . □
- *Fish Scales Formation* . . . . . ○
- *Westgate Formation* . . . . . ⊞

Figure 31. *Al/K versus Si/K diagram for bentonites and clay fraction of shale matrix for indicated formations. Inset shows the clay fraction sample used to calculate the regression for the Westgate (WG - solid line) and Second White Specks (SWS - dashed line) formations that intersects the bentonite fields for each formation in the upper part of the diagram. No regression was calculated for the Fish Scales because of the small number of data points. See Caritat et al. (1994) for Belle Fourche Formation data.*

shale diagenesis indicate that significant mineral reactions and mass transport of soluble species occur (i.e., Wintsch and Kvale, 1994, and references therein) whereas others show that little diagenetic alteration occurs in shales at depth (i.e., Bloch and Hutcheon, 1992). In Colorado Group shales, petrographic observations suggest that late diagenetic processes involve primarily the dissolution and precipitation of silicate minerals and fracture development. Significant fluid (aqueous and hydrocarbon) migration and soluble species transport may occur within fracture networks.

While early diagenetic kaolinization of silicates does occur, this process may extend well into the subsurface. Mechanical deformation of mica lathes may enhance kaolinization but not all deformed micas are pervasively altered (Plates 6b, 8d).

Well-preserved grain pseudomorphs indicate that kaolinization of feldspars (Plate 3) and perhaps volcanic clasts occurs after significant compaction and matrix stabilization.

Embayed quartz grains (Plates 1d, e, 2a) are commonly observed, suggesting that quartz dissolution is a pervasive process. Extensive dissolution that results in suturing is observed in one sample (Plates 4d–f). In this sample (#050940, 1496 m), quartz grains have extreme length to width ratios of up to 10 and are sutured in a bedding-parallel orientation. The intergranular matrix is enriched in Fe. These features are interpreted as reflecting framework dissolution by pore fluids near maximum burial depth. The rarity of these features suggests that this type of fluid movement is localized, perhaps controlled by fracture development or a localized increase in permeability due to a high silt content.

Feldspar dissolution (Plates 2d, 6a) is commonly observed in Colorado Group shales but it appears to be localized, and many K-feldspars are well preserved (Plates 1d, 7d). Plagioclase feldspar is not commonly observed and frequently shows alteration or replacement by calcite (Plate 6d).

Fe-rich carbonate is commonly observed rimming detrital (bioclastic) carbonate grains (Plate 6c). The timing of overgrowth development is difficult to discern from textural relationships but most likely follows sulphate reduction and significant concretion formation.

Fracture formation and sediment fluid isotopic compositions

Natural fractures are observed in core and outcrop, primarily in the Second White Specks Formation. Significant natural fracturing was found in only one core (Dome et al. Claresholm, Table 1). Rubble zones containing

common slickensides were noted in other cores but the origin of the slickensides and resulting rubble are unclear in many cases. Coring-induced fractures are also present (Plate 17).

Calcite-filled fractures are seen in concretionary horizons and are pervasive in some outcrops (Plates 18–21). The orientation and spacing of the fractures observed in outcrop indicate that they formed as a result of compressive (thrusting) tectonic stress and that the Second White Specks Formation behaved as a cohesive, brittle body with predictable fracture characteristics (Plates 18–20). In contrast, fractures observed in core indicate both brittle and ductile behaviour in response to compressive tectonic stress (Plate 21). Despite significant annealing in cataclastic zones, some good fracture porosity is preserved (Plate 21b, c).

The timing of fracture formation may be constrained using oxygen isotopic data from fracture cements and reasonable assumptions regarding the origin of these cements. Two sets of samples, consisting of fracture cement and host concretion calcite, were analyzed (Fig. 17). The difference in the $\delta^{18}O$ values of the host concretion and fracture cement calcite for both sets of samples is ~10.2‰. Utilizing calcite concretion $\delta^{18}O$ values and assuming an early diagenetic origin (3°C) for concretion calcite formation, calculated compositions of fluid from which concretions form are approximately -7‰ (Eq. 1, Fig. 32). If fracture-fill calcite is derived from the dissolution–precipitation of this early calcite, and fracture-fill cement is coeval with fracture formation, temperatures of between 40 and 50°C are indicated for fracture formation (Fig. 32). This suggests fracture formation at about 2.0–2.3 km of burial utilizing the present geothermal gradient for southwestern Alberta of 22°C/km (Majorowicz et al., 1985) and assuming a 0°C surface temperature. The low temperature of fracture formation indicates fracture development before the onset of local oil generation, but fractures could develop updip of mature source rock and therefore contribute to hydrocarbon migration. Fracture formation would occur at higher temperatures if the surface temperature were higher. By the Early Tertiary, nonmarine sediments were being deposited over much of the Western Interior suggesting surface temperatures of ~20°C.

The origin of the relatively enriched $\delta^{13}C$ values of the fracture-fill cement (Fig. 17) is not clear. The most likely source of $\delta^{13}C$-enriched carbonate is from OM maturation. Both biogenic and thermogenic gas generation result in ^{13}C enrichment in the residual OM. Oxidation of this residual material would result in dissolved bicarbonate with relatively high $\delta^{13}C$ values. Other possible sources include Paleozoic formation waters that migrated updip, or infiltrating meteoric waters.

Summary paragenesis

A generalized paragenesis for Colorado Group shales is summarized in Figure 33. Pyrite, calcite concretions, and possibly early siderite concretion growth resulted primarily from bacterial sulfate reduction and possibly dissolved bicarbonate sourced from underlying sediments undergoing methanogenesis. Most siderite formed in response to methanogenic activity. The temperature near the sediment–water interface is calculated to be about 3°C. Early kaolinite and I/S authigenesis resulted from the alteration of volcanic ash and most likely lowered pore-water $\delta^{18}O$ values by up to ~3‰. Some illitization of I/S may have occurred in response to increased burial. Quartz, plagioclase and localized K-feldspar dissolution occurred with continuing burial. Fe-carbonate overgrowths on bioclastic grains are inferred to postdate significant pyrite and siderite concretion growth. Localized, intensive grain dissolution occurred near maximum burial depths, presumably because of the migration or expulsion of fluids. In the Second White Specks, fracture development occurred in response to tectonic stress at temperatures of about 50°C.

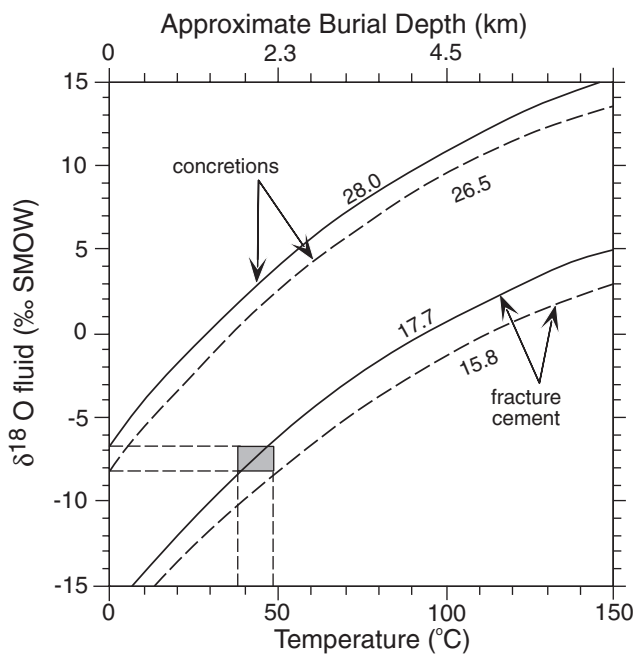

Figure 32. *Temperature and approximate burial depth versus calculated $\delta^{18}O$ values for fluids from which authigenic carbonate may have precipitated for paired samples shown in Figure 17 using the geothermometer of Friedman and O'Neil (1977). Stippled box indicates inferred temperature range of formation temperature for fracture-fill calcite cement assuming recrystallization of primary calcite concretion carbonate. $\delta^{18}O$ values of the carbonate cements used in the calculations are indicated on each curve. Solid line = LCD et al. Bashaw; dashed line = Bruin Creek.*

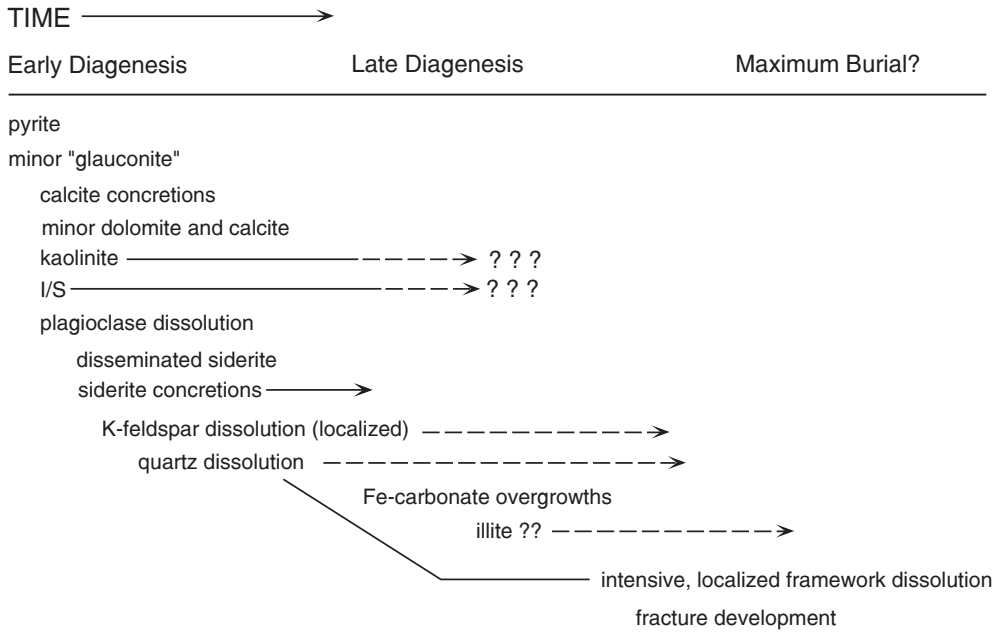

Figure 33. *Paragenetic summary of observed diagenetic processes.*

SOURCE ROCK POTENTIAL

The evaluation of sedimentary source rocks has become an integral component of hydrocarbon exploration and basin analysis. Clastic source rocks are commonly fine grained (> 50% silt- or clay-sized material) and can be defined on the basis of their organic matter content with a minimum value of about 0.5 wt% (Tissot and Welte, 1984). In the context of basinal petroleum systems, source rocks may be further subdivided into three types: *possible source rock*, that is, a sedimentary rock that may have generated hydrocarbons but is not yet evaluated; *effective source rock*, one that has generated and expelled hydrocarbons; and *potential source rock*, an immature sedimentary rock that is capable of generating hydrocarbons (Waples, 1984).

Distribution of organic matter

The present distribution of organic matter (OM) within the Colorado Group is controlled by depositional facies and diagenetic processes, including maturation and migration. The distribution of OM (as TOC) is shown for each formation on a basinal scale in Figure 34. Because of the small number of data points for the Westgate, Fish Scales, and Belle Fourche formations, the isopleths in these (and subsequent) figures should be considered tentative. The type of OM is also useful in evaluating the distribution and maturation of OM, and the HI values for each formation are shown in Figure 35. In addition, selected vertical profiles for TOC and HI are shown in Figures 36 and 37. The cross-section locations are shown in Figure 2.

The Westgate and Belle Fourche formations show broad areas of constant TOC content of between 1.5 to 2.0 wt%. In the Westgate, there is a slight increase in TOC in southern Alberta (Fig. 34). This increase occurs with an increase in HI (Fig. 35) and reflects the anomalously high TOC and HI values within the Westgate that occur in the area just east of the disturbed belt in the Keho Lake area (Fig. 37). A similar pattern is seen in the Fish Scales Formation (Fig. 34, 35). The Belle Fourche Formation shows an increase in HI values in the same area but no discernible increase in TOC. All three formations show a southwest to northeast decrease in HI values away from the disturbed belt.

In contrast, the Second White Specks shows an increase in both TOC and HI to the northeast. Where the sediments are immature, these values are interpreted as reflecting increased marine organic productivity in the well-developed marine environment that existed in the basin during Second White Specks deposition (Cadrin, 1992; Bloch et al., 1993; Schröder-Adams et al., 1996). Second White Specks organic matter was deposited primarily under anoxic bottom waters. Lower TOC and HI values in the other formations reflect more proximal marine sediments deposited under more shallow-water conditions. These environments were less productive and bottom waters were dominantly dysaerobic.

Maturation patterns

Maturation, as indicated by the pyrolysis temperature of maximum hydrocarbon generation (T_{max}), generally

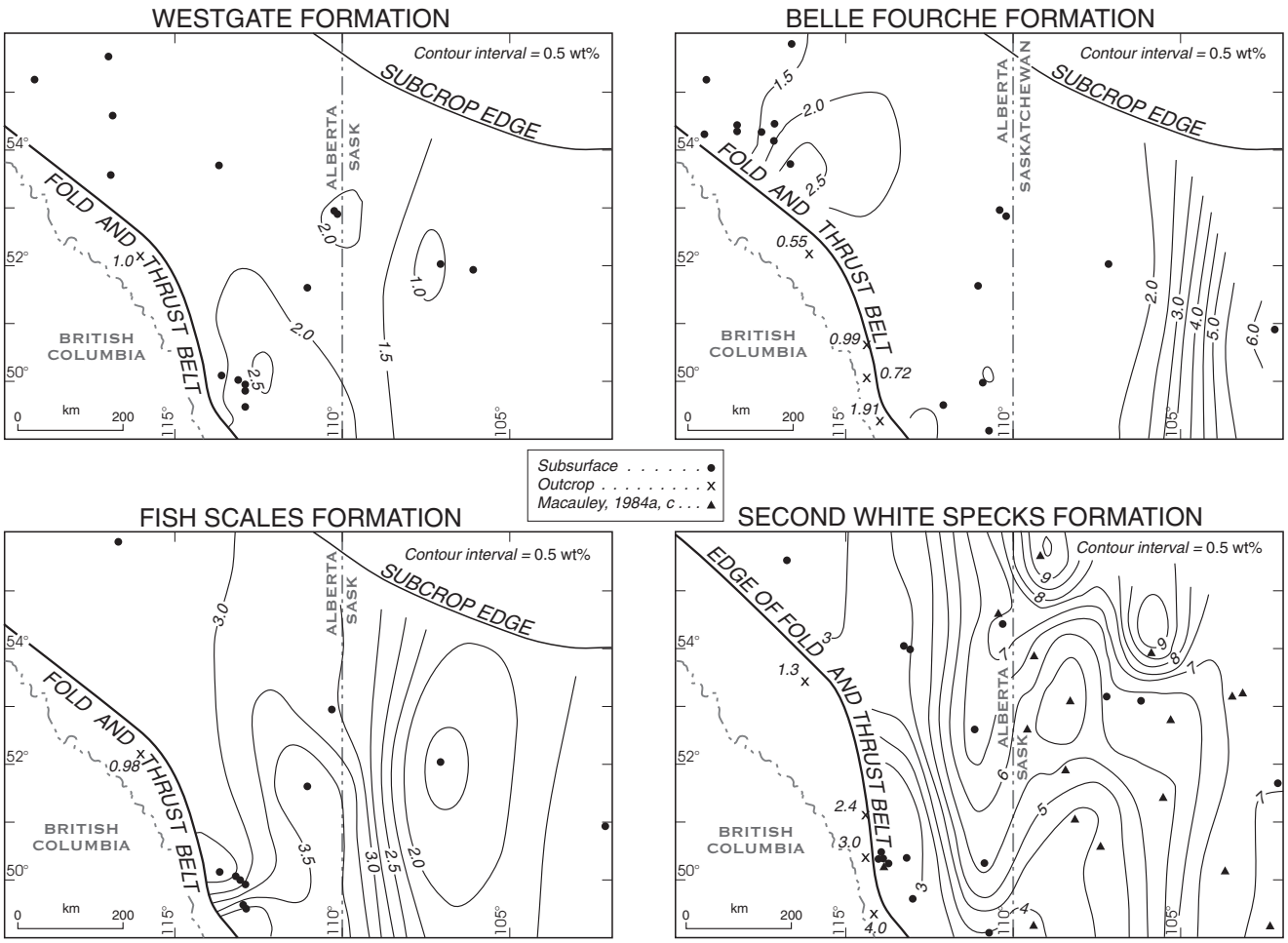

Figure 34. *Contour maps of TOC (wt%) values for the four formations of the lower Colorado Group.*

increases with depth (Fig. 38). Scatter in the data results from differential erosion during Tertiary uplift and variable mixtures of OM types. On a basinal scale, this translates into an east to west increase in maturation (Fig. 39). The onset of oil generation is generally considered to begin when T_{max} values reach 435°C (Tissot and Welte, 1984). This isotherm occurs at approximately 114° longitude in the Westgate and Belle Fourche formations and farther to the west, at about 115° longitude, for the Second White Specks. The data for the Fish Scales is too scattered to draw meaningful conclusions on a basinal scale, but in general, Fish Scales data are compatible with that from the other formations.

The occurrence of lower T_{max} values at equivalent depth in the Second White Specks suggests that oil generation may begin before the 435°C "threshold" is reached. Snowdon (1995) suggested that this "suppression" (lower T_{max} values at equivalent depth) may be related to a high sulphur content of the Second White Specks organic matter, similar to that documented in the Monterey Formation (Orr, 1986; Baskin and Peters, 1992; Zaback and Pratt, 1992). However, high sulphur in organic matter has not been documented in the Second White Specks. Further, sulphur incorporation into organic matter during early diagenesis occurs in iron-limited sediments (Sinninghe Damste and de Leeuw, 1990) and the Second White Specks is generally not iron-limited (Bloch et al., 1993). T_{max} suppression in the Second White Specks may result from the absence of refractory Type III or IV organic matter, which has higher T_{max} values (Peters, 1986). The degree of mixing of OM types within the Second White Specks, and resulting maturation characteristics, are largely a function of depositional facies and may be extremely variable (Mösle, 1995). The "suppression" within the Second White Specks appears to be about 10°C (Fig. 38) and, if oil generation is occurring at lower temperatures, then a much larger volume of Second White Specks sediment is in the oil window (Fig. 39).

The basinal scale data do not show a rapid increase in maturation just to the east of the fold and thrust belt in southwestern Alberta. Here, T_{max} values may increase by 15 to 20°C over a lateral distance of approximately 50 km

(Fig. 40). Steep maturation gradients are present in this hinge zone because of the increased burial depth resulting from loading by the Rocky Mountains directly to the west. The tectonically induced plunge in this zone also increases the potential for fracturing (Mallory, 1977).

Depositional controls on hydrocarbon distribution

Where Colorado Group sediments are immature (T_{max} < 435°C), the present distribution of OM is controlled by paleoenvironmental conditions and depositional processes. The entire Albian to Turonian interval east of approximately 114° longitude may be classified as potential source rock with significant internal variability. Isopleths generally trend north–south. This is, in part, an artifact of the location of the small number of sample control points that trend east–west. Additional data will undoubtedly complicate this simple picture. However, the north–south trends shown by the data are consistent with facies models of the Interior Seaway (Kauffman, 1977) that indicate a north–south strike for basinal facies that, to a large degree, are parallel to paleoshorelines.

The persistence of low HI values in central Saskatchewan is suggestive of a paleohigh in that area. However, the increased thickness of the Westgate Formation in the C.M.S. Vanscoy well (11-16-35-8W3, Fig. 29) indicates a depocentre from which this formation thins both to the east and the west. The thinning of the overlying units (Fish Scales, Belle Fourche, and Second White Specks) in this well suggest localized uplift in this area that occurred sometime in the Late Albian. The Morden Formation is not present in this area, and the Santonian First White Speckled Shale lies unconformably upon the Second White Specks, resulting in the single Speckled Shale of central Saskatchewan (Caldwell et al., 1978). This stratigraphic package, in contrast to those to the east and west, suggests the development of a localized topographic high in central Saskatchewan that developed over perhaps 2 m.y. in the Late Albian. The cause of this apparent basin-floor uplift remains elusive, but recent work (Leckie et al., in press) has

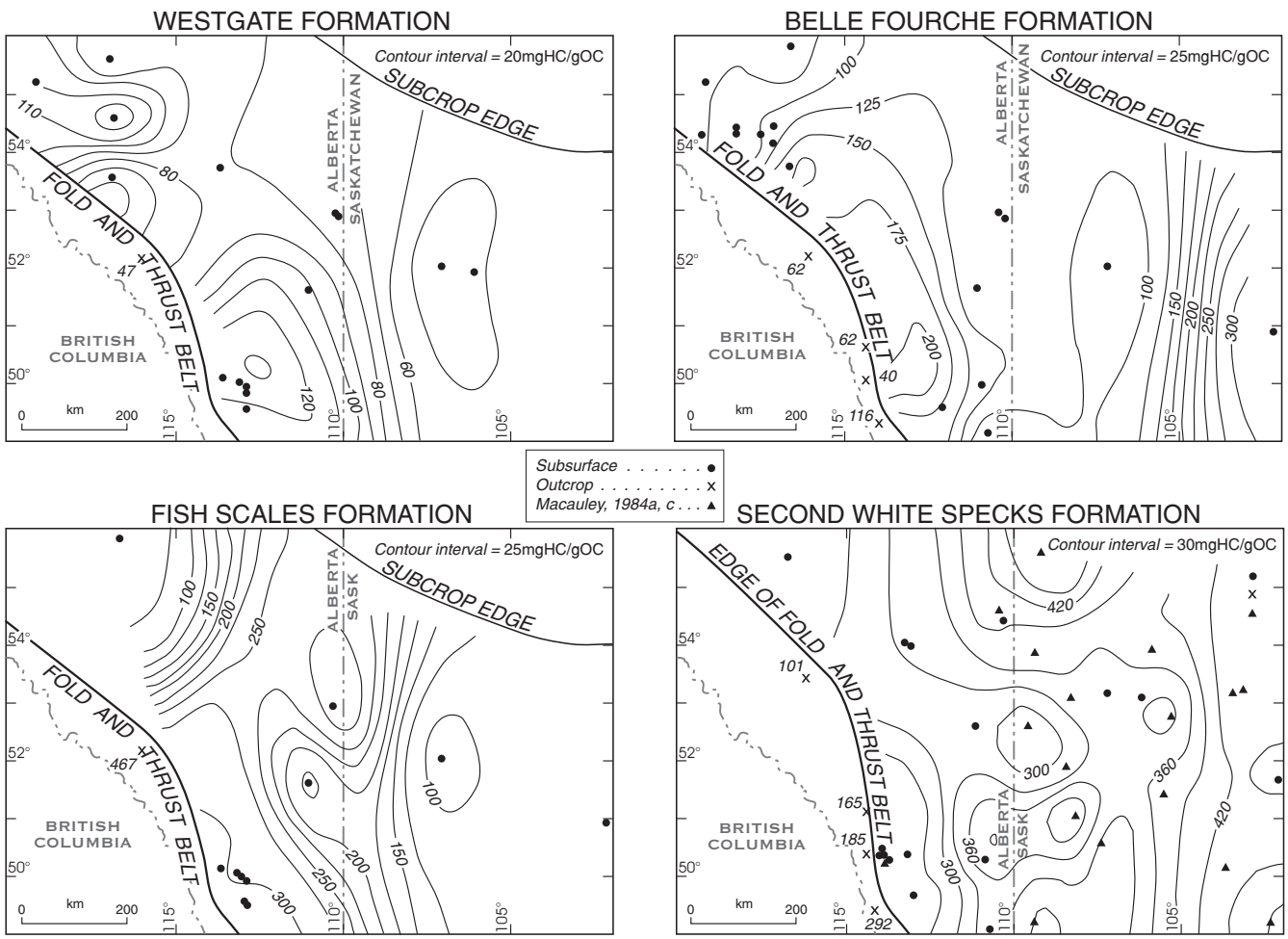

Figure 35. *Contour maps of Hydrogen Index (mgHC/gOC) values for the four formations of the lower Colorado Group.*

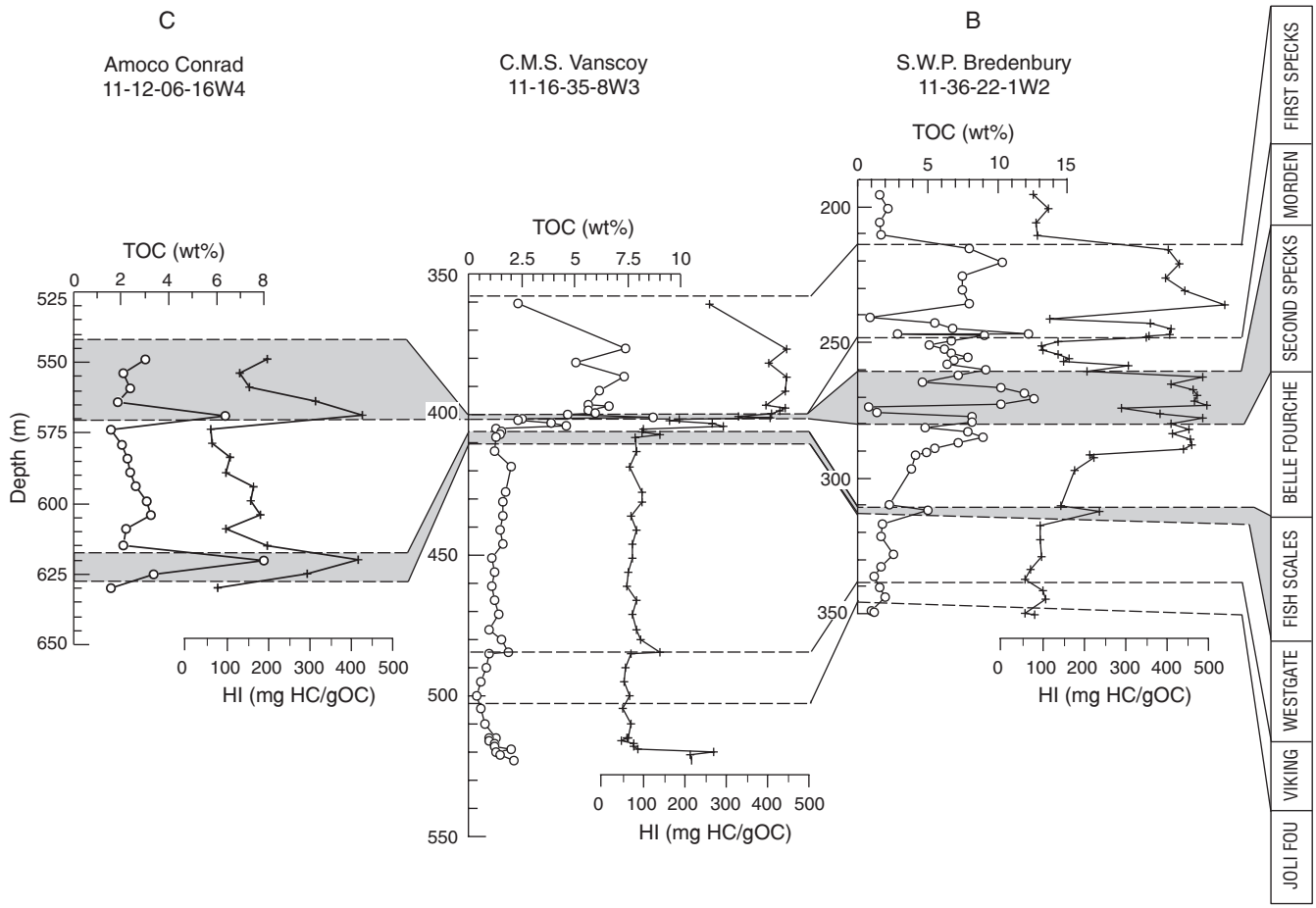

Figure 36. *TOC and HI profile B-C (see Figure 2).*

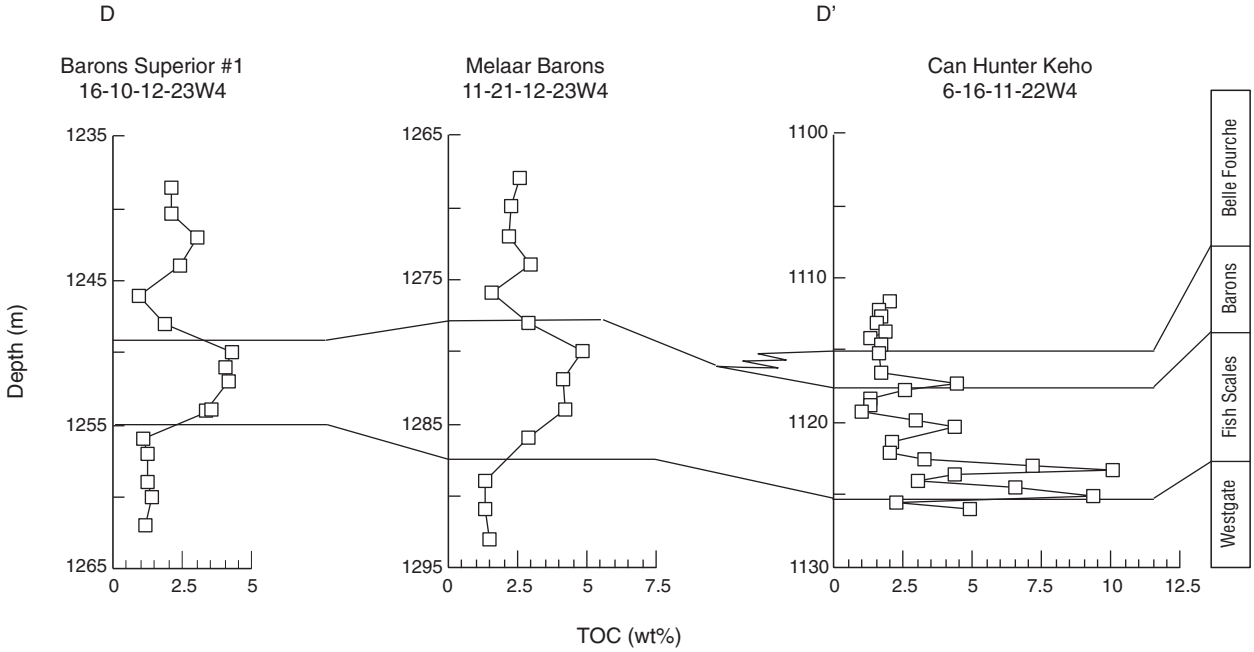

Figure 37. *TOC and HI profile D-D' in the Keho Lake area of southwestern Alberta (see Figure 2).*

documented the occurrence of kimberlites in central Saskatchewan that were emplaced at approximately 98 Ma. The complex internal geometry and compositional variability of this marine shale sequence indicate that the Cretaceous foreland basin was a dynamic depositional system and that source rocks may be much more heterogeneous than previously recognized.

The Second White Specks east of 114° longitude is a potential source rock and is the source of biogenic gas produced in some parts of southern Saskatchewan (Stasiuk and Goodarzi, 1988). The Westgate, Belle Fourche, and Fish Scales formations are also potential source rocks, but of a lesser quality. The greater abundance of Type III OM indicates that these formations are more gas prone.

Maturation effects

Primary (depositional) heterogeneous OM distribution is affected by maturation and diagenetic overprinting west of 114° longitude. The ratio of volatile hydrocarbons to the total hydrocarbons (S1/(S1+S2)) generated during pyrolysis, commonly called the production index (PI), provides information about the source of hydrocarbons within a sample and can discriminate between locally generated and migrated hydrocarbons or contamination.

Figures 41 to 44 show the PI (S1/(S1+S2)) plotted against T_{max} and depth for the four formations. PI values between 0.1 and 0.4 generally define the zone of oil generation (Tissot and Welte, 1984; Peters, 1986). On a plot of PI versus T_{max},

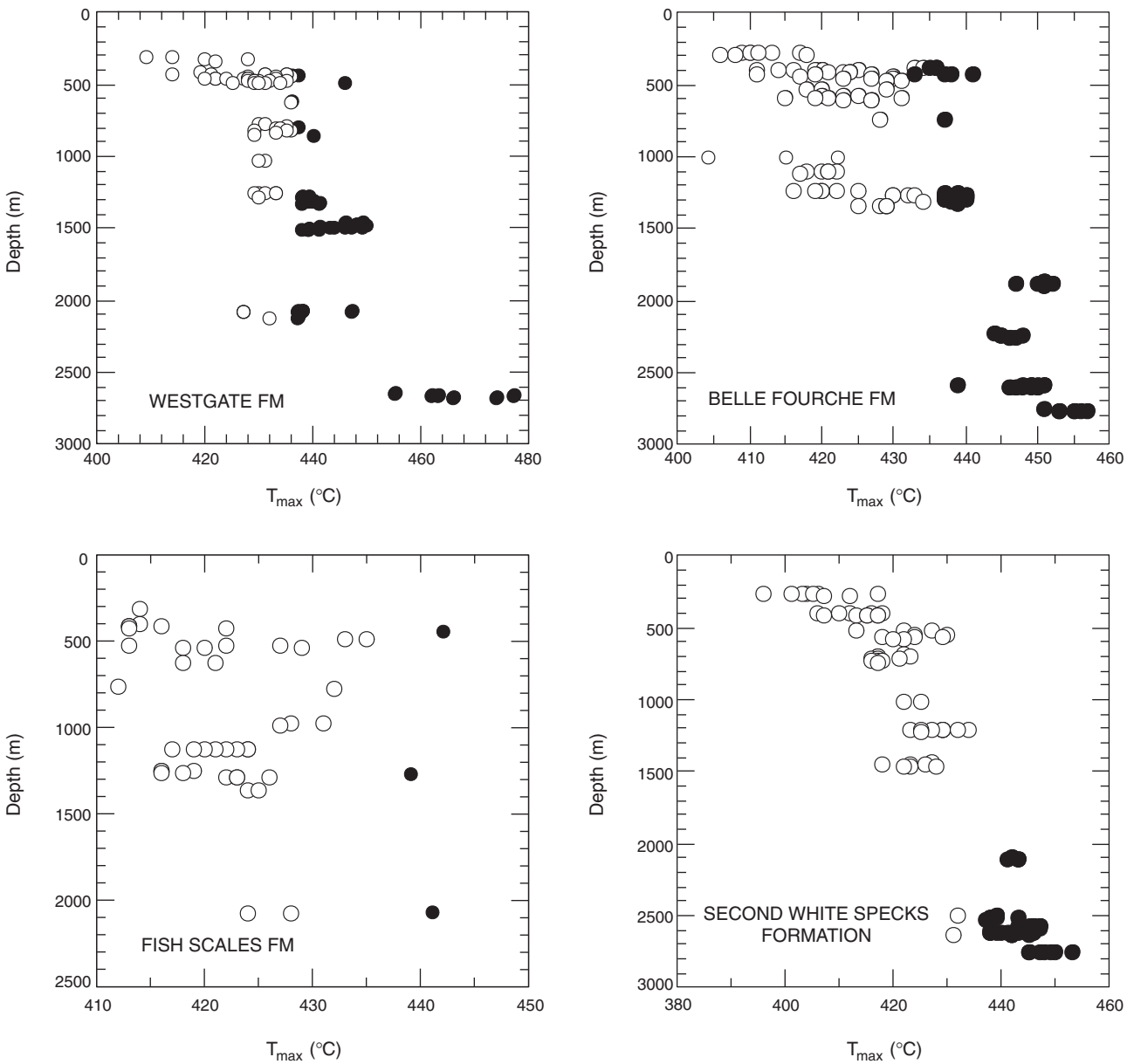

Figure 38. *T_{max} versus depth for the four formations of the lower Colorado Group. Open circles are T_{max} values <435°C; filled circles >435°C (see Table 2).*

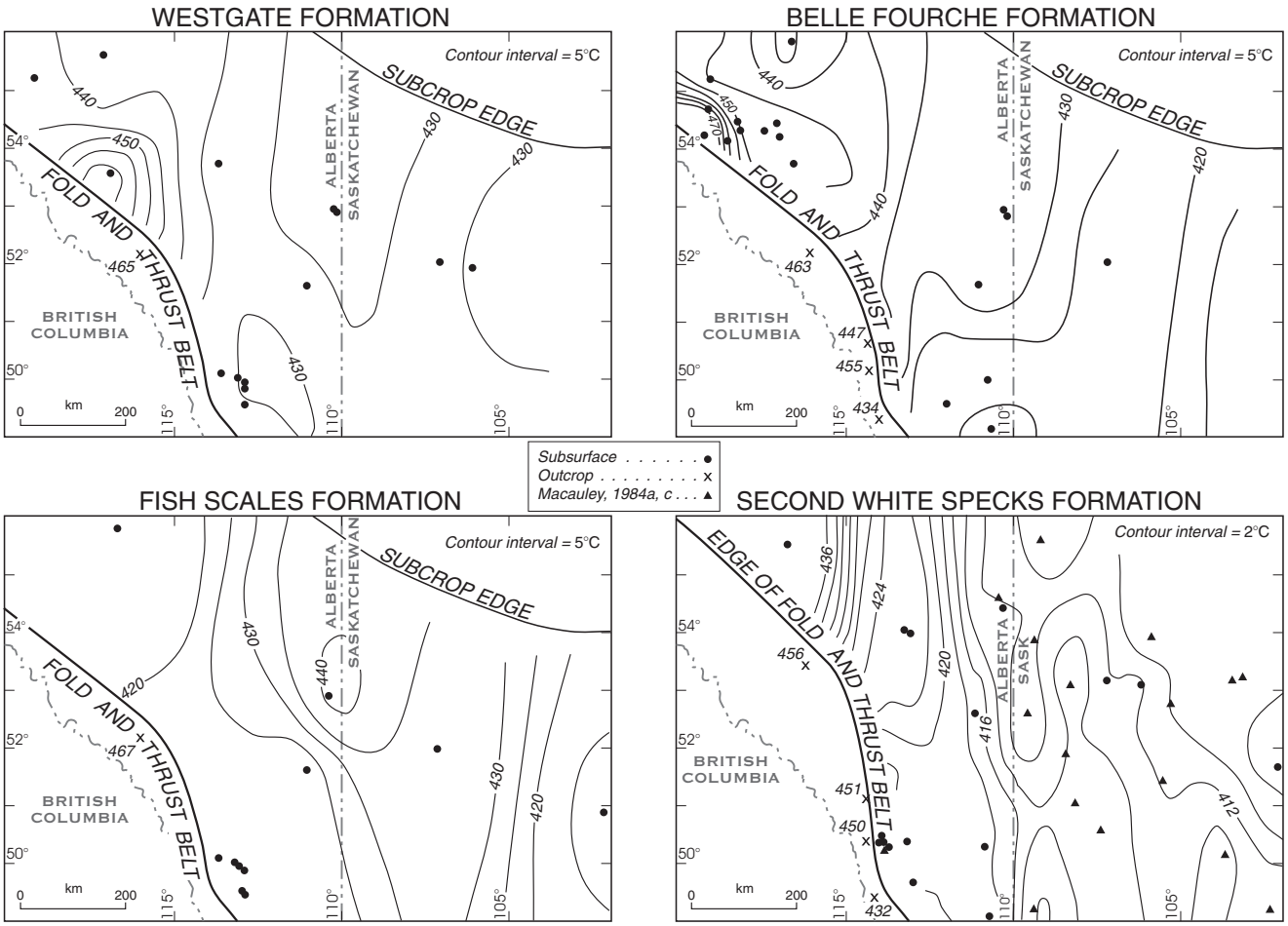

Figure 39. *T_{max} contour maps of the four formations of the lower Colorado Group.*

immature samples will plot in an area confined by values of < 0.1 and 435°C, respectively, and mature samples will plot at greater values. The Belle Fourche (Fig. 43) and Second White Specks (Fig. 44) formations show this relationship fairly well. However, in the Westgate Formation, a large number of immature samples plot at PI values greater than 0.1 (Fig. 41). These samples either contain migrated hydrocarbons or are contaminated with drilling lubricants.

There are a large number of samples from the Amoco Youngstown B-1 (6-34-30-8W4) well (Table 1) at approximately 700 m depth in both the Westgate and Second White Specks formations that are contaminated with drilling lubricant. This is confirmed by GC–GCMS data (M. Fowler, pers. comm.). Within the Westgate Formation, the remainder of samples with T_{max} less than 435°C and PI greater than 0.1 are primarily from two cores; the Anderson Husky Roros (10-35-45-2W4) and Imperial Kathleen #1 (5-1-77-20W5). In the case of the former, there is no evidence to suggest contamination and the high PI values are attributed to small amounts of migrated hydrocarbons. Many of these samples are from the basal Westgate and the hydrocarbons may have "leaked" up from the underlying Viking Formation. TOC and HI values are slightly elevated in the basal Westgate (see Bloch et al., 1993; their fig. 10), consistent with this interpretation.

The samples from the Imperial Kathleen #1 well, spudded in 1951, are taken from 1 inch diamond drill core. Water-based drilling fluids were used and therefore the possibility of contamination by hydrocarbons is small, but cannot be completely ruled out. However, a nearby well (Imperial Wembley; see Table 1) contains OM that is marginally mature (T_{max} to 440°C) with PI values to about 0.2. Together, these wells form a local trend distinct from other wells (Fig. 45) and suggest the presence of migrated hydrocarbons. The amount of migrated oil is small because the TOC (Fig. 34) and HI (Fig. 35) values show no significant increase from average formation values.

Immature samples at depths greater than 1000 m with PI values greater than 0.1 are also anomalous (Fig. 41). The presence of migrated hydrocarbons in mature samples lowers the T_{max} value (Peters, 1986). These samples are from wells located just west of Keho Lake (see Fig. 2). In these cores, visible oil-staining has been documented, particularly

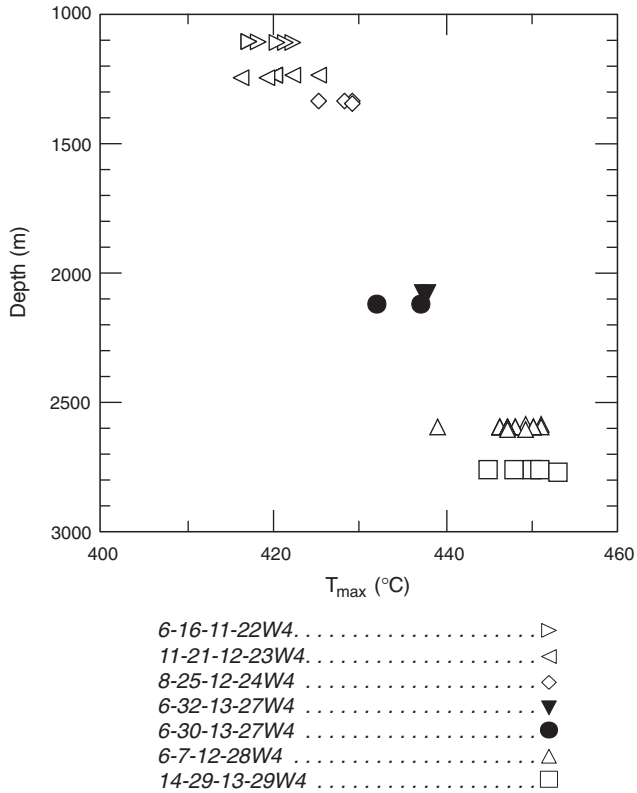

Figure 40. *T_{max} versus depth of Belle Fourche (open symbols) and Westgate (filled symbols) formations just west of the Keho Lake area (see Fig. 2 for location).*

in the Fish Scales Formation. Samples from the same cores characterized as immature occur at depth in the Fish Scales (Fig. 42), Belle Fourche (Fig. 43), and Second White Specks (Fig. 44). These data are interpreted as representing the presence of pervasive migrated oil through the section. Anomalously high TOC and HI values in the Westgate (Fig. 37) further support this interpretation.

The presence of migrated hydrocarbons in the Keho Lake area, and perhaps in the extreme northwest of the study area, affects regional patterns of hydrocarbon distribution, as shown in the HI and, to a lesser extent, the TOC contour maps. The Westgate and Fish Scales TOC maps (Fig. 34) show slightly higher values, and the HI values show a marked increase towards the fold and thrust belt that centers on the Keho Lake area. This is opposite to "normal" source rock trends that show a depletion in TOC and HI values with increasing maturity (Burtner and Warner, 1984). This characteristic trend is seen to the west of the fold and thrust belt where there is a distinct south to north increase in maturity (Fig. 39). The Second White Specks shows a "normal" source rock trend, in contrast to the other formations (Fig. 34, 35), where areas of higher maturity show a loss in hydrocarbon abundance and quality.

The Second White Specks has been identified as an effective source rock (Macauley, 1984a; Brooks et al., 1991; Creaney and Allan, 1992) and the regional trends shown herein suggests hydrocarbon generation has occurred west of 114° longitude. The enhanced stratigraphic resolution employed in this study indicates that migrated hydrocarbons, perhaps sourced from the Second White Specks, have infiltrated other shale units of the Colorado Group. This infiltration is localized areally and stratigraphically, occurring primarily along contacts with more permeable, intercalated sandstones (Barons, Viking Formation) or in siltstone-rich horizons within the shales. The regional

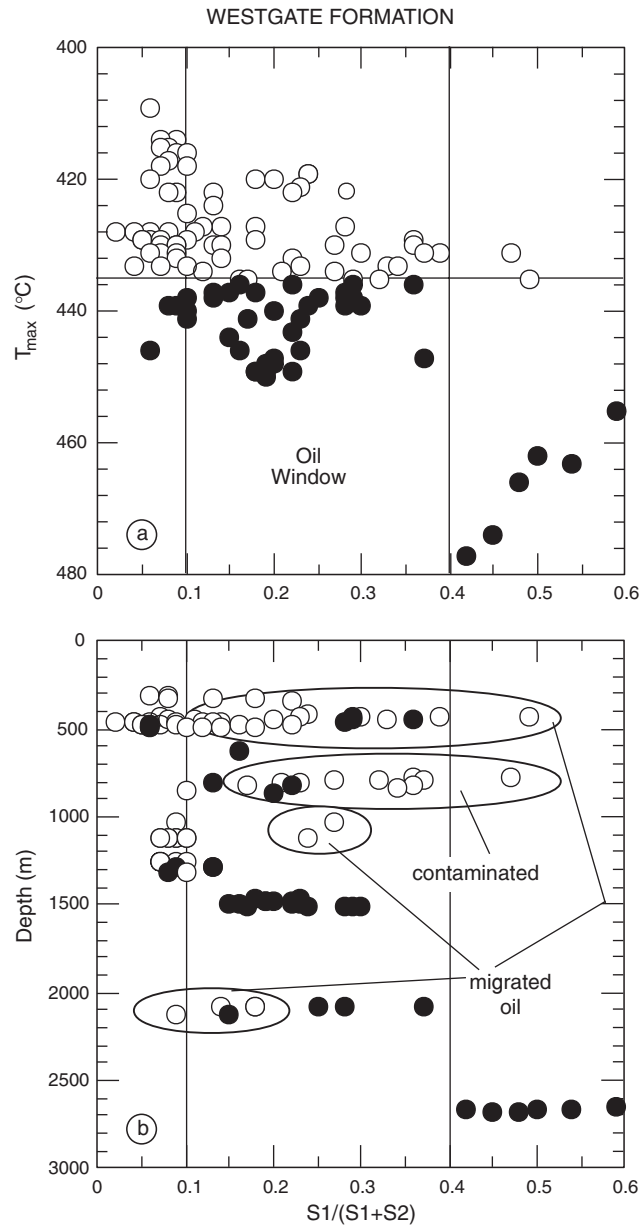

Figure 41. *Production index (S1/(S1+ S2)) versus T_{max} (a) and depth (b) for the Westgate Formation. Open circles are T_{max} values < 435°C; filled circles > 435°C (see Table 2). See text for discussion.*

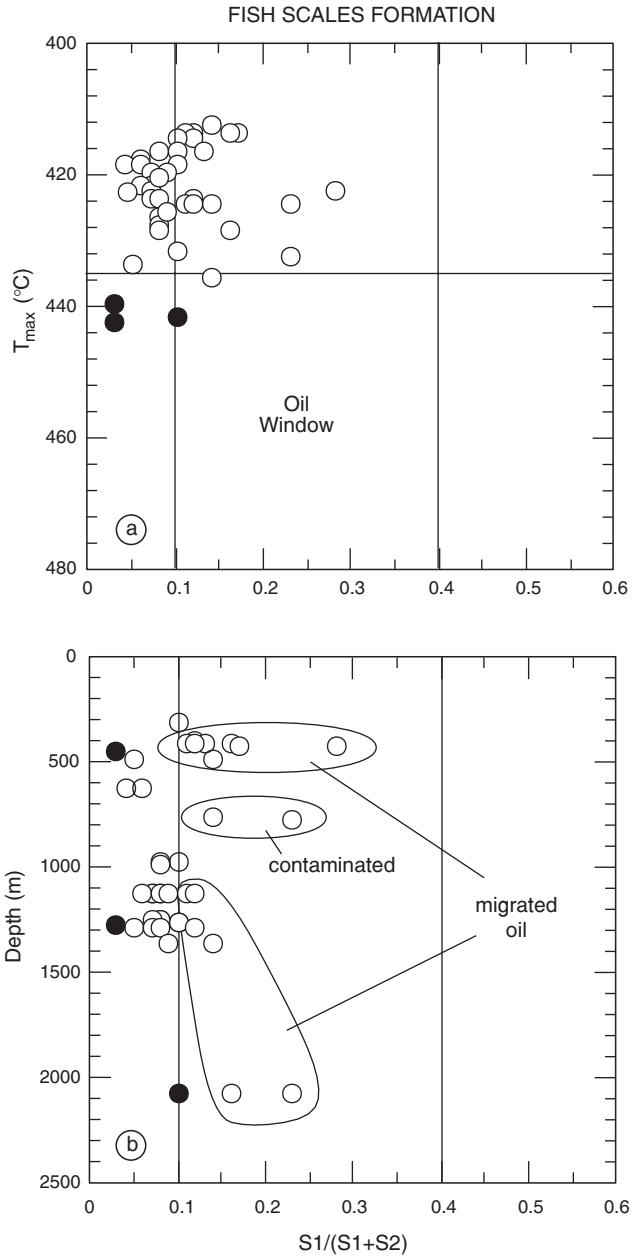

Figure 42. *Production index (S1/(S1+ S2)) versus T_{max} (a) and depth (b) for the Fish Scales Formation. Open circles are T_{max} values < 435°C; filled circles > 435°C (see Table 2). See text for discussion.*

patterns of hydrocarbon distribution indicate that migration has occurred, or is occurring, in the area west of Keho Lake and in northwestern Alberta on the southern flank of the Peace River Arch. Both of these areas are adjacent to the fold and thrust belt where maturation indices rapidly increase and most of the studied interval is within the oil window. The updip and cross-formation movement of evolved hydrocarbons within the Colorado Group is similar to other source rock studies that indicate source rock loss and accumulation of hydrocarbons in more porous and permeable units of basin-fill sediments (Burtner and Warner, 1984; Hagen and Surdam, 1984). The localization of hydrocarbon migration argues against widespread fluid movement through thick sections of fine grained sediment with low porosity and poor permeability. The areas that apparently contain migrated hydrocarbons are within or adjacent to tectonically disturbed belts where rapid changes in plunge or areas of overthrusting are common. Fractures are also associated with these zones. Current production

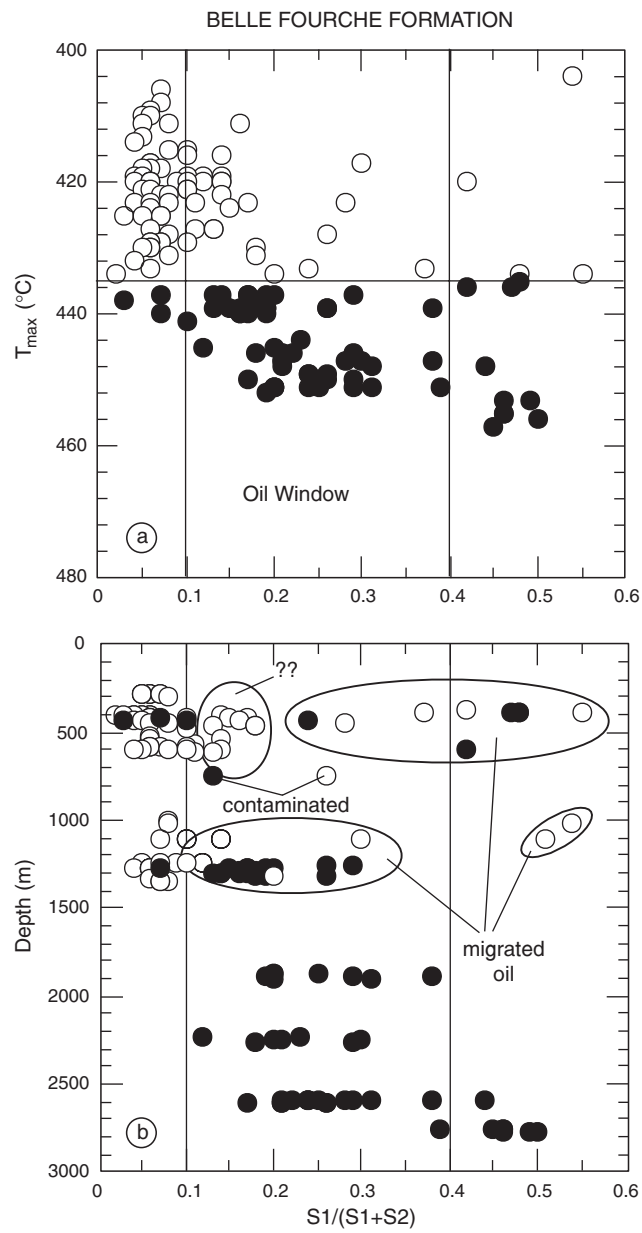

Figure 43. *Production index (S1/(S1+ S2)) versus T_{max} (a) and depth (b) for the Belle Fourche Formation. Open circles are T_{max} values < 435°C; filled circles > 435°C (see Table 2). See text for discussion.*

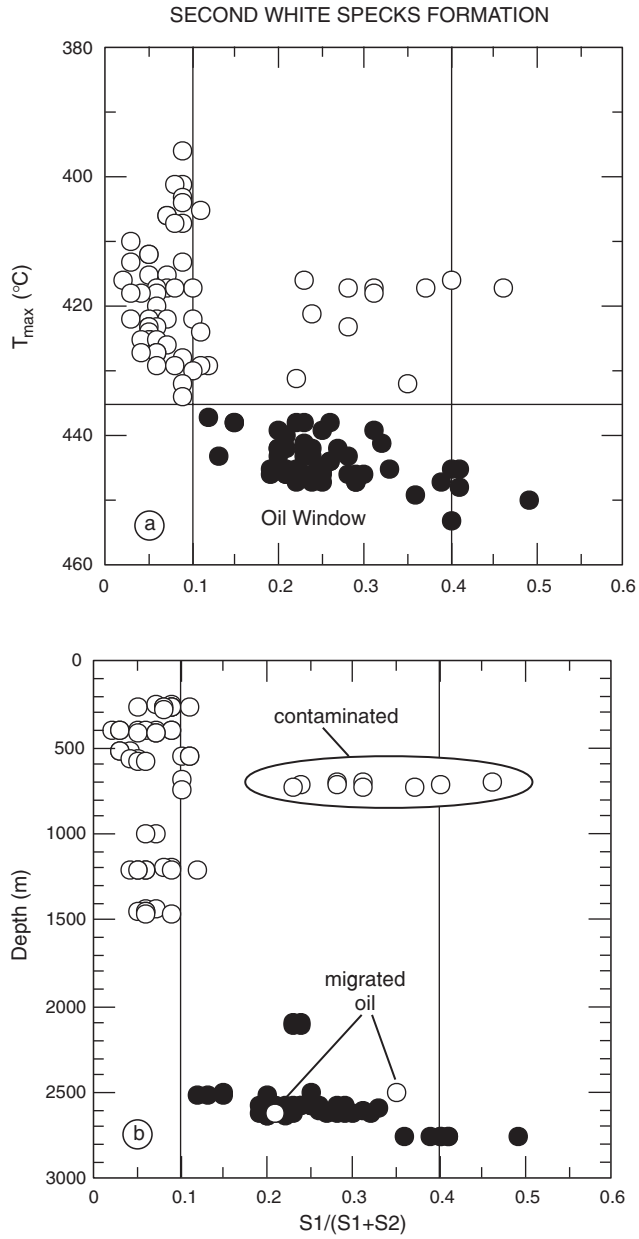

Figure 44. *Production index (S1/(S1+ S2)) versus T_{max} (a) and depth (b) for the Second White Specks Formation. Open circles are T_{max} values < 435°C; filled circles > 435°C (see Table 2). See text for discussion.*

from Colorado Group shales occurs in areas adjacent to this zone where there is significant structural deformation of the basin-fill sediments (Portigal et al., 1989). These circumstances suggest a fracture control on the migration and production of hydrocarbons from the Second White Specks Formation.

RESERVOIR POTENTIAL

Source rocks may also be considered reservoirs when hydrocarbons are extracted from them directly. Biogenic gas is commonly extracted from potential source rocks. With advances in completion and extraction technology, some effective source rocks may also be economic liquid and gaseous hydrocarbon reservoirs (Mallory, 1977). Therefore, the study of source rock reservoir characteristics, analogous to traditional reservoir rock (sandstone and carbonates) studies, should also be included in basin analysis, petroleum system, and hydrocarbon exploration studies.

The low porosity and permeability of shales result from the high proportion of clay minerals and a dominantly matrix-supported fabric that compacts significantly, resulting in very poor reservoir properties. Therefore, economic production generally requires the occurrence of significant fracture porosity and permeability. To develop and sustain a fracture system, shales must behave in a brittle manner. Economically viable fractured shale reservoirs include the Mancos, Niobrara, and Mowry (Mallory, 1977),

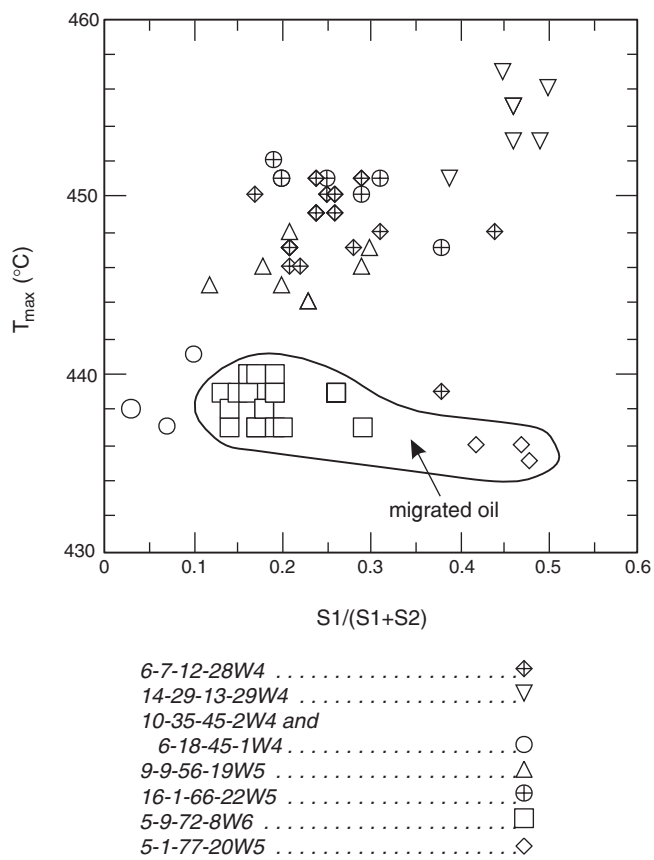

Figure 45. *Production Index (S1/(S1+S2)) versus T_{max} for the Westgate Formation from selected wells.*

Monterey (Graham and Williams, 1985), Bakken (Meissner, 1978), and Austin Chalk formations (Fritz et al., 1991). These units contain a high proportion of calcareous or siliceous material that imparts brittle characteristics to the rock. The only unit within the Colorado Group succession that contains considerable amounts of carbonate is the Second White Specks Formation (Table 9) and this unit is a proven producer (Portigal et al., 1989). Within the proposed stratigraphic nomenclature for the Colorado Group, considerable production identified to come from the "Second White Specks" actually comes from the siltstone interval in the uppermost Belle Fourche Formation. The relative importance of fracture porosity in production from calcareous and silt-rich intervals is not well understood but the variable and localized nature of "Second White Specks" production suggests that fracture porosity is a significant component. The distinct lithological (high proportion of quartz silt in the Belle Fourche) and mineralogical (calcareous nature of the Second White Specks) characteristics of the production interval within the Colorado Group suggest that mineralogy most likely is a factor in economic production from these units.

The relative effects of depositional and diagenetic controls on mineralogy and resulting rheological properties of Colorado Group shales are difficult to discern. Caritat et al. (1994a) demonstrated that diagenetic trends in mineralogy mimic depositional signals in the Belle Fourche Formation and this is probably applicable to other Colorado Group shale units. In the Belle Fourche, the illite content of I/S increases from east to west concomitant with an increase in maturity. However, the western portion of the basin is also the most proximal to the deltaic sediments of the equivalent Dunvegan Formation. These sediments are expected to contain a higher proportion of detrital illite as well as coarser grained quartz and feldspars. Therefore, depositional as well as diagenetic controls on mineralogy must be considered.

It is recognized from simple mass balance considerations that the formation of illite or illitic I/S from smectite or smectitic I/S results in the production of excess silica:

$$Na_{.28}K_{.18}Ca_{.04}[Al_{1.36}Fe^{3+}{}_{.34}Mg_{.33}]Si_{3.69}Al_{.31}O_{10}(OH)_2 + 0.4K^{+} + 0.37Al^{3+} \rightarrow \quad (6)$$

$$Na_{.28}K_{.58}Ca_{.04}[Al_{1.42}Fe^{3+}{}_{.20}Mg_{.33}]Si_{3.38}Al_{1.62}O_{10}(OH)_2 + 0.31Si^{4+} + 0.14Fe^{3+}$$

as shown by these mixed-layer clay compositions from the Belle Fourche Formation (Caritat et al., 1994a). This silica commonly precipitates as fine grained quartz within the matrix (see Caritat et al., 1994a; their fig. 10) or may contribute to quartz overgrowths that occur within the shale (Bloch and Hutcheon, 1992). Other studies have suggested that this silica is exported to adjacent sandstones where it may contribute to quartz cementation (Sibley and Blatt, 1976). The precipitation of authigenic quartz or quartz cement within the shale, however, will contribute to lithification and may enhance the brittle characteristics of the rock. This could be a factor in fracture formation within shales.

Some outcrop (Plate 19b) and core fracture surfaces show oil-staining. In outcrop, it is not clear whether the oil is locally sourced or migrated from downdip. In the subsurface, however, it is likely that fracture porosity is a critical component of liquid hydrocarbon migration and production in the Second White Specks Formation. It is also important to note that fracturing is observed only in areas where Colorado Group shales are considered mature (see below) and therefore have undergone a moderate to perhaps advanced degree of diagenetic alteration. The estimated depth (~ 2 km) and timing of fracture formation suggests that fractures developed before significant hydrocarbon generation or that fractures developed updip of mature source rocks. Fracture systems developing at this time could contribute to hydrocarbon migration and would provide storage capacity for generated hydrocarbons.

REFERENCES

Abbey, S.
1980: Studies in "standard samples" for use in the general analysis of silicate rocks and minerals - Part 6: 1979 edition of "useable" values. Geological Survey of Canada, Paper 80-14, 30 p.

Abercrombie, H.J.
1988: Water-rock interaction during diagenesis and thermal recovery, Cold Lake, Alberta. Unpublished Ph.D. thesis. The University of Calgary, Calgary, Alberta. 183 p.

Allan, J. and Creaney, S.
1988: Sequence stratigraphic control of source rocks: Viking - Belly River system. *In* Sequences, Stratigraphy, Sedimentology: Surface and Subsurface, D.P. James and D.A. Leckie (eds.). Canadian Society of Petroleum Geologists, Memoir 15, 575 p.

1991: Oil families of the Western Canada basin. Bulletin of Canadian Petroleum Geology, v. 39, p. 107-122.

Arthur, M.A., Dean, W.E., Pollastro, R.M., Claypool, G.E., and Scholle, P.A.
1985: A comparative geochemical study of two transgressive pelagic limestone units, Cretaceous western interior basin, U.S. *In* Fine-grained Deposits of Cyclic Sedimentary Processes, L.M. Pratt, E.G. Kauffman, and F.B. Zelt (ed.). Society of Economic Paleontologists and Mineralogists, 1985 midyear meeting, Golden, CO, Field Trip Guidebook 9.

Baedecker, P.A.
1987: Methods for geochemical analysis. United States Geological Survey, Bulletin 1770.

Bailey, S.W.
1982: Nomenclature for regular interstratifications. American Mineralogist 67, p. 394-398.

Ballantyne, B. and Harris, D.
1995: Alberta orientation: the big picture. *In* The Fourth Annual Calgary Mining Forum, Program and Abstracts.

Barclay, J.E. and Smith, D.G.
1992: Western Canada foreland basin oil and gas plays. *In* Foreland Basins and Fold Belts, R.W. Macqueen and D.A. Leckie (ed.). American Association of Petroleum Geologists, Memoir 55, p. 191-228.

Barss, M.S. and Williams, G.L.
1973: Palynology and nannofossil processing techniques. Geological Survey of Canada, Paper 73-26, 25 p.

Baskin, D.K. and Peters, K.E.
1992: Early generation characteristics of a sulfur-rich Monterey kerogen. American Association of Petroleum Geologists, Bulletin, v. 76, p. 1-13.

Beaumont, E.A.
1984: Retrogradational shelf sedimentation: Lower Cretaceous Viking Formation, central Alberta. *In* Siliciclastic Shelf Sediments, R.W. Tillman and C.T. Siemers (ed.). Society of Economic Paleontologists and Mineralogists, Special Publication 34, p. 163-177.

Bergquist, H.R.
1966: Micropaleontology of the Mesozoic rocks of Northern Alaska. U.S. Geological Survey Professional Paper 302-D, p. 93-227.

Berner, R.A.
1970: Sedimentary pyrite formation. American Journal of Science, v. 268, p. 1-23.

1980: Early Diagenesis. A Theoretical Approach. Princeton University Press, Princeton, N.J., 241 p.

Bhattacharya, J. and Walker, R.G.
1991: Allostratigraphic subdivision of the Upper Cretaceous Dunvegan, Shaftesbury and Kaskapau formations in the northwestern Alberta subsurface. Bulletin of Canadian Petroleum Geology, v. 39, p. 145-164.

Bloch, J. and Hutcheon, I.E.
1992: Shale diagenesis: A case study from the Albian Harmon Member (Peace River Formation), Western Canada. Clays and Clay Minerals, v. 40, no. 6, p. 682-699.

Bloch, J. and Leckie, D.A.
1993: Rock-Eval data of the Cretaceous Colorado Group, Western Canada Sedimentary Basin. Geological Survey of Canada, Open File Report # 2676, 22 p.

Bloch, J., Schröder-Adams, C., Leckie, D.A., McIntyre, D.J., Craig, J., and Staniland, M.
1993: Revised stratigraphy of the lower Colorado Group (Albian to Turonian), Western Canada. Bulletin of Canadian Petroleum Geology. v. 42, p. 325.

Brideaux, W.W.
1971: Palynology of the Lower Colorado Group, central Alberta, Canada. I. Introductory remarks, geology, and microplankton studies. Palaeontographica, Abt. B, Band 135, Liefg. 3-6, p. 53-114.

Brideaux, W.W. and McIntyre, D.J.
1975: Miospores and microplankton from Aptian-Albian rocks along Horton River, District of Mackenzie. Geological Survey of Canada, Bulletin 252, 85 p.

Brooks, P.W., Macqueen, R.W., Fowler, M.G., and Riediger, C.L.
1991: Source rock organic geochemistry and oil-source correlations, Western Canada Basin. 1991 CSPG Convention Abstracts, p. 37.

Burtner, R.L. and Warner, M.A.
1984: Hydrocarbon generation in Lower Cretaceous Mowry and Skull Creek shales of the northern Rocky Mountain area. *In* Hydrocarbon Source Rocks of the Greater Rocky Mountain Region, J. Woodward, F.F. Meissner, and J.L. Clayton (ed.). Rocky Mountain Association of Geologists, Symposium Volume, 1984. p. 449-467.

Cadrin, A.J.
1992: Geochemistry and palaeoenvironmental reconstruction of the Cretaceous Greenhorn marine cyclothem in the Western Interior Basin of Canada. University of Saskatchewan, Saskatoon, Ph.D. Thesis. 192 p.

Caldwell, W.G.E. (ed.)
1975: The Cretaceous System in the Western Interior of North America. Geological Association of Canada Special Paper Number 13, 666 p.

Caldwell, W.G.E., Diner, R., Eicher, D.L., Fowler, S.P., North, B.R., Stelck, C.R., and von Holdt Wilhelm, L.
1993: Foraminiferal Biostratigraphy of Cretaceous Marine Cyclothems. *In* Evolution of the Western Interior Basin, W.G.E. Caldwell, and E.G. Kauffman (ed.). Geological Association of Canada, Special Paper 39, p. 477-520.

Caldwell, W.G.E. and North B.R.
1984: Cretaceous stage boundaries in the southern Interior Plains of Canada. Bulletin of the Geological Society of Denmark, v. 33, p. 57-69.

Caldwell, W.G.E., North, B.R., Stelck,C.R., and Wall, J.H.
1978: A foraminiferal zonal scheme for the Cretaceous System in the Interior Plains of Canada. *In* Western and Arctic Canadian Biostratigraphy, C.R. Stelck and B.D.E. Chatterton (ed.). Geological Association of Canada, Special Paper Number 18, p. 495-575.

Campbell, F. A. and Oliver, T.A.
1968: Mineralogic and chemical composition of Ireton and Duvernay formations, central Alberta. Bulletin of Canadian Petroleum Geology, v. 16, p. 40-63.

Canfield, D.E., Raiswell, R., Westrich, J.T., Reaves, C.M., and Berner, R.A.
1986: The use of chromium reduction in the analysis of reduced inorganic sulfur in sediments and shales. Chemical Geology, v. 54, p. 149-155.

Caritat, P. de, Bloch. J., Hutcheon, I.E., and Longstaffe, F.J.
1994a: Compositional trends of a Cretaceous foreland basin shale (Belle Fourche Formation, Western Canada Sedimentary Basin) diagenetic and depositional controls. Clay Minerals, v. 29, p. 503-526.

1994b: LPNORM: A linear programming normative analysis code. Computers & Geosciences, v. 20, p. 313-347.

Carothers, W.W., Adami, L.H., and Rosenbauer, R.J.
1988: Experimental oxygen isotope fractionation between siderite-water and phosphoric acid liberated CO_2-siderite. Geochimica et Cosmochimica Acta, v. 52, p. 2445-2450.

Claypool, G.E. and Kaplan, I.R.
1974: The origin and distribution of methane in sediments. Plenum Press, New York, p. 99-139.

Cobban, W.A. and Kennedy, W.J.
1989: The ammonite *Metengonoceras* Hyatt, 1903, from the Mowry Shale (Cretaceous) of Montana and Wyoming. United States Geological Survey, Bulletin, 1878-L, 11 p.

Cobban, W.A., Merewether, E.A., Fouch, T.D., and Obradovich, J.D.
1994: Some Cretaceous shorelines in the Western Interior of the United States. *In* Mesozoic Systems of the Rocky Mountain Region, U.S.A., M.V. Caputo, J.A. Peterson, and K.J. Franczyk (ed.). Society for Sedimentary Geology (SEPM), Rocky Mountain Section, Denver, CO, U.S.A., p. 393-413.

Cobban, W.A. and Reeside, J.B.
1962: Correlation of the Cretaceous formations of the Western Interior of the United States. Bulletin of the Geological Society of America, v. 63, p. 1011-1044.

Creaney, S. and Allan, J.
1990: Hydrocarbon generation and migration in the Western Canada Sedimentary Basin. *In* Classic Petroleum Provinces, J. Brooks (ed.). Geological Society Special Publication No. 50, The Geological Society, London, p. 189-202.

1992: Petroleum systems in the Foreland Basin of Western Canada. *In* Foreland Basins and Fold Belts, R.W. Macqueen and D.A. Leckie (ed.). American Association of Petroleum Geologists, Memoir 55, p. 279-308.

Cumbaa, S.L.
1993: Pre-chalk fishes from the Western Interior Sea, North America. Mesozoic Fishes Systematics and Palaeoecology 1993, Jura-Museum Eichstätt, Germany, Abstracts.

Cumbaa, S.L., Tokaryk, T.T., and Jarzen, D.M.
1992: Paleoecology of a Late Cretaceous nearshore marine environment, Pasquia Hills, Saskatchewan. Canadian Paleontology Conference Ottawa 1992, Program and Abstracts, p. 11.

Dawson, G.M.
1874: Note on the occurrence of foraminifera, coccoliths etc. in the Cretaceous rocks of Manitoba. The Canadain Naturalist, v. 7, no. 5, p. 252-257.

1881: Report on an exploration from Port Simpson on the Pacific Coast to Edmonton on the Saskatchewan, embracing a portion of the northern part of British Columbia and the Peace River country. Geological Survey of Canada, Report on Progress 1879-1880, Part B, p. 1-77.

1886: On certain borings in Manitoba and the Northwest Territory. Proceedings and Transactions of the Royal Society of Canada, v. 4, sec. IV, p. 85-99.

Dixon, J.
1993: Regional unconformities in the Cretaceous of northwest Canada. Cretaceous Research, v. 14, p. 17-38.

Dixon, J., McNeil, D.H., Dietrich, J.R., and McIntyre, D.J.
1989: Barremian to Albian stratigraphy, Tuktoyaktuk Peninsula and South Mackenzie Delta, Northwest Territories. Geological Survey of Canada, Paper 89-15, 16 p.

Doerenkamp, A., Jardine, S., and Moreau, P.
1976: Cretaceous and tertiary palynomorph assemblages from Banks Island and adjacent areas (N.W.T.). Bulletin of Canadian Petroleum Geology, v. 24, p. 272-317.

Edwards, A.R.
1963: A preparation technique for calcareous nannoplankton. Micropaleontology, v. 9, p. 103-104.

Eicher, D.L.
1967: Foraminifera from Belle Fourche Shale and equivalents, Wyoming and Montana. Journal of Paleontology, v. 41, no. 1, p. 167-188.

Eicher, D.L.
1969: Cenomanian and Turonian planktonic foraminfera from the Western Interior of the United States. *In* Proceedings of the First International Conference on Planktonic Microfossils, Geneva, 1967, Leiden E. J. Brill, p. 163-174.

Eicher, D.L. and Diner, R.
1985: Foraminifera as indicators of water mass in the Cretaceous Greenhorn Sea, Western Interior. *In* Fine-grained deposits of Cyclic Sedimentary Processes, L.M. Pratt, E.G. Kauffman, and F.B. Zelt (ed.). Society of Economic Paleontologists and Mineralogists, 1985 midyear meeting, Golden, CO, Field Trip Guidebook 9, p. 60-71.

1989: Origin of the Cretaceous Bridge Creek Cycles in the Western Interior, United States. Palaeogeography, Palaeoclimatology, Palaeoecology, v. 74, p. 127-146.

Eicher, D.L. and Worstell, P.
1970: Cenomanian and Turonian foraminifera from the Great Plains, United States. Micropaleontology, v. 16, no. 3, p. 269-324.

Ekdale, A.A., Bromley, R.G., and Pemberton, S.G.
1984: Ichnology - Trace Fossils in Sedimentology and Stratigraphy. Society of Economic Paleontologists and Mineralogists Short Course 15, 317 p.

Embry, A.F. and Dixon, J.
1990: The breakup unconformity of the Amerasia Basin, Arctic Ocean Evidence from Arctic Canada. Geological Society of America, Bulletin, v. 102, p. 1526-1534.

Ericksen, M.C. and Slingerland, R.
1990: Numerical simulations of tidal and wind-driven circulation in the Cretaceous Interior Seaway of North America. Geological Society of America, Bulletin, v. 102, p. 1499-1516.

Espitalié, J., Laporte, J.L., Madec, M., Marquis, F., Leplat, P., Paulet, J., and Boutefeu, A.
1977: Méthode rapide de caractérisation des roches de méres de leur potentiel pétrolier et de leur degré d'évolution. Revue de Institute Francais Pétrolier, v. 32, p. 23-42.

Friedman, I. and O'Neil, J.R.
1977: Compilation of stable isotope fractionation factors of geochemical interest. United States Geological Survey Professional Paper #440-KK, 12 p.

Fritz, R.D., Horn, M.K., and Joshi, S.D.
1991: Geological aspects of horizontal drilling. American Association of Petroleum Geologists, Continuing Education Course Note Series #33, 561p.

Gartner, S.
1968: Coccoliths and related calcareous nannofossils from Upper Cretaceous deposits of Texas and Arkansas. University of Kansas Paleontological Contributions, Art. 1 (Protista), p. 1-56.

Gautier, D.L.
1986: Cretaceous shales from the Western Interior of North America: sulfur/carbon ratios and sulfur-isotope composition. Geology, v. 14, p. 225-228.

Gautier, D.L. and Claypool, G.E.
1984: Interpretation of methanic diagenesis in ancient sediments by analogy with processes in modern diagenetic environments. *In* Clastic Diagenesis, D.A. McDonald, and R.C. Surdam (ed.). American Association of Petroleum Geologists, Memoir 37, p. 111-126.

Gautier, D.L., Kharaka, Y.K., and Surdam, R.C.
1985: Relationship of organic matter and mineral diagenesis. Society of Economic Paleontologists and Mineralogists, Short Course #17 Notes, 232 p.

Gent, M.R.
1992: Diamonds and precious gems of the Phanerozoic Basin, Saskatchewan preliminary investigations. Saskatchewan Energy and Mines. Saskatchewan Geological Survey, Open File Report 92-2.

Gleddie, J.
1949: Upper Cretaceous in western Peace River plains, Alberta. American Association of Petroleum Geologists, Bulletin, v. 33, p. 511-532.

Goldhaber, M.B. and Kaplan, I.R.
1974: The sulfur cycle. *In* The Sea, v. 5, E.D. Goldburg (ed.). Wiley & Sons, N.Y., p. 569-656.

Graham, S.A. and Williams, L.A.
1985: Tectonic, depositional and diagenetic history of Monterey Formation (Miocene), central San Joaquin Basin, California. American Association of Petroleum Geologists, Bulletin, v. 69, p. 385-411.

Hagen, E.S. and Surdam, R.C.
1984: Maturation history and thermal evolution of Cretaceous source rocks of the Bighorn Basin, Wyoming and Montana. *In* Hydrocarbon Source Rocks of the Greater Rocky Mountain Region, J. Woodward, F.F. Meissner, and J.L. Clayton (ed.). Rocky Mountain Association of Geologists, Symposium Volume, 1984, p. 321-338.

Haq, B.U., Hardenbol, J., and Vail, P.R.
1988: Mesozoic and Cenozoic chronostratigraphy and cycles of sea level change. *In* Sea Level Changes: An Integrated Approach, C.K. Wilgus, B.S. Hastings, H. Posamentier, J. Van Wagoner, C.A. Ross, and C.G. St. C. Kendall (ed.). Society of Economic Paleontologists and Mineralogists, Special Publication 42, p. 71-108.

Hattin, D.E.
1965: Upper Cretaceous stratigraphy, paleontology, and paleoecology of western Kansas (with section on Pierre Shale by W.A. Cobban). Geological Society of America, Field Conference Guidebook, 69 p.

1982: Stratigraphy and depositional environment of Smoky Hill Chalk Member, Niobrara Chalk (Upper Cretaceous) of the type area, Western Kansas. Kansas Geological Survey, Bulletin 225, p. 71-83.

1986: Carbonate substrates of the Late Cretaceous Sea, Central Great Plains and Southern Rocky Mountains. Palaios, v. 1, p. 347-367.

Hay, W.W.
1989: Marginal seas as source of an oceanic oxygen minimum and origin of organic carbon-rich deposits. American Association of Petroleum Geologists, Bulletin, v. 73, p. 362.

Hay, W.W., Eicher, D.L., and Diner, R.
1993: Physical oceanography and water masses in the Cretacous Western Interior Seaway. *In* Evolution of the Western Interior Basin, W.G.E. Caldwell and E.G. Kauffman (ed.). Geological Association of Canada, Special Paper 39, p. 297-318.

Hoefs, J.
1987: Stable Isotope Geochemistry. Third edition, Springer-Verlag, New York, 241 p.

Houghton, S.D.
1991: Calcareous nannofossils. *In* Calcareous Algae and Stromatolites. R. Riding (ed.). Springer-Verlag, Berlin, p. 217-266.

Hower, J. and Mowatt, T.C.
1966: The mineralogy of illites and mixed-layer illite/ montmorillonites. The American Mineralogist, v. 51, p. 825-854.

Huggett, J.M.
1994: Diagenesis of mudrocks and concretions from the London Clay Formation in the London Basin. Clay Minerals, v. 29, p. 693-707.

Irwin, H., Coleman, M., and Curtis, C.D.
1977: Isotopic evidence for source of diagenetic carbonates formed during burial of of organic-rich sediments. Nature, v. 269, p. 209-213.

Jeletzky, J.A.
1968: Macrofossil zones of the marine Cretaceous of the Western Interior of Canada and their correlation with the zones and stages of Europe and the Western Interior of the United States. Geological Survey of Canada Paper 67-72, p. 66.

Jones, R.W. and Charnock, M.A.
1985: "Morphogroups" of agglutinated foraminifera. Their life positions and feeding habits and potential applicability in (paleo)ecological studies. Revue De Paléobiologie, v. 4, no. 2, p. 311-320.

Kauffman, E.G.
1969: Cretaceous marine cycles of the Western Interior. Mountain Geologist, v. 6. p. 227-245.

1977: Geological and biological overview: Western Interior Cretaceous Basin. *In* Cretaceous Facies, Faunas, and Paleoenvironments across the Western Interior Basin, E.G. Kauffman (ed.). Mountain Geologist, Rocky Mountain Association of Geologists, v. 14, no. 3, 4, p. 75-99.

1988: The case of the missing community: Low-oxygen adapted Paleozoic and Mesozoic bivalves ("flat clams") and bacterial symbioses in typical Phanerozoic seas. *In* Centennial Meeting, Denver, Colorado, Geological Society America, Abstract with Programs A48.Kauffman, E.G., Sageman, B.B., Kirkland, J.I., Elder, W.P., Harries, P.J., and Villamil, T.
1993: Molluscan Biostratigraphy of the Cretaceous Western Interior Basin, North America. *In* Evolution of the Western Interior Basin, W.G.E. Caldwell and E.G. Kauffman (ed.). Geological Association of Canada, Special Paper 39, p. 397-434.

1984: Paleogeography and evolutionary response dynamic in the Cretaceous Western Interior Seaway of North America. *In* Jurassic-Cretaceous Biochronology and Paleogeography of North America, G.E.G. Westerman (ed.), Geological Association of Canada, Special Paper 27, p. 273-306.

Koutsoukos, E.A.M., Leary, P.N., and Hart, M.B.
1990: Latest Cenomanian-earliest Turonian low-oxygen tolerant benthonic foraminifera: a case-study from the Sergipe basin (N.E. Brazil) and the western Anglo-Paris basin (southern England). Palaeogeography, Palaeoclimatology, Palaeoecology, v. 77, p. 145-177.

Kowallis, B.J., Christiansen, E.H., Deino, A.L., Kunk, M.J., and Heaman, L.M.
1995: Age of the Cenomanian-Turonian boundary in the Western Interior of United States. Cretaceous Research, v. 16, p. 109-129.

Kulander, B.R., Dean, S.L., and Ward, B.J.
1990: Fractured core analysis: interpretation, logging and use of natural and induced fractures in core. American Association of Petroleum Geologists, Methods in Exploration Series 8, 88 p.

Lambeck, K., Cloetingh, S., and McQueen, H.
1987: Intraplate stress and apparent changes in sea level: the basins of northwestern Europe. *In* Sedimentary Basins and Basin-forming Mechanisms, C. Beaumont and A.J. Tankard (eds.). Canadian Society of Petroleum Geologists, Memoir 12, p. 259-268.

Lang, H.R. and McGugan, A.
1988: Cretaceous (Albian-Turonian) foraminiferal biostratigraphy and paleogeography of northern Monatana and southern Alberta. Canadian Journal of Earth Science, v. 25, p. 316-342.

Leckie, D.A.
1986: Tidally influenced, transgressive shelf sediments in the Viking Formation, Caroline, Alberta. Bulletin of Canadian Petroleum Geologists, v. 34, p. 111-125.

Leckie, D.A., Bhattacharya, J., Bloch, J., Gilboy, C.F., and Norris, B.
1994: Cretaceous Colorado/Alberta Group strata of the Western Canada Sedimentary Basin. *In* Geological Atlas of the Western Canada Sedimentary Basin, G. Mossop and I. Shetsen (comp.). Canadian Society of Petroleum Geology and the Alberta Research Council, p. 335-352.

Leckie, D.A., Kjarsgaard, B.A., Bloch, J., McIntyre, D., McNeil, D., Stasiuk, L., and Heaman L.
1997: Emplacement and reworking of Cretaceous, diamond-bearing, crater facies kimberlite of central Saskatchewan, Canada. Geological Society of America, Bulletin 109, p. 1000-1020.

Leckie, D.A., Singh, C., Bloch, J., Wilson, M., and Wall, J.H.
1992: An anoxic event at the Albian-Cenomanian Boundary: the Fish Scale marker bed, northern Alberta, Canada. Paleogeography, Paleoecology, Paleoclimatology, v. 92, p. 139-166.

Leckie, D.A. and Smith, D.G.
1992: Regional setting, evolution, and depositional cycles of the Western Canada Foreland Basin. *In* Foreland Basins and Fold Belts, R.W. Macqueen and D.A. Leckie (ed.). Amercian Association of Petroleum Geologists, Memoir 55, p. 9-46.

Leckie, D.A. and Reinson, G.E.
1993: Effects of middle to Late Albian sea-level fluctuations in the Cretaceous interior seaway, Western Canada. *In* Evolution of the Western Interior Basin, W.G.E. Caldwell and E.G. Kauffman (ed.). Geological Association of Canada, Special Paper 39, p. 151-175.

Leckie, R.M.
1987: Paleoecology of mid-Cretaceous planktonic foraminifera: a comparison of open ocean and epicontinental sea assemblages. Micropaleontology, v. 33. p. 164-176.

Leckie, R.M., Schmidt, M.G., Finkelstein, D., and Yuretich, R.
1991: Paleoceanographic and paleoclimatic interpretations of the Mancos Shale (Upper Cretaceous), Black Mesa Basin, Arizona. Geological Society of America, Special Paper 260, p. 139-152.

Lehnert-Theil, K., Loewer, R., Orr, R.G., and Robertshaw, P.
1992: Diamond-bearing kimberlites in Saskatchewan, Canada: the Fort à la Corne case history. Exploration and Mining Geology, v. 1, p. 391-403.

Leythaeuser, D.
1973: Effects of weathering on organic matter in shales. Geochimica et Cosmochimica Acta, v. 37, p. 113-120.

Loeblich, A.R., Jr.
1946: Foraminfera from the type Pepper Shale of Texas. Journal of Paleontology, v. 20, p. 130-139.

Longstaffe, F.J.
1987: Stable isotope studies of diagenetic processes. *In* Stable Isotope Geochemistry of Low Temperature Fluids, Volume 13, T.K. Kyser (ed.). Mineralogical Association of Canada, Short Course, p. 187-257.

Loutit, T.S., Hardenbol, J., Vail, P.R., and Baum, G.R.
1988: Condensed sections: the key to age determination and correlation of continental margin sequences. *In* Sea Level Changes: an Integrated Approach, C.K. Wilgus, B.S. Hastings, C.G. St.C. Kendall, H.W. Posamentier, C.A. Ross, and J.C. Van Wagoner (ed.). Society of Economic Paleontologists and Mineralogists, Special Publication No. 42, p. 183-213.

Macauley, G.
1984a: Geology of the oil shale deposits of Canada. Geological Survey of Canada, Paper 81-25, 65 p.

1984b: Cretaceous oil shale potential in Saskatchewan. *In* Oil and Gas in Saskatchewan, L.J.A Lorsong and M.A. Wilson (ed.). Special Publication of the Saskatchewan Geological Society, v. 7, p. 255-269.

1984c: Cretaceous oil shale potential of the prairie provinces, Canada. Geological Survey of Canada, Open File Report OF-977, 61 p.

Macauley, G., Snowdon, L.R., and Ball, F.D.
1985: Geochemistry and geological factors governing exploitation of selected Canadian oil shale deposits. Geological Survey of Canada, Paper 85-13, p. 65.

Machemer, S.D. and Hutcheon, I.E
1988: Geochemistry of early carbonate cements in the Cardium Formation, central Alberta. Journal of Sedimentary Petrology, v. 58, p. 136-147.

Macqueen, R.W. and Leckie, D.A. (ed.)
1992: Foreland Basins and Fold Belts. American Association of Petroleum Geologists, Memoir 55, 460 p.

Majorowicz, J., Jones, F., Lam, H., and Jessop, A.
1985: Terrestrial heat flow and geothermal gradients in relation to hydrodynamics in the Alberta basin, Canada. Journal of Geodynamics, v. 4, p. 265-283.

Malloch, G.S.
1911: Bighorn coal basin, Alberta. Canada Department of Mines, Geological Survey Branch Memoir Number 9E, 66 p.

Mallory, W.W.
1977: Oil and gas from fractured shale reservoirs in Colorado and northwest New Mexico. Rocky Mountain Association of Geologists, Special Publication 1, 38 p.

May, F.E.
1979: Dinoflagellate and acritarch assemblages from the Naunshuk Group (Albian-Cenomanian) and the Torok Formation (Albian), Umiat Test Well 11, National Petroleum Reserve in Alaska, Northern Alaska. *In* Preliminary Geologic, Petrologic and Paleontologic Results of the Study of Nanushuk Group Rocks, North Slope, Alaska, T.S. Ahlbrandt (ed.). Geological Survey Circular 794, p. 113-127.

May, F.E. and Stein, J.A.
1979: Dinoflagellate and acritarch assemblages from the Grandstand Formation (Middle to Upper Albian) of the Nanushuk Group, Simpson Core Test 25, National Petroleum Reserve in Alaska, Northern Alaska. *In* Preliminary Geologic Petrologic and Paleontologic Results of the Study of Nanushuk Group Rocks, North Slope, Alaska, Ahlbrandt, T.S. (ed.). Geological Survey Circular 794, p. 128-145.

McLearn, F.H.
1944: Revision of the Lower Cretaceous of the Western Interior of Canada. Geological Survey of Canada, Paper 44-17.

McMechan, M.E. and Thompson, R.I.
1993: The Canadian Cordilleran Fold and Thrust Belt south of 66°N and its influence on the Western Interior Basin. *In* Evolution of the Western Interior Basin, W.G.E. Caldwell and E.G. Kauffman (eds.). Geological Association of Canada, Special Paper 39, p. 477-520.

McNeil, D.H.
1984: The eastern facies of the Cretaceous System in the Canadian Western Interior. *In* The Mesozoic of North America, D.F. Stott and D.J. Glass, (eds.). Canadian Society of Petroleum Geologists, Memoir 9, p. 145-171.

McNeil, D.H. and Caldwell, W.G.E.
1981: Cretaceous Rocks and Their Foraminifera in the Manitoba Escarpment. Geological Association of Canada, Special Paper 21, 439 p.

Meissner, F.F.
1978: Petroleum geology of the Bakken Formation Williston Basin, North Dakota and Montana. Williston Basin Symposium, The Montana Geological Society 24th Annual Conference Proceedings. Reprinted *In* Petroleum Geochemistry and Basin Evaluation, G. Demaison and R.F. Murris (eds.). American Association of Petroleum Geologists, Memoir 35 (1984), p. 159-179.

Moore, D.M. and Reynolds, R.C., Jr.
1989: X-ray Diffraction and the Identification and Analysis of Clay Minerals. Oxford University Press, New York, 332 p.

Mösle, B.
1995: Faziesanalytische Untersuchungen am organischen Material in Sedimenten aus der Lower Colorado Group (Alb-Turon) im Westkanadischen Sedimentären Becken (Südalberta, Kanada). Ph.D. thesis, RWTH Aachen, Germany. Mahaliac Scientific Studies, G2. Edition Prairie, 162 p.

Mossop G. and Shetsen, I. (comp.)
1994: Geological Atlas of the Western Canada Sedimentary Basin. Canadian Society of Petroleum Geologists and the Alberta Research Council, 507 p.

Nadeau, P.H. and Reynolds, R.C. Jr.
1981: Volcanic components in pelitic sediments. Nature, v. 294, p. 72-74.

North, B.R. and Caldwell, W.G.E.
1975: Foraminiferal faunas in the Cretaceous System in Saskatchewan. *In* The Cretaceous System in the Western Interior of North America, W.G.E. Caldwell (ed.). Geological Association of Canada, Special Paper 13, p. 303-331.

Obradovich, J.D.
1991: A revised Cenomanian-Turonian time scale based on studies from the Western Interior United States. Abstracts with Programs, Geological Society of America, 1991 Annual Meeting, San Diego, CA., p. A296.

1993: A Cretaceous time scale in Evolution of the Western Interior Basin, W.G.E. Caldwell and E.G. Kauffman (eds.). Geological Association of Canada, Special Paper 39, p. 379 - 396.

Oremland, R.S. and Taylor, B.F.
1978: Sulfate reduction and methanogenesis in marine sediments. Geochimica et Cosmochimica Acta, v. 42, p. 209-214.

Orr, W.L.
1986: Kerogen/asphaltene/sulfur relationships in sulfur-rich Monterey oils. Organic Geochemistry, v. 10, p. 499-516.

Pearce, T.H.
1967: A contribution to the theory of variation diagrams. Contributions to Mineralogy and Petrology, v. 19, p. 142-157.

Peters, K.E.
1986: Guidelines for evaluating petroleum source rock using programmed pyrolysis. American Association of Petroleum Geologists, Bulletin, v. 70, p. 318-329.

Pollastro, R.M.
1981: Authigenic kaolinite and associated pyrite in chalk of the Cretaceous Niobrara Formation, eastern Colorado. Journal of Sedimentary Petrology, v. 51, p. 553-562.

Porter, J.W.
1992a: Early surface and subsurface investigations of the Western Canada Sedimentary Basin. *In* Foreland Basins and Fold Belts, R.W. Macqueen and D.A. Leckie (ed.). American Association of Petroleum Geologists, Memoir 55, p. 125-158.

1992b: Conventional hydrocarbon reserves of the Western Canada Foreland Basin. *In* Foreland Basins and Fold Belts, R.W. Macqueen and D.A. Leckie (ed.). American Association of Petroleum Geologists, Memoir 55, p. 159-190.

Portigal, M.H., Creed, R.M., Hogg, J.H., and Hewitt, M.D.
1989: Oil and gas developments in Western Canada in 1987. Bulletin of Canadian Petroleum Geology, v. 37, p. 334-345.

Pratt, L.M.
1984: Influence of paleoenvironmental factors on preservation of organic matter in Middle Cretaceous Greenhorn Formation, Pueblo, Colorado. American Association of Petroleum Geologists, Bulletin, v. 68, p. 1146-1159.

Pratt. L.M., Comer, J.B., and Brassell, S.C.
1992: Geochemistry of Organic Matter in Sediments and Sedimentary Rocks. Society of Economic Paleontologists and Mineralogists, Short Course #27 Notes. 100 p.

Reeside, J.B., Jr. and Cobban, W.A.
1960: Studies of the Mowry Shale (Cretaceous) and contemporary formations in the United States and Canada. United States Geological Survey Professional Paper 355, 126 p.

Rosenbaum, J. and Sheppard, S.M.F.
1986: An isotopic study of siderites, dolomites, and ankerites at high temperatures. Geochimica et Cosmochimica Acta, v. 50, p. 1147-1150.

Ross, C.S. and Hendricks, S.B.
1945: Minerals of the montmorillonite group, their origin and relation to soils and clays. United States Geological Survey, Professional Paper 205B, p. 23-72.

Rubey, W.W.
1931: Lithologic studies of fine-grained Upper Cretaceous sedimentary rocks of the Black Hills region. United States Geological Survey, Professional Paper 165-A, 54 p.

Sageman, B.B.
1989: The benthic boundary biofacies model Hartland Shale Member, Greenhorn Formation (Cenomanian), Western Interior, North America. Palaeogeography, Palaeoclimatology, Palaeoecology, v. 74, p. 87-110.

Sageman, B.B. and Arthur, M.A.
1994: Early Turonian paleogeographical/paleobathymetric map western interior. *In* Mesozoic Systems of the Rocky Mountain Region, USA, M.V. Caputo, J.A. Peterson, and K.J. Franczyk (ed.), p. 457-469.

Savin, S.M and Yeh, H-W.
1981: Stable isotopes in ocean sediments. *In* The Sea, Volume 7, The Oceanic Lithosphere, C. Emiliani (ed.). John Wiley and Sons, New York, p. 1521-1554.

Schröder-Adams, C.L., Bloch, J.D., Leckie, D.A., Craig, J., McIntyre, D.J., and Adams, P.J.
1996: Paleoenvironmental changes in the Cretaceous (Albian to Turonian) Colorado Group of western Canada: microfossil, sedimentological and geochemical evidence. Cretaceous Research, v. 17, p. 311-365.

Schultz, L.G., Tourtelot, H.A., Gill, J.R., and Boerngen, J.G.
1980: Composition and properties of the Pierre Shale and equivalent rocks, Northern Great Plains region. United States Geological Survey, Professional Paper 1064-B, 114 p.

Selwyn, A.R.C.
1877: Report on exploration in British Columbia. Geological Survey of Canada, Report of Progress for 1875-1876, p. 28-86.

Sibley, D.F. and Blatt, H.
1976: Intergranular pressure solution and cementation of the Tuscarora Orthoquartzite. Journal of Sedimentary Petrology, v. 46, p. 881-896.

Simpson, F.
1982: Sedimentology, paleoecology and economic geology of Lower Colorado (Cretaceous) strata of west-central Saskatchewan. Saskatchewan Energy and Mines, Saskatchewan Geological Survey Report 150, 182 p.

Singh, C.
1971: Lower Cretaceous microfloras of the Peace River area, northwestern Alberta. Research Council of Alberta, Bulletin 28, 542 p.

1983: Cenomanian microfloras of the Peace River area, northwestern Alberta. Alberta Research Council, Bulletin 44, 322 p.

Sinninghe Damsté, J.S. and de Leeuw, J.W.
1990: Analysis, structure and geochemical significance of organically-bound sulphur in the geosphere: State of the art and future research. Organic Geochemistry, v. 16, p. 1077-1101.

Sliter, W.V.
1979: Cretaceous foraminifers from the north slope of Alaska. *In* Preliminary Geologic Petrologic and Paleontologic Results of the Study of Nanushuk Group Rocks, North Slope, Alaska, T.S. Ahlbrandt (ed.). Geological Survey Circular 794, p. 147-158.

Smith, C.C.
1981: Calcareous nannoplankton and stratigraphy of Late Turonian, Coniacian, and early Santonian age of the Eagle Ford and Austin Groups of Texas. United States Geological Survey, Professional Paper 1075, 96 p, 16 pl.

Snowdon, L.R.
1995: Rock-Eval T_{max} suppression: documentation and amelioration. American Association of Petroleum Geologists, Bulletin, v. 79, p. 1337 -1348.

Srodon, J.
1980: Precise identification of illite/smectite interstratifications by X-ray powder diffraction. Clays and Clay Minerals, v. 28, p. 401-411.

Stasiuk, L.D. and Goodarzi, F.
1988: Organic petrology of Second White Speckled Shale, Saskatchewan, Canada - possible link between bituminite and biogenic gas? Bulletin of Canadian Petroleum Geology, v. 36, p. 397-406.

Stelck, C.R.
1975: The Upper *Miliammina manitobensis* Zone in northeastern British Columbia. *In* The Cretaceous System in the Western Interior of North America, W.G.E. Caldwell (ed.). Geological Association of Canada, Special Paper Number 13, p. 253-276.

Stelck, C.R. and Wall, J.H.
1954: Kaskapau foraminifera from Peace River area of Western Canada. Research Council of Alberta Report 68, 38 p.

Stelck, C.R. and Armstrong, J.
1981: *Neogastroplites* from southern Alberta. Bulletin of Canadian Petroleum Geology, v. 29, p. 399-407.

Stelck, C.R. and Koke, K.R.
1987: Foraminiferal zonation of the Viking interval in the Hasler Shale (Albian), northeastern British Columbia. Canadian Journal of Earth Sciences, v. 24, p. 793-798.

Stelck, C.R., Wall, J.H. and Wetter, R.E.
1958: Lower Cenomanian Foraminifera from Peace River area, Western Canada. Research Council of Alberta, Bulletin 2, Part I, p. 1-35.

Stott, D.F.
1963: The Cretaceous Alberta Group and equivalent rocks, Rocky Mountain Foothills, Alberta. Geological Survey of Canada, Memoir 317, p. 306.

1967: The Cretaceous Smoky Group, Rocky Mountain Foothills, Alberta and British Columbia. Geological Survey of Canada, Bulletin 132, 133 p.

1982: Lower Cretaceous Fort St. John Group and Upper Cretaceous Dunvegan Formation of the foothills and plains of Alberta, British Columbia, District of Mackenzie and Yukon Territory. Geological Survey of Canada, Bulletin 328, 124 p.

Stover, L.E.
1966: Cretaceous coccoliths and associated nannofossils from France and the Netherlands, Micropaleontology, v. 12, p. 133-167.

Tappan, H.
1962: Cretaceous Foraminifera; part 3 of Foraminifera from the Arctic slope of Alaska. United States Geological Survey, Professional Paper 236-C, p. 91-209.

Taylor, K.G. and Curtis, C.D.
1995: Stability and facies association of early diagenetic mineral assemblages: an example from a Jurassic ironstone-mudstone succession. United Kingdom Journal of Sedimentary Research, v. A65, p. 358-368.

Then, D.R. and Dougherty, B.J.
1983: A new procedure for extracting foraminfera from indurated organic shale. *In* Current Research, Part B, Geological Survey of Canada, Paper 83-1B, p. 413-414.

Thierstein, H.R.
1976: Mesozoic calcareous nannoplankton biostratigraphy of marine sediments. Marine Micropaleontology, v. 1, p. 325-362.

Thode, H.G., Kleerekoper, H., and McElcheran, D.
1951: Isotopic fractionation in the bacterial reduction of sulfate. Research, v. 4, p. 581-582.

Tissot, B.P. and Welte, D.H.
1984: Petroleum Formation and Occurrence, 2nd Edition. Springer-Verlag, Berlin. 699 p.

Tuttle, M.L., Goldhaber, M.B., and Williamson, D.L.
1986: An analytical scheme for determining forms of sulphur in oil shales and associated rocks. Talanta, v. 33, no. 12, p. 953-961.

Ueda, A. and Krouse, H.R.
1986: Direct conversion of sulphide and sulphate minerals to SO_2 for isotope analyses. Geochemical Journal, v. 20, p. 209-212.

Wall, J.H.
1967: Cretaceous foraminifera of the Rocky Mountain Foothills, Alberta. Research Council of Alberta, Bulletin 20. p. 185.

Wall, J.H. and Germundson, R.K.
1963: Microfaunas, megafaunas, and rock-stratigraphic units in the Alberta Group (Cretaceous) of the Rocky Mountain Foothills. Bulletin of Canadian Petroleum Geology, v. 11, p. 327-349.

Waples, D.W.
1984: Modern approaches in source rock evaluation. *In* Hydrocarbon Source Rocks of the Greater Rocky Mountain Region. J. Woodward, F.F. Meissner, and J.L. Clayton (eds.). Rocky Mountain Association of Geologists, Symposium Volume, 1984, p. 35-50.

Warren, P.S. and Stelck, C.R.
1969: Early *Neogastroplites*, Fort St. John Group, Western Canada. Bulletin of Canadian Petroleum Geology, v. 17, p. 529-547.

Whittaker, S.G., Kyser, T.K., and Caldwell, W.G.E.
1987: Paleoenvironmental geochemistry of the Claggett marine cycothem in south-central Saskatchewan. Canadian Journal of Earth Sciences, v. 24, p. 967-984.

Wickenden, R.T.D.
1945: Mesozoic stratigraphy of the eastern plains, Manitoba and Saskatchewan. Geological Survey of Canada, Memoir 239, 87 p.

Wickenden, R.T.D. and Shaw, G.
1943: Stratigraphy and structure in Mount Hulcross-Commotion Creek map-area, British Columbia. Geological Survey of Canada, Paper 43-13, 14 p.

Williams, G.D. and Bayliss, P.
1988: Mineralogy of the Cretaceous shales in southeastern Saskatchewan. Bulletin of Canadian Petroleum Geology, v. 36, p. 145-157.

Williams, G.D. and Stelck, C.R.
1975: Speculations on the Cretaceous palaeogeography of North America. *In* The Cretaceous System in the Western Interior of North America, W.G.E. Caldwell (ed.). Geological Association of Canada, Special Paper 13, p. 1-20.

Wintsch, R.P. and Kvale, C.M.
1994: Differential mobility of elements in burial diagenesis of siliclastic rocks. Journal of Sedimentary Research A64, p. 349-361.

Yoder, H.S. and Eugster, H.P.
1955: Synthetic and natural muscovites. Geochimica et Cosmochimica Acta, v. 8, p. 225-280.

Zaback, D.A. and Pratt, L.M.
1992: Isotopic composition and speciation of sulfur in the Miocene Monterey Formation: Reevaluation of sulfur reactions during early diagenesis in marine environments. Geochimica et Cosmochimica Acta, v. 56, p. 763-774.

Appendix A

Lithostratigraphic logs

Imperial Wembley 5-9
05-09-72-08W6

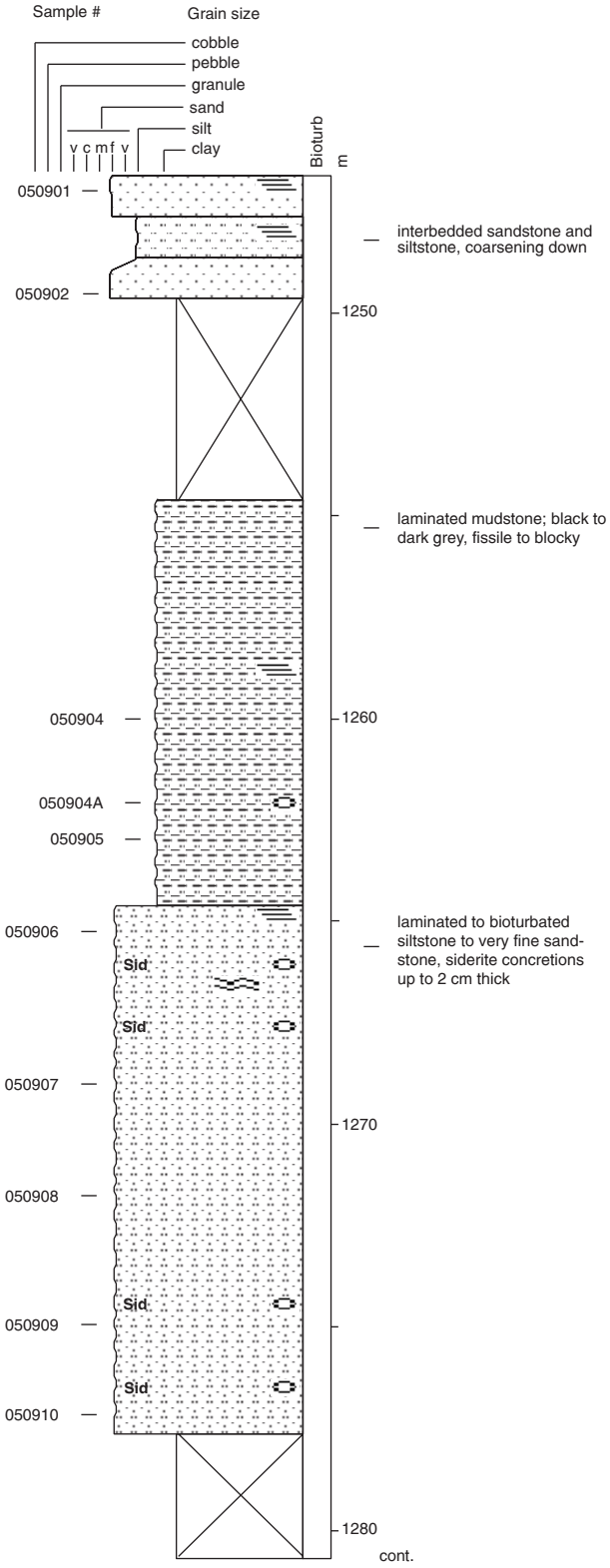

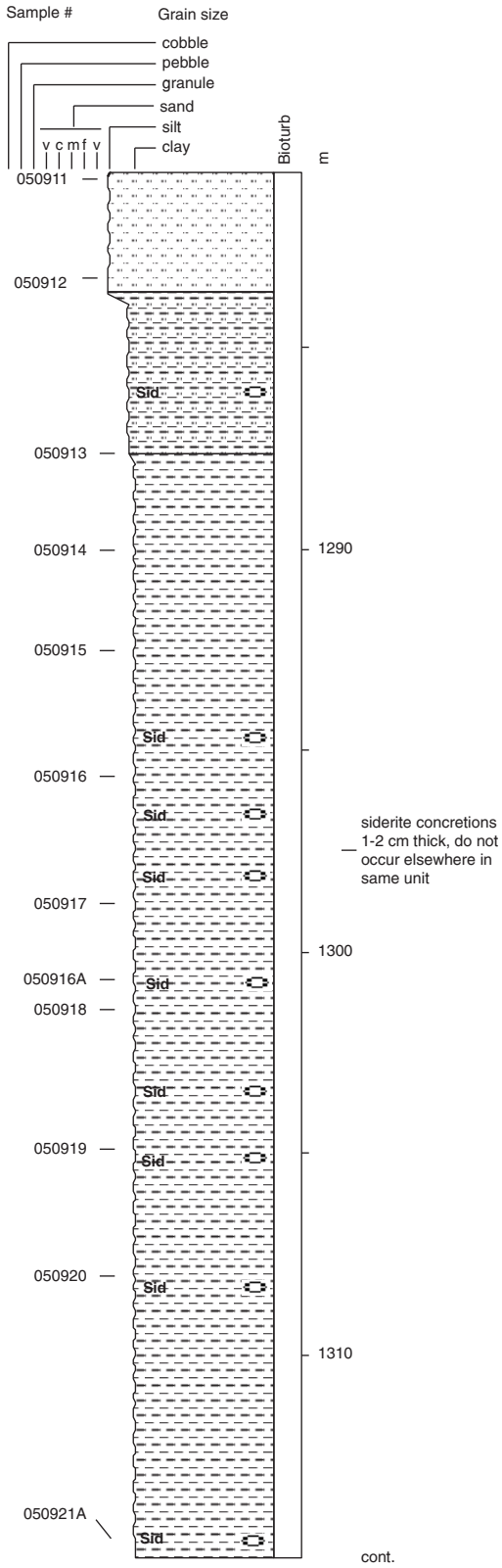

Imperial Wembley 5-9
05-09-72-08W6

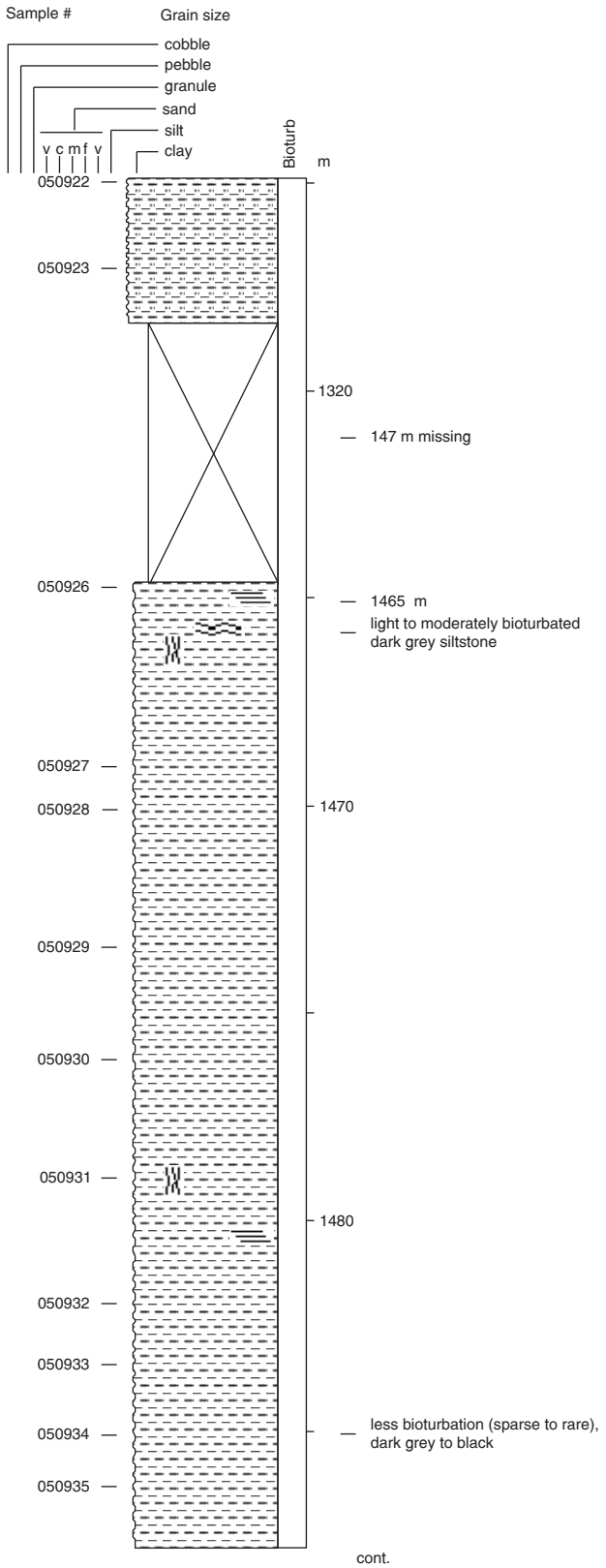

cont.

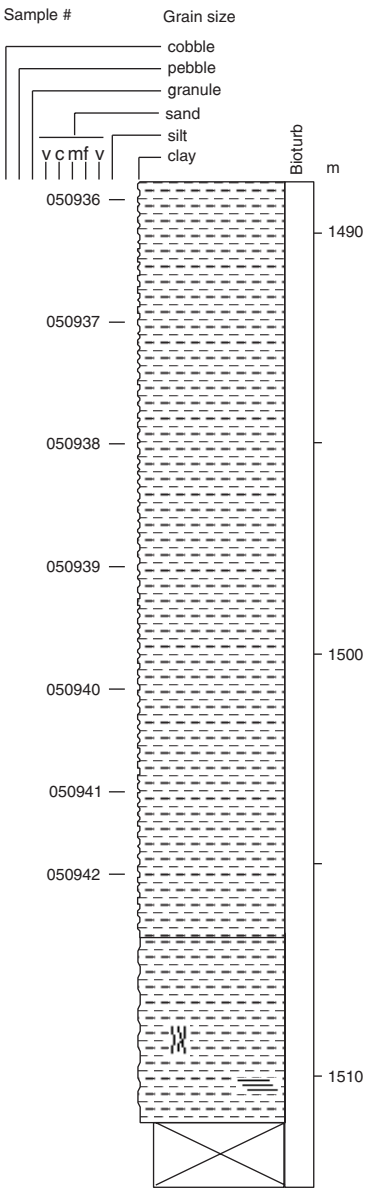

Amoco Bigstone 16-1
16-01-61-22W5

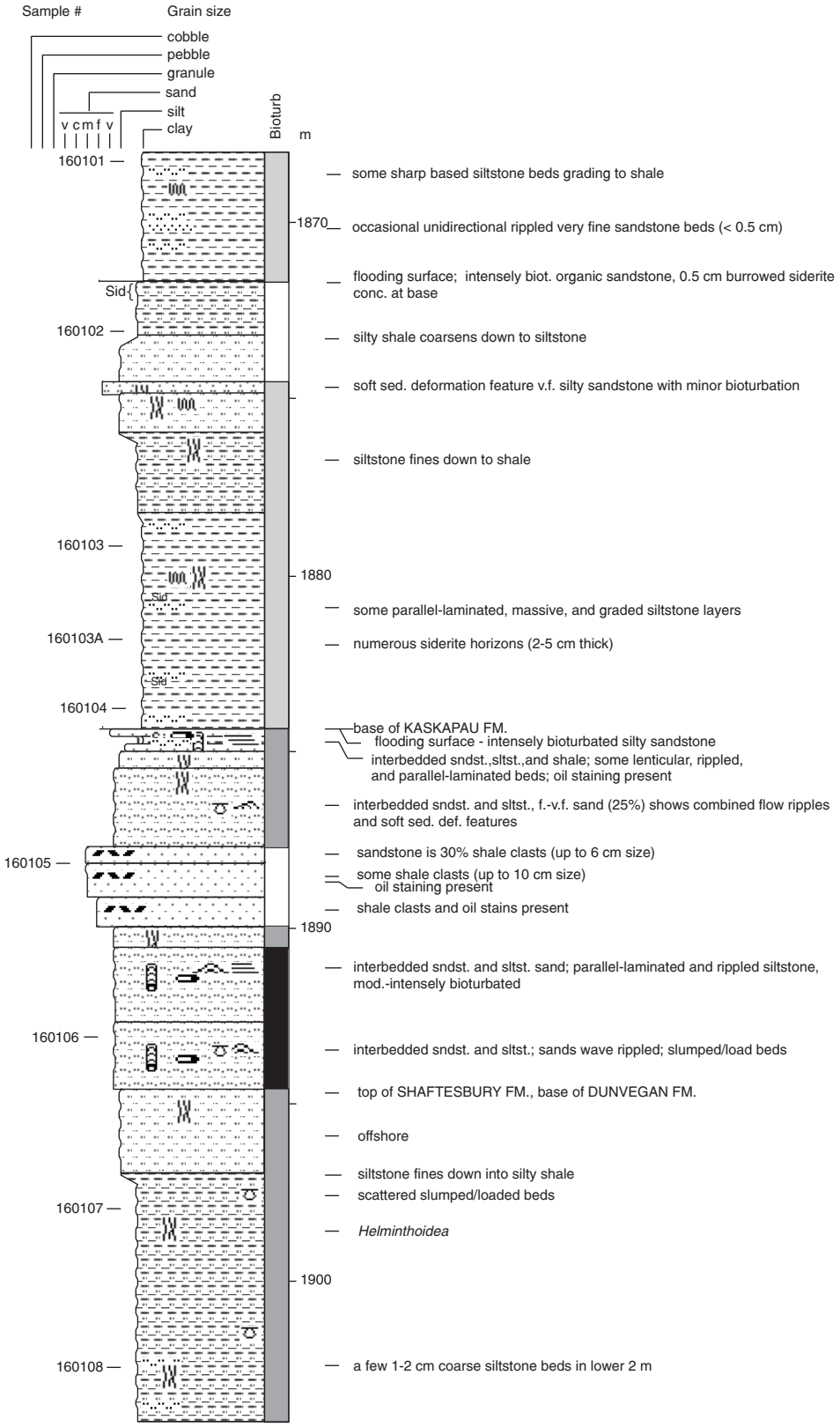

Imperial Kathleen #1, 5-1
05-01-77-20W5

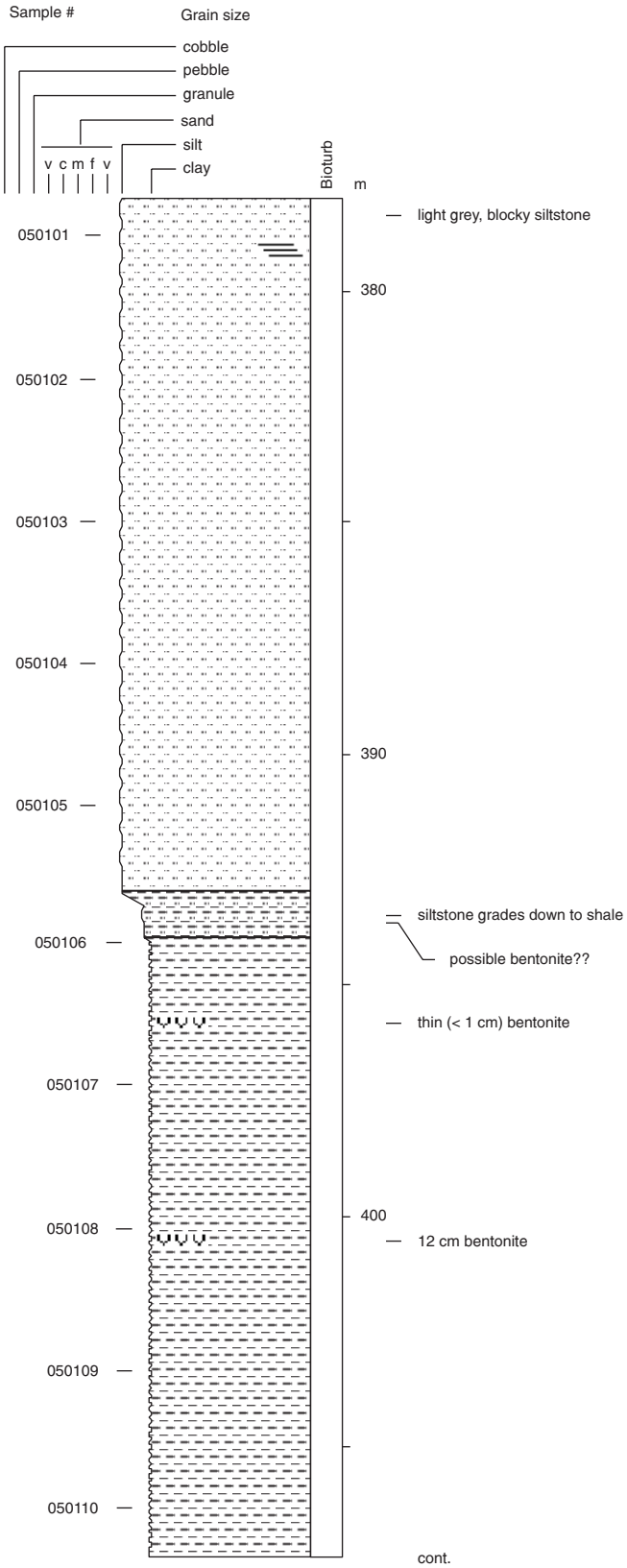

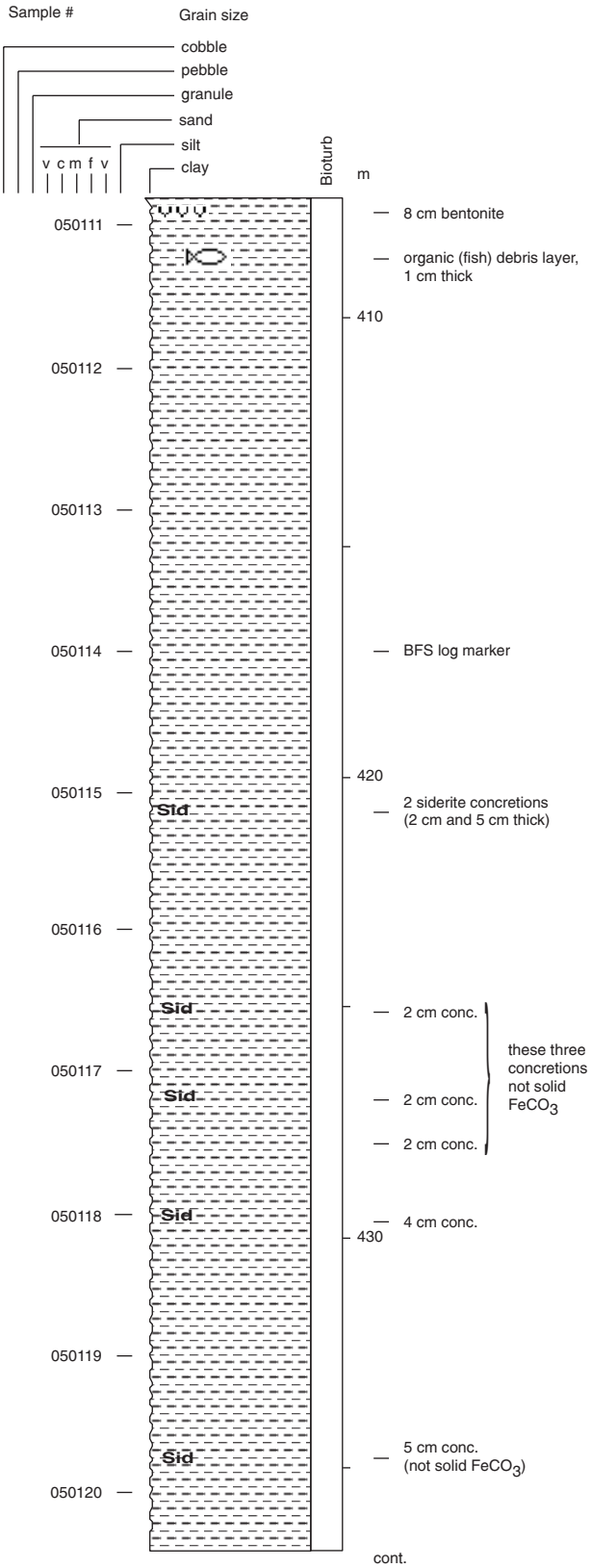

Imperial Kathleen #1, 5-1
05-01-77-20W5

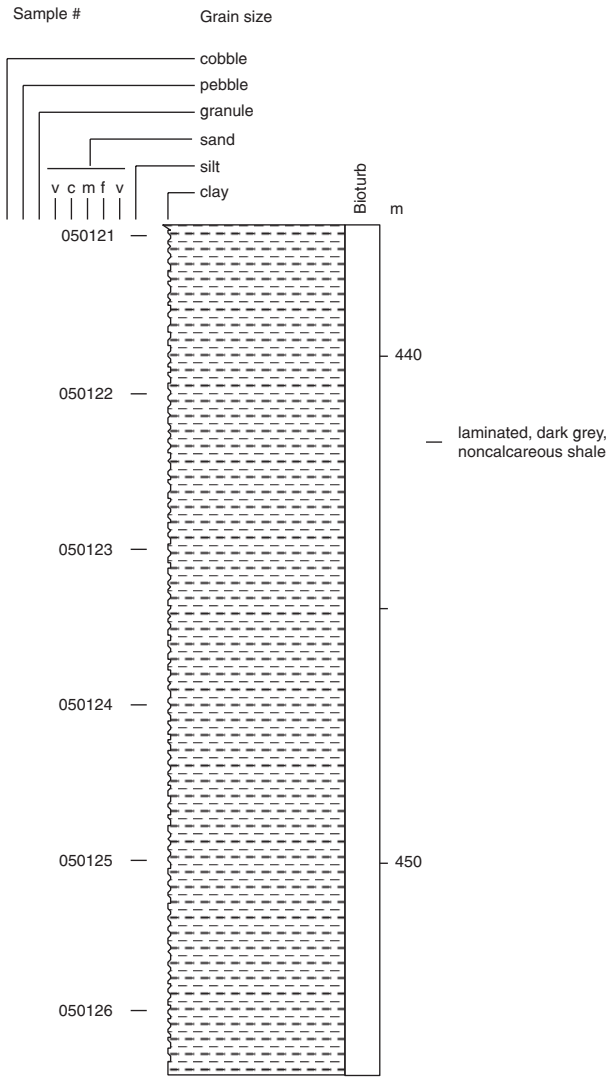

Sabine et al. Iosegun 10-25
10-25-65-20W5

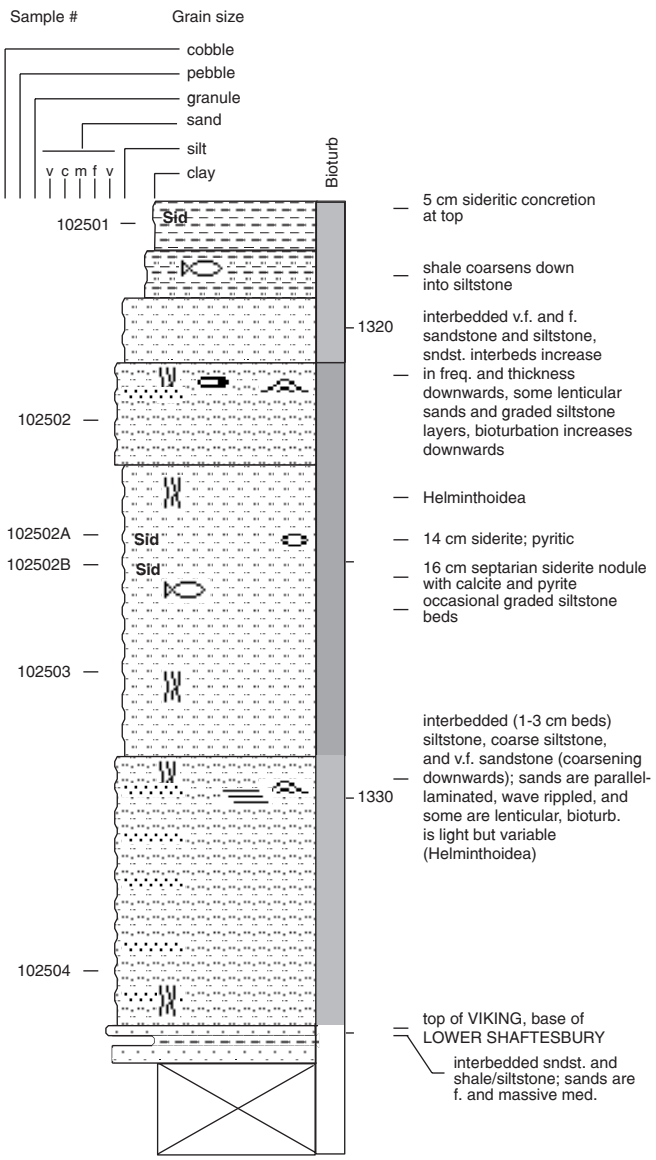

H.B. Galloway
10-5-53-20W5

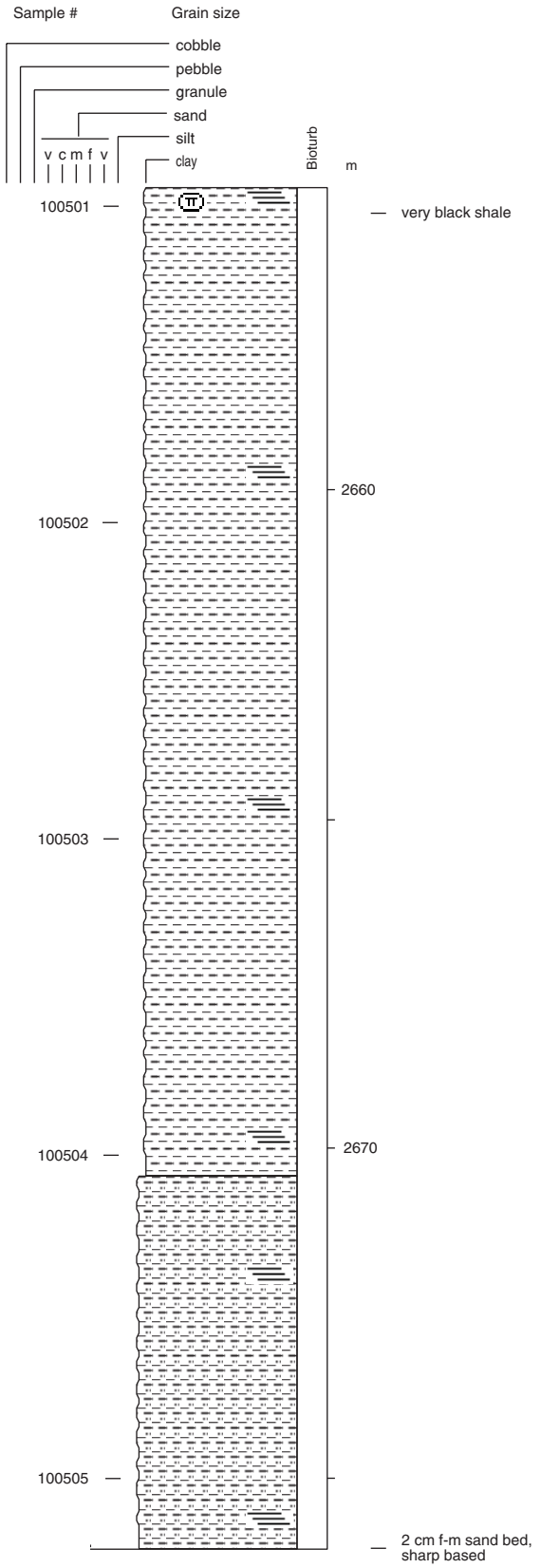

cont.

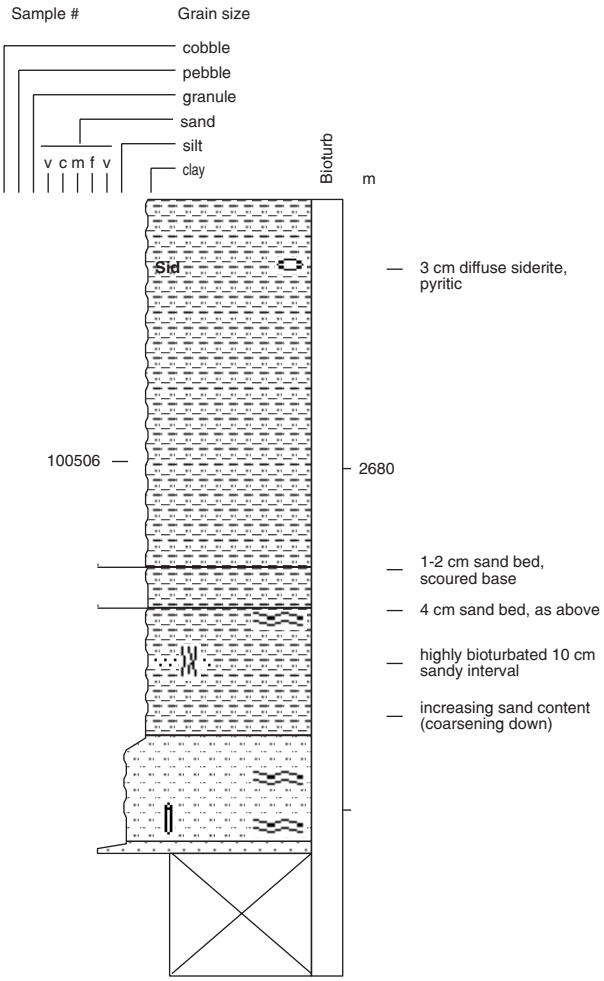

HCS et al. Beaver Creek 9-9
09-09-56-19W5

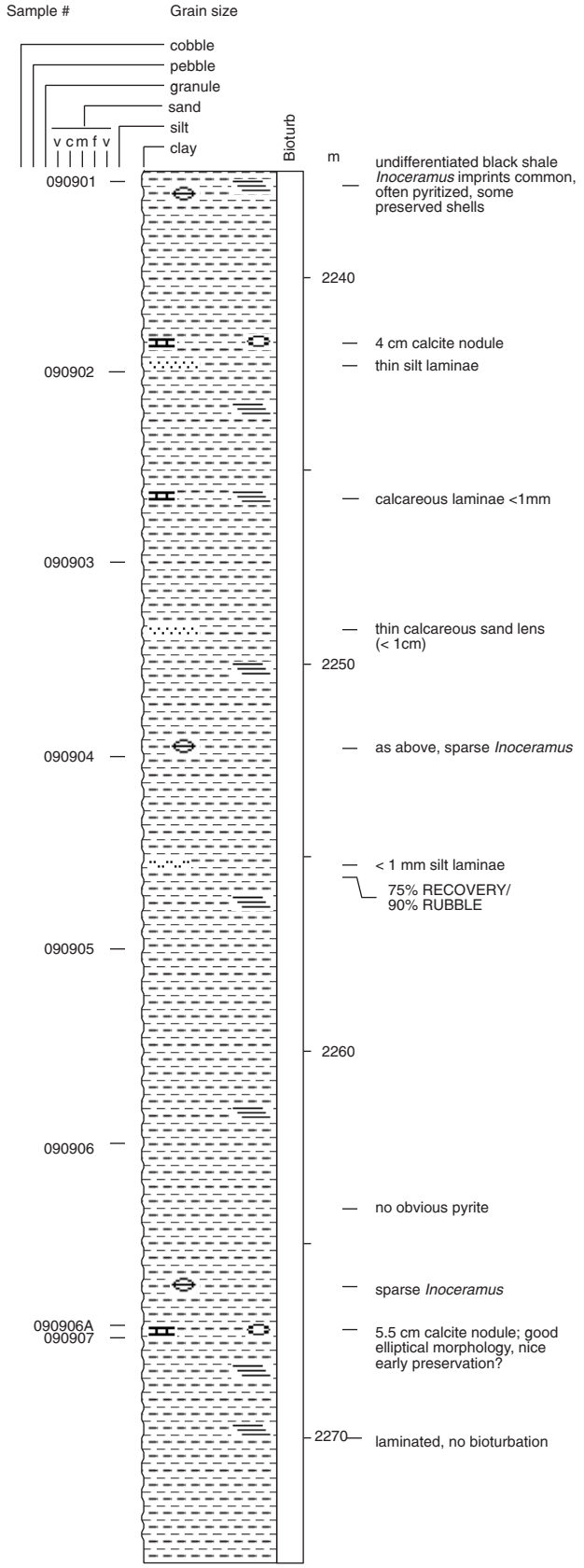

Texex Edson
04-13-54-18W5

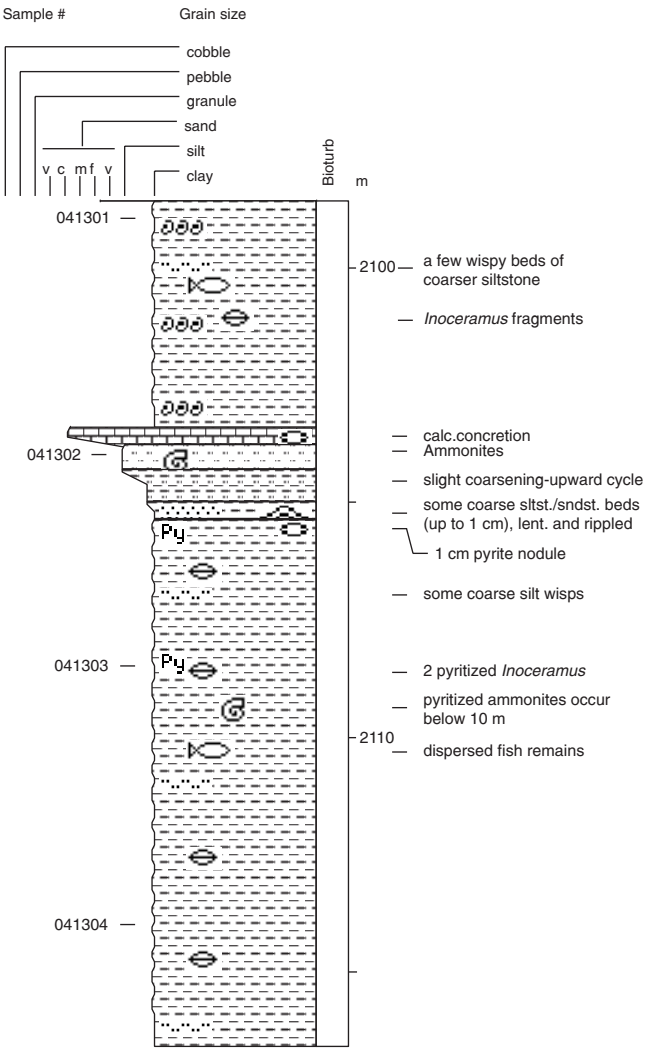

Dome et al. Claresholm 14-29
14-29-11-28W4

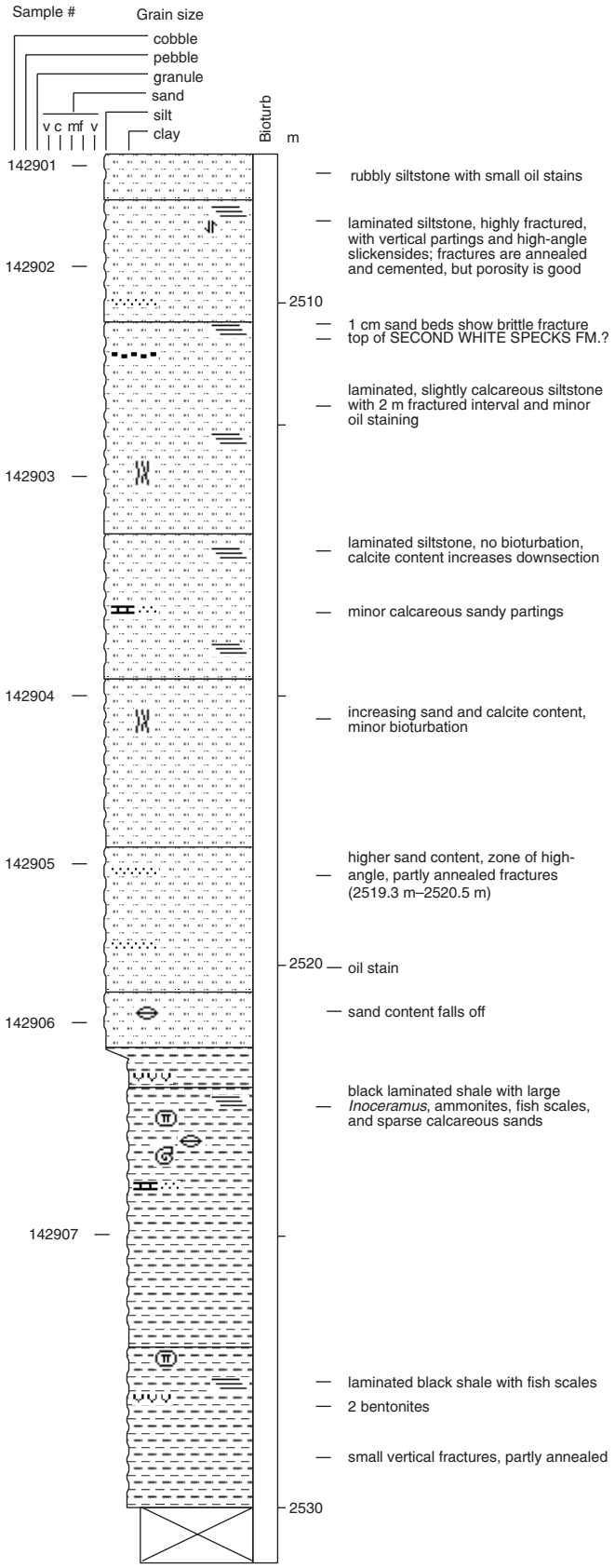

Ajax Morinville 6-21
06-21-55-25W4

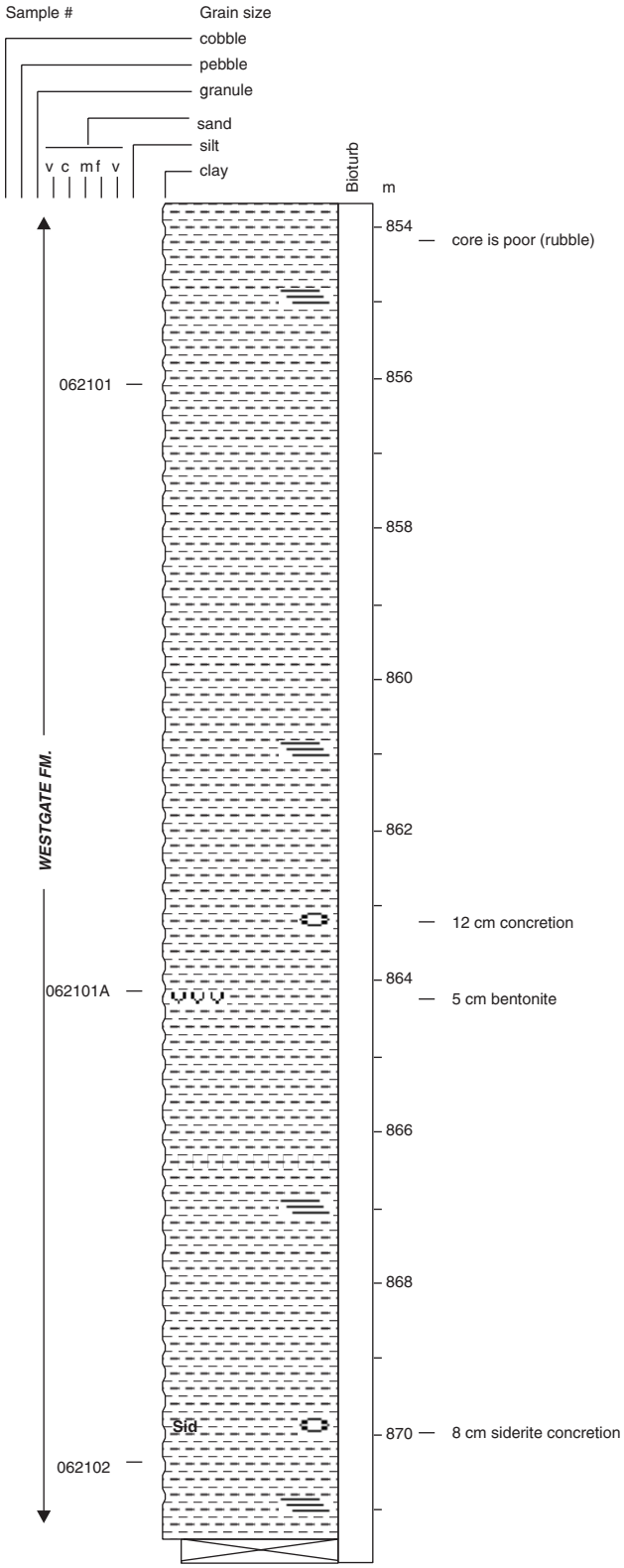

Pennwest et al. Barons
8-25-12-24W4

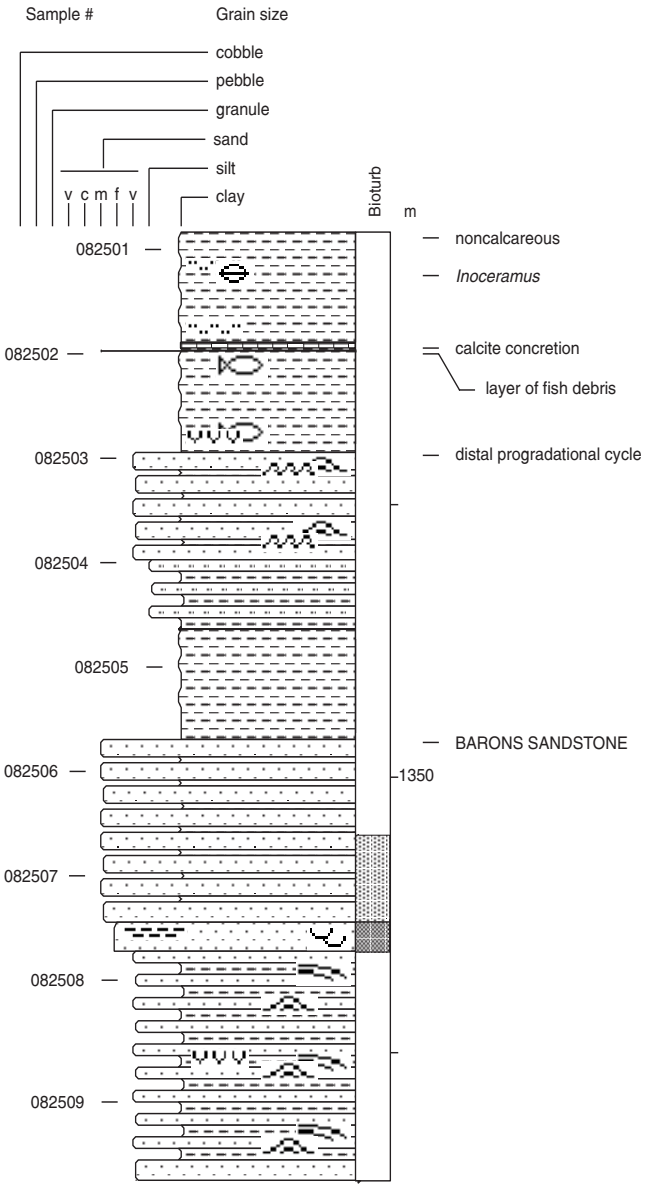

Melaar Barons 11-21
11-21-12-23W4

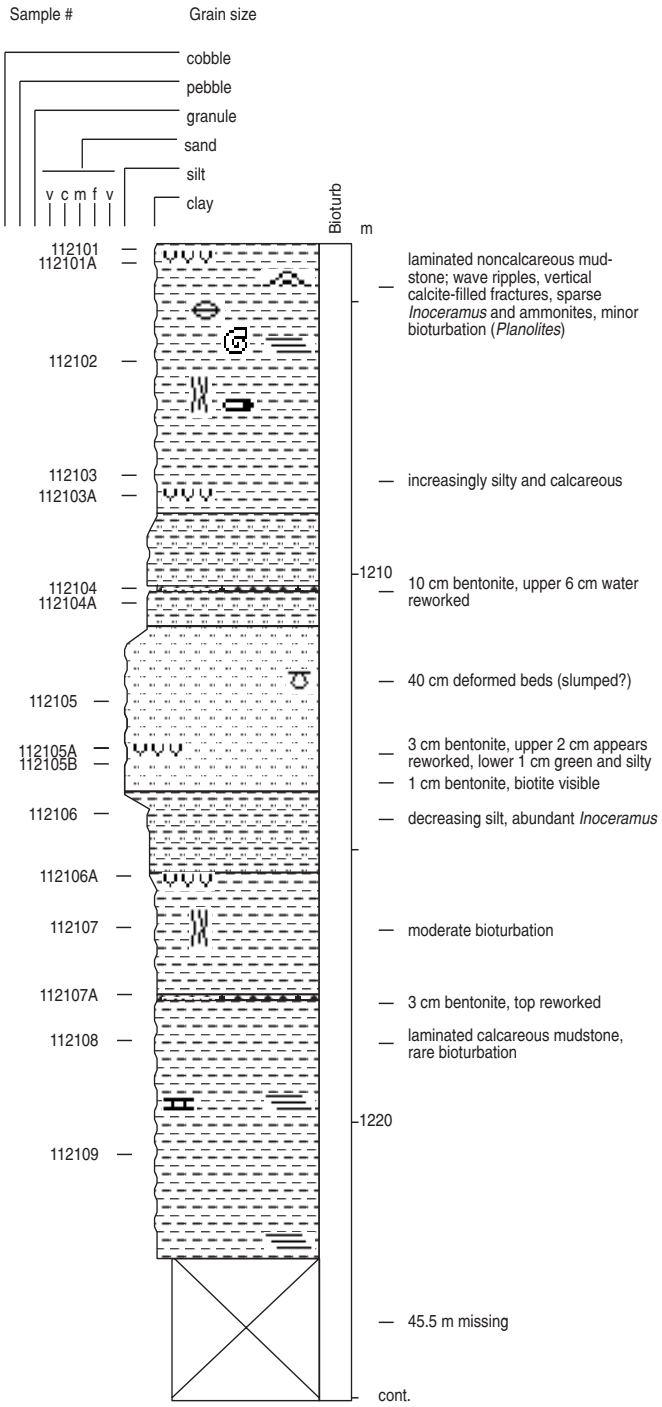

Melaar Barons 11-21
11-21-12-23W4

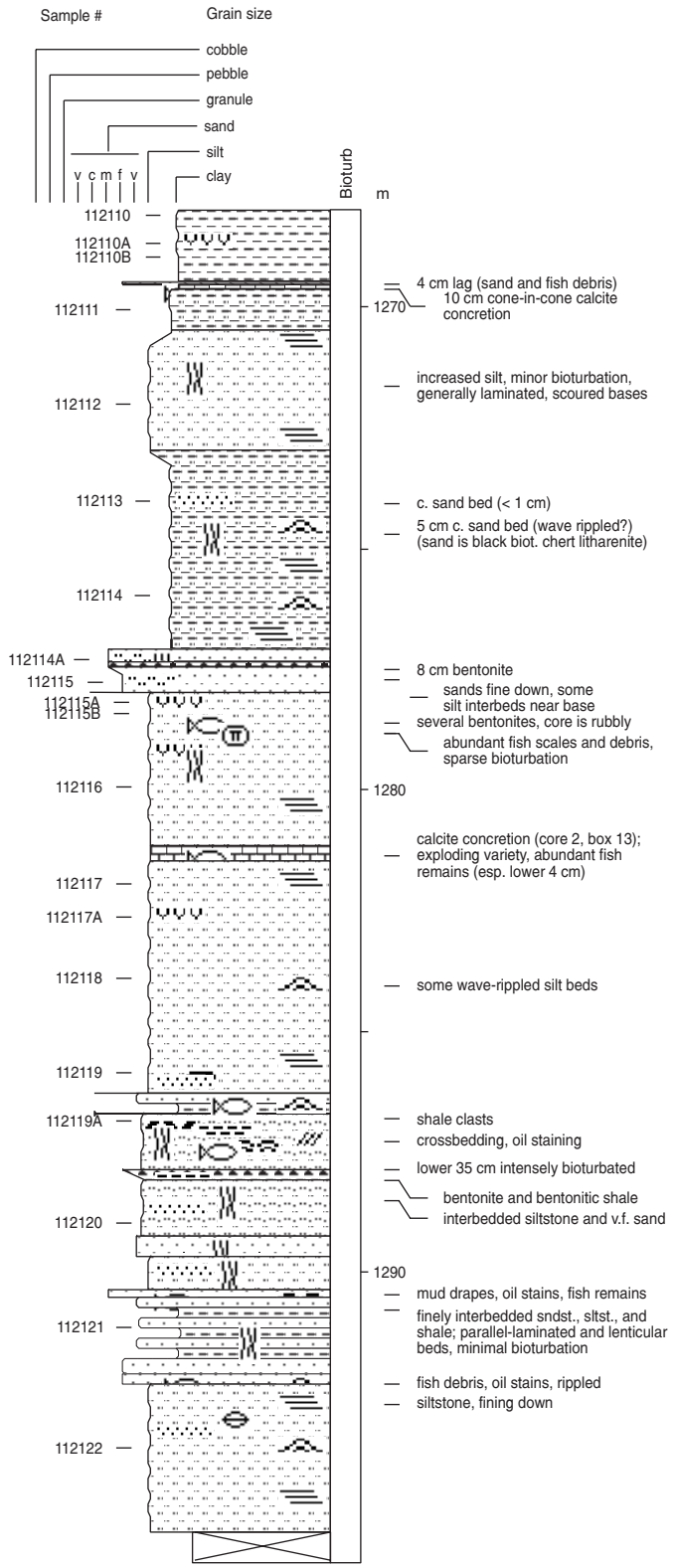

Canhunter Keho
6-16-11-22W4

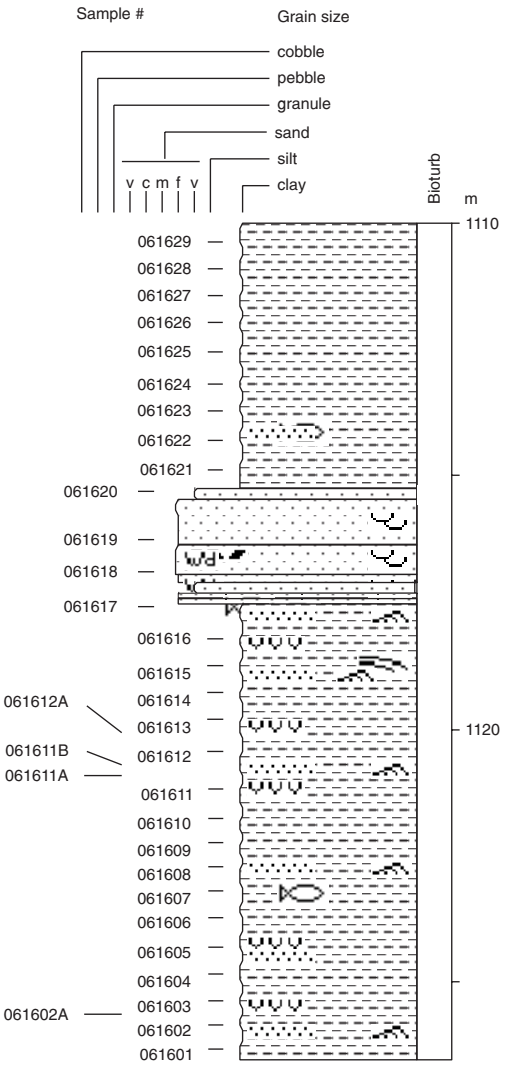

LCD et al. Bashaw 10-34
10-34-42-22W4

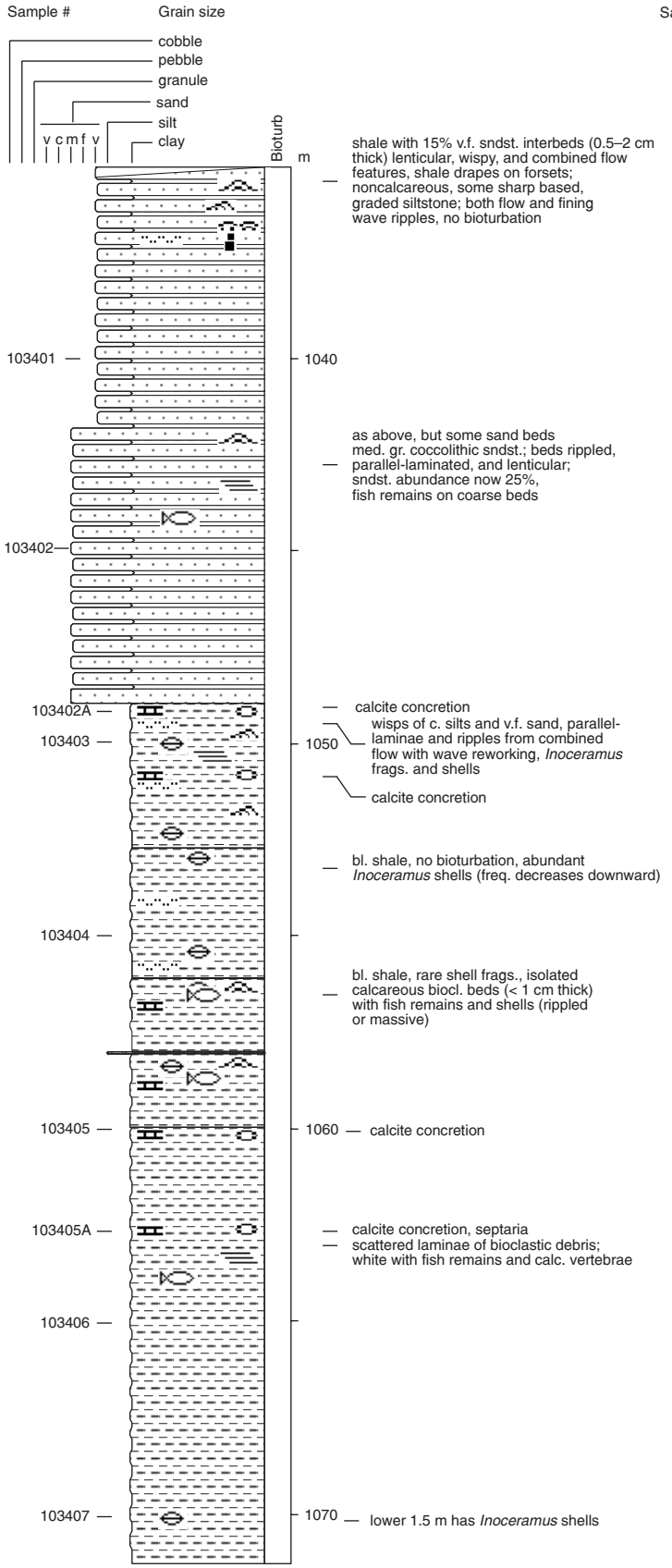

LCM et al. Buff Lk. N. 7-12
07-12-42-21W4

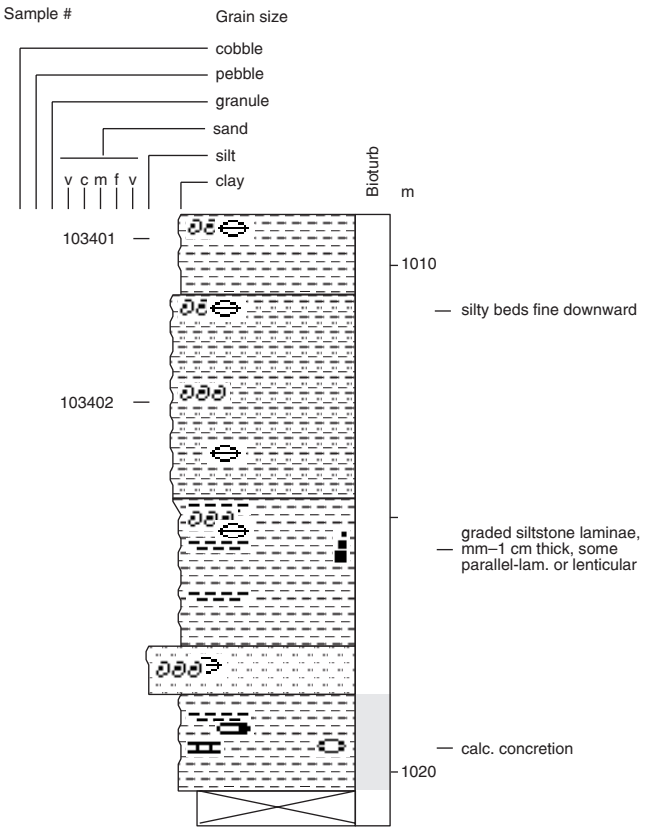

Amoco Conrad
11-12-6-16W4

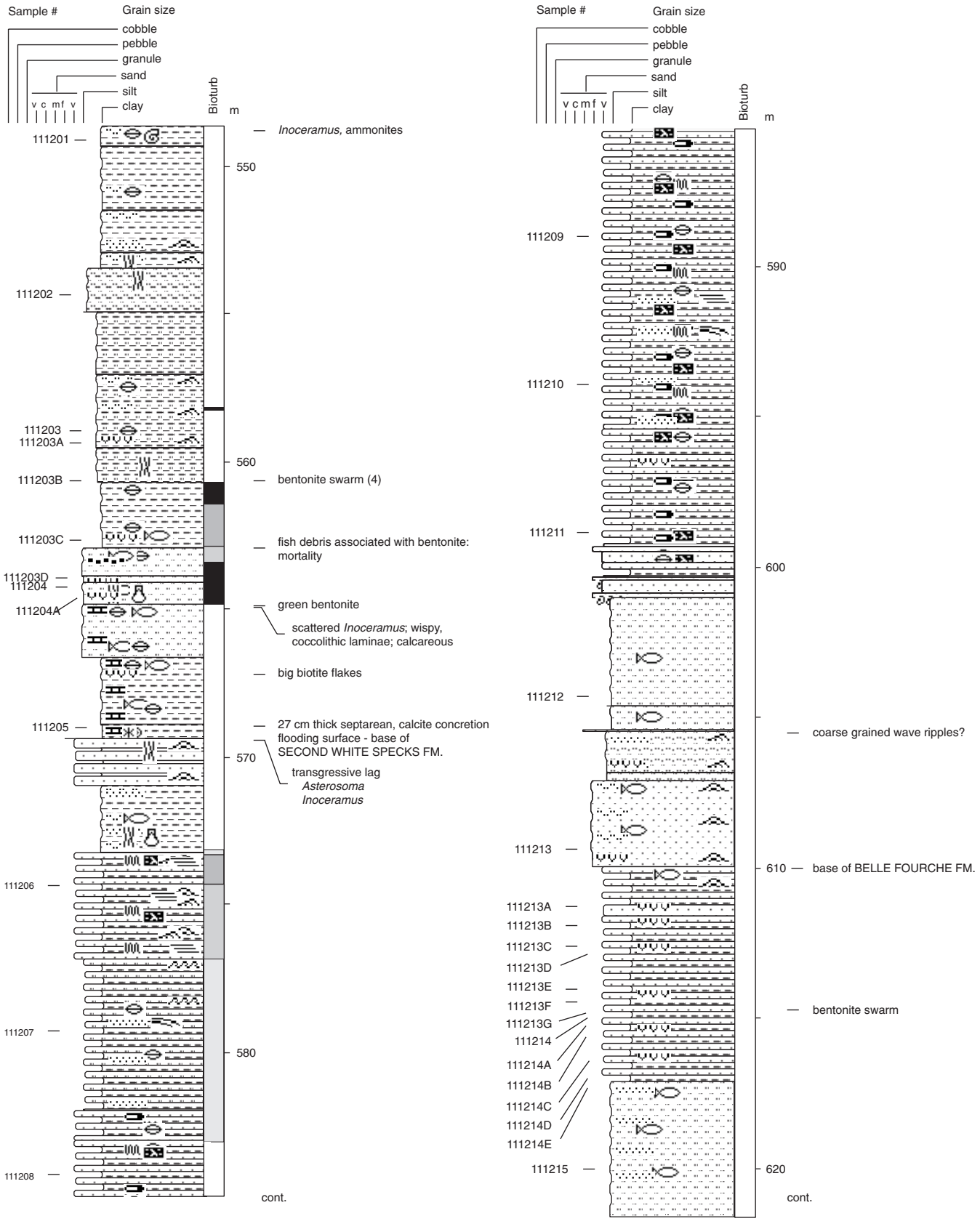

Amoco Conrad (cont.)
11-12-6-16W4

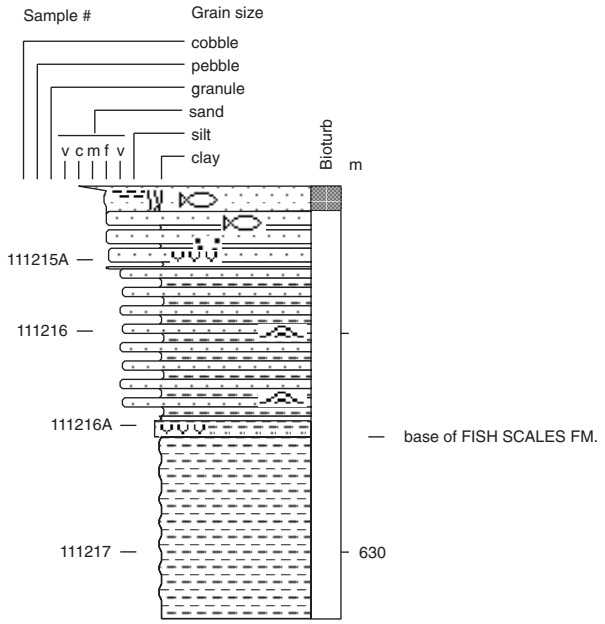

Pan Am A1 Handhills 6-29
06-29-30-16W4

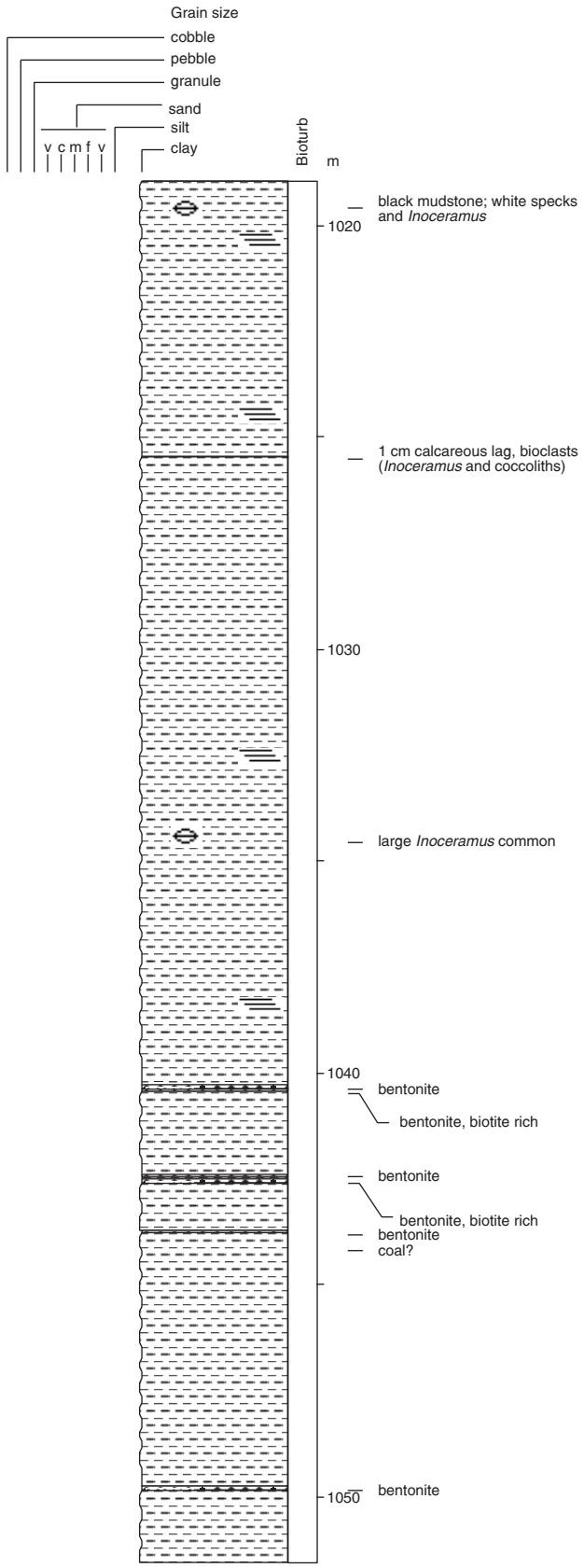

Pan Am A1 Handhills 6-29 (cont.)
06-29-30-16W4

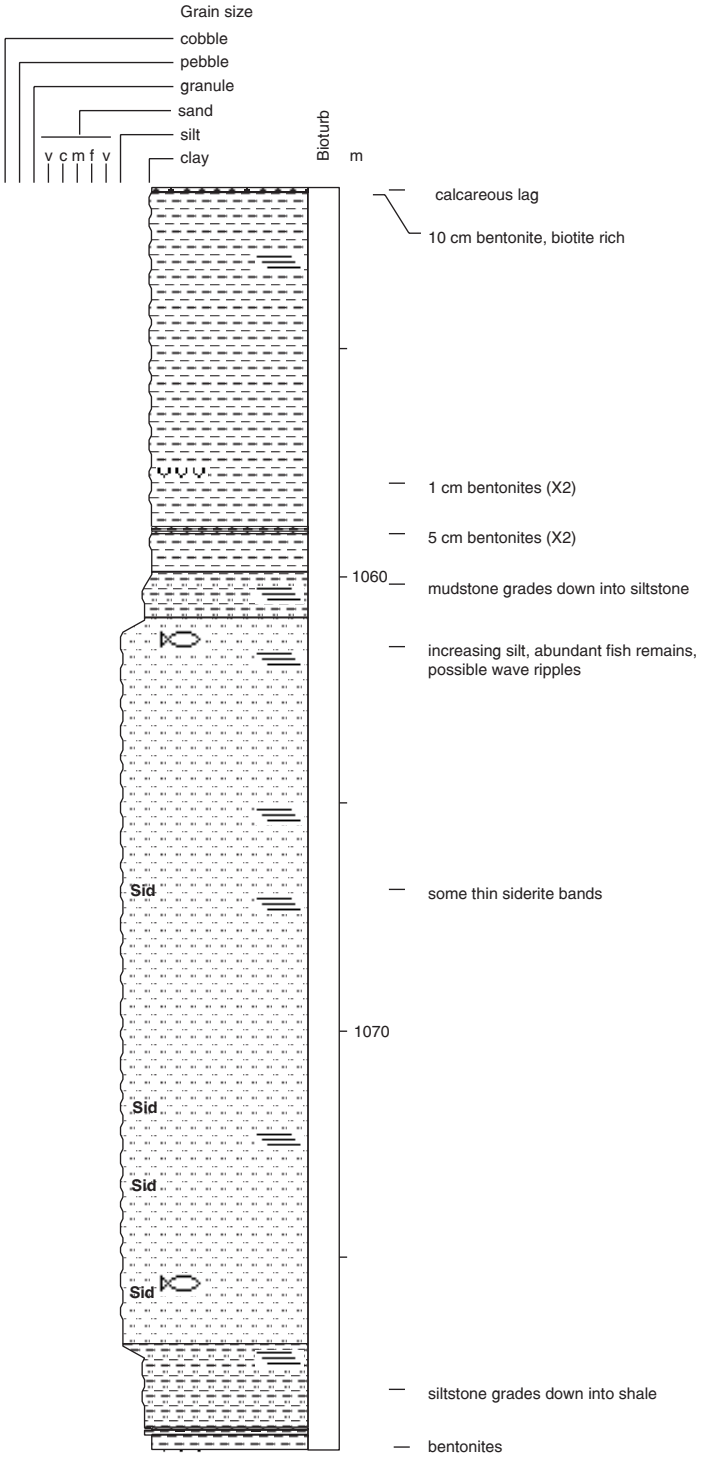

cont.

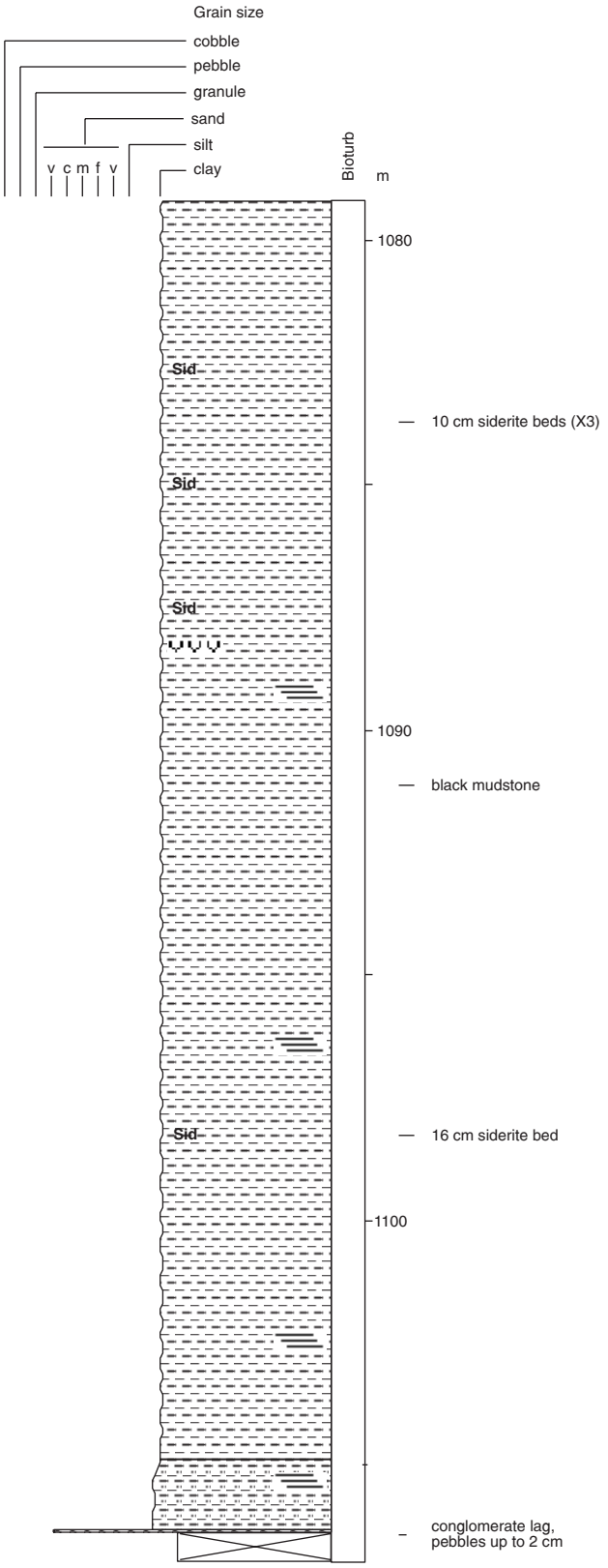

Gulf Mohawk Blood 6-16
06-16-06-22W4

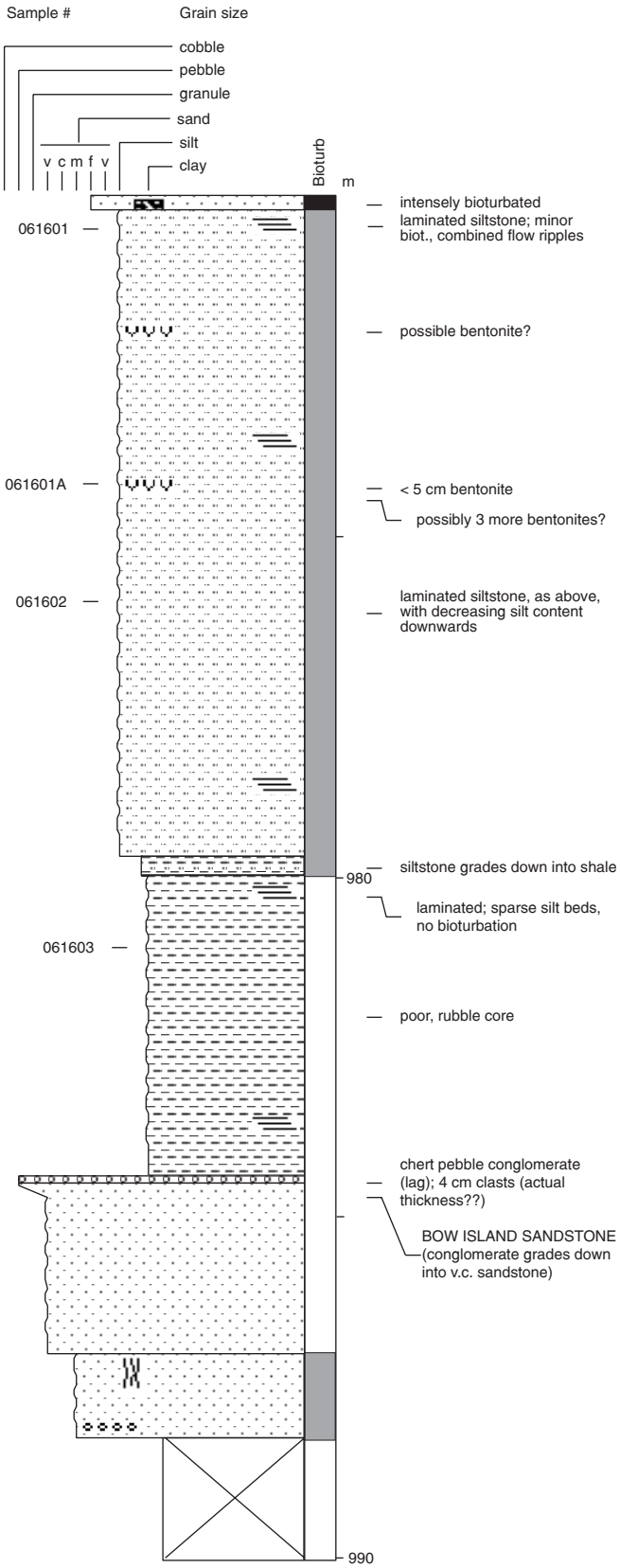

Amoco B-1 Youngstown
6-34-30-8W4

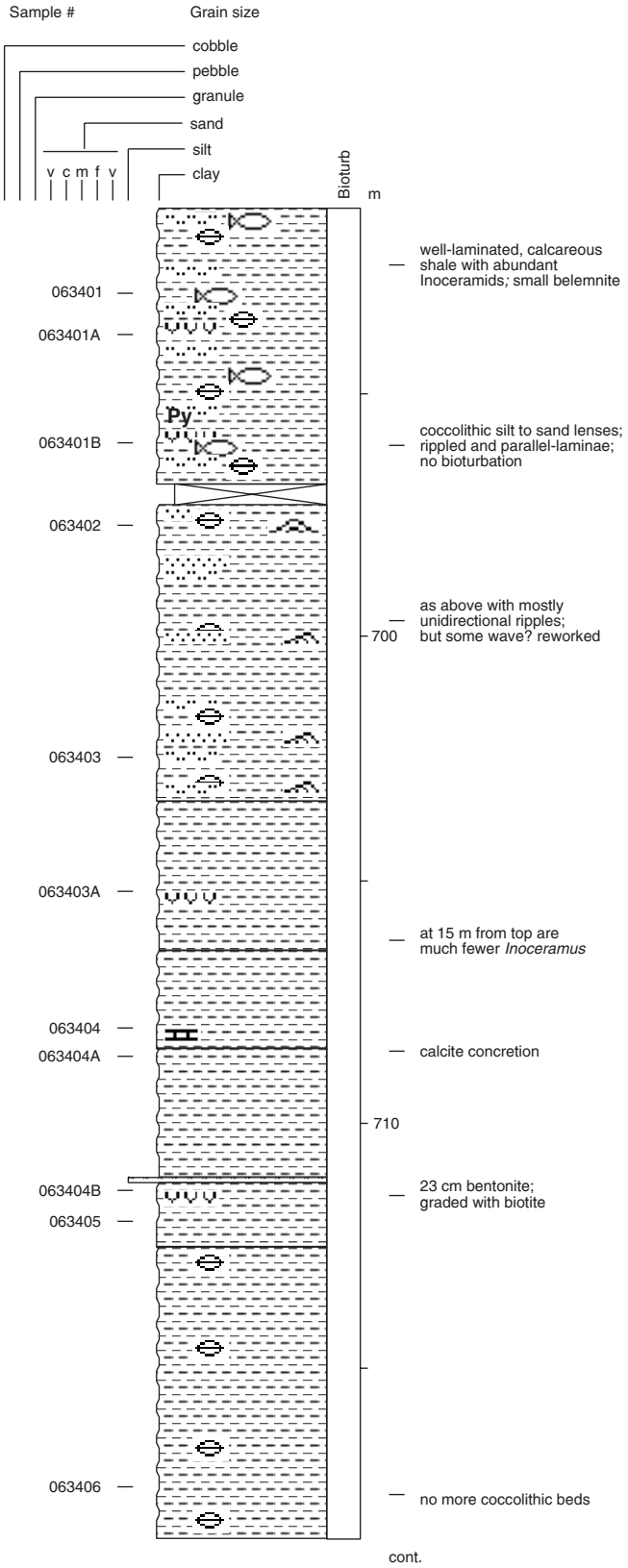

cont.

Amoco B-1 Youngstown (cont.)
6-34-30-8W4

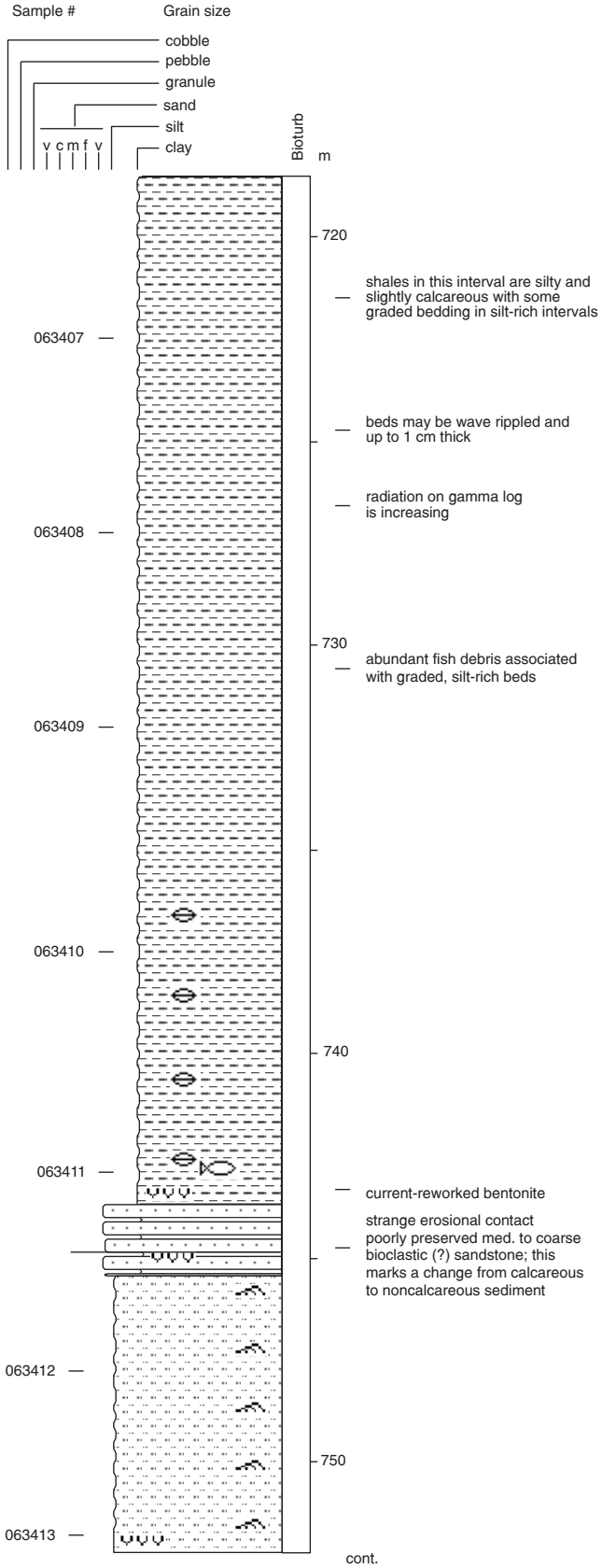

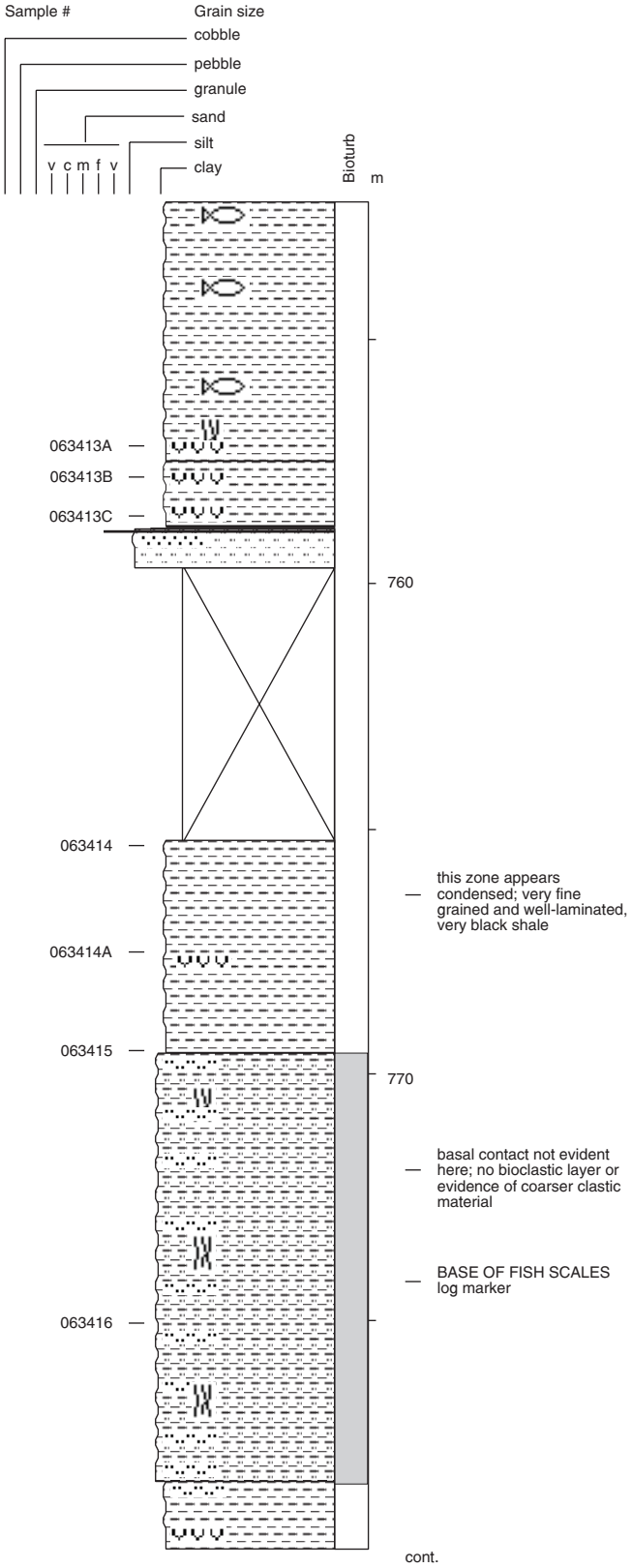

Amoco B-1 Youngstown (cont.)
6-34-30-8W4

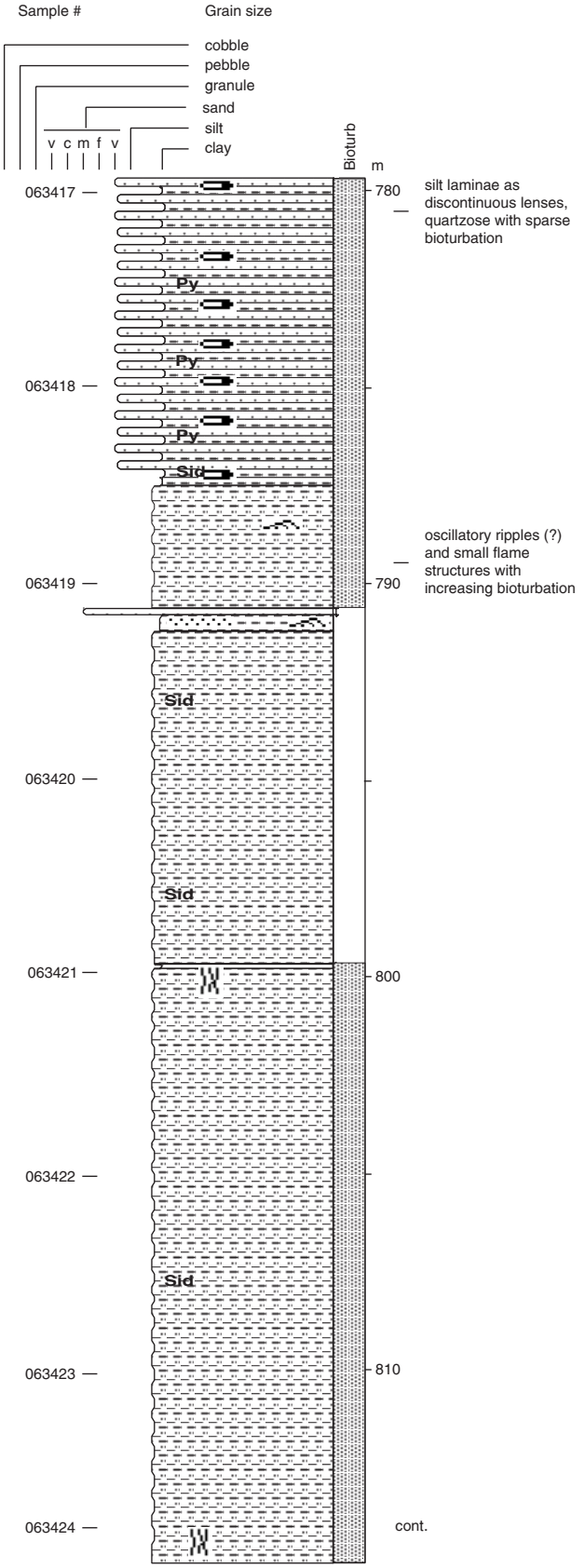

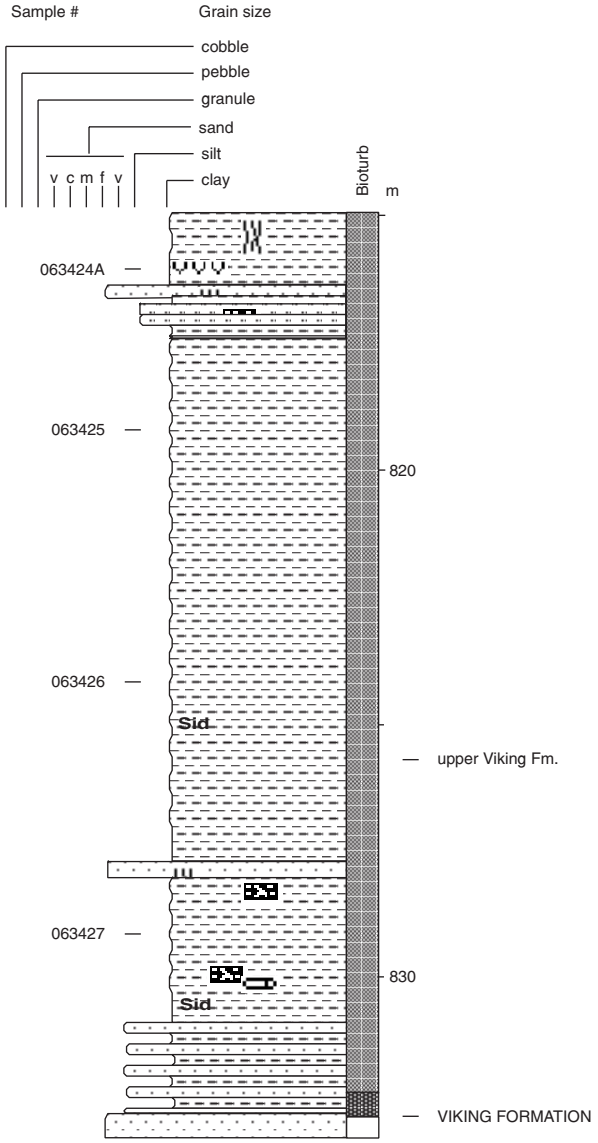

G. Basin Bux. Med. Hat 6-22
06-22-11-06W4

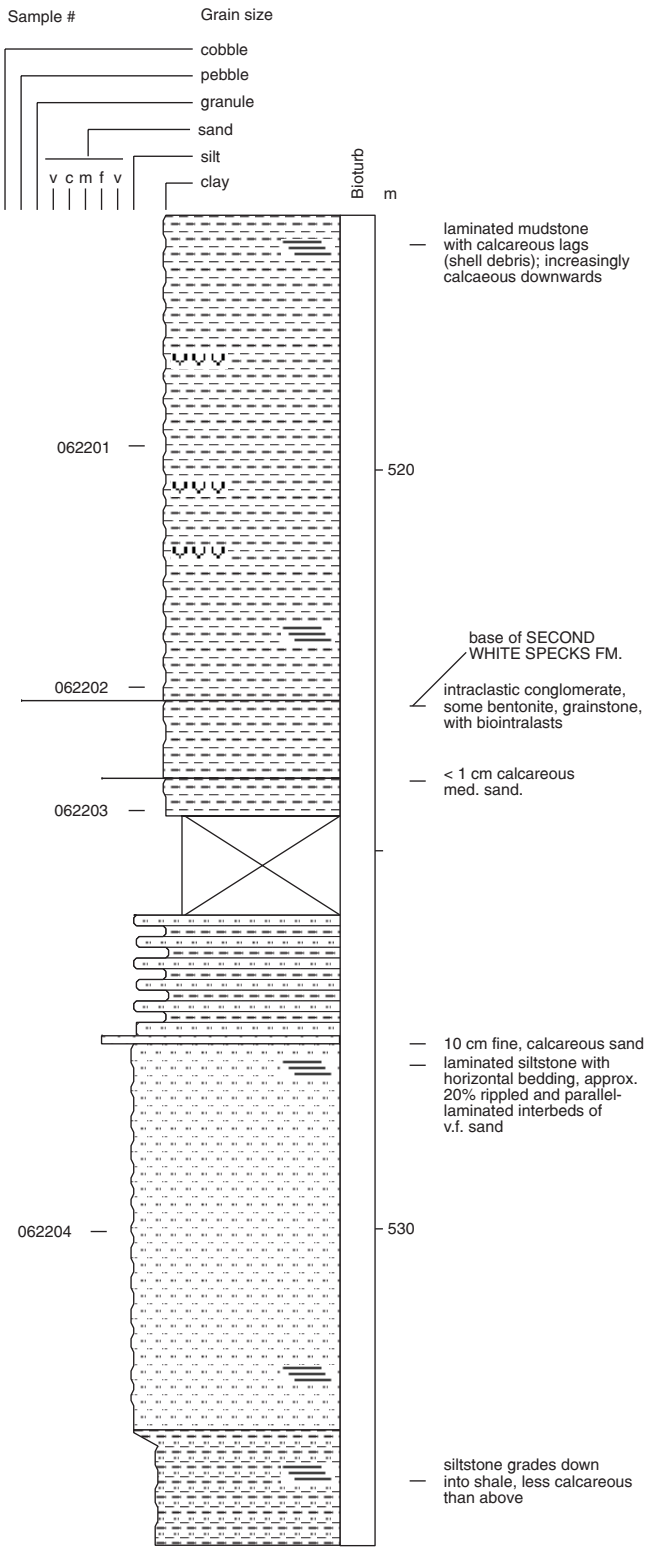

cont.

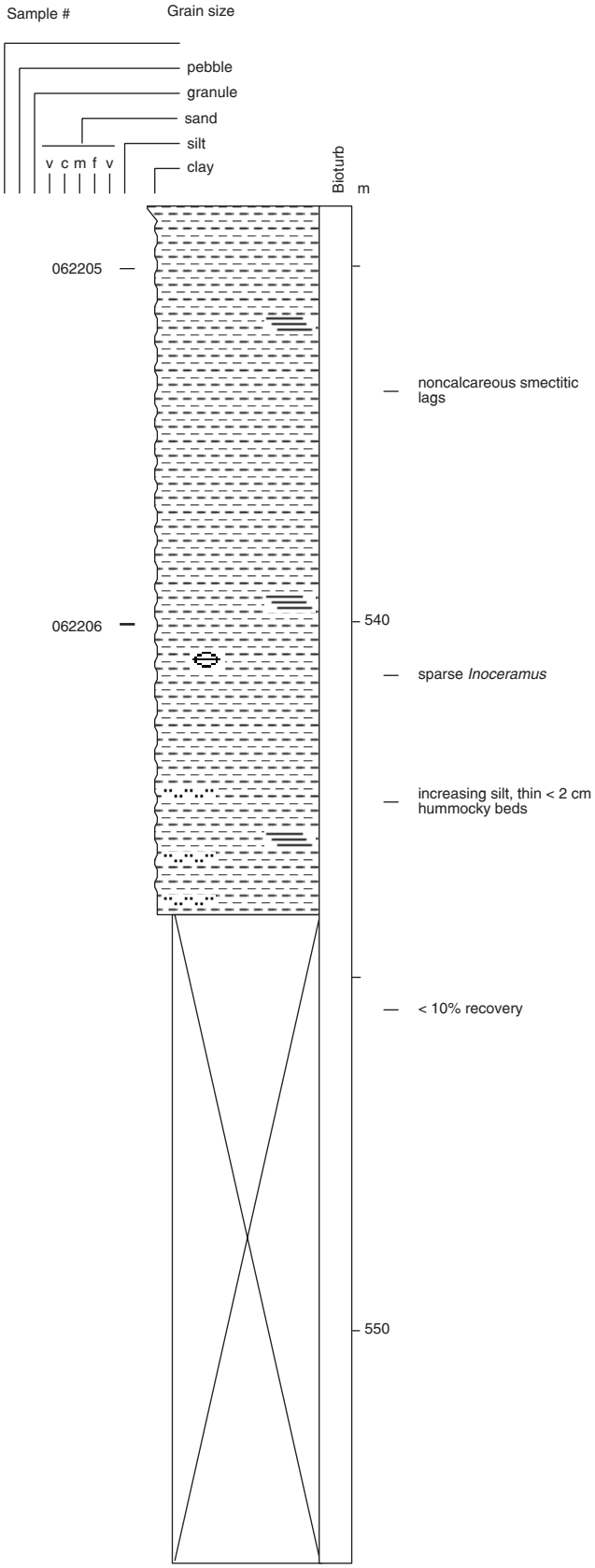

Pac. Amoco Sapphire 7-14
07-14-01-05W4

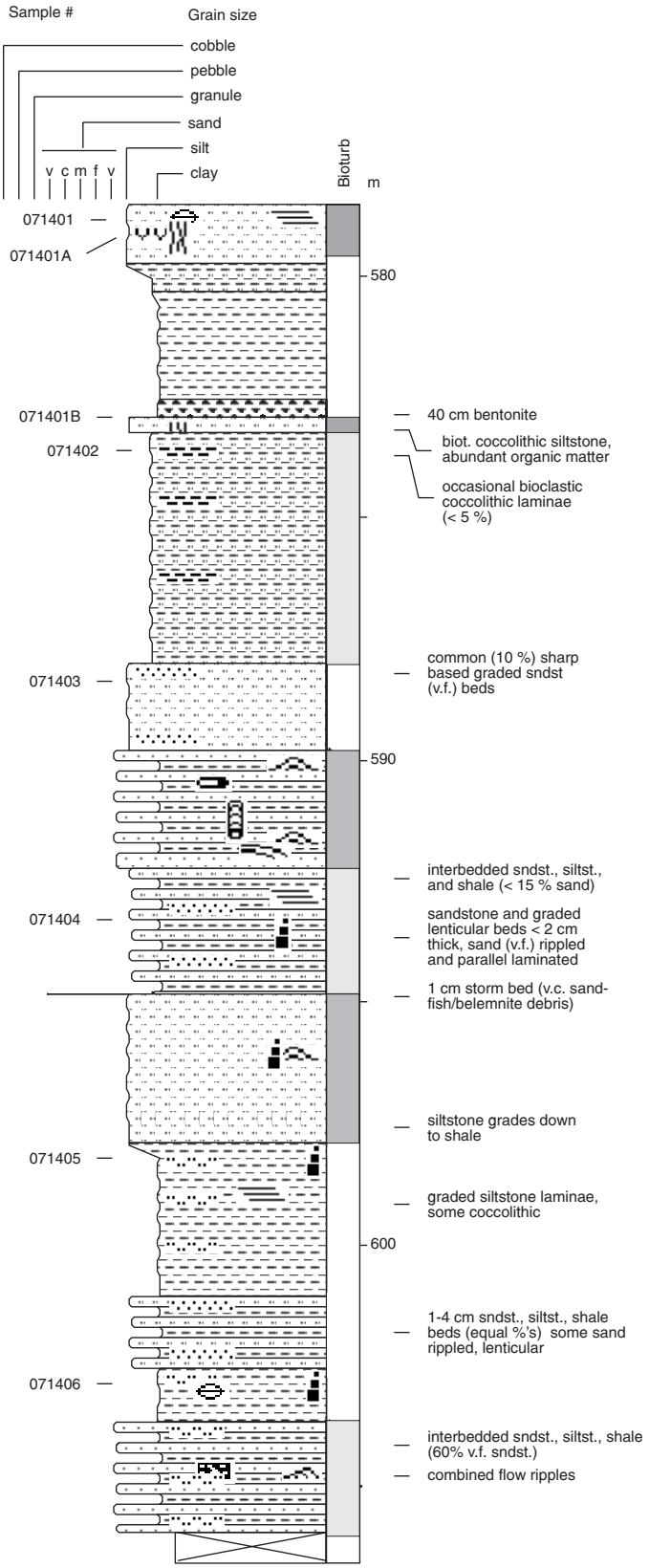

Anderson Husky Roros
10-35-45-2W4

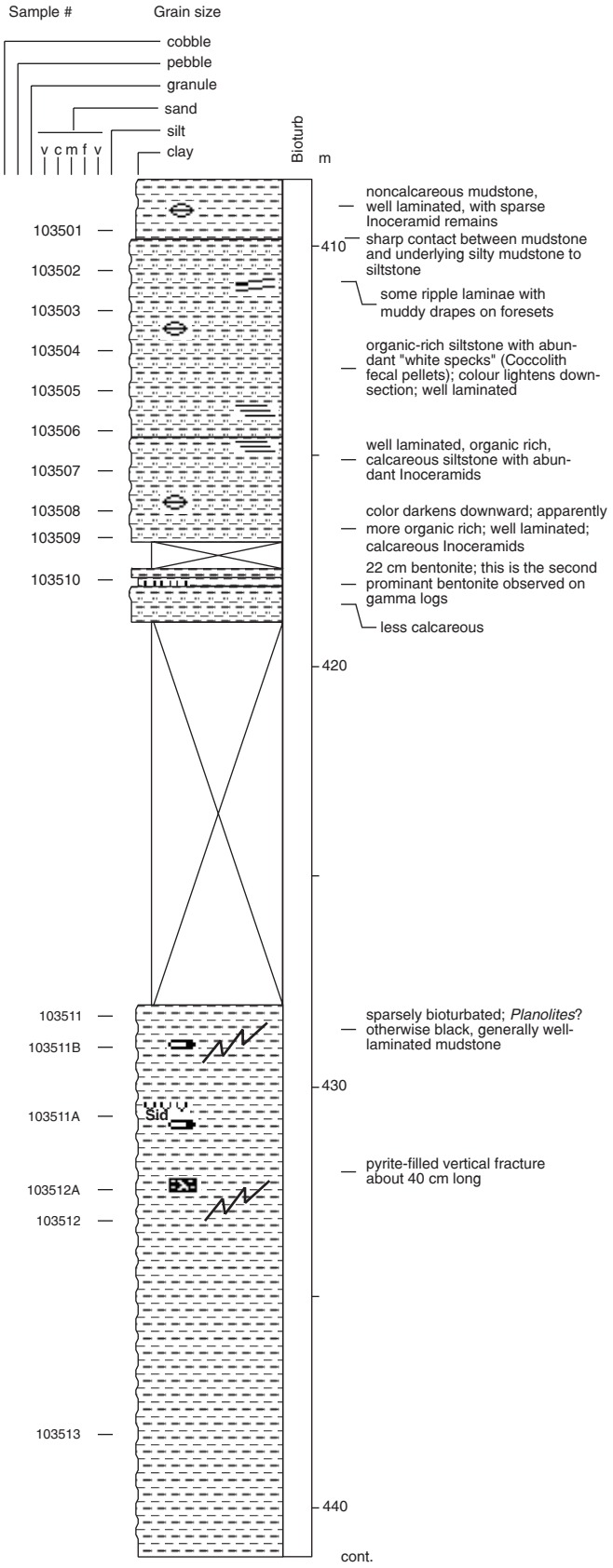

cont.

Anderson Husky Roros (cont.)
10-35-45-2W4

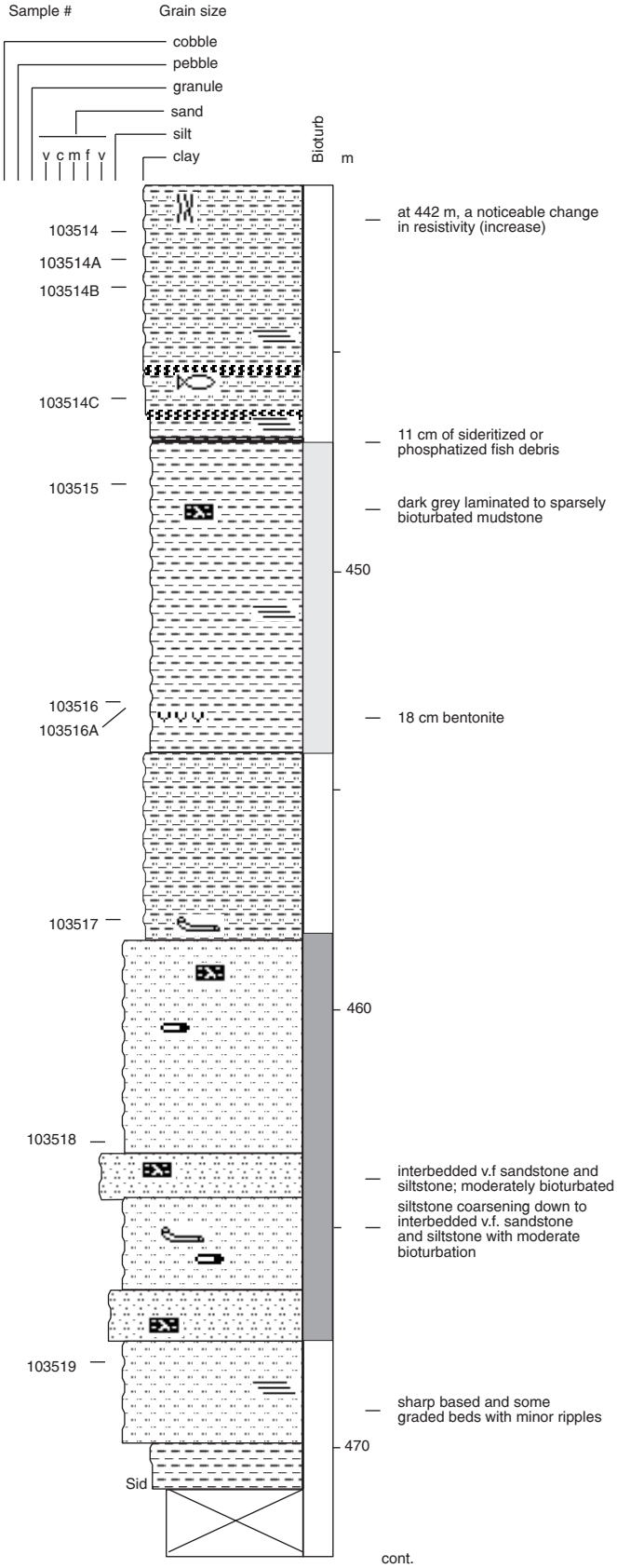

cont.

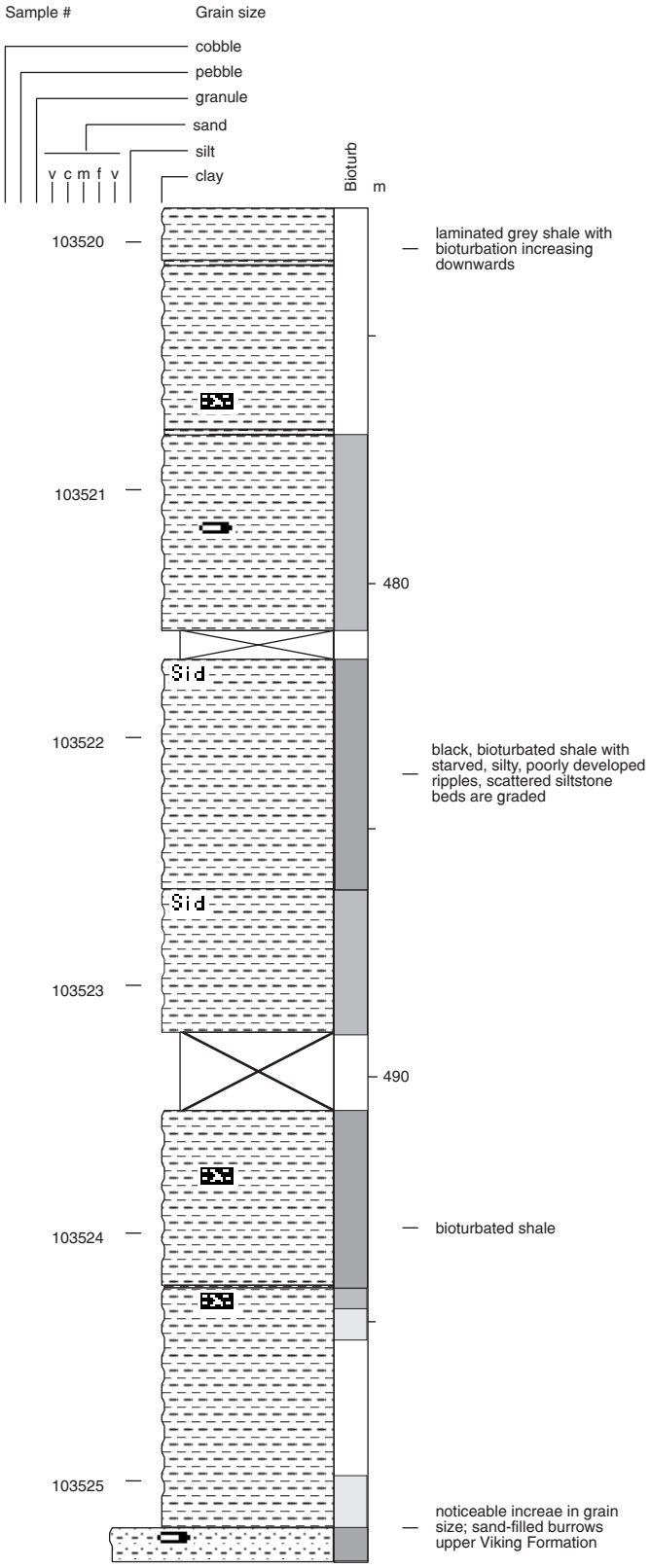

Anderson et al. Ribstone
6-18-45-1W4

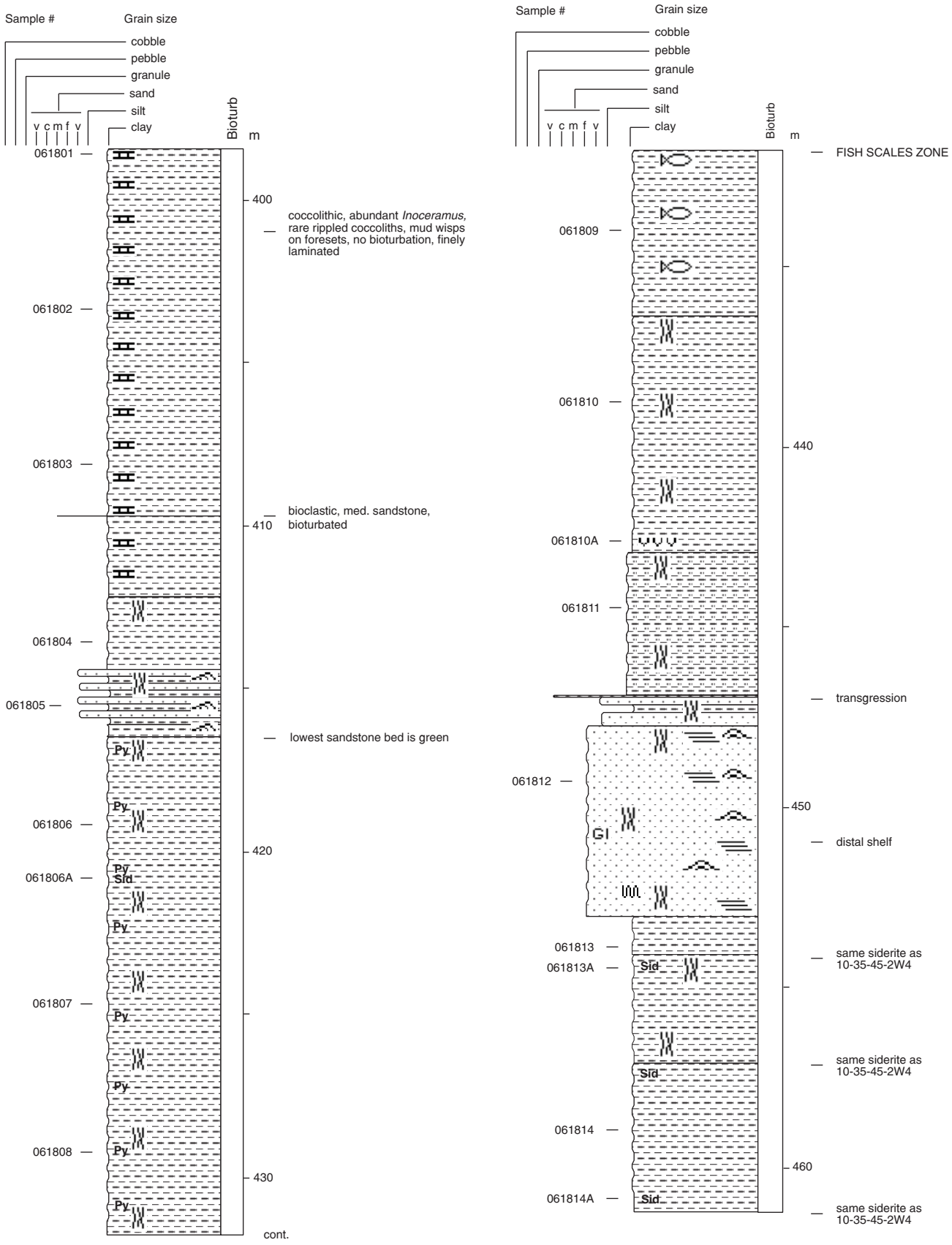

Campana Watrous 4-16
04-16-31-24W2

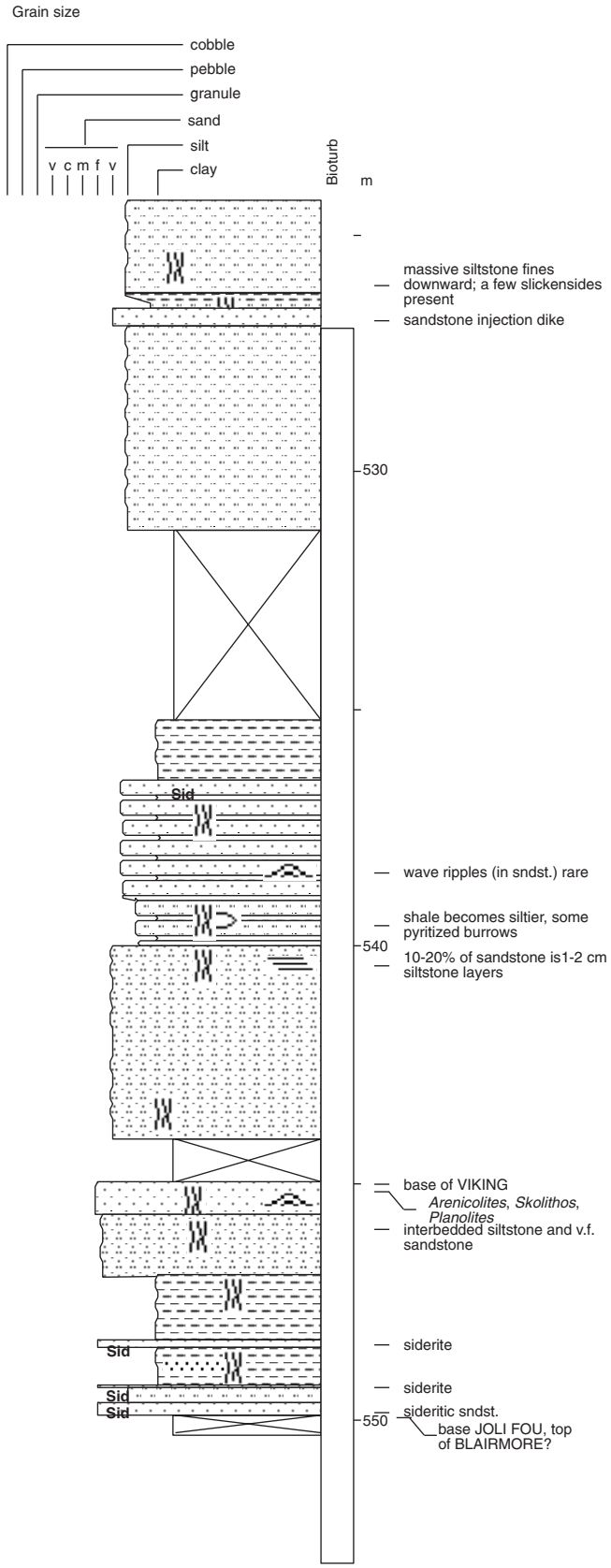

Appendix B

Foraminiferal species count

Amoco Conrad 11-12-6-16W4

	Second White Specks Formation												
Depth (m)	549.64	550.64	551.64	552.64	553.64	554.14	554.64	555.64	556.64	557.64	558.64	559.64	560.64
Barren		X	X		X	X	X	X	X	X	X	X	X
Foraminiferal species													
Trochammina rainwateri	275												
Trochammina ribstonensis	1												
Pseudobolivina sp.				1									
Gavelinella dakotensis													
Neobulimina albertensis													
Heterohelix globulosa													
Hedbergella delrioensis													
Hedbergella amabilis													
Hedbergella loetterlei													
Hedbergella planispira													
Hedbergella portsdownensis													
Whiteinella aprica													
Heterohelix pulchra													
Pseudobolivina rollaensis													
Gavelinella sp.?													
Verneuilinoides sp.													
Ammobaculites sp.													
Bathysiphon sp.													
Spiroplectammina ammovitrea													
Trochammina spp.													
Reophax sp.													
Trochammina rutherfordi													
Trochammina depressa													
Pseudobolivina variana													
Pseudobolivina sp. 1													
planktonic foram. fragments													
agglutinated foram. fragments	20												
Miscellaneous components													
Inoceramus prisms	A	F	A	A		F	C	F	F	F	F-C	R	C
Fish debris						F				R			F
Algal cysts				F	C	F		R			F		
Lignite				F	A	C			F		F	R	R
Pyrite													

A = abundant; C = common; F = few; R = rare

Amoco Conrad 11-12-6-16W4 (cont.)

Second White Specks Formation										Belle Fourche Formation						
561.64	562	562.64	563.14	563.4	563.64	564.64	566.64	567.64	568.64	569.64	570.64	571.64	572.14	572.64	574.64	576.64
				X					X					X	X	
								7		8						78
1																
7	5					86	4									
2	8	50	>100		>100	>100	12	2								
21		>100	>100		>100	>100	12									
	25	>100	>100		20	>100										
	>100	>100	>100		>100	>100	4									
	A	>100	>100		>100	>100										
	15	>100	>100		>100	>100										
		10	>100		25	>100	8									
						75										
							4	2			3					
								2								
								1								
										1						
										2						
											10	24				38
												1	1			
											2					
											5					
											2					
													1			
													3			
	A	A	A		A	A	A									
											F					
	F	A	A	A	A	A		C	F			F-C		F		F
C	C	F	F	F	F	F				F-C						F
A	C				F						F					A
										C	F	F	F		F	
	A															

SWP Bredenbury 11-36-22-1W2

	Morden Formation			Second White Specks Formation												
Depth (m)	255.4	256.3	258.3	260.3	262.3	264.9	266.9	268.9	270.9	272.7	273.7	275.6	277.5	279.4	281.3	283.2
Barren	X	X														
Foraminiferal Species																
Haplophragmoides hendersonense			5													
Haplophragmoides spp.			4													
Pseudobolivina rollaensis			4													
Trochammina ribstonensis			4													
Ataxophragmiidae			5													
*Hedbergell*a spp.				1				24				37				
Heterohelix globulosa					37	11	>100	>100	>100	>100	>100		>100	>100	50	
Hedbergella amabilis									10	>100	>100		>100	>100	>100	>100
Hedbergella delrioensis									>100	>100	>100		>100	>100	>100	>100
Hedbergella loetterlei									>100	>100	>100		>100	>100	>100	>100
Hedbergella planispira									>100	>100	>100		>100	>100	>100	>100
Hedbergella portsdownensis									12	>100	>100		>100	>100	>100	40
Whiteinella aprica									>100	>100	>100		>100	>100	>100	10
Heterohelix pulchra													9			
Clavihedbergella subcretacea														>100	>100	>100
Clavihedbergella simplex															14	1
Bathysiphon sp.																
Hippocrepina sp.																
Trochammina rainwateri																
Verneuilinoides perplexus																
Spiroplectammina sp.																
Placentammina s. 1																
Trochammina wetteri																
Verneuilina canadensis																
Trochammina spp.																
Gaudryina irenensis																
Haplophragmoides howardense																
Haplophragmoides linki																
Textularia sp.																
Ammobaculites tyrelli																
Gaudryina canadensis																
Haplophragmoides rota																
Miliammina manitobensis																
Psamminopelta browsheri																
Uvigerammina manitobensis																
Saccammina alexanderi																
Ammobaculites fragmentarius																
Haplophragmoides postis																
Haplophragmoides kirki																
Haplophragmoides topagorukensis																
Hyperammina emacerata																
Haplophragmium engleri																
Haplophragmoides gilberti																
planktonic foram. fragments								A	A	A	A	F	A	A	A	
aggl. foram. fragments																
Miscellaneous components																
Fish debris	C	R		A	A	C		C	F	C	C		C	C	F	F
Inoceramus prisms					A	A	A	A		C	A	C	A	C	A	A
Radiolarians												C				
Pyrite														F		
Algal cysts																A
Diatoms																

SWP Bredenbury 11-36-22-1W2 (cont.)

Belle Fourche Formation			Fish Scales Formation		Westgate Formation									Viking Formation		
285.1	287	288.9	290.8	291.7	296.7	309.7	311.8	316.8	321.8	328.1	332.6	336.3	340.5	343.8	348.8	349.3
			X	X		X							X	X		
	3															
3	2															
1																
2					1											
1	1															
28	11															
2																
		3														
					3					6					2	1
					12				2							
					6		1	10	3	3	4	2				
							1				4					
								34	4							
								3				1				
								4		6					3	
								2								
									3	1	1					
									1						2	
									1			1				
									4	4	3					
									3	5	2					
									4						3	
										2						
										1	1				14	
											3	2			7	
											3					
												14				
												3				
															3	
															2	
C	R							C	F	C	C	F				
A	A	C					F		R		R	F	C	R	C	R
			F	F												
		A				F									F	
A	A	F		F	F	F	F		R	C					C	R
												R			R	

Anderson Husky Roros 10-35-45-2W

.			Second White Specks Fm							Belle Fourche Fm				Fish Scales		Westgate Fm			
Depth (m)	408.4	410	411	411.8	412.7	413.6	414	415.6	417	428	433	438.2	442.5	442.9	443	448.3	452.8	454.4	456.4
Barren	X	X									X	X	X	X	X				
Foraminiferal species																			
Hedbergella delrioensis			1	160	>100	23	>100	102	15										
Hedbergella amabilis				5	>100	8	>100	3	9										
Hedbergella loetterlei				390	>100	>100	>100	10	117										
Heterohelix globulosa				60	30	56	>100	11	23										
Whiteinella aprica				6		4	>100												
Hedbergella planispira					>100	15	>100												
Hedbergella portsdownensis					12	9	>100												
Trochammina rutherfordi mellariolum										4									
Ammobaculites sp.																2			
Ammodiscus sp.																1			
Haplophragmoides howardense																2			
Miliammina manitobensis																4		18	18
Placentammina sp. 1																3		1	
Verneuilina canadensis																5		16	38
Psamminopelta browsheri																	1		
Ammobaculites fragmentarius																		8	16
Ammobaculites wenonahae																		7	2
Arenobulimina paynei																		10	11
Gaudryina canadensis																		2	8
Haplophragmoides collyra var. bullocki																		5	5
Haplophragmoides hendersonense																		10	13
Haplophragmoides spiritense																		2	
Hippocrepina sp.																		3	
Saccammina alexanderi																		5	1
Trochammina sp. 1																		4	
Ammobaculites albertensis																			6
Haplophragmoides kirki																			3
Gaudryina irinensis																			8
Psamminopelta sp.																			2
Pseudobolivina sp.																			1
Reophax incompta																			8
Reophax minuta																			7
Reophax spp.																			3
Saccammina complanata																			1
Trochammina wetteri																			16
Flabellammina spp.																			
Miliammina ischnia																			
Textularia gravenori																			
Trochammina diagonis																			
Trochammina rutherfordi																			
Uvigerammina sp. 1																			
Reophax troyeri																			

Anderson Husky Roros 10-35-45-2W (cont.)

Westgate Fm																							
458.4	460.4	462.4	464.4	466.4	467	468.4	470.4	472.4	474.4	476.4	477	478.4	480.4	482.4	484.4	486.4	488.4	490.7	492.4	492.5	494.4	496.4	498.4
											X				X								
	10									12													
13	8	6	7	5	4		14	4	15	18		1	13	3		3	6	6	5	4	1	5	11
		4				4				1			2	2				5	3	1			5
75	17	12	1	2		21	8		19													11	31
	4							1		4		1	2			2							1
5	10	100	11	12	11	13	49										1		25	4	1	16	23
						3				10													
7																							
3	5	2																					
2	11	3	3				1																
																							1
	2	6	1	4	3	5				11			7				5	12	6			16	19
2																							
2		1																					
3																							
				1		10	1											3	5	1			
									10				1				1						9
3							3																
	2																						
	2																						
	3																						
	10	10																					
	1			1																			
		7					8	13															

Anderson Husky Roros 10-35-45-2W4 (cont.)

			Second White Specks Fm							Belle Fourche Fm				Fish Scales		Westgate Fm			
Depth (m)	408.4	410	411	411.8	412.7	413.6	414	415.6	417	428	433	438.2	442.5	442.9	443	448.3	452.8	454.4	456.4
Barren	X	X									X	X	X	X	X				
Foraminiferal species																			
Trochammina depressa																			
Trochammina sp. 2																			
Trochammina spp.																			
Bathysiphon sp.																			
Flabellammina warreni																			
Haplophragmoides spp.																			
Haplophragmoides neolinki																			
Textularia sp.																			
Trochammina cf. *whittingtoni*																			
Flabellammina hendersonensis																			
Haplophragmoides sp. 1																			
Haplophragmoides topagorukensis																			
Thuramminoides septagonalis																			
Ammobaculites sp. a																			
Textularia topagorukensis																			
Bathysiphon brosgei																			
Ammobaculites petilus																			
Verneuilinoides fischeri																			
Ammotium sp.																			
Haplophragmoides sp. 2																			
Haplophragmoides postis goodrichi																			
Miliammina awunensis																			
Verneuilinoides sp.																			
Psammosphaera sp.																			
Reophax texanus																			
Haplophragmoides gilberti																			
Rhabdammina sp.																			
Reophax tundraensis																			
Pseudobolivina variana																			
planktonic foram. fragments				A	A	A	A	C											
aggl. foram. fragments																F		C	A
Miscellaneous components																			
Inoceramus prisms	C	F	A	A	R	R	A	F	A										
Fish debris	C	F	A	C	A	F	C								F	R			F
Algal cysts		F	R	F	F	F		A	A				R	R	C	R			R
Ostracods										R									
Pyrite										F	F								
Radiolarians															R				
Diatoms																		C	F

Anderson Husky Roros 10-35-45-2W4 (cont.)

Westgate Fm																							
458.4	460.4	462.4	464.4	466.4	467	468.4	470.4	472.4	474.4	476.4	477	478.4	480.4	482.4	484.4	486.4	488.4	490.7	492.4	492.5	494.4	496.4	498.4
											X				X								
		1																					
		2																					
			1	6				2	30	35												20	
				6		5	1	2	5	3							1						
				2																			
				5			1	2	27	5			3					4	5	5	3	19	
					5	3																	
					1																		
					2																		
						3																	
						20		5	20	12													
							5	2															
								2															
								20	110	13													
								5															
									3	44								1			1		35
									5														
									25	18													
										1													
										28													
													3				4	7					26
													5										
													3			1	1						
																			4	1		6	6
																					3		
																						5	
																							1
																							10
																							1
A	A	F				A			A	C		R		R			F					F	C
R	F	R		R	R	F		R		R			C	F			R	C					C
	F			R				R		F					C	R	F	C					
C	C															R		R					

Anderson et al. Ribstone 6-18-45-1W4

	Second White Specks Formation											Belle Fourche Formation										FSF	Westgate Formation					
Depth (m)	398.3	398.5	400	401.5	403	404.5	406	407.52	408.52	409.52	410.52	412.52	414.1	415.25	416.4	418	419.1	421	424.1	427.2	429.1	434.1	439.1	444.1	449.1	449.5	454.1	459.1
Barren	X	X	X										X	X			X	X				X						
Foraminiferal Species																												
Hedbergella amabilis				15																								
Hedbergella delrioensis				115	12	40	25	1		10																		
Hedbergella loetterlei				135	30	28	30			2																		
Hedbergella planispira				60	15	25	9			2																		
Hedbergella portsdownensis				140	12	50	20			2																		
Heterohelix globulosa				640	60	186	10	1	15	54	20					1												
Heterohelix pulchra				30	3	18					4																	
Whiteinella aprica				170	9	125	50	7	15																			
Neobulimina albertensis						10		2	42	8																		
Haplophragmoides howardense var. manifestatum								5																				
Saccammina lathrami								1																				
Trochammina sp.								1																				
Spiroplectammina ammovitrea									3																			
Trochammina depressa									3																			
Trochammina rainwateri									21			12			1												3	
Bathysiphon sp.												2														2		
Psamminopelta browsheri												1															1	
Saccammina alexanderi												1							2		1							2
Verneuilinoides perplexus												24																
Uvigerammina sp.																			1									
Placentammina sp. 1																			1					1			1	
Verneuilina sp.																					1							1
Ammodiscus rotalarius																							1					
Haplophragmoides linki																							3	3				
Miliammina manitobensis																							4	1		1	1	1
Spiroplectammina sp.																							1					
Trochammina wetteri																							2				3	
Arenobulimina paynei																								12	2			
Haplophragmoides spp																								4		3		4
Verneuilina canadensis																									1	3		
Gaudryina bearpawensis																										2		
Haplophragmoides kirki																										1		
Ammobaculites fragmentarius																											1	
Pseudobolivina variana																												2
Bathysiphon brosgei																												1
planktonic foram. fragments				A	C	A	A			C																		
aggl. foram. fragments									F			F				R				R				F	F	F	F	
Miscellaneous components																												
Inoceramus prisms	A	F		A	C	C	C	F	A	C																		
Fish debris	F	R		F	R	F	F	A	A	A	A			C	C			R				R						
Algal cysts				C	A	A	A	F	F		F	C																
Pyrite													A	A		F					R	R				A		
Diatoms																								F		R		

Saskoil Willow Creek 10-25-1-27W3

	Second White Specks Formation										Belle Fourche Formation						
Depth (m)	838	839	840	841	842	843	844	845	846	847	848	849	850	851	852	853	854
Barren	X	X	X	X	X					X							
Foraminiferal species																	
Hedbergella amabilis						220		24									
Hedbergella delrioensis						130	2	560									
Hedbergella loetterlei						60	2	584									
Hedbergella portsdownensis						38		80									
Heterohelix globulosa						734	17	1580									
Whiteinella aprica						24	3	120									
?*Praeglobotruncana delrioensis*									1								
Placentammina sp. 1											2						
Saccammina lathrami											6						
Miliammina sp. fragment											1						
Spiroplectammina ammovitrea											15	6	2		11		22
Verneuilinoides sp.											2	1			1		
Reophax pepperensis												4					
Trochammina rainwateri												2					14
Bathysiphon sp.														2			
Trochammina rutherfordi														31			4
Saccammina alexanderi																	2
Ammobaculites fragmentarius																	2
Haplophragmoides sp.																	2
planktonic foram. fragments						240	27	400									
aggl. foram. fragments																3	
Miscellaneous components																	
Inoceramus prisms	A	A	A	C	C	C	F	C	C								F
Radiolarians			F		C												
Fish debris			C			C	F	F	C				A				F
Algal cysts						C											
Lignite										F	A					F	F

C.M.S. Vanscoy 11-16-36-8W3

	First White Speckled Shale										SWSF	Belle Fourche Formation							FSF
Depth (m)	360.7	376.3	381.3	386.3	391.3	396.3	397.3	398.3	399.4	400.35	401	401.7	402.2	403.2	404.2	405.2	406.2	407.2	408.2
Barren		X															X		X
Foraminiferal species																			
Arenobulimina sp. 1	1																		
Gaudryina sp. 1	1																		
Neobulimina painoides	4		36																
Placentammina sp. 1	1											2		12	8			3	
Praebulimina reussi	1																		
Globigerinelloides bentonensis	16																		
Hedbergella loetterlei	5			1		2	2			21									
Hedbergella planispira	2																		
Heterohelix globulosa	2		3	1	11	1	2			3	>100								
Gavelinella henbesti			309	179	9	18	208			4									
Globigerinelloides messinae			18	3	11	3	22		2										
Haplophragmoides collyra			3	15	4														
Flabellammina magna				4	1		2												
Glomospirella inconstans				2		1													
Pseudobolivina rollaensis				8	2	19	10												
Pseudobolivina sp. 1				28	19	1			5										
Neobulimina albertensis					6														
Dorothia smokyensis						24				1									
Trochammina ribstonensis						14	104	17	8	4									
Ammodiscus planus							10	1		5									
Heterohelix moremani							256			1									
Hedbergella amabilis							8												
Hedbergella spp.							6			>100									
Ataxophragmiidae							18	5		3			10	13	7				
Bathysiphon sp.										7				5	2				
Cassidella tegulata										5									
Dorothia sp.										1									
Saccammina lathrami										1									
Saccammina sp.										1				1	1				
Hedbergella portsdownensis											>100								
Whiteinella aprica											54								
Pseudobolivina variana												2	20	23	5				
Reophax troyeri												1	4	3					
Trochammina wetteri												6	17	5					
Verneuilinoides perplexus												38	115	111	66				
Haplophragmoides spp.													4	6	17				
Pseudobolivina sp.													10						
Gaudryina sp.														1					
Hippocrepina sp.														2					
Textularia sp. 1														1					
Trochammina rainwateri														2	36			1	
Trochammina spp.															2				
Saccammina alexanderi																		2	
Ammobaculites spp.																			
Gaudryina canadensis																			
Gravellina sp.																			
Haplophragmium engleri																			
Haplophragmoides postis goodrichi																			
Miliammina manitobensis																			

C.M.S. Vanscoy 11-16-36-8W3 (cont.)

Westgate Fm																		Viking	Joli Fou Fm	
413.2	418.2	427.3	430.8	435.8	440.8	445.8	450.8	455.8	460.8	465.8	476.4	470.8	479.8	484.3	484.8	489.9	494.8	499.8	504.6	510
											X									
6					1							7	7		7					
															2				1	
3			6											4						
				1	1		1		1	2			2	6	5		3		1	2
																				4
										1				1						
2	5	6		7	7				8	3		6			2		2			6
										1		1								
													2			9	1		1	
														1						
								3	1	6		8	4	6	4	10	2		37	27
2		4	4						6					1						
20									1	2				2	1	10	2		13	7
4		1																		
1																				
22		16	8																	
4			4				2		12	2		15	4	4	19	2	2			

C.M.S. Vanscoy 11-16-35-8W3 (cont.)

	First White Speckled Shale										SWSF	Belle Fourche Fm							FSF
Depth (m)	360.7	376.3	381.3	386.3	391.3	396.3	397.3	398.3	399.4	400.35	401	401.7	402.2	403.2	404.2	405.2	406.2	407.2	408.2
Barren		X															X		X
Foraminiferal species																			
Uvigerammina manitobensis																			
Verneuilina canadensis																			
Verneuilinoides sp.																			
Ammobaculites tyrelli																			
Trochammina depressa																			
Haplophragmoides bonanzaense																			
Placentammina sp. 2																			
Ammobaculites fragmentarius																			
Haplophragmoides howardense																			
Haplophragmoides kirki																			
Trochammina uminiatensis																			
Haplophragmoides linki																			
Haplophragmoides sp. 1																			
Flabellammina gleddiei																			
Ammobaculites whitneyi																			
Textularia topagorukensis																			
Reophax incompta																			
Ammodiscus kiowensis																			
Psamminopelta browsheri																			
Haplophragmoides spiritense																			
Ammodiscus anthosatus																			
Flabellammina sp.																			
Bathysiphon brosgei																			
Hyperammina sp.																			
Gaudryina irenensis																			
Haplophragmoides rota																			
Gaudryina bearpawensis																			
Haplophragmoides gigas																			
Haplophragmoides sp. 2																			
Pseudobolivina sp. 2																			
Ammobaculites pertilus																			
Haplophragmoides cushmani																			
Reophax sp.																			
Arenobulimina paynei																			
Ammomarginulina sp. 1																			
Ammomarginulina sp. 2																			
Psammosphaera sp.																			
Haplophragmoides lapillosus																			
Verneuilinoides tailleuri																			
Reophax troyeri																			
planktonic foram. fragments											A								
aggl. foram. fragments															F				
Miscellaneous components																			
Fish debris	F	F	F				F	F	R				F						
Algal cysts	F	F	F	F	C		F	C	F	F	C							F	
Inoceramus prisms											C								
Diatoms													F						
Pyrite																	C	A	F

C.M.S. Vanscoy 11-16-35-8W3 (cont.)

Westgate Formation																		Viking	Joli Fou	
413.2	418.2	427.3	430.8	435.8	440.8	445.8	450.8	455.8	460.8	465.8	476.4	470.8	479.8	484.3	484.8	489.9	494.8	499.8	504.6	510
											X									
							2													
1					5			2												
14	2	1	4	6	4	1	3	5	6	13		6	2	5	1				1	
4																				
		4			3				4										12	22
		1							1	3		2								
			16	2														2		
			2											2	2					
					20			2					1				2	19	18	18
					3															
					3															
					4		3	4	3											
								1	2								1		15	1
								8	3								1	4		
								1												
									1							1				3
									1								2	1		1
										2			3		4	9				
												1								
												8	1			7				
													2							
															1					
															1					
																5				
																3	2	1		
																1				
																7				
																	1			
																		2	6	6
																		4		
																		2	3	
																			4	1
																			73	15
																			2	
																			1	
																				3
																				4
																				2
																				2
																				3
																				1
F				F			F	F	C	F		F	F	C	C	F	C	R	C	C
F					R		R	R	F		C	R								
F	R	R	R	R				R	F					F		R				
									F						R				F	
							R	R		C	F		F		F		A		R	

Amoco B1-Youngstown 6-34-30-8W4

		Second White Specks Formation										Belle Fourche		FSF	Westgate Formation												
Depth (m)	693.2	698.2	703	708	713.2	718.2	723.2	728.2	733.2	738.2	743.2	748.2	753.2	765.4	769.7	774.7	779.7	784.7	789.7	794.7	799.7	804.2	809.7	814.4	819.4	824.4	829.4
Barren		X									X			X								X			X		
Foraminiferal species																											
Placentammina sp. 1	6												4		1	2	1			1	3					16	2
Pseudobolivina rollaensis	18																										
Trochammina rainwateri	38		3																								
Trochammina spp.	5														1									2			
Verneuilinoides perplexus	5												124														
Hedbergella delrioensis				>100				10																			
Hedbergella loetterlei				>100						2																	
Hedbergella spp.				>100	4			60																			
Heterohelix globulosa				>100	3		10	8																			
Whiteinella aprica				90				6																			
Textularia sp.					2				5																		
Trochammina ribstonensis					15																						
Haplophragmoides collyra						2																					
Saccammina alexanderi						3						3			1	2	3	15	6	16	5			3		26	7
Spiroplectammina ammovitrea						16		5	7	5																	
Ataxophragmiidae						10			8	10		5									5						
Hedbergella planispira								3																			
Ammomarginulina asperata								1																			
Pseudobolivina variana									2																		
Psammosphaera sp.												1					9	5		2							
Saccammina globosa												1	2								1					1	
Haplophragmoides hendersonense													1														
Haplophragmoides spp.													3		3		5	3					5	1		2	7
Hippocrepina sp.													6		1					8							
Reophax incompta													7														
Trochammina wetteri													11			9											
Gaudryina canadensis																		3									
Psamminopelta browsheri															1		2	7		19						2	
Miliammina manitobenesis															1		7	14		10	2			1		18	11
Verneuilinoides sp.															3		1			7							
Arenobulimina paynei																2											
Ammobaculites erectus																1											
Haplophragmoides rota																3											
Textularia topagorukensis																9	1	3	2		6					3	

Amoco B1-Youngstown 6-34-30-8W4 (cont.)

		Second White Specks Formation										Belle Fourche		FSF	Westgate Formation												
Depth (m)	693.2	698.2	703	708	713.2	718.2	723.2	728.2	733.2	738.2	743.2	748.2	753.2	765.4	769.7	774.7	779.7	784.7	789.7	794.7	799.7	804.2	809.7	814.4	819.4	824.4	829.4
Barren		X									X			X								X			X		
Foraminiferal species																											
Verneuilina canadensis																6	15	5	2								
Saccammina lathrami																	1										
Haplophragmoides postis goodrichi																	8	3			10						
Bathysiphon brosgei																	1	7									10
Haplophragmium swareni																	3										
Ammomarginulina sp.																	3										
Trochammina alcanensis																	1										2
Pseudobolivina sp.																	3										
Uvigerammina manitobenesis																	3										
Reophax sikanniensis																		15	8							6	4
Ammobaculites sp.																		1		4	4					6	
Haplophagmoides gilberti																		3									
Verneuilinoides fischeri																		3									2
Ammobaculites fragmentarius																		15									26
Rhabdammina sp.																			11							4	3
Ammotium sp.																			2								
Reophax troyeri																				3							3
Verneuilinoides borealis																					6					1	
Trochammina albertensis																					1						
Miliammina awunensis																										7	5
Reophax tundraensis																											1
planktonic foram. fragments				A				C																			
aggl. foram. fragments							R									F	C	A	F				F		C	A	A
Miscellaneous components																											
Fish debris	R	A	R		F		F	C	C	R				F		F	R	R			F				R	C	
Algal cysts	R			F		R	A	A	A	A	A	F		F	A	F	R			F	F			C	R	F	
Inoceramus prisms	A	A	A	A	C	A	A	F	F	F																	
Pyrite												A	F														
Radiolarian												C															
Diatoms																F	F										

Appendix C

Coccolith species count

Saskoil Willow Creek 10-25-1-27W3

	First White Speckled Shale					Second White Specks Fm				Belle Fourche Fm				
Depth (m)	838	839	840	841	842	843	844	845	846	847	848	849	850	854
Barren			X	X	X					X	X	X	X	X
Coccolith species														
Ahmuellerella octoradiata	3					4		4						
Arkhangelskiella cymbiformis						2	5	4	2					
Biscutum constans		1				4	13	9	3					
Braarudosphaera bigelowii	9	5				4	1	2	4					
Broinsonia parca						2								
Chiastozygus plicatus	1					5	11	4	6					
Corollithion asymmetricum							1							
Corollithion exiguum								2						
Corollithion rhombicum							1							
Corollithion signum							2							
Costacentrum horticum									1					
Cretarhabdus conicus		2				1	5	8	2					
Cretarhabdus crenulatus	9	21					1	9	4					
Cribrosphaerella ehrenbergi	2	3				20	3	4	4					
Eiffellithus eximius	1					6		3	2					
Eiffellithus trabeculatus		1				3	1	15	1					
Eiffellithus turriseiffeli		1				15	30	29	20					
Gartnerago costatum						1								
Gartnerago segmentatum	2	5												
Kamptnerius magnificus	1	1												
Lithastrinus floralis	1	3				7	8	5	4					
Lithastrinus grilli						2	3		1					
Lithraphidites carniolensis						1	9	7						
Marthasterites furcatus	1													
Markalius circumradiatus						3		2	2					
Microrhabdulus decoratus	1	1				1								
Micula staurophora	1	1					5	1	2					
Parhabdolithus angustus						2		3	1					
Parhabdolithus granulatus	1					1	2	1						
Predicosphaera cretacea	3	4				52	40	75	173					
Predicosphaera spinosa						3	1	4	2					
Scapholithus fossilis						1	1	2						
Stephanolithion laffittei						1	4	4	3					
Tertalithus gothicus						1								
Tetralithus obscurus	7	16												
Vagalapilla matalosa	1	1				47	5	5						
Vekshinella elliptica	2	2				1	5	5	1					
Watznaueria barnesae	20	20				63	82	65	65					
Zygodiscus acanthus						1								
Zygodiscus crux								2						
Zygodiscus diplogrammus	27	33				48	47	130	61					
Zygodiscus orionatus	1													
TOTAL NO. SPECIMENS	94	121				302	286	404	365					

Anderson Husky Roros 10-35-45-2W4

			Second White Specks Fm						Belle Fourche Fm		
Depth (m)	408	410	411	411	412	413	414	417	428	433	438
Barren	X	X							X	X	X
Coccolith species											
Ahmuellerella octoradiata			26	21	46	65	18	49			
Arkhangelskiella cymbiformis						3	1	13			
Biscutum constans			47	26	32	35	30	238			
Braarudosphaera bigelowii			1								
Chiastozygus plicatus			5	11	6	1	8	5			
Corollithion exiguum								1			
Corollithion signum			1					2			
Cretarhabdus conicus				9	3	4	2	8			
Cretarhabdus crenulatus				2	5			1			
Cribrosphaerella ehrenbergi				1	12	17	2	5			
Eiffellithus eximius			2	5	5	1	1	2			
Eiffellithus trabeculatus				2	5	1	1	1			
Eiffellithus turriseiffeli			8	24	85	28	39	38			
Gartnerago costatum			6	5	9	11	2	2			
Lithastrinus floralis			5	1	7	12	4	2			
Lithastrinus grilli				1							
Lithraphidites carniolensis			8	2	4	7	3	2			
Markalius circumradiatus			2	2							
Microrhabdulus decoratus					1						
Micula decussata			3								
Micula staurophora			4			1		5			
Parhabdolithus angustus				1	1			2			
Predicosphaera cretacea			9	17	22	21	8	6			
Predicosphaera spinosa			17	3	7	20	4	8			
Stephanolithion laffittei			2	4	11	1	2	2			
Vagalapilla matalosa			9	6	31	41	20	60			
Watznaueria barnesae			117	36	121	122	119	71			
Zygodiscus acanthus			21	54	173	92	30	53			
Zygodiscus crux			2	2	13	2	2	4			
Zygodiscus diplogrammus			172	258	313	70	68	47			
Zygodiscus orionatus			5	3	6	15	5	1			
TOTAL NO. SPECIMENS			472	496	919	570	369	628			

Amoco Conrad 11-12-6-16W4

			Second White Specks Fm					Belle Fourche Fm							
Depth (m)	562	563	564	565	566	567	569	570	571	572	572	560	560.6	561	562
Barren	X								X	X	X	X	X	X	X
Coccolith species															
Ahmuellerella octoradiata			1	34	6			2							
Arkhangelskiella cymbiformis		3	4	2	4		1								
Biscutum constans		41	6	81	39			3							
Braarudosphaera bigelowii		1				3									
Chiastozygus cuneatus				1											
Chiastozygus plicatus		1	1	1											
Corollithion signum					1										
Cretarhabdus conicus								1							
Cretarhabdus crenulatus		1	2	1			1								
Cribrosphaerella ehrenbergi				2				1							
Eiffellithus eximius		1		6	2			1							
Eiffellithus trabeculatus				7		1		1							
Eiffellithus turriseiffeli		1	2	5	3	1									
Gartnerago costatum		1		1											
Lithastrinus floralis		16	7	4			3	4							
Microrhabdulus decoratus				1											
Micula staurophora			5												

Amoco Conrad 11-12-6-16W4 (cont.)

			Second White Specks Fm					Belle Fourche Fm							
Depth (m)	562	563	564	565	566	567	569	570	571	572	572	560	560.6	561	562
Barren	X								X	X	X	X	X	X	X
Coccolith species															
Parhabdolithus angustus				1											
Predicosphaera cretacea		1	2	3	2	24		1							
Predicosphaera spinosa		3	1	1		1		2							
Stephanolithion laffittei		5	2	1	4			7							
Vagalapilla matalosa		27	3	1	3	3	1								
Watznaueria barnesae		150	118	67	73	11	4	17							
Zygodiscus acanthus				2	11			3							
Zygodiscus angustus								8							
Zygodiscus crux		1		1											
Zygodiscus diplogrammus		50	36	17	18	4	1	31							
Zygodiscus orionatus		1		1											
TOTAL NO. SPECIMENS		343	190	240	167	48	11	82							

S.W.P. Bredenbury 11-36-22-1W2

	Morden Fm			Second White Specks Fm												Belle Fourche		Fish Scales	
Depth (m)	255.4	256.3	258.3	260.3	262.3	264.9	265.9	268.9	272.7	273.7	275.6	277.5	279.4	281.3	283.2	285.1	288.9	290.8	291.7
Barren	X	X	X	X	X	X					X					X		X	X
Coccolith species																			
Ahmuellerella octoradiata							5	9	3	8		7	13	8	15		1		
Arkhangelskiella cymbiformis								1	1	2		5	6	6	2		1		
Biscutum constans							35	11	17	11		9	54	182	169		22		
Braarudosphaera bigelowii								1											
Broinsonia bevieri							1												
Chiastozygus plicatus							3	1	1	7		3	12	14	10		21		
Corollithion achylosum																	1		
Corollithion completum															1				
Costacentrum horticum										1									
Cretarhabdus conicus							4	1		3		5	30	7	11		14		
Cretarhabdus crenulatus													19	13	10		30		
Cribrosphaerella ehrenbergi							1	2	17	3		2	4	11	11		2		
Cylindralithus asymmetricus														1			2		
Eiffellithus eximius							2	1		2		4	48	8	7				
Eiffellithus trabeculatus										3			10	5	1				
Eiffellithus turriseiffeli							3	4	13	29		5	39	18	27		2		
Gartnerago costatum							1								1				
Gartnerago segmentatum									1			1	1	2					
Gartnerago zipperum							1												
Kamptnerius magnificus								1											
Kamptnerius punctatus														1					
Lithastrinus floralis								5		3		2	56	11	51		59		
Lithastrinus grilli								4											
Lithraphidites carniolensis							8	7	11	12		5	10	17	23		5		
Lucianorhabdus cayeuxi													4						
Manivitella pemmatoidea										1			2	1			32		
Markalius circumradiatus									1	5		1	2	1	1		3		
Micula staurophora							3	87	2	1		1	4						
Parhabdolithus sp.							1												
Parhabdolithus angustus								1		1			1	1	3		2		
Parhabdolithus embergeri													1						
Parhabdolithus granulatus								21	4	4			1	1	1		2		
Phanulithus ovalis												2	2	4	1		1		
Predicosphaera cretacea							32	11	107	28		78	122	107	290		71		
Predicosphaera spinosa									2	18		3	4	9	11		5		
Rhabdolithus intermedius														1					

S.W.P. Bredenbury 11-36-22-1W2 (cont.)

	Morden Fm			Second White Specks Fm												Belle Fourche		Fish Scales	
Depth (m)	255.4	256.3	258.3	260.3	262.3	264.9	265.9	268.9	272.7	273.7	275.6	277.5	279.4	281.3	283.2	285.1	288.9	290.8	291.7
Barren	X	X	X	X	X	X					X					X		X	X
Coccolith species																			
Scapholithus fossilis														5	6				
Stephanolithion laffittei							2	1		2			5	10	5				
Tetralithus gothicus																	15		
Vagalapilla matalosa							5	52	3	2		1	2		48		3		
Vekshinella ara													3	2					
Vekshinella dibrachiata															3		1		
Vekshinella elliptica									1	7		1	11						
Watznaueria barnesae							72	58	55	55		89	476	130	105		316		
Zygodiscus acanthus							18	20	54	36		4							
Zygodiscus compactus							7												
Zygodiscus crux								2	5										
Zygodiscus diplogrammus							46	24	41	73		69	279	110	162		325		
Zygodiscus elegans								2	1	1									
Zygodiscus orionatus							4	5	2			1	7	1	6		1		
TOTAL NO. SPECIMENS							254	332	342	318		300	1232	689	982		937		

Anderson et al. Ribstone 6-18-45-1W4

	Second White Specks Fm												Belle Fourche Fm			
Depth (m)	398.3	398.5	400	400.37	401.4	402.4	404.5	406	407.5	408.5	409.5	410.5	412.5	414.1	415.3	416.4
Barren	X	X	X										X	X	X	X
Coccolith species																
Ahmuellerella octoradiata				13	11	5	20	3	1			2				
Arkhangelskiella cymbiformis					2	5	4	8			1	2				
Biscutum constans				2	5	1	17	3	4	6	9	5				
Braarudosphaera bigelowii				4	6											
Chiastozygus litterarius							2				1					
Chiastozygus plicatus				1	2	1	1				4	1				
Cretarhabdus conicus					1		3	2		1	2	2				
Cretarhabdus crenulatus				4	3	6	2	3		2	3					
Cribrosphaerella ehrenbergi					3		25	1	1		2	1				
Eiffellithus eximius					1	2			2		1					
Eiffellithus trabeculatus					3						2	1				
Eiffellithus turriseiffeli				25	13	3	20	3	2		4	3				
Gartnerago costatum				1		2	2	9								
Gartnerago segmentatum							1	1			1					
Lithastrinus floralis				2	5	4	3	2	8	10	4	9				
Lithastrinus grilli							2			1		1				
Lithraphidites carniolensis					2		10	4								
Manivitella pemmatoidea						2	2				2	1				
Markalius circumradiatus						1			1	1						
Microrhabdulus decoratus						1										
Micula staurophora				3			1	2		1	4	6				
Parhabdolithus angustus					1											
Phanulithus ovalis												1				
Predicosphaera cretacea				2	5		90	17	1	1	2	2				
Predicosphaera spinosa				1	11	2	6	5	4	3	5	4				
Stephanolithion laffittei				1	3	9	10	2	3		10					
Vagalapilla matalosa				17	10	3	20	21	4	1	3	7				
Watznaueria barnesae				83	54	38	85	186	28	116	500	180				
Zygodiscus acanthus				25	3	1	43	42	1	1	2	4				
Zygodiscus compactus												1				
Zygodiscus crux					5	5	5	1	4			1				
Zygodiscus diplogrammus				58	122	23	70	70	32	14	50	160				
Zygodiscus orionatus				1	1	4	1	5				6				
TOTAL NO. SPECIMENS				243	272	118	445	390	96	158	611	400				

Amoco B1-Youngstown 6-34-30-8W4

		Second White Specks Fm													Belle Fourche Fm	
Depth (m)	693.2	698.2	703	708	708.4	709.3	710.3	713.2	718.7	723.2	728.2	733.2	738.2	743.2	748.2	753.2
Barren	X	X	X	X										X	X	X
Coccolith species																
Ahmuellerella octoradiata					15	1	7	1		34	6	25	3			
Arkhangelskiella cymbiformis					4	1	3	2	2	3						
Biscutum constans					7	4	7		1	84	168	73	43			
Braarudosphaera bigelowii										2						
Chiastozygus plicatus					2	2	2	1	2	7	5	2	5			
Corollithion exiguum							6									
Costacentrum horticum					2							1				
Cretarhabdus conicus					4	4	3			13	11	5	7			
Cretarhabdus crenulatus					11	11	7	5	2		17	6	7			
Cretarhabdus decorus											1					
Cribrosphaerella ehrenbergi					9		5		2	10	20	1	2			
Cylindralithus coronatus					5											
Discolithus fessus					2											
Eiffellithus eximius					7	3	10				3	1				
Eiffellithus trabeculatus					3	2	8			2		5				
Eiffellithus turriseiffeli					8	3	10	3		6	17	9	6			
Gartnerago costatum							3	1	1	2	2	1				
Lithastrinus floralis					4	3	4	7	4	11	14	10	3			
Lithraphidites carniolensis					1		3				3	6	1			
Manivitella pemmatoidea					1				2							
Markalius circumradiatus					14				4		5	2	4			
Micula staurophora					1			2	1			1	2			
Parhabdolithus angustus					1		2				1	2				
Phanulithus ovalis										1		1				
Predicosphaera cretacea					4		3			12	3	15	7			
Predicosphaera spinosa					8	2	14	4		6	7	9	4			
Scapholithus fossilis													7			
Stephanolithion laffittei					2		10	3	5	5	1	7	1			
Vagalapilla matalosa					26	9	22	8	1	3	14	51	14			
Watznaueria barnesae					52	43	97	49	95	87	95	113	5			
Watznaueria communis											3					
Zygodiscus acanthus					7	1	2			6	11	20	11			
Zygodiscus compactus							2					1	5			
Zygodiscus crux					3		2			3	2	1	3			
Zygodiscus diplogrammus					26	16	56	11	6	53	54	42	26			
Zygodiscus orionatus					4	9	2				7	3				
TOTAL NO. SPECIMENS					232	114	290	97	128	350	474	420	166			

C.M.&S. Vanscoy 11-16-35-8W3

	First White Speckled Shale										SWS Fm	Belle Fourche Fm		
Depth (m)	360.7	376.3	381.3	386.3	391.3	396.3	397.3	398.4	399.4	400.4	400.85	401.7	402.2	403.2
Barren												X	X	X
Coccolith species														
Ahmuellerella octoradiata	21	47	26	20	20	22	22	1	11	9	17			
Arkhangelskiella cymbiformis	2	6	12	10	4	7	2			6	17			
Biscutum constans	99	20	74	30	22	39	44	2	18	14	71			
Braarudosphaera bigelowii	73	3	13		7		11		5		1			
Broinsonia bevieri		1	5		2									
Broinsonia parca				1	1	4	6		2					
Chiastozygus plicatus	15	8	35	22	11	17	8		14	11	10			
Corollithion rhombicum						1								
Corollithion signum	1	1	10	9										
Cretarhabdus conicus		2	3	3	1	10	2		3	1	3			
Cretarhabdus crenulatus	2		1		1		1				3			
Cretarhabdus decorus			1						1	2				

C.M.&S. Vanscoy 11-16-35-8W3 (cont.)

	First White Speckled Shale										SWS Fm	Belle Fourche Fm		
Depth (m)	360.7	376.3	381.3	386.3	391.3	396.3	397.3	398.4	399.4	400.4	400.85	401.7	402.2	403.2
Barren												X	X	X
Coccolith species														
Cribrosphaerella ehrenbergi	6	1	5	8	4	4	4	1	3	7	38			
Cyclolithus redemiculatus				2		1								
Cylindralithus asymmetricus				1		5	3		2		1			
Cylindralithus sculptus				3										
Eiffellithus eximius	10	17	123	12	1	5	7		4	2	3			
Eiffellithus trabeculatus	1		9	2	1		1		1		10			
Eiffellithus turriseiffeli	3	9	12	12	8	7	5	1	4	2	10			
Gartnerago costatum		1	3	2	3	21	14		6	2				
Gartnerago segmentatum			1		2	3	2		1		3			
Gartnerago zipperum			2	2	3									
Kamptnerius magnificus	4	17	26	14	11	10	6		2	2				
Kamptnerius punctatus							1							
Lithastrinus floralis			2	4		2	1			1	8			
Lithastrinus grilli			2	10		2	2	1		2	1			
Lithraphidites carniolensis	1	3	13	18	8	2					40			
Lucianorhabdus cayeuxi					1						1			
Manivitella pemmatoidea	3					7	5	1		3				
Marthasterites furcatus	1	11	16	44	6	21	20	3	3	6				
Marthasterites simplex				2		1				2	1			
Markalius circumradiatus	2	3	16	4	8	8	1			1	4			
Microrhabdulus decoratus	1	1	2	2	2	1	1		1					
Micula staurophora	12	68	90	105	25	106	73	24	67	111	2			
Parhabdolithus angustus			1	1							5			
Parhabdolithus granulatus	2	1	3											
Phanulithus ovalis											4			
Predicosphaera cretacea	61	110	208	91	26	41	20		22	8	84			
Predicosphaera spinosa	4	5	15	15	5	7	6		4	4	10			
Stephanolithion laffittei			1	1	1	3	5		1	5	12			
Tetralithus aculeus							1							
Tetralithus nitidus			2											
Tetralithus pyramidus		1	4	4			1							
Vagalapilla matalosa	7	2	4	3	2	17	12	1	4	3	11			
Vekshinella elliptica	3	2	9	8	10	15	11		1	16				
Watznaueria barnesae	69	155	192	170	48	297	203	14	110	212	142			
Zygodiscus acanthus	1	80	28	22	23	6	3		3	3	70			
Zygodiscus compactus		25	11	2	2	2	3				2			
Zygodiscus crux		2	12	8	13	11	6		7	9	9			
Zygodiscus diplogrammus	34	94	82	87	34	101	76	3	26	23	77			
Zygodiscus orionatus			4	1			1				16			
Zygodiscus theta		2	8	2	1	2	1							
TOTAL NO. SPECIMENS	438	705	1088	757	317	808	592	52	326	467	690			

Appendix D

Dinoflagellate Plates

Plates A to D

(All figures x500)

Slides containing the figured dinoflagellates are curated in the type collection of the Geological Survey of Canada, Ottawa, Ontario but are currently located at the Geological Survey of Canada, Calgary, Alberta. For each specimen the GSC locality number (C-), palynology slide number (P) and GSC type number (GSC) are recorded. Stage coordinates and England Finder readings are on file with the specimens.

Plate A

Figure 1. *Discorsia nanna* (Davey, 1974) Duxbury, 1977 C-167137, P3546-37b, GSC 103422

Figure 2. *Protoellipsodinium spinocristatum* Davey and Verdier, 1971 C-167144, P3548-1c, GSC 103432

Figure 3. *Wigginsiella grandstandica* Lucas-Clark, 1987 C-167144, P3548-1b, GSC 109902

Figure 4. *Oligosphaeridium totum* Brideaux, 1971 C-167136, P3545-18b, GSC 109903

Figure 5. *Ginginodinium evittii* Singh, 1983 C-167135, P3545-13f, GSC 109904

Figure 6. *Ginginodinium evittii* Singh, 1983 C-167137, P3546-36b, GSC 103433

Figure 7. *Fromea amphora* Cookson and Eisenack, 1958 C-167136, P3545-13e, GSC 109905

Figure 8. *Ovoidinium verrucosum* (Cookson and Hughes, 1964) Davey, 1970 C-167137, P3546-36b, GSC 103425

Figure 9. *Ovoidinium scabrosum* (Cookson and Hughes, 1964) Davey, 1970 C-167136, P3545-14d, GSC 112919

Figure 10. *Pseudoceratium expolitum* Brideaux, 1971 C-167136, P3545-16b, GSC 112920

Figure 11. *Catastomocystis spinosa* Singh, 1983 C-167144, P3548-1b, GSC 103440

Figure 12. *Dingodinium cerviculum* Cookson and Eisenack, 1958; emend. Mehrotra and Sarjeant, 1984; emend. Khowaja-Ateequzzaman, 1990 C-167144, P3548-1c, GSC 103423

Figure 13. *Gardodinium trabeculosum* (Gocht, 1959) Alberti, 1961 C-167144, P3548-1c, GSC 103424

Figure 14. *Batioladinium jaegeri* (Alberti, 1961) Brideaux, 1975 C-167136, P3545-18b, GSC 112921

Figure 15. *Odontochitina singhii* Morgan, 1980 C-167136, P3545-17b, GSC 112922

Figure 16. *Hystrichosphaerina schindewolfei* Alberti, 1961 C-167135, P3544-6b, GSC 103420

Figure 17. *Luxadinium propatulum* Brideaux and McIntyre, 1975 C-167136, P3545-17b, GSC 112923

Figure 18. *Ascostomocystis gigantea* Singh, 1983 C-167136, P3545-15b, GSC 112924

Figure 19. *Ascostomocystis maxima* Singh, 1971 C-167136, P3545-17b, GSC 112925

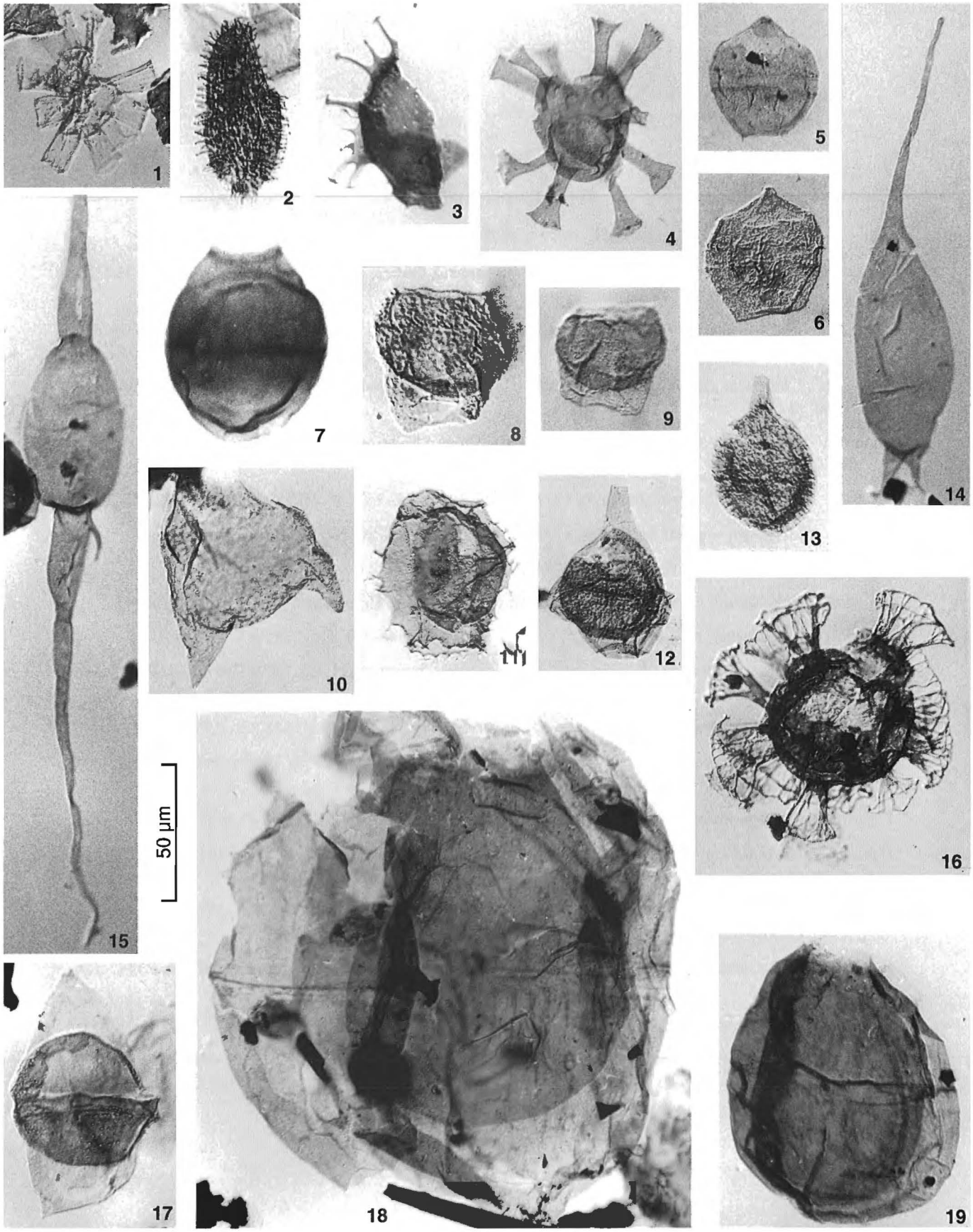
1
2
3
4
5
6
7
8
9
10
11
12
13
14
15
16
17
18
19
50 µm

Plate B

Figure 1. *Bourkidinium psilatum* Singh, 1983 C-167144, P3548-1b, GSC 103429

Figure 2. *Palaeoperidinium cretaceum* Pocock, 1962 emend. Davey, 1970 emend. Harding, 1990 C-167136, P3545-14b, GSC 112926

Figure 3. *Chichaouadinium vestitum* (Brideaux, 1971) Bujak and Davies, 1983 C-167137, P3546-37b, GSC 103421

Figure 4. *Chichaouadinium vestitum* (Brideaux, 1971) Bujak and Davies, 1983 C-167144, P3548-1c, GSC 112927

Figure 5. *Fromea fragilis* (Cookson and Eisenack, 1962) Stover and Evitt, 1978 C-167136, P3545-18b, GSC 112928

Figure 6. *Florentinia cooksoniae* (Singh, 1971) Duxbury, 1980 C-167136, P3545-15b, GSC 112929

Figure 7. *Florentinia verdieri* Singh, 1983 C-167144, P3548-1b, GSC 103434

Figure 8. *Alterbidinium* sp. C-167144, P3548-1b, GSC 112930

Figure 9. *Stephodinium australicum* Cookson and Eisenack, 1962 C-167136, P3545-17b, GSC 103435

Figure 10. *Apteodinium reticulatum* Singh, 1971 C-167136, P3545-21b, GSC 112931

Figure 11. *Cribroperidinium exilicristatum* (Davey, 1969) Stover and Evitt, 1978 C-167136, P3545-14b, GSC 112932

Figure 12. *Pseudoceratium eisenackii* (Davey, 1969) Bint, 1986 C-167136,P3545-22b, GSC 112933

Figure 13. *Oligosphaeridium pulcherrimum* (Deflandre and Cookson, 1955) Davey and Williams, 1966 C-167136, P3545-15b, GSC 112934

Figure 14. *Cribroperidinium intricatum* Davey, 1969 C-167136, P3545-15b, GSC 112935

Figure 15. *Ovoidinium verrucosum* (Cookson and Hughes, 1964) Davey, 1970 C-167136, P3545-11e, GSC 112936

Figure 16. *Oligosphaeridium complex* (White, 1842) Davey and Williams, 1966 C-167136, P3545-15b, GSC 112937

Figure 17. *Cribroperidinium edwardsii* (Cookson and Eisenack, 1958) Davey, 1969 C-167136, P3545-14b, GSC 112938

Figure 18. *Nyktericysta* sp. C-167136, P3545-17b, GSC 112939

Figure 19. *Limbicysta octopediformis* MacRae et al., 1996 C-167136, P3545-10b, GSC 112940

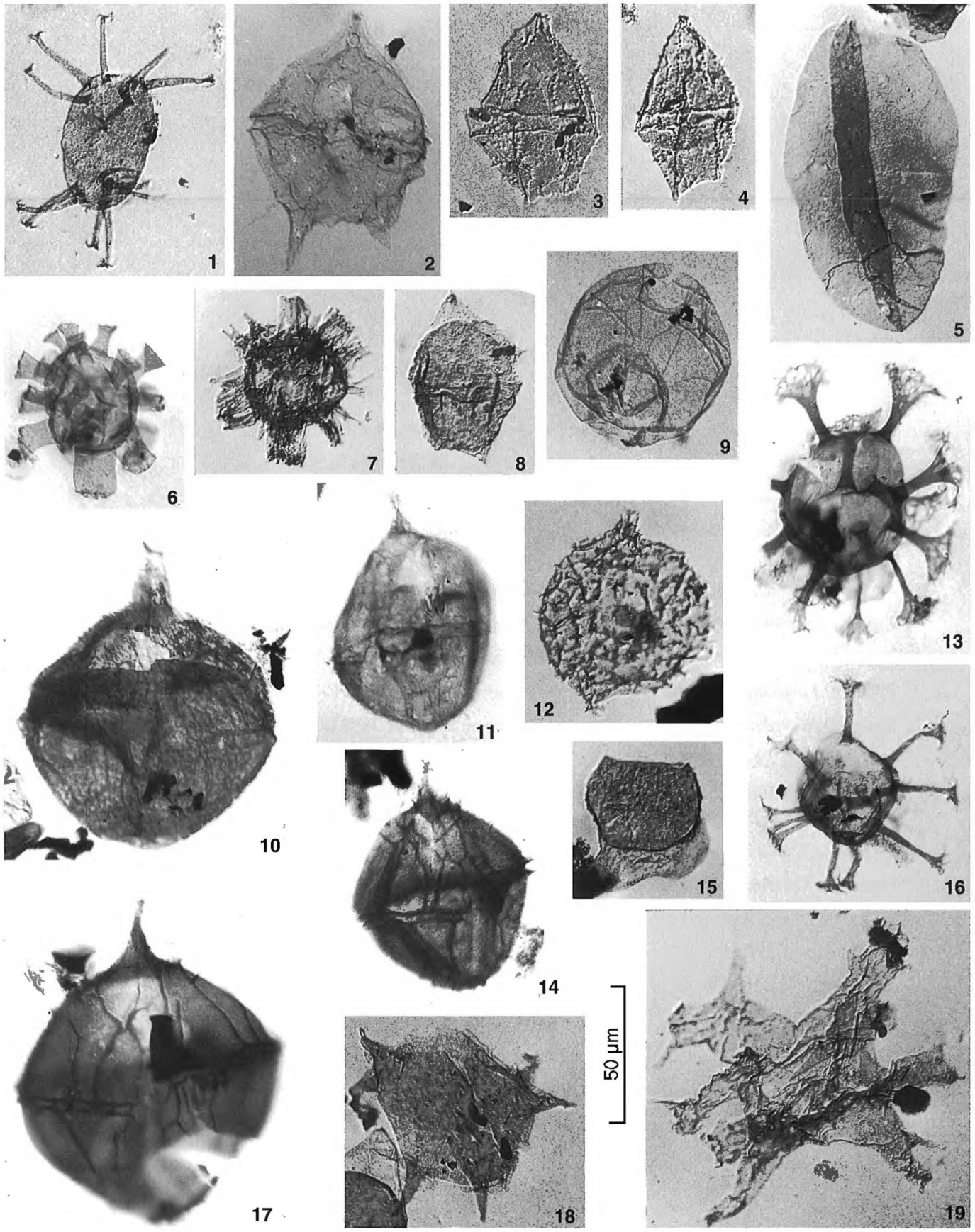
1
2
3
4
5
6
7
8
9
10
11
12
13
14
15
16
17
18
19
50 µm

Plate C

Figure 1. *Odontochitina operculata* (Wetzel, 1933) Deflandre and Cookson, 1955 C-167136, P3545-12e, GSC 112941

Figure 2. *Odontochitina singhii* Morgan, 1980 C-167135, P3544-3b, GSC 112942

Figure 3. *Florentinia cooksoniae* (Singh, 1971) Duxbury, 1980 C-167136, P3545-12e, GSC 112943

Figure 4. *Trichodinium spinosum* Singh, 1971 C-167136, P3545-11e, GSC 112944

Figure 5. *Leberidocysta defloccata* (Davey and Verdier, 1973) Stover and Evitt, 1978 C-167136, P3545-12e, GSC 112945

Figure 6. *Isabelidinium magnum* (Davey, 1970) Stover and Evitt, 1978 C-167146, P3550-1a, GSC 103438

Figure 7. *Ascostomocystis gigantea* Singh, 1983 C-167144, P3548-1b, GSC 112946

Figure 8. *Pseudoceratium* sp. C-167136, P3545-12e, GSC 114450

Figure 9. *Eurydinium glomeratum* (Davey, 1970) Stover and Evitt, 1978 C-167146, P3550-2b, GSC 103439

Figure 10. *Eurydinium glomeratum* (Davey, 1970) Stover and Evitt, 1978 C-167146, P3550-2b, GSC 114451

Figure 11. *Alterbidinium "daveyi"* Stover and Evitt, 1978 C-167136, P3545-8e, GSC 114452

Figure 12. *Wallodinium luna* (Cookson and Eisenack, 1960) Lentin and Williams, 1973 C-167136, P3545-8e, GSC 114453

Figure 13. *Isabelidinium magnum* (Davey, 1970) Stover and Evitt, 1978 C-167136, P3545-7e, GSC 114454

Figure 14. *Leberidocysta defloccata* (Davey and Verdier, 1973) Stover and Evitt, 1978 C-167136, P3545-5e, GSC 114455

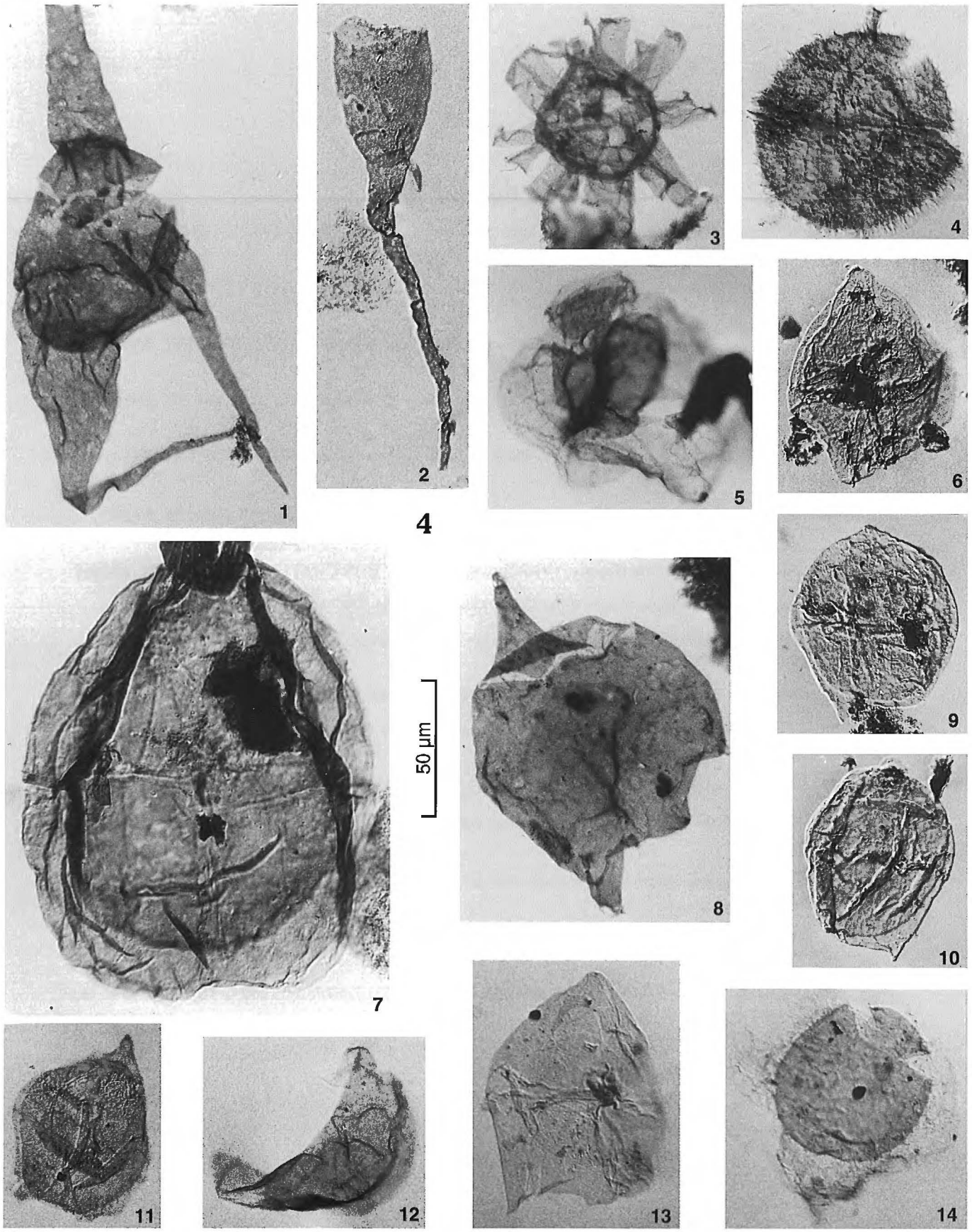
1
2
3
4
5
6
4
7
50 µm
8
9
10
11
12
13
14

Plate D

Figure 1. *Kallosphaeridium ringnesiorum* (Manum and Cookson, 1964) Helby, 1987 C-167136, P3545-5e, GSC 114456

Figure 2. *Chatangiella granulifera* (Manum, 1963) Lentin and Williams, 1976 C-167136, P3545-1e, GSC 114457

Figure 3. *Chatangiella granulifera* (Manum, 1963) Lentin and Williams, 1976 C-167136, P3545-2e, GSC 114458

Figure 4. *Chatangiella ditissima* (McIntyre, 1975) Lentin and Williams, 1976 C-167136, P3545-1e, GSC 114459

Figure 5. *Isabelidinium globosum* (Davey, 1970) Lentin and Williams, 1977 C-167136, P3545-1e, GSC 114460

Figure 6. *Isabelidinium globosum* (Davey, 1970) Lentin and Williams, 1977 C-167136, P3545-1e, GSC 114461

Figure 7. *Eurydinium glomeratum* (Davey, 1970) Stover and Evitt, 1978 C-167136, P3545-5e, GSC 114462

Figure 8. *Trithryodinium dubium* Singh, 1983 C-167136, P3545-8e, GSC 114463

Figure 9. *Surculosphaeridium longifurcatum* (Firtion, 1952) Davey et al., 1956 C-167136, P3545-8e, GSC 114464

Figure 10. *Dorocysta litotes* Davey, 1970 C-167136, P3545-4e, GSC 114465

Figure 11. *Trigonopyxidia ginella* (Cookson and Eisenack, 1960) Downie and Sarjeant, 1965 C-167136, P3545-2e, GSC 114466

Figure 12. *Dinopterygium cladoides* Deflandre, 1935 C-167136, P3545-8e, GSC 114467

Figure 13. *Trithyrodinium suspectum* (Manum and Cookson, 1964) Davey, 1969 C-167136, P3545-2e, GSC 114468

Figure 14. *Trithyrodinium suspectum* (Manum and Cookson, 1964) Davey, 1969 C-167136, P3545-2e, GSC 114469

Figure 15. *Heterosphaeridium difficile* (Manum and Cookson, 1964) Ioannides, 1986 C-167136, P3545-2e, GSC 114470

Figure 16. *Circulodinium distinctum* (Deflandre and Cookson, 1955) Jansonius, 1986 C-167136, P3545-8e, GSC 114471

Figure 17. *Florentinia cooksoniae* (Singh, 1971) Duxbury, 1980 C-167136, P3545-2e, GSC 114472

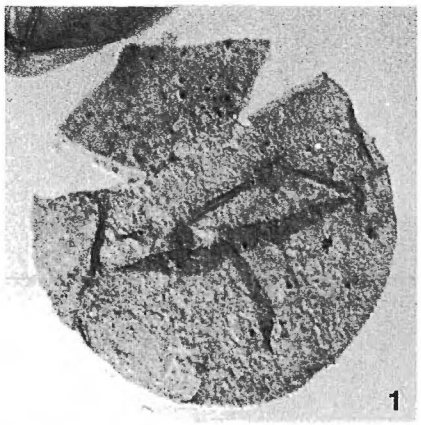

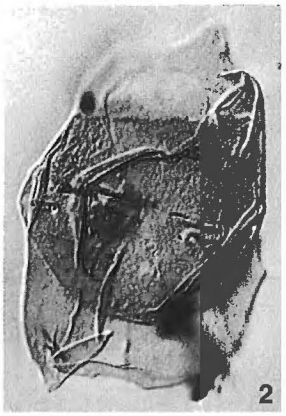

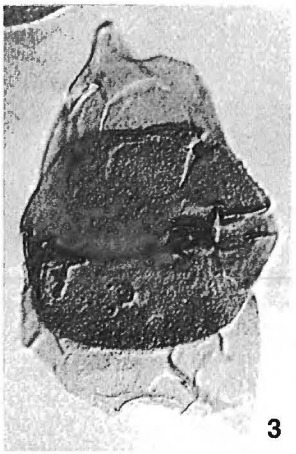

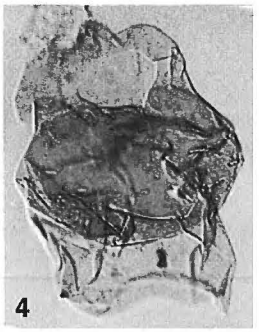

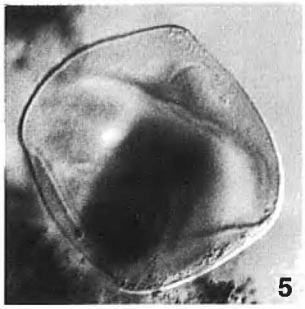

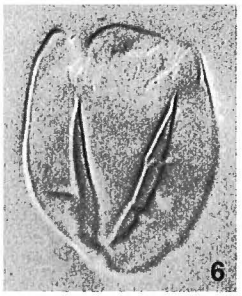

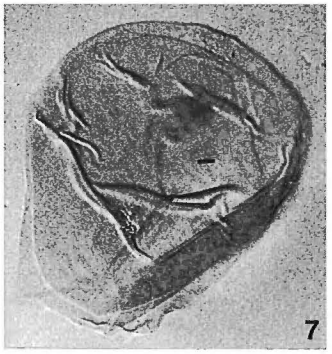

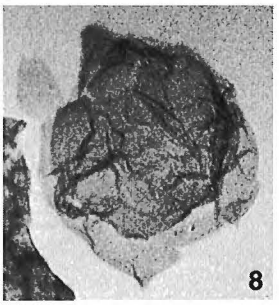

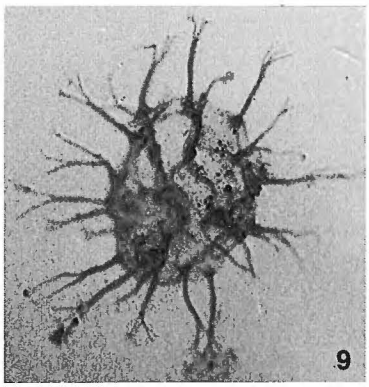

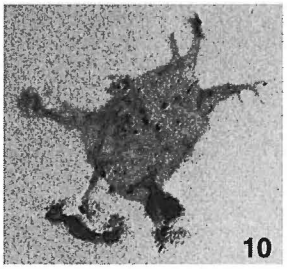

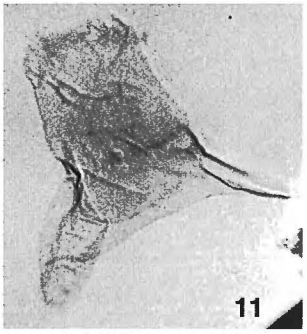

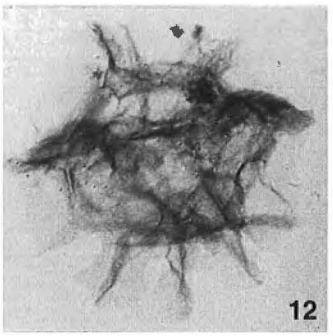

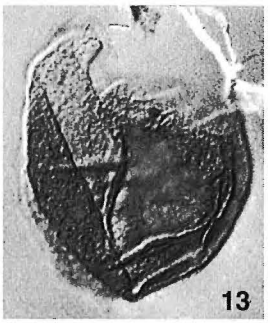

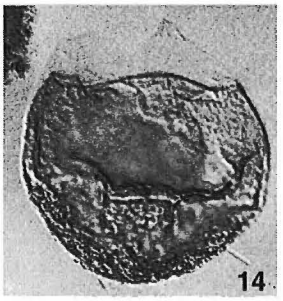

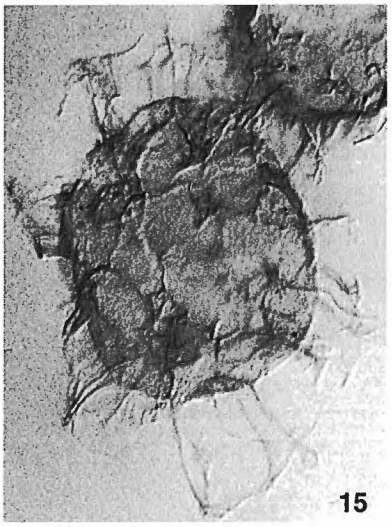

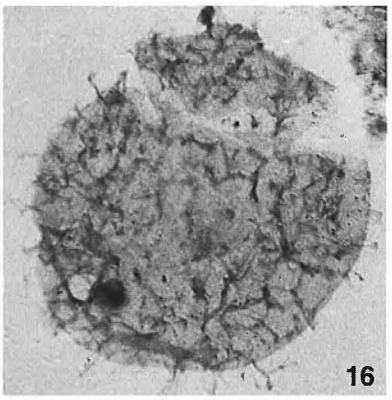

50 µm

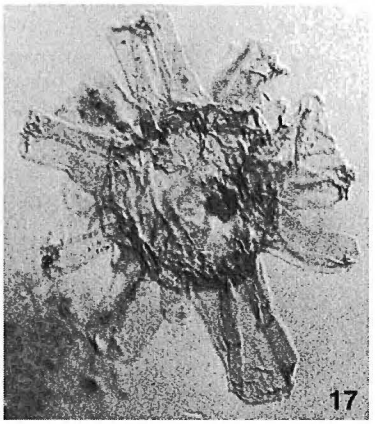

Appendix E

Rock-Eval pyrolysis data

Formation	Depth (m)	Sample #	Tmax	S1	S2	S3	PI	S2/S3	PC	TOC	HI	OI
05-09-72-08 W6, C-167134												
Westgate	1513.64	050943	441	1.06	5.21	0.52	0.17	10.11	0.52	3.14	166	16
Westgate	1511.50	050942	438	1.46	3.60	0.46	0.29	8.00	0.42	3.26	110	14
Westgate	1510.28	050941	439	0.99	3.22	0.41	0.24	7.84	0.35	2.05	157	20
Westgate	1507.24	050940	439	1.13	2.64	0.41	0.30	6.52	0.31	2.34	113	17
Westgate	1504.19	050939	439	1.01	2.63	0.30	0.28	8.94	0.30	2.70	97	11
Westgate	1501.14	050938	443	0.60	2.21	0.23	0.22	9.89	0.23	2.19	101	10
Westgate	1498.09	050937	447	0.54	2.20	0.25	0.20	8.82	0.23	1.88	117	13
Westgate	1495.04	050936	441	0.52	1.80	0.22	0.23	8.16	0.19	2.09	86	10
Westgate	1494.13	050935	444	0.52	3.12	0.25	0.15	12.72	0.30	2.12	147	11
Westgate	1491.69	050934	446	0.40	2.10	0.53	0.16	3.96	0.20	1.75	120	30
Westgate	1490.78	050933	449	0.40	1.81	0.58	0.19	3.12	0.18	1.62	112	35
Westgate	1487.73	050932	448	0.41	1.74	0.29	0.19	6.03	0.17	1.49	117	20
Westgate	1484.68	050931	449	0.35	1.67	0.47	0.18	3.57	0.17	1.54	108	31
Westgate	1482.24	050930	450	0.43	1.85	0.24	0.19	7.88	0.19	1.67	111	14
Westgate	1479.19	050929	449	0.50	1.84	0.20	0.22	9.22	0.19	1.59	116	12
Westgate	1477.67	050928	448	0.39	1.54	0.12	0.20	12.83	0.16	1.55	99	7
Westgate	1472.49	050927	449	0.42	1.93	0.08	0.18	11.75	0.19	1.62	119	5
Westgate	1469.44	050926	446	0.49	1.68	0.10	0.23	22.93	0.18	1.55	108	6
Belle Fourche	1326.18	050925	439	0.30	0.87	0.05	0.26	21.50	0.09	1.42	61	3
Belle Fourche	1323.44	050924	434	0.38	1.55	0.15	0.20	5.43	0.16	1.65	94	9
Belle Fourche	1317.35	050923	438	0.21	0.96	0.44	0.18	2.19	0.10	1.28	74	34
Belle Fourche	1314.30	050922	439	0.17	0.71	0.79	0.19	0.90	0.07	1.22	58	65
Belle Fourche	1311.25	050921	439	0.19	1.00	0.66	0.16	1.52	0.09	1.44	69	45
Belle Fourche	1308.20	050920	439	0.16	1.10	0.55	0.13	1.99	0.10	1.38	79	40
Belle Fourche	1305.15	050919	437	0.13	0.80	0.84	0.14	0.95	0.07	1.36	58	61
Belle Fourche	1302.11	050918	438	0.16	0.99	1.11	0.14	0.89	0.09	1.57	63	70
Belle Fourche	1299.06	050917	437	0.20	0.98	1.67	0.17	0.58	0.10	1.62	60	103
Belle Fourche	1296.92	050916	440	0.28	1.25	1.90	0.19	0.65	0.13	2.03	61	93
Belle Fourche	1291.74	050915	437	0.29	1.31	1.49	0.19	0.88	0.13	1.98	66	75
Belle Fourche	1288.69	050914	440	0.21	1.11	1.51	0.16	0.74	0.11	1.84	60	82
Belle Fourche	1285.65	050913	440	0.16	0.81	0.69	0.16	1.17	0.08	1.29	62	53
Belle Fourche	1284.12	050912	438	0.21	0.97	1.32	0.18	0.73	0.09	1.49	65	88
Belle Fourche	1280.46	050911	437	0.15	0.77	0.90	0.17	0.86	0.07	1.31	59	68
Belle Fourche	1277.42	050910	439	0.25	1.12	1.25	0.19	0.89	0.11	1.55	72	81
Belle Fourche	1274.37	050909	437	0.23	0.95	1.02	0.20	0.93	0.10	1.49	63	68
Belle Fourche	1271.93	050908	439	0.15	0.91	1.48	0.15	0.61	0.09	1.60	57	92
Belle Fourche	1268.88	050907	440	0.14	0.73	1.57	0.17	0.46	0.07	1.40	52	112
Belle Fourche	1258.52	050904	437	0.41	1.00	1.92	0.29	0.52	0.11	1.71	58	112
Belle Fourche	1255.24	050902	439	0.19	0.56	0.70	0.26	0.80	0.06	1.06	53	66
16-01-66-22W5, C-167143												
Belle Fourche	1903.00	160108	451	0.27	1.12	0.15	0.20	7.43	0.11	1.34	83	11
Belle Fourche	1898.00	160107	451	0.24	0.57	1.13	0.31	0.50	0.07	1.18	47	95
Belle Fourche	1893.00	160106	450	0.40	1.00	1.42	0.29	0.70	0.11	1.49	66	95
Belle Fourche	1888.00	160105	447	0.52	0.85	1.18	0.38	0.72	0.11	1.31	65	90
Belle Fourche	1884.00	160104	452	0.26	1.18	0.23	0.19	5.17	0.12	1.44	82	16
Belle Fourche	1879.00	160103	451	0.15	0.63	0.53	0.20	1.19	0.06	1.24	50	42
Belle Fourche	1873.00	160102	451	0.23	0.70	0.99	0.25	0.70	0.07	1.43	48	69
Belle Fourche	1868.00	160101	451	0.21	0.84	0.17	0.20	4.95	0.08	1.21	69	14
05-01-77-20W5, C-167135												
Westgate	451.10	050125	436	0.37	0.66	0.37	0.36	1.81	0.08	1.50	44	24
Westgate	448.06	050124	436	0.48	1.18	0.36	0.29	3.26	0.13	1.89	62	19
Westgate	445.01	050123	427	0.23	0.58	0.36	0.28	1.63	0.06	1.62	35	22
Westgate	441.96	050122	437	0.59	1.52	0.42	0.28	3.61	0.17	2.03	75	21
Westgate	438.91	050121	433	0.53	1.11	0.41	0.33	2.74	0.13	1.96	56	20
Westgate	435.86	050120	435	0.44	1.09	0.48	0.29	2.30	0.13	1.81	60	26
Westgate	432.82	050119	431	0.44	0.72	0.40	0.39	1.79	0.09	1.81	39	22
Westgate	430.07	050118	435	1.21	1.26	0.50	0.49	2.55	0.20	1.88	67	26
Westgate	427.02	050117	431	0.48	1.16	0.43	0.30	2.68	0.13	1.77	65	24

Formation	Depth (m)	Sample #	Tmax	S1	S2	S3	PI	S2/S3	PC	TOC	HI	OI
Westgate	423.98	050116	421	0.36	1.20	0.54	0.23	2.23	0.13	2.15	55	25
Westgate	421.23	050115	419	0.42	1.34	0.56	0.24	2.39	0.15	2.31	58	24
Fish Scales	419.40	050114	422	0.43	1.14	0.60	0.28	1.93	0.13	2.04	56	29
Fish Scales	417.58	050113	413	0.33	1.68	0.95	0.17	1.77	0.17	2.96	57	32
Fish Scales	414.53	050112	413	0.37	2.72	1.00	0.12	2.72	0.25	3.20	85	31
Fish Scales	411.48	050111	413	0.35	2.87	1.12	0.11	2.57	0.27	3.19	89	35
Fish Scales	408.43	050110	413	0.26	1.41	1.04	0.16	1.36	0.14	2.62	53	39
Fish Scales	405.38	050109	416	0.22	1.53	1.10	0.13	1.39	0.14	2.61	59	42
Fish Scales	402.34	050108	414	0.22	1.61	0.98	0.12	1.65	0.15	2.62	61	37
Belle Fourche	399.29	050107	416	0.18	1.16	0.62	0.14	1.88	0.11	2.23	52	27
Belle Fourche	396.24	050106	434	0.68	0.74	0.61	0.48	1.21	0.12	1.26	58	48
Belle Fourche	393.19	050105	435	0.74	0.80	0.86	0.48	0.93	0.13	1.23	64	70
Belle Fourche	390.14	050104	436	0.67	0.75	1.34	0.47	0.56	0.11	1.30	57	103
Belle Fourche	387.10	050103	434	0.59	0.50	1.07	0.55	0.47	0.09	1.13	44	94
Belle Fourche	384.05	050102	433	0.27	0.47	1.41	0.37	0.38	0.06	1.16	40	120
Belle Fourche	381.00	050101	436	0.27	0.38	2.96	0.42	0.12	0.05	1.07	35	277
10-25-65-20W5, C-167144												
Westgate	1334.00	102504	438	0.57	5.04	0.27	0.10	19.58	0.47	2.29	220	11
Westgate	1327.00	102503	441	0.27	2.53	0.29	0.10	8.71	0.23	1.85	136	15
Westgate	1322.00	102502	440	0.34	2.93	0.31	0.10	9.59	0.27	1.77	165	17
Westgate	1317.00	102501	439	0.24	2.70	0.26	0.08	10.40	0.24	1.86	145	14
10-05-53-20W5, C-167145												
Westgate	2680.00	100506	466	0.62	0.70	0.01	0.48	68.00	0.11	1.58	44	0
Westgate	2675.00	100505	474	0.48	0.59	0.06	0.45	9.83	0.08	1.35	44	4
Westgate	2671.00	100504	477	0.48	0.67	0.16	0.42	4.44	0.09	1.43	46	11
Westgate	2666.00	100503	463	0.36	0.32	0.07	0.54	4.57	0.05	1.71	18	4
Westgate	2661.00	100502	462	0.57	0.59	0.10	0.50	7.08	0.09	1.62	36	6
Westgate	2656.00	100501	455	1.15	0.82	0.25	0.59	4.57	0.16	3.18	25	7
09-09-56-19W5, C-167147												
Belle Fourche	2268.00	090907	446	2.40	10.88	0.59	0.18	18.95	1.10	4.08	266	14
Belle Fourche	2262.00	090906	446	1.63	3.99	0.56	0.29	7.19	0.46	2.32	172	24
Belle Fourche	2257.00	090905	447	1.23	2.97	0.53	0.30	5.65	0.35	1.99	149	26
Belle Fourche	2252.00	090904	445	2.02	8.00	0.62	0.20	13.03	0.83	3.43	233	18
Belle Fourche	2247.00	090903	448	1.93	7.23	0.60	0.21	12.21	0.76	3.22	225	18
Belle Fourche	2242.00	090902	445	1.69	12.08	0.53	0.12	23.01	1.14	4.31	280	12
Belle Fourche	2237.00	090901	444	2.46	8.56	0.57	0.23	15.22	0.92	3.48	246	16
04-13-54-18W5, C-167146												
Second White Specks	2114.00	041304	443	2.42	8.30	0.55	0.23	15.10	0.89	3.13	265	17
Second White Specks	2109.00	041303	443	3.63	11.36	0.65	0.24	17.73	1.25	3.83	297	17
Second White Specks	2104.00	041302	441	4.15	14.28	0.51	0.23	28.87	1.53	4.83	296	10
Second White Specks	2099.00	041301	442	1.32	4.23	0.27	0.24	17.38	0.46	2.17	195	12
14-29-13-29W4, C-205701												
Belle Fourche	2770.00	142915	456	0.67	0.68	0.25	0.50	2.79	0.11	1.26	54	19
Belle Fourche	2769.00	142914	455	0.49	0.59	0.24	0.46	2.48	0.09	1.77	39	16
Belle Fourche	2768.00	142913	453	0.61	0.65	0.31	0.49	2.13	0.10	1.21	54	25
Belle Fourche	2767.00	142912	455	0.63	0.75	0.33	0.46	2.30	0.11	1.23	61	26
Belle Fourche	2766.00	142911	457	0.56	0.70	0.34	0.45	2.07	0.10	1.08	64	31
Belle Fourche	2765.00	142910	453	1.14	1.39	0.60	0.46	2.33	0.21	1.42	98	42
Belle Fourche	2763.00	142909	451	2.33	3.67	0.84	0.39	4.36	0.50	3.21	114	26
Second White Specks	2762.00	142908	448	2.50	3.70	0.77	0.41	4.83	0.52	3.19	115	24
Second White Specks	2761.00	142907	449	2.93	5.29	0.90	0.36	5.95	0.68	3.81	139	23
Second White Specks	2760.00	142906	445	2.90	4.11	0.75	0.41	5.52	0.58	3.11	132	24
Second White Specks	2759.00	142905	445	2.98	4.60	0.82	0.40	5.68	0.63	3.38	136	24
Second White Specks	2758.00	142904	450	1.57	1.65	0.75	0.49	2.20	0.27	1.74	95	43
Second White Specks	2757.00	142903	0	0.00	0.00	0.00	0.00	0.00	0.00	0.02	0	0
Second White Specks	2756.00	142902	453	0.98	1.52	0.59	0.40	2.58	0.20	1.71	88	34
Second White Specks	2755.00	142901	447	1.21	1.97	0.73	0.39	2.67	0.26	1.81	108	40
10-36-11-29W4, C-205702												
Second White Specks	2638.00	103624	431	3.20	11.21	0.44	0.22	25.60	1.20	3.87	292	11
Second White Specks	2636.00	103623	442	2.66	11.02	0.68	0.20	16.91	1.14	3.69	298	18
Second White Specks	2634.00	103622	442	1.50	6.00	0.72	0.20	8.41	0.62	2.35	256	30
Second White Specks	2632.00	103621	442	1.68	6.50	0.47	0.21	13.96	0.68	2.66	244	17

Formation	Depth (m)	Sample #	Tmax	S1	S2	S3	PI	S2/S3	PC	TOC	HI	OI
Second White Specks	2630.00	103620	445	1.20	5.02	0.39	0.19	12.88	0.51	2.48	203	15
Second White Specks	2626.00	103619	446	0.53	1.31	0.41	0.29	3.21	0.15	1.12	116	36
Second White Specks	2624.00	103618	446	1.03	2.42	0.53	0.30	4.53	0.29	1.82	134	29
Second White Specks	2623.00	103617	443	0.41	1.11	0.26	0.28	4.32	0.12	1.02	109	25
Second White Specks	2622.00	103616	442	1.14	3.75	0.53	0.23	7.10	0.41	1.93	195	27
Second White Specks	2621.00	103615	440	1.37	5.13	0.59	0.21	8.77	0.54	2.31	222	25
Second White Specks	2621.00	103614	438	1.38	4.95	0.58	0.22	8.55	0.53	2.26	220	25
Second White Specks	2620.00	103613	442	0.89	2.41	0.41	0.27	5.86	0.27	1.51	164	28
Second White Specks	2618.00	103612	441	0.51	1.12	0.29	0.32	3.84	0.13	1.11	100	26
Second White Specks	2616.00	103611	438	2.35	8.04	0.59	0.23	13.96	0.86	3.02	266	19
Second White Specks	2614.00	103610	439	0.86	1.96	0.38	0.31	5.30	0.23	1.33	147	28
Second White Specks	2612.00	103609	438	1.86	5.47	0.50	0.26	11.30	0.61	2.23	245	22
Haven Mbr.?	2610.00	103608	443	0.60	1.34	0.30	0.31	4.47	0.16	1.27	106	23
Haven Mbr.?	2608.00	103607	443	0.45	1.44	0.27	0.24	5.31	0.15	1.12	129	24
Haven Mbr.?	2606.00	103606	441	0.67	2.14	0.40	0.24	5.40	0.23	1.39	155	28
Haven Mbr.?	2604.00	103605	441	0.32	0.55	0.25	0.37	2.25	0.07	0.64	86	38
Haven Mbr.?	2602.00	103604	442	0.51	1.67	0.34	0.24	4.96	0.18	1.20	141	28
Haven Mbr.?	2600.00	103603	440	0.88	3.10	0.49	0.22	6.38	0.33	1.69	183	28
Haven Mbr.?	2598.00	103602	441	0.84	2.55	0.47	0.25	5.43	0.28	1.67	152	28
Haven Mbr.?	2597.00	103601	438	0.87	2.70	0.51	0.24	5.34	0.29	1.75	154	28
06-07-12-28W4, C-190616, 1-35												
Belle Fourche	2606.00	060736	450	0.45	1.28	0.20	0.26	6.40	0.14	0.63	203	31
Belle Fourche	2605.00	060735	449	0.31	0.86	0.19	0.26	4.64	0.09	0.36	238	51
Belle Fourche	2604.00	060734	447	0.50	1.86	0.27	0.21	7.01	0.19	0.71	262	37
Belle Fourche	2603.00	060733	450	0.51	2.52	0.26	0.17	9.69	0.25	0.80	315	32
Belle Fourche	2602.00	060732	447	0.42	1.58	0.24	0.21	6.72	0.17	0.66	239	35
Belle Fourche	2601.00	060731	447	0.23	0.60	0.20	0.28	3.09	0.07	0.26	236	77
Belle Fourche	2600.00	060730	446	0.50	1.85	0.30	0.21	6.29	0.19	0.72	256	42
Belle Fourche	2599.00	060729	448	0.32	0.72	0.25	0.31	2.96	0.08	0.39	188	64
Belle Fourche	2598.00	060728	446	0.46	1.65	0.29	0.22	5.73	0.17	0.77	215	38
Belle Fourche	2597.00	060727	448	0.15	0.20	0.18	0.44	1.11	0.02	0.07	278	250
Belle Fourche	2596.00	060726	449	0.39	1.24	0.28	0.24	4.42	0.13	0.56	222	50
Belle Fourche	2595.00	060725	450	0.31	0.95	0.27	0.25	3.58	0.10	0.50	190	53
Belle Fourche	2594.00	060724	439	3.27	5.49	0.65	0.38	8.47	0.73	4.57	120	14
Belle Fourche	2593.50	060723	451	0.55	1.37	0.33	0.29	4.20	0.16	0.65	210	50
Belle Fourche	2593.00	060722	451	0.31	1.01	0.30	0.24	3.42	0.11	0.57	177	52
Belle Fourche	2592.00	060721	449	0.55	1.78	0.43	0.24	4.14	0.19	0.74	241	58
Second White Specks	2591.00	060720	446	2.25	8.37	0.69	0.21	12.13	0.88	2.44	343	28
Second White Specks	2590.00	060719	445	2.41	8.54	0.77	0.22	11.18	0.91	2.33	366	32
Second White Specks	2589.00	060718	444	1.31	3.73	0.68	0.26	5.54	0.42	1.29	291	52
Second White Specks	2588.00	060717	445	4.41	9.00	0.80	0.33	11.25	1.12	3.00	300	26
Second White Specks	2587.00	060716	447	2.35	5.74	0.61	0.29	9.45	0.67	1.83	314	33
Second White Specks	2586.00	060715	446	3.50	13.01	0.66	0.21	19.75	1.37	3.48	374	19
Second White Specks	2585.00	060714	445	3.70	11.42	0.65	0.25	17.70	1.26	3.05	375	21
Second White Specks	2584.00	060713	446	3.56	11.57	0.63	0.24	18.37	1.26	2.90	399	21
Second White Specks	2583.00	060712	445	3.20	9.75	0.55	0.25	18.07	1.08	2.58	379	21
Second White Specks	2582.00	060711	447	3.65	11.04	0.55	0.25	20.08	1.22	2.77	399	20
Second White Specks	2581.00	060710	446	2.93	7.74	0.47	0.28	16.74	0.89	2.13	364	22
Second White Specks	2580.00	060709	446	3.60	11.26	0.63	0.25	18.78	1.23	2.97	379	21
Second White Specks	2579.00	060708	445	1.09	4.13	0.48	0.21	8.62	0.43	0.82	507	59
Second White Specks	2578.00	060707	443	1.31	5.51	0.71	0.20	7.76	0.57	1.51	365	47
Second White Specks	2577.00	060706	444	0.88	2.51	0.44	0.26	6.05	0.28	0.73	345	61
Second White Specks	2576.00	060705	446	2.51	10.61	0.37	0.19	28.67	1.09	2.59	410	14
Second White Specks	2575.00	060704	446	3.40	11.33	0.66	0.23	18.26	1.23	2.81	403	23
Second White Specks	2574.00	060703	447	1.38	3.47	0.51	0.29	7.03	0.40	1.29	270	39
Second White Specks	2573.00	060702	447	1.89	6.78	0.48	0.22	14.28	0.72	1.95	348	24
Second White Specks	2572.00	060701	447	2.01	6.61	0.49	0.24	13.62	0.71	1.89	350	26
14-29-11-28W4, C-205706												
Second White Specks	2525.00	142907	437	1.26	9.84	0.62	0.12	15.89	0.92	3.06	321	20
Second White Specks	2522.00	142906	443	0.93	6.26	0.59	0.13	10.78	0.60	2.35	267	25
Second White Specks	2518.00	142905	438	1.01	5.91	0.66	0.15	8.95	0.57	2.35	251	28
Second White Specks	2515.00	142904	439	0.91	3.62	0.61	0.20	5.98	0.38	1.78	203	34

Formation	Depth (m)	Sample #	Tmax	S1	S2	S3	PI	S2/S3	PC	TOC	HI	OI
Second White Specks	2511.00	142903	438	0.90	5.35	0.64	0.15	8.36	0.52	1.88	284	34
Second White Specks	2507.00	142902	432	1.39	2.63	0.76	0.35	3.48	0.33	1.41	187	54
Second White Specks	2505.00	142901	439	1.12	3.50	0.65	0.25	5.70	0.38	1.85	189	35
06-30-13-27W4, C-179967, 1-2												
Westgate	2121.00	063001	437	0.20	1.14	0.15	0.15	7.85	0.11	1.25	91	11
Westgate	2122.80	063002	432	0.33	3.35	0.29	0.09	11.55	0.30	1.68	199	17
06-29-13-27W4, C-179966, 1-2												
Westgate	2083.00	062902	427	0.98	6.12	0.49	0.14	12.51	0.59	2.12	290	23
Westgate	2081.00	062901	427	0.51	2.39	0.34	0.18	7.14	0.24	1.44	166	23
4-8-13-27W4												
Westgate	2081.80	040804	447	0.48	0.83	0.30	0.37	2.77	0.11	1.21	68	24
Westgate	2079.50	040803	438	0.29	0.86	0.24	0.25	3.64	0.10	0.88	99	27
Fish Scales	2071.40	040802	428	2.04	10.66	0.79	0.16	13.63	1.06	3.25	328	24
Fish Scales	2068.50	040801	441	0.35	3.18	0.28	0.10	11.57	0.29	1.46	218	18
6-32-13-27W4												
Bow Island	2091.00	063206	0	0.11	0.00	0.07	1.00	0.00	0.00	0.18	0	36
Bow Island	2087.00	063205	437	0.25	3.50	0.25	0.07	14.68	0.31	1.81	194	13
Bow Island	2084.00	063204	438	0.26	3.40	0.21	0.07	16.62	0.30	1.72	198	12
Westgate	2081.25	063203	438	0.28	0.74	0.11	0.28	7.05	0.08	0.93	80	11
Westgate	2079.50	063202	437	0.23	1.08	0.17	0.18	6.53	0.11	1.11	97	15
Fish Scales	2076.50	063201	424	1.98	6.76	0.50	0.23	14.71	0.73	2.13	317	23
06-21-55-25W4, C-167142, 1-2												
Westgate	870.00	062102	440	0.35	1.44	0.52	0.20	2.81	0.15	1.77	81	29
Westgate	856.00	062101	429	0.15	1.45	0.56	0.10	2.61	0.13	1.88	77	29
8-25-12-24W4, C-205707												
Fish Scales	1356.00	082509	425	0.25	2.60	0.41	0.09	6.41	0.23	0.93	280	43
Fish Scales	1354.00	082508	424	1.22	7.66	0.52	0.14	14.73	0.74	2.79	275	18
Barons	1352.00	082507	438	0.99	7.37	0.46	0.12	16.02	0.70	1.92	384	23
Barons	1350.00	082506	428	0.50	4.88	0.39	0.10	12.49	0.44	2.05	237	19
Belle Fourche	1348.00	082505	429	0.37	4.95	0.34	0.07	14.56	0.44	2.06	240	16
Belle Fourche	1346.00	082504	429	0.36	4.64	0.34	0.07	13.64	0.42	1.83	253	19
Belle Fourche	1344.00	082503	428	0.25	2.80	0.33	0.08	8.59	0.25	1.44	194	22
Belle Fourche	1342.00	082502	429	0.26	3.99	0.32	0.06	12.65	0.35	1.69	237	18
Belle Fourche	1340.00	082501	425	0.46	6.51	0.37	0.07	17.57	0.58	2.24	290	16
11-21-12-23W4, C-167150, 16-22												
Westgate	1293.00	112122	439	0.11	1.12	0.26	0.09	4.39	0.10	1.48	76	17
Westgate	1291.00	112121	438	0.18	1.19	0.23	0.13	5.27	0.11	1.30	91	17
Westgate	1289.00	112120	430	0.32	2.28	0.35	0.13	6.58	0.21	1.34	170	26
Fish Scales	1286.00	112119	423	1.41	10.00	0.55	0.12	18.19	0.95	2.91	344	19
Fish Scales	1284.00	112118	426	1.34	15.91	0.42	0.08	37.89	1.43	4.22	377	10
Fish Scales	1282.00	112117	423	1.20	16.46	0.45	0.07	36.98	1.47	4.13	398	10
Fish Scales	1280.00	112116	422	1.10	21.14	0.78	0.05	27.98	1.85	4.83	438	16
Fish Scales	1278.00	112115	439	0.38	11.39	0.50	0.03	23.01	0.98	2.89	395	17
Belle Fourche	1276.00	112114	440	0.19	2.38	0.26	0.07	9.35	0.21	1.54	154	16
Belle Fourche	1274.00	112113	433	0.55	9.31	0.50	0.06	18.90	0.82	2.99	312	16
Belle Fourche	1272.00	112112	430	0.34	5.45	0.48	0.06	11.38	0.48	2.18	250	22
Belle Fourche	1270.00	112111	430	0.53	8.15	0.52	0.06	15.66	0.72	2.26	360	23
Belle Fourche	1268.00	112110	432	0.39	9.17	0.44	0.04	21.11	0.79	2.58	356	17
Second White Specks	1220.00	112109	425	1.29	25.15	0.60	0.05	42.30	2.20	4.51	558	13
Second White Specks	1218.00	112108	425	1.39	32.95	0.65	0.04	50.86	2.86	5.32	620	12
Second White Specks	1216.00	112107	423	1.41	27.42	0.83	0.05	33.95	2.40	5.31	516	16
Second White Specks	1214.00	112106	432	0.36	3.74	0.49	0.09	7.62	0.34	1.99	187	24
Second White Specks	1212.00	112105	427	0.83	12.48	0.80	0.06	15.68	1.11	3.43	364	23
Second White Specks	1210.00	112104	429	0.35	2.66	0.37	0.12	7.26	0.25	1.07	249	34
Second White Specks	1208.00	112103	429	0.63	10.92	0.72	0.06	15.57	0.96	2.94	371	24
Second White Specks	1206.00	112102	429	0.46	5.25	0.50	0.08	10.60	0.47	2.22	236	22
Second White Specks	1204.00	112101	434	0.57	6.14	0.41	0.09	15.11	0.55	2.52	244	16
16-10-12-23W4, C-205703												
Westgate	1262.00	161016	433	0.08	0.76	0.25	0.10	3.02	0.07	1.17	65	21
Westgate	1260.00	161015	431	0.08	1.09	0.23	0.07	4.82	0.10	1.36	79	16
Westgate	1259.00	161014	429	0.08	1.10	0.19	0.07	6.08	0.10	1.28	87	14
Westgate	1257.00	161013	433	0.08	1.18	0.17	0.07	6.94	0.10	1.22	96	14

Formation	Depth (m)	Sample #	Tmax	S1	S2	S3	PI	S2/S3	PC	TOC	HI	OI
Westgate	1256.00	161012	430	0.08	0.85	0.17	0.09	5.15	0.08	1.12	76	15
Fish Scales	1254.00	161011	416	1.36	12.11	0.70	0.10	22.83	1.12	3.36	360	21
Fish Scales	1254.00	161010	418	1.30	12.75	0.54	0.10	26.37	1.17	3.52	363	15
Fish Scales	1252.00	161009	419	1.28	17.36	0.59	0.07	34.51	1.55	4.12	422	14
Fish Scales	1251.00	161008	416	1.40	17.95	0.72	0.08	32.10	1.61	4.06	445	17
Fish Scales	1250.00	161007	416	1.42	17.74	0.74	0.08	29.41	1.60	4.29	414	17
Belle Fourche	1248.00	161006	416	0.71	6.45	0.65	0.10	10.04	0.59	1.89	341	34
Belle Fourche	1246.00	161005	419	0.45	3.38	0.57	0.12	5.93	0.32	0.91	372	63
Belle Fourche	1244.00	161004	420	0.49	5.18	0.55	0.09	9.60	0.47	2.40	216	23
Belle Fourche	1242.00	161003	420	0.99	7.46	0.52	0.12	14.33	0.70	3.05	245	17
Belle Fourche	1240.40	161002	425	0.31	6.33	0.35	0.05	18.41	0.55	2.08	304	16
Belle Fourche	1238.50	161001	422	0.32	4.82	0.38	0.07	12.70	0.43	2.06	234	18
10-34-42-22W4, C-167138												
Second White Specks	1470.00	103407	422	1.09	18.74	1.13	0.06	16.61	1.65	4.78	392	23
Second White Specks	1465.00	103406	428	0.68	7.38	0.73	0.09	10.23	0.67	3.05	242	24
Second White Specks	1460.00	103405	423	1.10	18.99	1.11	0.06	17.22	1.67	4.61	412	24
Second White Specks	1455.00	103404	423	1.18	22.57	1.11	0.05	20.33	1.98	5.24	431	21
Second White Specks	1450.00	103403	418	1.56	26.24	1.16	0.06	22.63	2.31	6.15	427	18
Second White Specks	1445.00	103402	426	0.48	6.60	0.74	0.07	8.97	0.59	2.80	236	26
Second White Specks	1440.00	103401	427	0.52	7.94	0.52	0.06	15.68	0.70	2.81	282	18
06-16-11-22W4, C-179965												
Belle Fourche	1111.60	061628	418	0.27	3.45	0.36	0.07	9.62	0.31	1.99	174	18
Belle Fourche	1112.10	061627	420	0.24	1.55	0.31	0.14	5.00	0.14	1.58	98	19
Belle Fourche	1112.60	061626	421	0.22	2.09	0.32	0.10	6.51	0.19	1.68	124	19
Belle Fourche	1113.10	061625	422	0.44	2.69	0.46	0.14	6.09	0.26	1.49	182	32
Belle Fourche	1113.60	061624	421	0.35	3.27	0.49	0.10	6.74	0.30	1.85	177	26
Belle Fourche	1114.10	061623	417	1.01	2.38	0.54	0.30	4.55	0.28	1.32	181	41
Belle Fourche	1114.60	061622	384	0.31	1.43	0.91	0.51	4.28	0.14	1.68	86	53
Barons Sst.	1115.10	061621	428	0.25	2.22	0.77	0.10	2.98	0.20	1.62	137	47
Barons Sst.	1116.50	061620	413	14.31	5.26	1.16	0.74	4.84	1.63	1.66	317	70
Barons Sst.	1117.20	061619	423	0.73	7.40	1.51	0.09	4.91	0.68	4.45	166	34
Fish Scales	1117.75	061618	424	0.49	4.06	1.35	0.11	3.01	0.38	2.52	161	53
Fish Scales	1118.25	061617	424	0.22	1.61	1.02	0.12	1.58	0.15	1.31	122	77
Fish Scales	1118.75	061616	423	0.22	2.51	1.16	0.08	2.16	0.22	1.28	197	91
Fish Scales	1119.25	061615	422	0.20	2.60	1.04	0.07	2.52	0.23	0.95	273	109
Fish Scales	1119.75	061614	421	0.41	5.43	1.59	0.07	3.42	0.48	2.96	184	53
Fish Scales	1120.25	061613	417	0.60	8.96	1.81	0.06	4.96	0.79	4.32	207	41
Fish Scales	1121.35	061612	420	0.34	3.79	1.52	0.08	2.49	0.34	2.05	184	74
Fish Scales	1122.00	061611	419	0.34	3.54	1.44	0.09	2.46	0.32	1.96	180	73
Westgate	1122.50	061610	418	0.66	8.28	1.35	0.07	6.19	0.74	3.27	253	41
Westgate	1123.00	061609	416	1.93	20.58	1.16	0.09	17.77	1.87	7.17	287	16
Westgate	1123.25	061608	414	2.99	30.51	1.74	0.09	17.97	2.79	10.01	306	17
Westgate	1123.50	061607	417	0.86	9.96	1.29	0.08	7.72	0.90	4.34	229	30
Westgate	1124.00	061606	418	0.69	6.21	0.96	0.10	6.72	0.57	2.97	209	32
Westgate	1124.50	061605	415	1.56	17.72	0.91	0.08	19.59	1.61	6.54	271	13
Westgate	1125.00	061604	415	1.98	25.89	1.23	0.07	21.93	2.32	9.30	278	13
Westgate	1125.50	061603	419	1.48	4.82	1.00	0.24	4.85	0.52	2.19	220	45
Westgate	1126.00	061602	416	1.15	10.61	1.06	0.10	10.07	0.98	4.89	217	21
6-34-10-22W4, C-205705												
Viking	1050.00	439	0.08	13.24	0.22	0.01	61.59	1.11	2.62	506	8	
Viking	1048.50	436	0.14	1.56	0.15	0.09	10.40	0.14	1.44	108	10	
Westgate	1037.00	430	0.27	0.73	0.21	0.27	3.45	0.08	1.10	66	19	
Westgate	1032.00	431	0.12	1.27	0.24	0.09	5.42	0.11	1.37	93	17	
Fish Scales	1017.50	415	0.67	7.52	0.53	0.08	14.32	0.68	2.33	322	22	
Barons	1012.50	404	3.21	2.75	0.63	0.54	5.27	0.49	0.87	316	24	
Barons	1010.00	422	0.19	2.15	0.28	0.08	8.15	0.19	1.56	138	18	
06-16-06-22W4, C-167149												
Fish Scales	981.00	061603	427	1.71	19.19	0.52	0.08	36.88	1.74	5.30	362	10
Fish Scales	976.00	061602	428	0.99	12.63	0.47	0.08	26.85	1.13	3.21	393	15
Fish Scales	971.00	061601	431	0.52	4.94	0.37	0.10	13.36	0.45	2.07	239	18
07-12-42-21W4, C-167139												
Second White Specks	1012.00	071202	425	1.19	19.95	0.86	0.06	23.19	1.76	5.41	369	16

Formation	Depth (m)	Sample #	Tmax	S1	S2	S3	PI	S2/S3	PC	TOC	HI	OI
Second White Specks	1009.00	071201	422	0.78	10.92	0.77	0.07	14.32	0.97	4.12	265	18
11-12-06-16W4, C-167148												
Westgate	630.00	111217	436	0.23	1.21	0.34	0.16	3.63	0.12	1.57	77	21
Fish Scales	625.00	111216	421	0.65	9.98	0.70	0.06	14.36	0.88	3.39	294	20
Fish Scales	620.00	111215	418	1.42	33.04	1.08	0.04	30.91	2.87	7.96	415	13
Belle Fourche	615.00	111214	427	0.46	4.13	0.52	0.11	7.93	0.38	2.09	197	25
Belle Fourche	609.00	111213	427	0.33	2.20	0.44	0.13	4.99	0.21	2.23	98	19
Belle Fourche	604.00	111212	423	0.25	5.87	0.52	0.04	11.39	0.51	3.26	180	16
Belle Fourche	599.00	111211	421	0.23	4.82	0.47	0.05	10.25	0.42	3.07	157	15
Belle Fourche	594.00	111210	431	0.37	4.35	0.40	0.08	11.07	0.39	2.64	164	15
Belle Fourche	589.00	111209	423	0.16	2.35	0.32	0.06	7.45	0.20	2.37	99	13
Belle Fourche	584.00	111208	420	0.15	2.44	0.36	0.06	6.77	0.21	2.29	106	16
Belle Fourche	579.00	111207	425	0.10	1.31	0.33	0.07	4.04	0.12	2.04	64	16
Belle Fourche	574.00	111206	423	0.12	0.94	0.36	0.11	2.65	0.09	1.56	60	23
Second White Specks	569.00	111205	418	0.93	27.22	1.01	0.04	27.00	2.34	6.37	427	16
Second White Specks	564.00	111204	424	0.31	5.77	0.82	0.05	7.08	0.50	1.85	313	44
Second White Specks	559.00	111203	429	0.45	3.66	0.53	0.11	6.90	0.34	2.37	154	22
Second White Specks	554.00	111202	424	0.34	2.73	0.47	0.11	5.88	0.25	2.08	131	22
Second White Specks	549.00	111201	430	0.66	5.95	0.42	0.10	14.26	0.55	3.03	196	13
06-22-11-06W4, C-179954												
Belle Fourche	540.00	062206	429	0.21	3.23	0.70	0.06	4.61	0.28	2.66	122	26
Belle Fourche	535.00	062205	420	0.27	1.64	0.61	0.14	2.68	0.15	1.60	102	38
Belle Fourche	530.00	062204	418	0.24	3.65	0.65	0.06	5.65	0.32	1.90	192	34
Second White Specks	525.00	062203	413	1.58	53.55	1.69	0.03	31.73	4.59	9.88	544	17
Second White Specks	523.00	062202	422	0.59	22.99	1.32	0.03	17.41	1.96	5.23	442	25
Second White Specks	520.00	062201	427	0.44	10.94	1.01	0.04	10.95	0.94	2.86	383	35
06-34-30-08W4, C-167141												
Westgate	829.00	063427	433	1.11	2.15	1.20	0.34	1.79	0.27	1.57	136	76
Westgate	824.00	063426	435	0.63	3.09	0.66	0.17	4.71	0.31	2.07	149	32
Westgate	819.00	063425	436	0.80	2.90	0.72	0.22	4.05	0.31	2.22	130	32
Westgate	814.00	063424	429	0.44	0.78	0.32	0.36	2.46	0.10	1.08	72	29
Westgate	810.00	063423	434	0.37	1.39	0.84	0.21	1.65	0.14	1.90	73	44
Westgate	805.00	063422	437	0.28	1.95	0.74	0.13	2.65	0.18	1.90	103	38
Westgate	800.00	063421	433	0.55	1.88	0.48	0.23	3.92	0.20	1.57	119	30
Westgate	795.00	063420	435	0.61	1.31	0.60	0.32	2.19	0.16	1.90	68	31
Westgate	790.00	063419	434	0.61	1.72	0.78	0.27	2.21	0.19	1.56	110	50
Westgate	785.00	063418	431	1.07	1.82	0.57	0.37	3.19	0.24	1.61	113	35
Westgate	780.00	063417	431	1.70	1.97	0.60	0.47	3.31	0.30	1.83	107	32
Westgate	775.00	063416	430	0.78	1.37	0.48	0.36	2.87	0.18	1.71	80	28
Fish Scales	770.00	063415	432	0.57	1.89	0.72	0.23	2.66	0.20	2.03	93	35
Fish Scales	765.00	063414	412	2.11	12.77	1.41	0.14	9.09	1.24	5.57	229	25
Belle Fourche	753.00	063413	437	0.30	2.04	0.59	0.13	3.48	0.19	1.88	108	31
Belle Fourche	748.00	063412	428	0.60	1.76	0.62	0.26	2.83	0.19	1.75	100	35
Second White Specks	743.00	063411	417	3.88	35.61	1.73	0.10	20.58	3.29	8.73	408	20
Second White Specks	738.00	063410	416	8.44	27.54	1.75	0.23	15.78	3.00	8.21	335	21
Second White Specks	733.00	063409	418	9.65	21.97	1.58	0.31	13.97	2.63	7.26	302	21
Second White Specks	728.00	063408	417	14.75	25.65	1.78	0.37	14.43	3.36	8.11	316	22
Second White Specks	723.00	063407	421	5.30	17.08	1.35	0.24	12.66	1.86	5.88	290	23
Second White Specks	718.00	063406	417	5.84	15.07	1.19	0.28	12.71	1.74	5.26	286	22
Second White Specks	713.00	063405	416	11.72	17.88	1.20	0.40	14.96	2.46	6.26	285	19
Second White Specks	708.00	063404	417	18.76	21.79	1.63	0.46	13.37	3.37	7.39	295	22
Second White Specks	703.00	063403	417	8.65	19.97	1.28	0.31	15.60	2.38	6.19	322	20
Second White Specks	698.00	063402	423	7.11	18.60	1.26	0.28	14.76	2.14	5.77	322	22
Second White Specks	693.00	063401	422	1.44	13.00	1.18	0.10	11.01	1.20	5.04	258	23
07-14-01-05W4, C-179953												
Belle Fourche	603.00	071406	419	0.24	1.49	0.44	0.14	3.42	0.14	1.93	77	23
Belle Fourche	598.00	071405	420	0.12	1.04	0.38	0.10	2.76	0.09	1.96	53	19
Belle Fourche	593.00	071404	420	0.18	0.25	0.12	0.42	2.16	0.03	0.42	60	29
Belle Fourche	589.00	071403	415	0.23	2.14	0.65	0.10	3.28	0.20	2.70	79	24
Second White Specks	583.00	071402	420	0.93	15.79	1.20	0.06	13.21	1.39	4.30	367	28
Second White Specks	579.00	071401	422	0.45	8.32	0.90	0.05	9.29	0.73	2.13	390	42
10-35-45-02W4, C-167136												

Formation	Depth (m)	Sample #	Tmax	S1	S2	S3	PI	S2/S3	PC	TOC	HI	OI
Westgate	498.00	103525	430	0.26	1.59	0.40	0.14	4.02	0.15	2.12	75	18
Westgate	493.00	103524	434	0.21	1.63	0.42	0.12	3.87	0.15	1.98	82	21
Westgate	488.00	103523	425	0.08	0.81	0.44	0.10	1.87	0.07	1.85	43	23
Westgate	483.00	103522	435	0.28	1.46	0.43	0.16	3.39	0.14	1.88	77	22
Westgate	478.00	103521	430	0.06	0.64	0.34	0.09	1.89	0.06	1.44	44	23
Westgate	473.00	103520	432	0.15	0.53	1.03	0.22	0.51	0.05	1.32	40	78
Westgate	468.00	103519	424	0.05	0.34	0.36	0.13	0.94	0.03	1.10	30	32
Westgate	463.00	103518	422	0.04	0.41	0.44	0.09	0.94	0.03	1.28	32	34
Westgate	458.00	103517	422	0.18	0.46	0.41	0.28	1.12	0.05	1.12	41	36
Westgate	448.00	103516	420	0.32	1.33	0.51	0.20	2.63	0.14	1.94	68	26
Fish Scales	443.00	103515	442	0.24	8.84	0.79	0.03	11.20	0.75	2.98	296	26
Belle Fourche	438.00	103513	441	0.32	3.14	1.14	0.10	2.76	0.28	1.85	169	62
Belle Fourche	428.00	103511	433	0.46	1.48	0.54	0.24	2.75	0.16	1.57	94	34
Second White Specks	417.00	103510	417	1.94	27.39	2.89	0.07	9.49	2.44	8.48	323	34
Second White Specks	414.00	103507	415	1.62	29.60	3.09	0.05	9.58	2.60	7.90	375	39
Second White Specks	413.00	103506	415	1.82	24.72	2.41	0.07	10.25	2.21	6.08	406	39
Second White Specks	412.00	103505	413	2.38	24.96	2.65	0.09	9.44	2.28	6.81	367	39
Second White Specks	411.00	103504	417	1.43	20.85	2.24	0.06	9.33	1.85	5.73	364	39
Second White Specks	410.00	103503	407	1.60	16.82	1.50	0.09	11.22	1.53	6.97	241	21
06-18-45-01W4, C-167137												
Westgate	459.00	061814	427	0.08	0.57	0.34	0.12	1.67	0.05	1.36	42	25
Westgate	454.00	061813	432	0.09	0.58	0.42	0.14	1.40	0.05	1.27	46	33
Westgate	449.00	061812	428	0.20	1.58	0.48	0.11	3.29	0.14	1.87	84	26
Westgate	439.00	061811	422	0.14	1.67	0.61	0.08	2.76	0.15	2.04	81	29
Westgate	434.00	061810	414	0.86	11.06	1.30	0.07	8.52	0.99	5.83	189	22
Belle Fourche	429.00	061809	438	0.17	6.00	1.12	0.03	5.37	0.51	2.49	241	45
Belle Fourche	424.00	061808	437	0.24	3.11	0.58	0.07	5.40	0.28	1.99	155	29
Belle Fourche	419.00	061807	424	0.19	1.13	0.38	0.15	3.00	0.11	1.59	71	23
Belle Fourche	416.00	061806	423	0.11	0.53	0.70	0.17	0.77	0.05	1.06	50	66
Belle Fourche	414.00	061805	419	0.12	1.10	0.65	0.10	1.69	0.10	2.08	53	31
Second White Specks	408.00	061804	418	0.76	28.97	2.42	0.03	11.99	2.47	7.50	386	32
Second White Specks	403.00	061803	410	1.73	50.77	3.48	0.03	14.63	4.37	12.08	420	29
Second White Specks	398.00	061802	412	0.71	14.86	1.54	0.05	9.65	1.30	5.59	266	27
10-25-01-27W3 Saskoil Willow Creek, C-179958												
First White Specks	839.00	102504	418	0.46	19.45	1.51	0.02	12.88	1.65	5.68	342	26
First White Specks	838.00	102503	415	0.52	20.66	1.39	0.02	14.88	1.76	3.53	587	39
First White Specks	837.00	102502	421	0.25	9.83	1.05	0.03	9.43	0.84	3.68	267	28
First White Specks	836.00	102501	413	0.47	16.06	1.12	0.03	14.40	1.37	3.15	511	35
11-16-35-8W3 C.M.S. Vanscoy, C-179956												
Pense	523.15	111601	433	1.39	3.96	0.39	0.26	10.14	0.44	2.08	190	19
Pense	520.90	111602	431	0.32	2.74	0.29	0.10	9.46	0.25	1.47	187	20
Joli Fou	519.90	111603	432	0.23	3.12	0.25	0.07	12.75	0.28	1.28	244	19
Joli Fou	518.90	111604	422	0.16	1.31	0.36	0.11	3.69	0.12	2.00	65	18
Joli Fou	517.90	111605	418	0.11	0.65	0.27	0.14	2.47	0.06	1.18	55	22
Joli Fou	516.90	111606	418	0.11	0.65	0.29	0.14	2.24	0.06	1.21	54	24
Joli Fou	515.90	111607	416	0.05	0.23	0.35	0.19	0.67	0.02	0.93	24	37
Joli Fou	514.90	111608	419	0.18	0.35	0.27	0.34	1.30	0.04	0.97	36	28
Joli Fou	514.80	111609	428	0.05	0.51	0.22	0.09	2.42	0.04	1.25	41	17
Joli Fou	510.00	111610	421	0.04	0.34	0.21	0.11	1.62	0.03	0.73	47	29
Joli Fou	504.60	111611	431	0.00	0.15	0.17	0.00	0.91	0.01	0.55	27	30
Viking	499.80	111612	438	0.01	0.17	0.02	0.06	12.00	0.01	0.38	43	4
Westgate	494.80	111613	446	0.01	0.18	0.03	0.06	6.00	0.01	0.57	31	5
Westgate	489.90	111614	431	0.02	0.26	0.06	0.06	4.33	0.02	0.78	34	7
Westgate	484.80	111615	429	0.10	0.46	0.10	0.18	4.81	0.04	0.93	49	10
Fish Scales	484.30	111616	435	0.36	2.19	0.39	0.14	5.60	0.21	1.86	117	21
Fish Scales	479.80	111617	433	0.06	1.05	0.15	0.05	7.24	0.09	1.52	69	9
Belle Fourche	476.40	111618	429	0.06	0.56	0.08	0.10	7.11	0.05	0.94	59	8
Belle Fourche	470.80	111619	431	0.16	0.74	0.12	0.18	6.12	0.07	1.40	52	8
Belle Fourche	465.80	111620	430	0.17	0.76	0.10	0.18	7.97	0.07	1.22	61	8
Belle Fourche	460.80	111621	427	0.06	0.41	0.05	0.13	8.54	0.04	1.06	38	4
Belle Fourche	455.80	111622	423	0.04	0.47	0.04	0.08	11.75	0.04	1.17	40	3
Belle Fourche	450.80	111623	423	0.22	0.57	0.07	0.28	8.81	0.06	1.08	52	6

Formation	Depth (m)	Sample #	Tmax	S1	S2	S3	PI	S2/S3	PC	TOC	HI	OI
Belle Fourche	445.80	111624	417	0.05	0.85	0.26	0.06	3.31	0.07	1.62	52	16
Belle Fourche	440.80	111625	430	0.05	0.91	0.15	0.05	6.29	0.08	1.47	62	10
Belle Fourche	435.80	111626	419	0.03	0.74	0.21	0.04	3.61	0.06	1.56	47	13
Belle Fourche	430.80	111627	411	0.24	1.22	1.81	0.16	0.67	0.12	1.62	75	111
Belle Fourche	427.30	111628	427	0.08	1.29	0.21	0.06	6.16	0.11	1.73	75	12
Belle Fourche	418.50	111629	421	0.06	0.88	0.34	0.06	2.59	0.08	1.97	44	17
Belle Fourche	413.20	111630	424	0.04	0.72	0.17	0.06	4.21	0.06	1.20	59	14
Belle Fourche	408.20	111631	425	0.02	0.72	0.12	0.03	6.28	0.06	1.26	57	9
Belle Fourche	407.20	111632	434	0.04	1.72	0.27	0.02	6.41	0.14	1.48	116	18
Belle Fourche	406.20	111633	420	0.05	1.13	0.32	0.04	3.58	0.10	1.50	75	21
Belle Fourche	405.20	111634	419	0.05	1.01	0.33	0.05	3.12	0.08	1.28	78	25
Belle Fourche	404.20	111635	411	0.57	12.30	1.23	0.05	9.99	1.07	4.61	267	26
Belle Fourche	403.20	111636	414	0.39	9.30	1.15	0.04	8.08	0.81	3.88	239	29
Belle Fourche	402.20	111637	420	0.19	3.17	0.68	0.06	4.66	0.28	2.30	138	29
Belle Fourche	401.70	111638	420	0.26	4.02	0.71	0.06	5.75	0.36	2.47	163	28
Second White Specks	401.00	111639	406	2.35	32.86	2.26	0.07	14.53	2.93	8.67	379	26
Second White Specks	400.25	111640	416	0.33	14.02	1.38	0.02	10.19	1.19	4.62	303	30
First White Specks	399.40	111641	412	0.76	22.62	1.56	0.03	14.50	1.95	5.94	381	26
First White Specks	398.40	111642	415	0.70	22.39	1.43	0.03	15.71	1.92	5.60	400	25
First White Specks	397.25	111643	413	1.18	27.04	1.86	0.04	14.54	2.35	6.56	412	28
First White Specks	396.30	111644	416	0.60	20.52	1.55	0.03	13.28	1.76	5.60	367	27
First White Specks	391.30	111645	411	1.02	25.20	1.58	0.04	16.00	2.18	6.11	412	25
First White Specks	386.30	111646	412	1.59	30.46	1.95	0.05	15.67	2.67	7.30	418	27
First White Specks	381.30	111647	413	0.78	18.95	1.56	0.04	12.15	1.64	5.06	375	31
First White Specks	376.30	111648	410	1.56	30.52	2.00	0.05	15.26	2.67	7.34	416	27
First White Specks	360.70	111649	421	0.30	5.39	2.33	0.05	2.31	0.47	2.31	233	100
05-22-34-1W3 U.S. Borax & Chemical, C-179955												
Pense	517.60	052241	431	0.07	1.41	0.45	0.05	3.13	0.12	1.11	127	41
Pense	515.50	052240	433	0.02	0.87	2.97	0.02	0.29	0.07	0.69	127	433
Joli Fou	507.80	052239	427	0.20	4.67	0.67	0.04	7.03	0.40	1.40	335	47
Joli Fou	506.80	052238	421	0.03	0.30	0.50	0.08	0.73	0.02	1.21	25	41
Joli Fou	505.80	052237	419	0.00	0.08	0.55	0.00	0.19	0.00	0.16	52	348
Joli Fou	504.50	052236	412	0.02	0.14	0.28	0.13	0.48	0.01	0.77	18	39
Joli Fou	502.80	052235	416	0.04	0.16	0.62	0.20	0.26	0.01	0.64	25	98
Joli Fou	501.80	052234	415	0.09	0.19	0.22	0.32	0.88	0.02	0.70	30	33
Joli Fou	499.60	052233	410	0.03	0.09	0.78	0.28	0.11	0.01	0.33	25	237
Joli Fou	498.60	052232	397	0.01	0.07	0.31	0.15	0.22	0.00	0.40	20	85
Joli Fou	497.50	052231	415	0.01	0.09	0.17	0.10	0.55	0.00	0.43	23	43
Joli Fou	496.50	052230	318	0.00	0.01	1.29	0.00	0.00	0.00	0.30	3	470
Joli Fou	494.50	052229	417	0.00	0.08	0.08	0.00	0.93	0.00	0.43	18	20
Joli Fou	493.50	052228	420	0.00	0.11	0.85	0.00	0.13	0.01	0.51	23	185
Joli Fou	492.60	052227	421	0.01	0.10	0.29	0.04	0.34	0.01	0.37	27	79
Joli Fou	491.20	052226	370	0.01	0.05	0.33	0.01	0.15	0.01	0.41	12	81
Joli Fou	490.10	052225	424	0.02	0.31	0.35	0.06	0.88	0.02	0.86	35	40
Joli Fou	489.10	052224	423	0.02	0.20	0.32	0.08	0.62	0.01	0.73	27	43
Joli Fou	488.10	052223	421	0.02	0.14	0.28	0.11	0.49	0.01	0.73	19	37
Joli Fou	487.10	052222	422	0.01	0.18	0.34	0.06	0.53	0.01	0.78	23	43
Joli Fou	486.10	052221	417	0.02	0.12	0.35	0.14	0.34	0.01	0.73	16	48
Joli Fou	485.10	052220	420	0.01	0.14	0.36	0.07	0.39	0.01	0.72	19	50
Joli Fou	484.10	052219	425	0.01	0.14	0.26	0.07	0.52	0.01	0.76	18	34
Joli Fou	483.10	052218	390	0.00	0.02	0.70	0.00	0.02	0.00	0.34	4	209
Joli Fou	482.10	052217	424	0.01	0.16	0.29	0.06	0.56	0.01	0.74	21	38
Joli Fou	481.10	052216	426	0.01	0.10	0.27	0.09	0.37	0.01	0.55	18	50
Joli Fou	480.20	052215	423	0.03	0.21	0.28	0.12	0.75	0.02	0.85	25	33
Joli Fou	479.10	052214	423	0.02	0.19	0.33	0.10	0.57	0.01	0.77	24	43
Joli Fou	478.20	052213	423	0.02	0.22	0.29	0.09	0.75	0.02	0.78	27	36
Viking	476.25	052212	430	0.03	0.47	0.34	0.06	1.38	0.04	0.92	51	37
Viking	475.25	052211	429	0.06	0.70	0.37	0.07	1.90	0.06	1.21	57	30
Viking	474.50	052210	429	0.05	0.80	0.32	0.06	2.52	0.07	1.38	57	23
Westgate	473.20	052209	429	0.06	0.91	0.57	0.06	1.59	0.08	1.62	56	35
Westgate	472.20	052208	429	0.04	0.81	0.42	0.05	1.93	0.07	1.58	51	26
Westgate	471.20	052207	430	0.06	0.91	0.51	0.07	1.79	0.08	1.52	59	33

Formation	Depth (m)	Sample #	Tmax	S1	S2	S3	PI	S2/S3	PC	TOC	HI	OI
Westgate	470.00	052206	428	0.04	0.64	0.47	0.06	1.36	0.05	1.56	41	30
Westgate	468.90	052205	429	0.04	0.73	0.30	0.05	2.42	0.06	1.34	54	22
Westgate	467.90	052204	428	0.03	0.78	0.35	0.04	2.26	0.06	1.67	46	21
Westgate	466.80	052203	428	0.02	0.73	0.24	0.02	3.04	0.06	1.33	55	18
Westgate	465.80	052202	420	0.05	0.74	0.33	0.06	2.24	0.06	1.68	44	20
Westgate	464.80	052201	433	0.04	1.08	0.65	0.04	1.67	0.09	1.52	71	42
White Specks	398.20	052242	412	1.49	31.09	1.84	0.05	16.89	2.71	8.18	380	22
White Specks	397.20	052243	414	1.12	26.88	1.58	0.04	17.01	2.33	6.67	403	23
White Specks	396.20	052244	413	1.23	28.76	1.79	0.04	16.06	2.50	7.31	393	24
White Specks	395.20	052245	414	1.27	29.68	1.93	0.04	15.47	2.58	7.94	374	24
White Specks	394.20	052246	422	0.62	17.01	1.09	0.04	15.68	1.46	4.16	409	26
White Specks	393.20	052247	415	1.10	23.93	1.65	0.04	14.55	2.08	6.12	391	27
White Specks	392.50	052248	413	0.73	13.57	1.65	0.05	8.25	1.19	4.42	307	37
White Specks	390.20	052249	415	0.82	15.37	1.58	0.05	9.72	1.35	4.41	349	35
White Specks	388.00	052250	415	0.77	14.88	1.64	0.05	9.10	1.30	4.36	341	37
White Specks	387.00	052251	411	0.96	21.17	1.91	0.04	11.11	1.84	6.04	350	31
White Specks	385.90	052252	411	0.94	19.85	2.08	0.05	9.54	1.73	6.24	318	33
White Specks	384.90	052253	413	1.22	19.81	2.45	0.06	8.36	1.75	5.74	345	43
White Specks	383.90	052254	417	0.53	9.05	2.95	0.05	3.07	0.79	4.86	186	61
White Specks	382.90	052255	419	0.40	11.41	2.03	0.03	5.63	0.98	4.67	244	43
White Specks	382.00	052256	409	0.39	6.41	1.38	0.06	4.66	0.56	3.05	210	45
White Specks	381.13	052257	409	2.65	38.19	2.33	0.06	16.49	3.40	9.92	385	23
11-36-22-1W2 S.W.P Bredenbury, C-179957												
Joli Fou	349.30	113652	420	0.05	0.68	0.17	0.07	3.97	0.06	1.27	53	13
Joli Fou	348.80	113651	418	0.03	0.34	0.57	0.08	0.60	0.03	1.07	32	53
Viking	343.80	113650	419	0.28	1.62	0.43	0.15	3.77	0.16	2.03	79	21
Viking	340.50	113649	419	0.23	1.11	0.89	0.17	1.25	0.11	1.57	71	56
Westgate	336.30	113648	422	0.11	0.39	0.56	0.22	0.69	0.04	1.20	32	47
Westgate	332.60	113647	420	0.16	0.76	1.03	0.18	0.73	0.07	1.71	44	60
Westgate	328.10	113646	422	0.27	1.83	0.69	0.13	2.67	0.17	2.64	69	26
Westgate	321.80	113645	428	0.09	1.14	0.43	0.08	2.67	0.10	1.69	67	25
Westgate	316.80	113644	414	0.10	1.19	0.55	0.08	2.20	0.10	1.81	65	30
Westgate	311.80	113643	409	0.70	10.42	1.31	0.06	7.99	0.93	5.09	204	26
Fish Scales	309.70	113642	414	0.30	2.65	0.80	0.10	3.30	0.24	2.34	113	34
Belle Fourche	296.70	113641	411	0.50	5.75	1.16	0.08	4.95	0.52	3.91	147	29
Belle Fourche	291.70	113640	406	0.60	8.02	1.26	0.07	6.39	0.71	4.20	191	30
Belle Fourche	290.80	113639	408	0.67	8.98	1.51	0.07	5.95	0.80	4.95	181	30
Belle Fourche	288.90	113638	418	1.19	22.07	2.13	0.05	10.38	1.93	5.51	401	38
Belle Fourche	287.00	113637	413	1.59	30.37	1.96	0.05	15.50	2.66	7.22	421	27
Belle Fourche	285.10	113636	410	1.78	37.74	2.44	0.05	15.46	3.29	8.99	419	27
Belle Fourche	283.20	113635	409	1.85	29.59	2.43	0.06	12.17	2.62	7.87	375	30
Belle Fourche	281.30	113634	417	1.29	20.24	1.75	0.06	11.58	1.79	4.88	415	36
Belle Fourche	279.40	113633	410	1.92	30.47	2.09	0.06	14.58	2.70	8.17	373	25
Second White Specks	277.50	113632	407	3.23	36.32	2.55	0.08	14.25	3.29	8.14	446	31
Second White Specks	275.60	113631	412	0.25	4.85	1.22	0.05	3.99	0.42	1.40	346	87
Second White Specks	273.70	113630	417	0.17	2.10	0.93	0.08	2.26	0.19	0.82	255	113
Second White Specks	272.70	113629	401	4.55	46.40	2.54	0.09	18.26	4.24	10.20	455	25
Second White Specks	270.90	113628	401	4.58	53.99	2.57	0.08	21.03	4.88	12.62	429	20
Second White Specks	268.90	113627	405	6.28	51.91	2.31	0.11	22.47	4.84	11.95	434	19
Second White Specks	266.90	113626	403	4.09	43.39	2.32	0.09	18.70	3.95	10.26	423	22
Second White Specks	264.90	113625	404	1.78	17.36	1.86	0.09	9.33	1.59	4.65	374	40
Second White Specks	262.30	113624	406	2.20	32.30	2.54	0.07	12.77	2.87	7.23	447	35
Second White Specks	260.30	113623	396	1.58	16.14	2.27	0.09	7.13	1.48	9.14	177	24
Morden	258.30	113622	411	1.14	17.71	1.59	0.06	11.27	1.57	6.46	274	24
Morden	256.30	113621	401	0.76	8.30	3.89	0.09	2.13	0.75	6.91	120	56
Morden	255.40	113620	401	1.09	10.60	4.08	0.09	2.59	0.97	7.91	134	52
Morden	253.90	113619	400	1.05	7.24	3.42	0.13	2.12	0.69	6.75	107	50
Morden	252.40	113618	398	0.63	4.53	3.32	0.12	1.36	0.43	6.21	73	53
Morden	250.80	113617	404	0.63	3.64	2.82	0.15	1.29	0.35	5.15	70	54
Morden	249.30	113616	398	0.90	7.29	3.09	0.11	2.36	0.68	6.75	108	46
First White Specks	247.49	113615	412	2.39	28.74	3.67	0.08	7.84	2.59	9.11	316	40
First White Specks	247.02	113614	412	0.62	9.19	2.05	0.07	4.47	0.82	2.87	320	71

Formation	Depth (m)	Sample #	Tmax	S1	S2	S3	PI	S2/S3	PC	TOC	HI	OI
First White Specks	246.65	113613	410	3.85	45.04	4.22	0.08	10.69	4.07	12.17	370	34
First White Specks	244.65	113612	414	1.47	25.36	3.46	0.06	7.34	2.23	6.78	374	51
First White Specks	242.65	113611	416	1.04	17.76	3.47	0.06	5.12	1.57	5.51	323	63
First White Specks	240.65	113610	413	0.12	0.79	0.79	0.14	1.00	0.07	0.89	88	89
First White Specks	235.65	113609	415	1.93	39.68	3.32	0.05	11.97	3.46	7.98	497	41
First White Specks	230.65	113608	415	1.79	30.38	3.65	0.06	8.32	2.68	7.51	405	48
First White Specks	225.65	113607	413	1.67	26.92	2.77	0.06	9.74	2.38	7.50	359	37
First White Specks	220.65	113606	413	2.70	40.69	5.15	0.06	7.90	3.61	10.39	391	49
First White Specks	215.50	113605	422	1.14	29.48	3.33	0.04	8.91	2.55	8.02	367	41
Lea Park	210.50	113604	427	0.15	1.00	0.76	0.13	1.32	0.10	1.69	59	44
Lea Park	205.50	113603	420	0.22	0.94	0.56	0.19	1.67	0.10	1.64	57	34
Lea Park	200.50	113602	427	0.20	1.88	0.81	0.09	2.32	0.17	2.16	87	37
Lea Park	195.40	113601	420	0.16	0.79	0.69	0.17	1.14	0.07	1.59	49	43

Petrographic and foraminiferal plates

Plate 1

BSEM photomicrographs. GSC # = Geological Survey of Canada, Calgary photographic file number; # followed by six digits = sample number. Westgate Formation **a)** siltstone laminae overlain by a claystone laminae. Arrow indicates contact (#111618, 484.3 m - GSC #4072-77). **b)** matrix-supported fabric with quartz (q) and kaolinized biotite (arrow) (#111618, 484.3 m - GSC #4072-81). **c)** sand-sized K-feldspar grains in laminae of a starved ripple (#111618, 484.3 m - GSC #4072-78). **d)** K-feldspar (K), microcline (M), biotite (B), quartz (Q), and zircon (Z) in a sandy laminae (#111618, 484.3 m - GSC #4072-85). **e)** argillaceous rock fragment (F) with K-feldspar (K) and a rounded polycrystalline quartz grain (Q) (#111618, 484.3 m - GSC #4072-84). **f)** Detrital chamosite (C) (#050120, 436 m - GSC #3680-30).

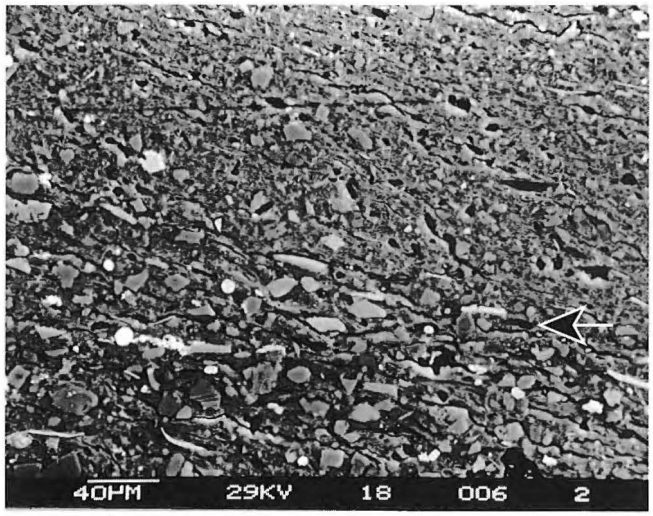
40PM 29KV 18 006 2

a

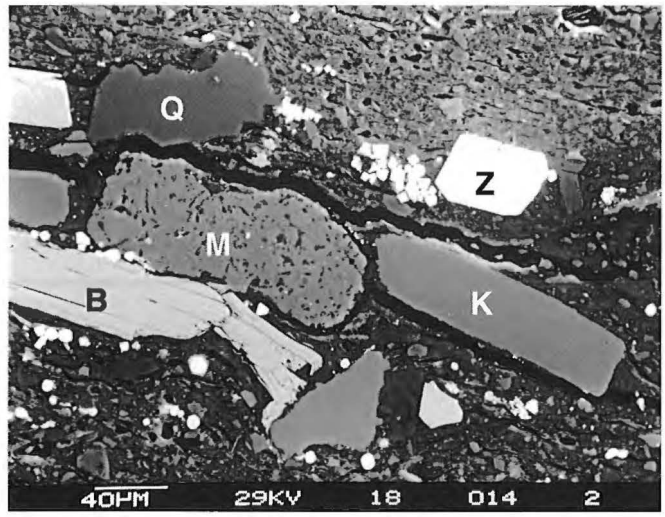
Q
Z
M
B
K
40PM 29KV 18 014 2

d

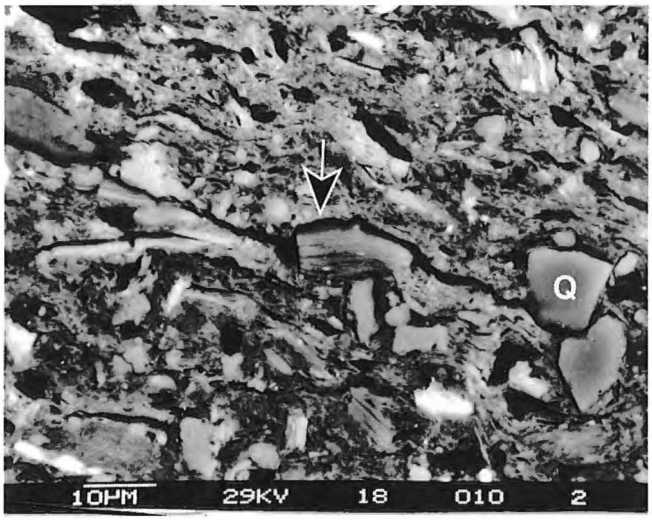
Q
10PM 29KV 18 010 2

b

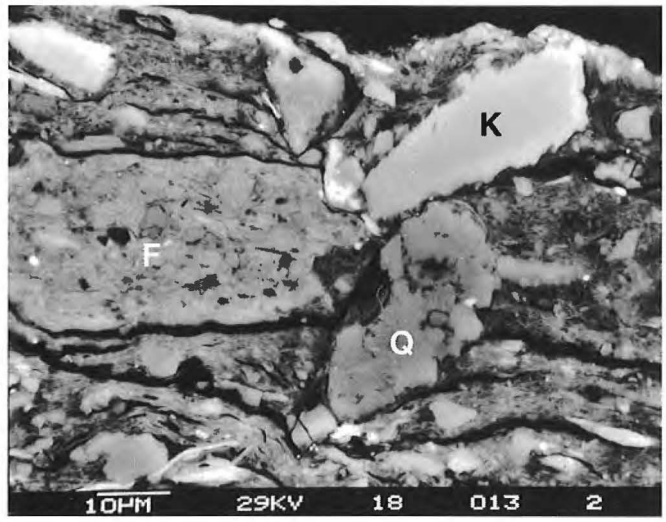
K
F
Q
10PM 29KV 18 013 2

e

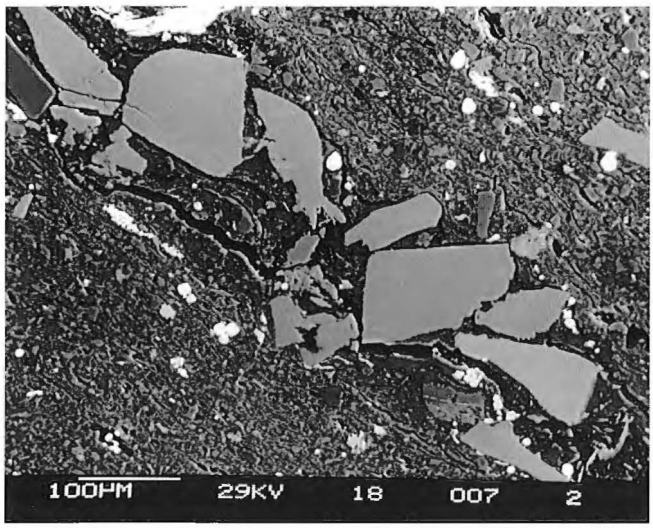
100PM 29KV 18 007 2

c

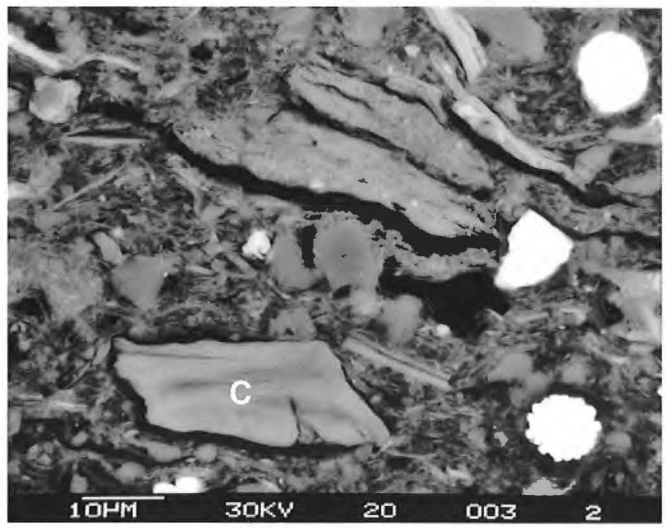
C
10PM 30KV 20 003 2

f

Plate 2

Westgate Formation. **a)** quartz (Q) and pyroclastic plagioclase (P) (#111618, 484.3 m - GSC #4072-80). **b)** volcanic rock fragment with K-rich (light grey) and K-poor (dark grey) zones (#111618, 484.3 m - GSC #4072-82). **c)** zoned volcanic rock fragment with K-rich (light grey) and K-depleted (dark grey) zones. Bright rim is due to edge effects (#111614, 489.9 m - GSC #4072-62). **d)** sand-sized microcline (M) and K-feldspar (K). Note difference in dissolution characteristics. Microcline is pitted and K-feldspar is dissolved at the edge (high magnification of 1D). **e)** silica replaced foraminifera test. This sample is extensively bioturbated. Compare homogeneous matrix fabric with those of 1a and 1b (#111610, 510 m - GSC #4072-60).

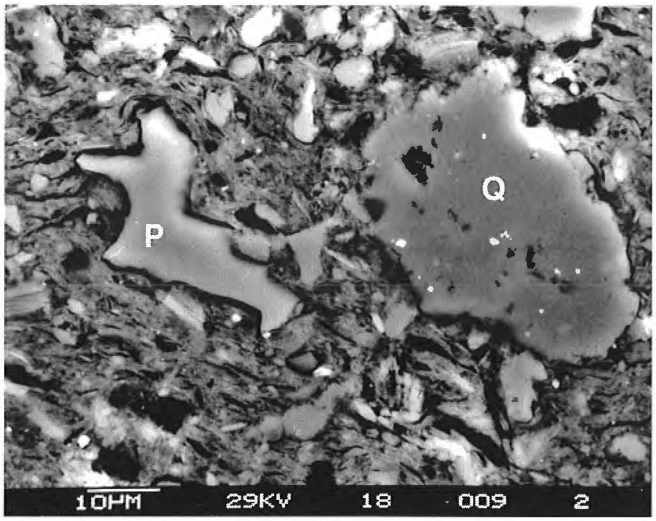
P
Q
10PM 29KV 18 009 2

a

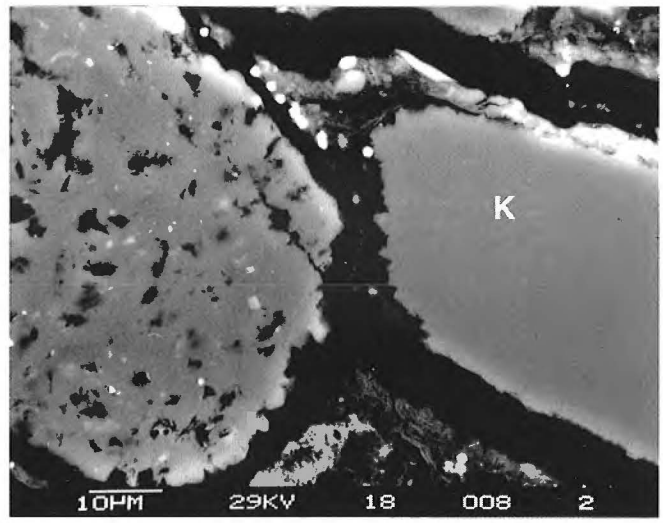
K
10PM 29KV 18 008 2

d

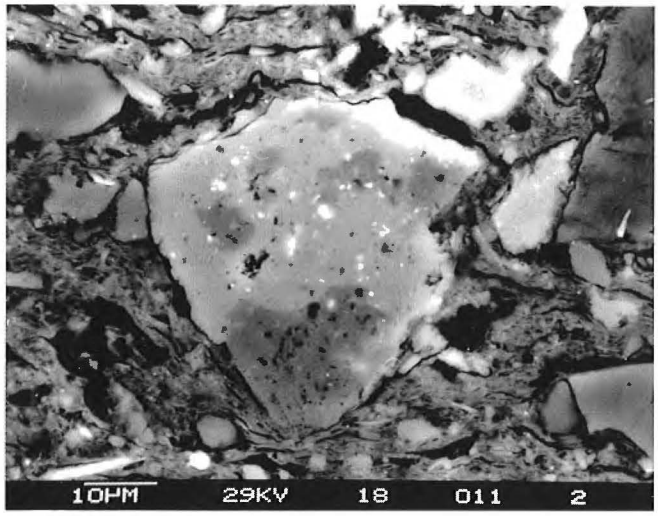
10PM 29KV 18 011 2

b

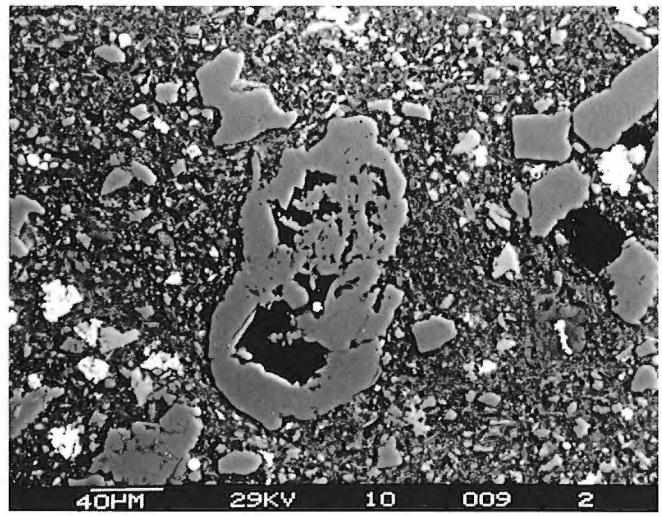
40PM 29KV 10 009 2

e

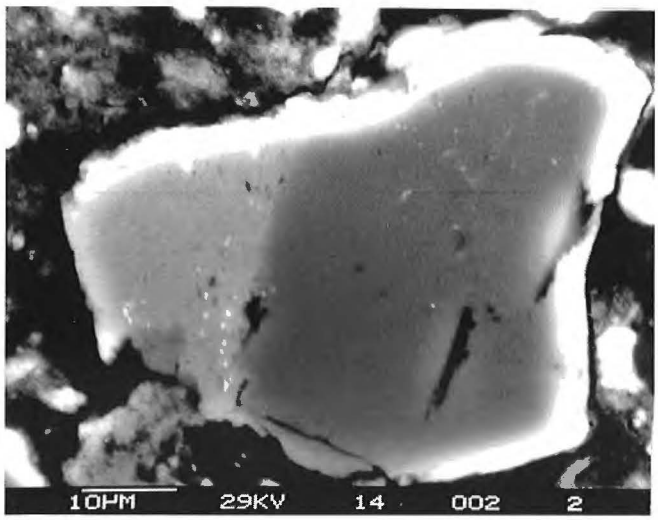
10PM 29KV 14 002 2

c

Plate 3

Westgate Formation. **a)** I/S in a quartz "vug"(#111610, 510 m - GSC #4072-57). **b)** high magnification (~10K) of "a". Fibrous habit of I/S indicates an authigenic origin (GSC #4072-56). **c)** authigenic kaolinite shows large vermicular habit (bottom) and a fine-grained pseudomorphic habit (arrows), probably after plagioclase feldspar (#050941A, 1503 m - GSC #3680-115). **d)** kaolinite pseudomorph of a detrital grain, presumably feldspar (#050941A, 1503 m -GSC #3680-113). **e)** kaolinite replacing K-feldspar (arrow) (#050926, 1466 m - GSC #3680-97). **f)** authigenic kaolinite (arrow) replacing a mica(?). Detrital muscovite (M) appears unaltered (#102503, 1327 m - GSC #3680-34).

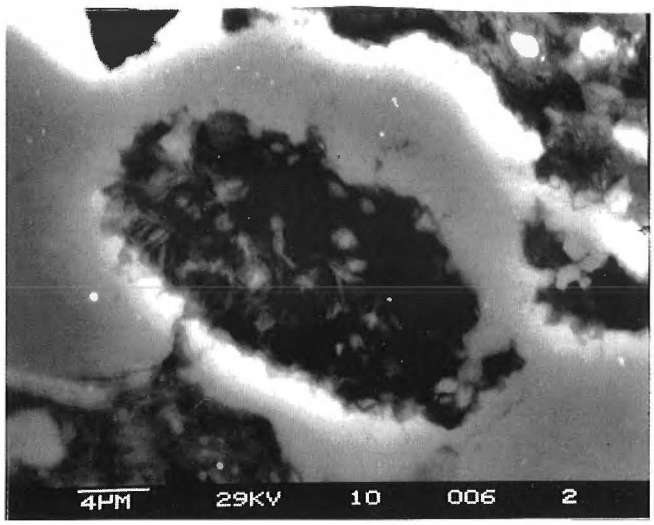
4μM 29KV 10 006 2

a

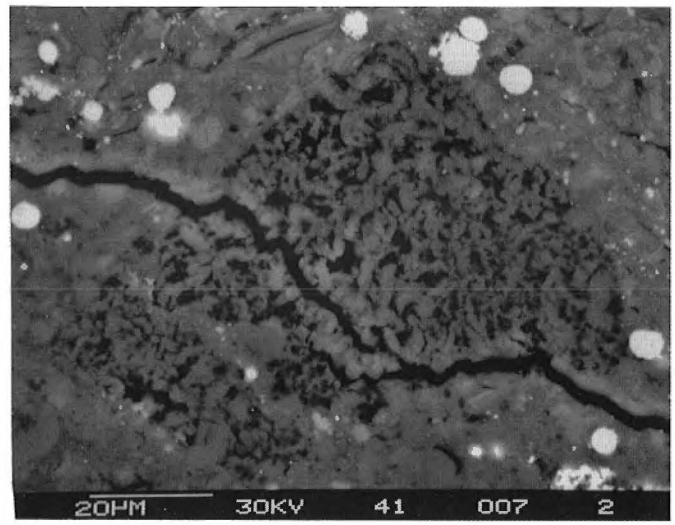
20μM 30KV 41 007 2

d

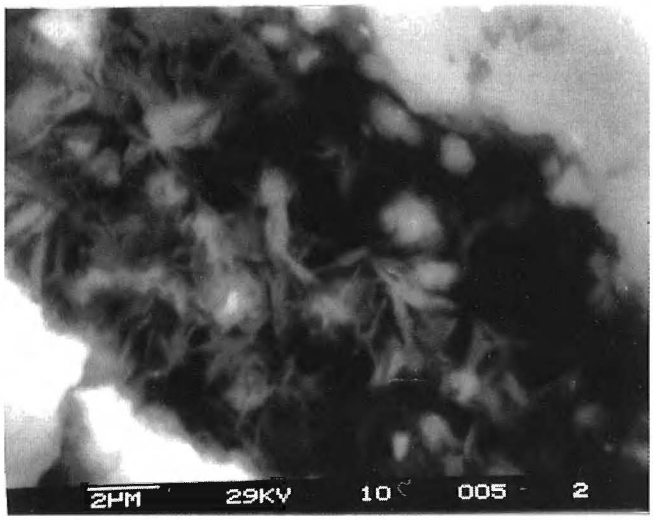
2μM 29KV 10 005 2

b

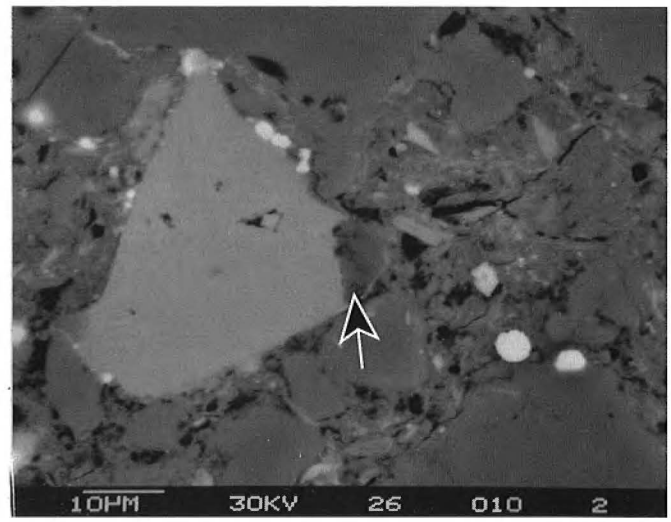
10μM 30KV 26 010 2

e

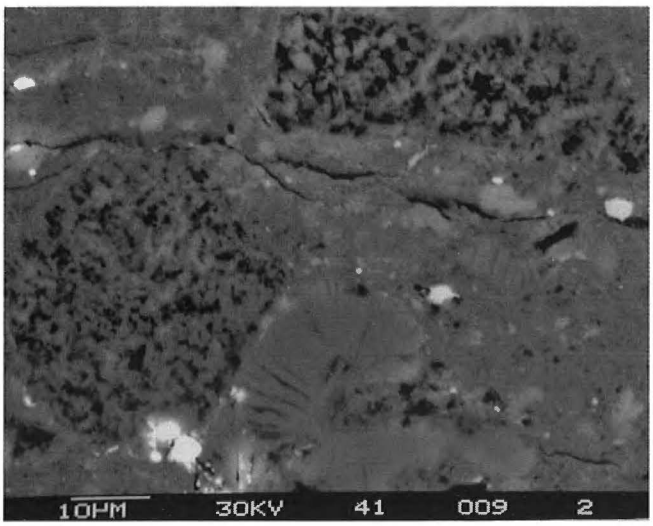
10μM 30KV 41 009 2

c

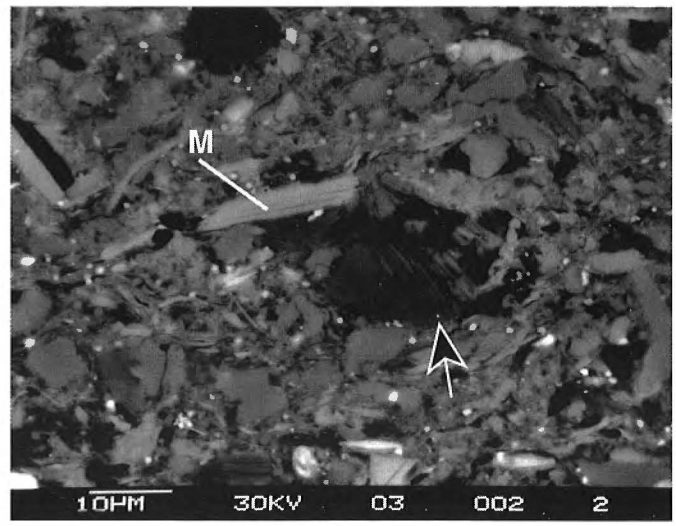
M
10μM 30KV 03 002 2

f

Plate 4

Westgate Formation. **a)** glauconite (G) with quartz (dark grey) grains and K-feldspar (arrow) in a bioturbated siltstone (#111610, 510 m - GSC #4072-60). **b)** "glauconite" grain shows an inclusion-rich, fibrous crystal habit (#111610, 510 m - GSC #4072-52). **c)** bone fragment composed of collophane (dark grey) and crystalline apatite (white inclusions) (#100501, 2566 m - GSC #3680-37). **d)** siltstone matrix with pyrite framboids (white spheres). Matrix shows extensive dissolution and is Fe-rich in top half (#050940, 1496 m - GSC #3680-101). **e)** extensive framework dissolution has occurred in bright zone where the matrix is Fe-rich (#050940, 1496 m - GSC #3680-103). **f)** sutured quartz grains in a zone of intensive dissolution (#050940, 1496 m - GSC #3680-98).

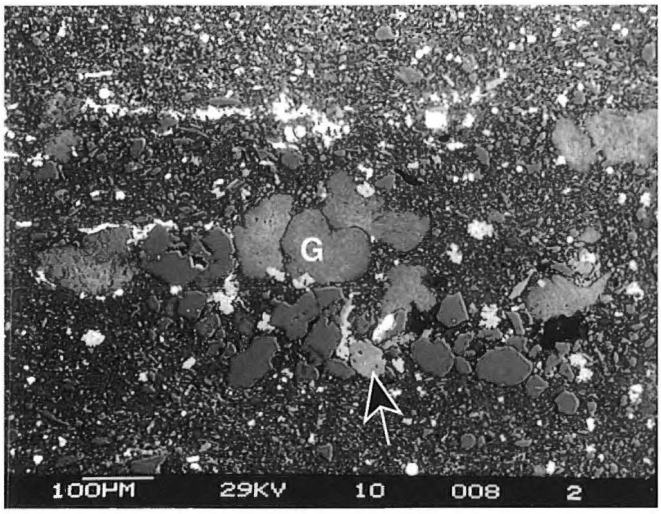
G
100µM 29KV 10 008 2

a

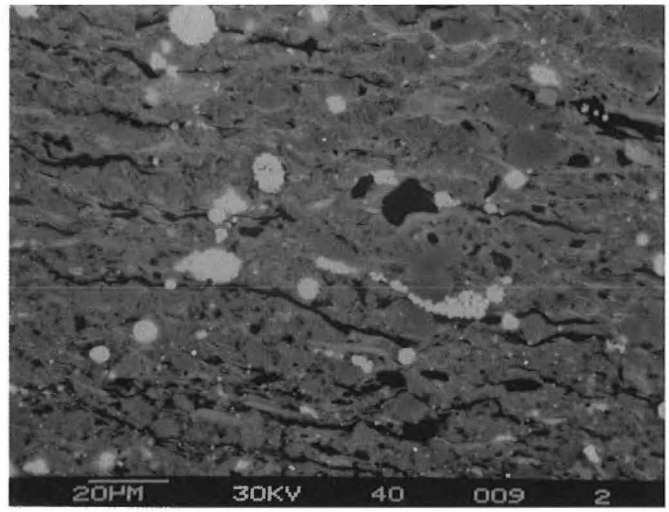
20µM 30KV 40 009 2

d

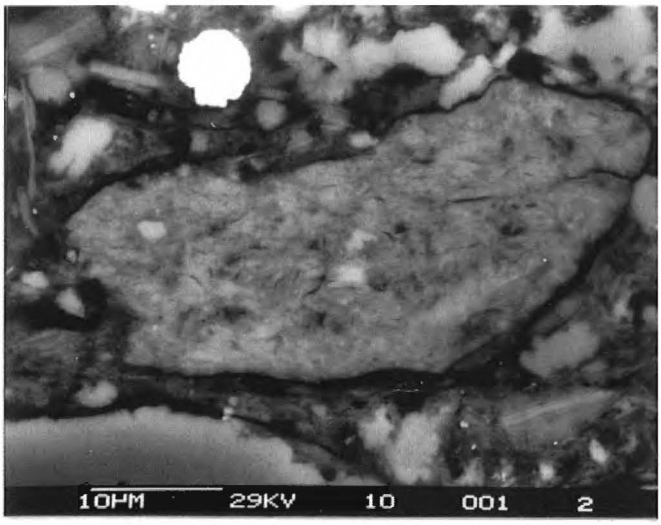
10µM 29KV 10 001 2

b

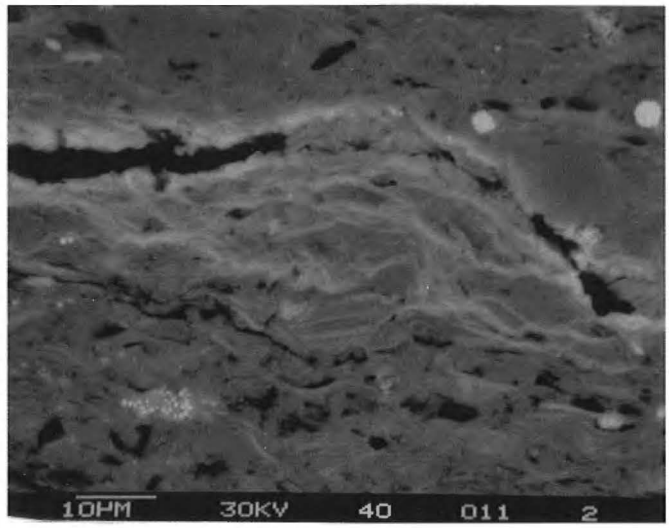
10µM 30KV 40 011 2

e

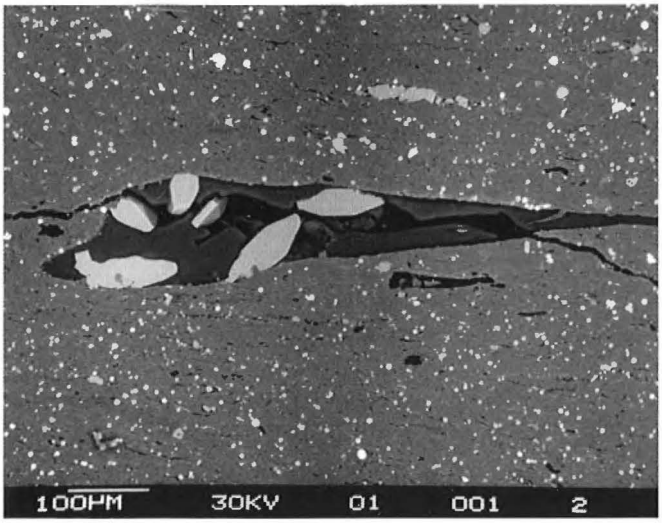
100µM 30KV 01 001 2

c

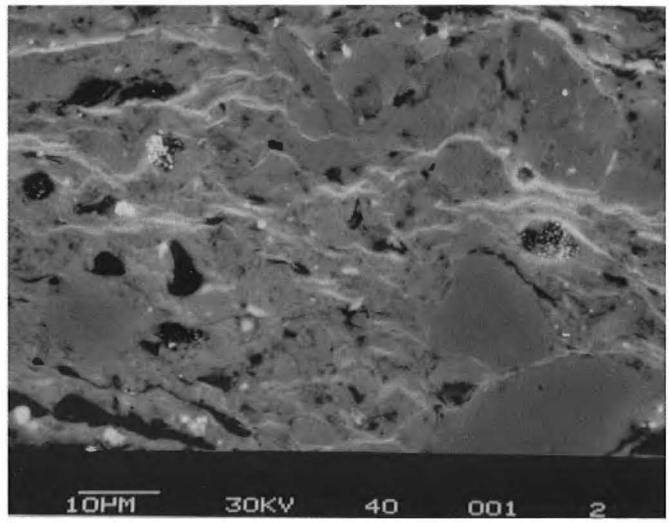
10µM 30KV 40 001 2

f

Plate 5

Westgate Formation. **a)** heterogeneous pyrite distribution in claystone. Abundant pyrite in bottom replaces fish debris. Less abundant pyrite in top is dominantly framboidal (#050941A, 1503 m - GSC #3680-108). **b)** pyrite aggregate in siltstone (#111618, 476.4 m - GSC #4072-74). **c)** reduced contrast, high magnification of aggregate in "b" showing pyrite pseudomorphs of feldspars (F) and "exploded" micas (M) as well as framboidal and octahedral pyrite (#111618, 476.4 m - GSC #4072-74). **d)** framboid aggregate showing random, cubic, and closest-packing arrangements (#111618, 476.4 m - GSC #4072-83). **e)** partial pyrite replacement of a bone fragment (#111618, 476.4 m - GSC #4072-72). **f)** partly dissolved detrital TiO_2 grain, probabaly rutile (#111614, 489.9 m - GSC #4072-70).

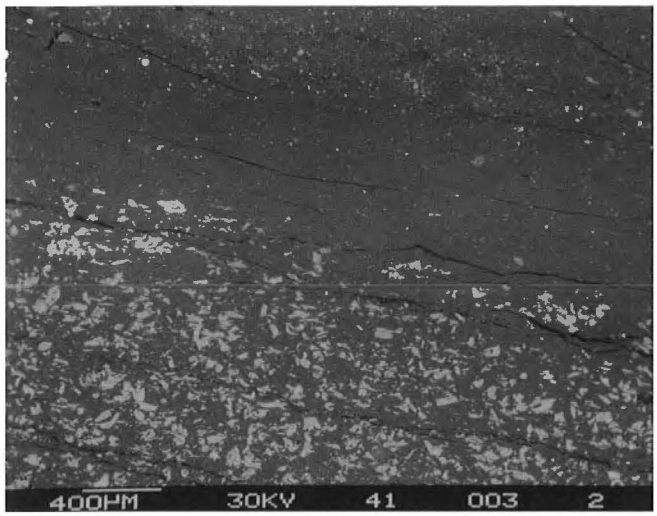
400µM 30KV 41 003 2

a

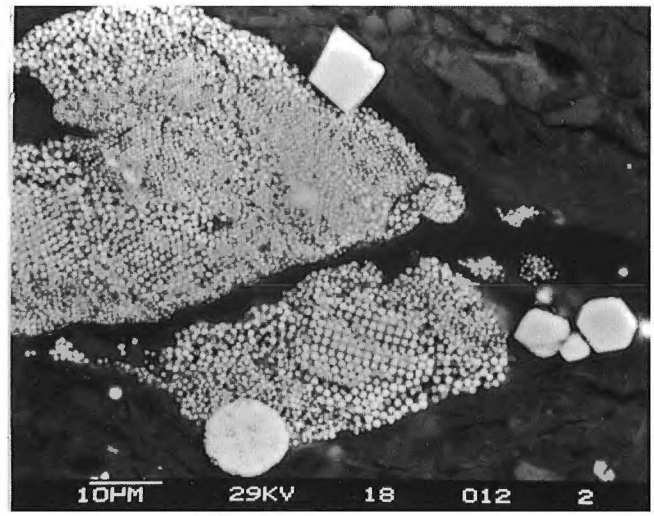
10µM 29KV 18 012 2

d

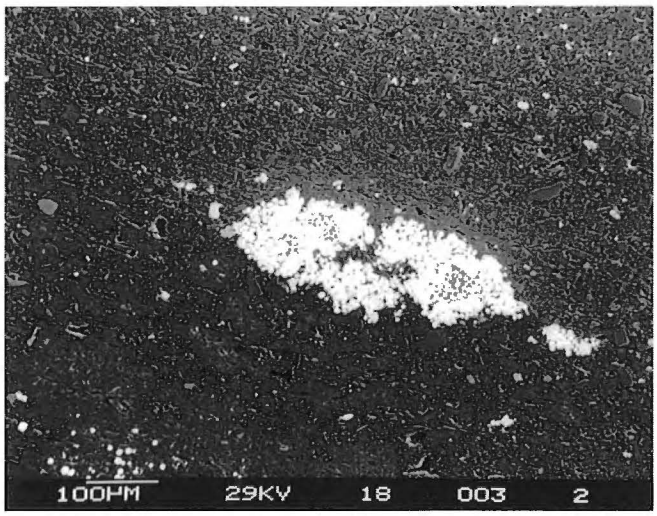
100µM 29KV 18 003 2

b

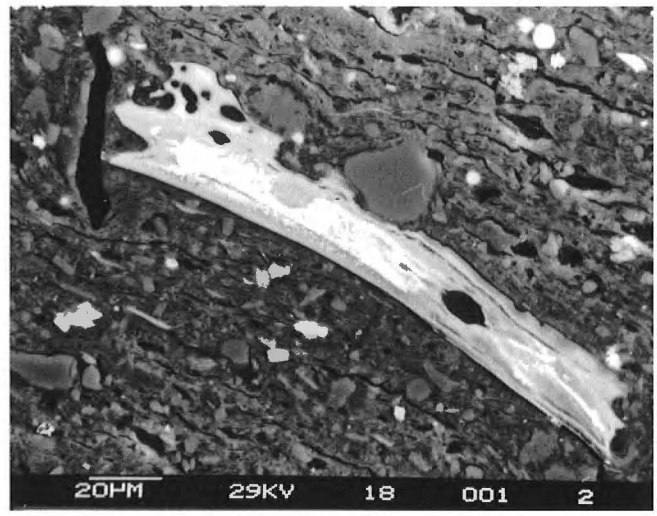
20µM 29KV 18 001 2

e

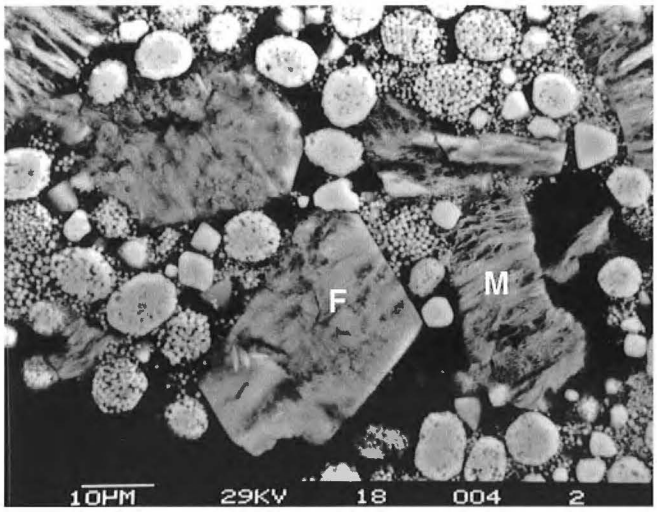
F
M
10µM 29KV 18 004 2

c

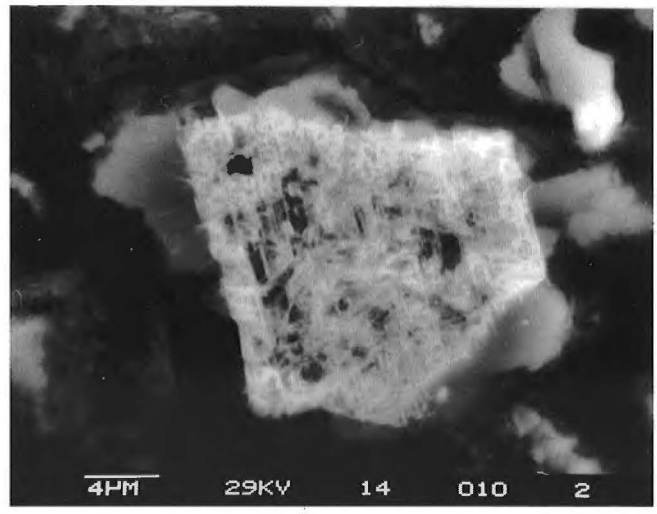
4µM 29KV 14 010 2

f

Plate 6

Westgate Formation. **a)** authigenic siderite (S) and partly dissolved K-feldspar (K) in bioturbated matrix (#111614, 489.9 m - GSC #4072-66). **b)** authigenic siderite between laths of muscovite (#111610, 510 m - GSC #4072-53). **c)** Fe-rich carbonate rimming a detrital carbonate bioclast (#102503, 1327 m - GSC #3680-33). **d)** Calcite (C) replacing plagioclase (P) (#050926, 1466 m - GSC #3680-89). **e)** Siderite replaces the cell wall structure and pyrite fills the cells of these algal bodies (#102523, 483 m - GSC #3680-15). **f)** siderite microconcretion, probably replacing a burrow structure (#102503, 1327 m - GSC #3680-85).

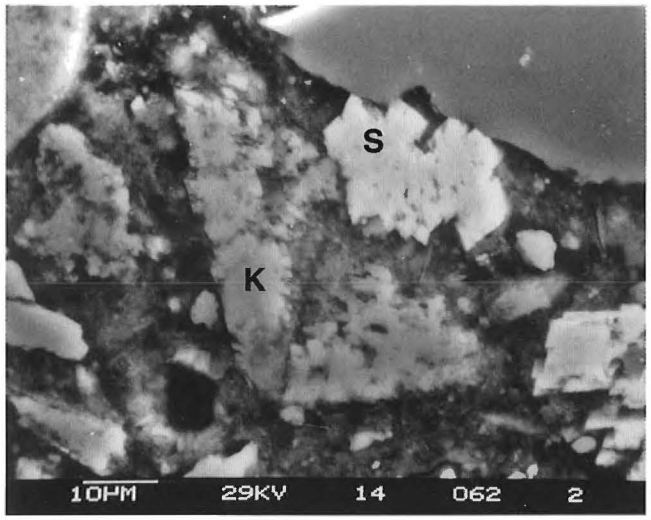
S
K
10µM 29KV 14 062 2

a

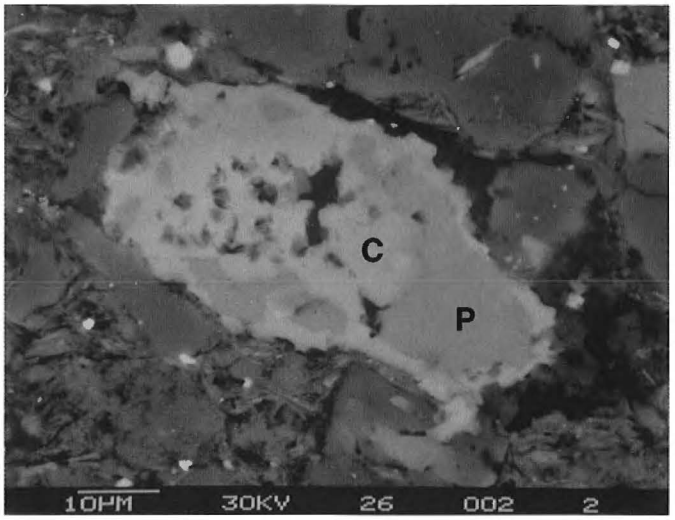
C
P
10µM 30KV 26 002 2

d

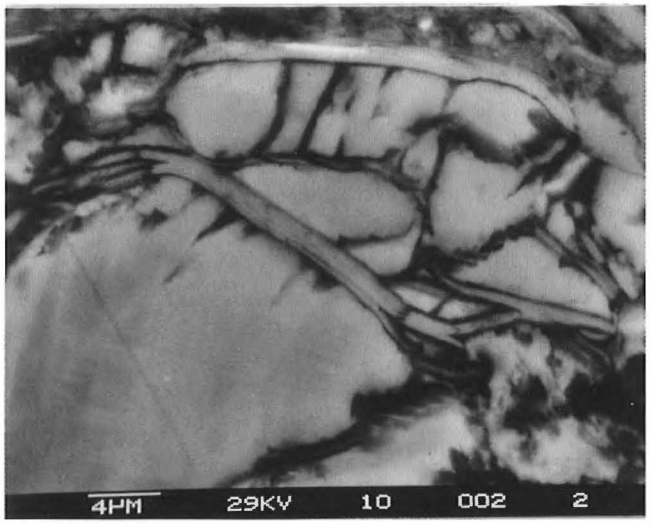
4µM 29KV 10 002 2

b

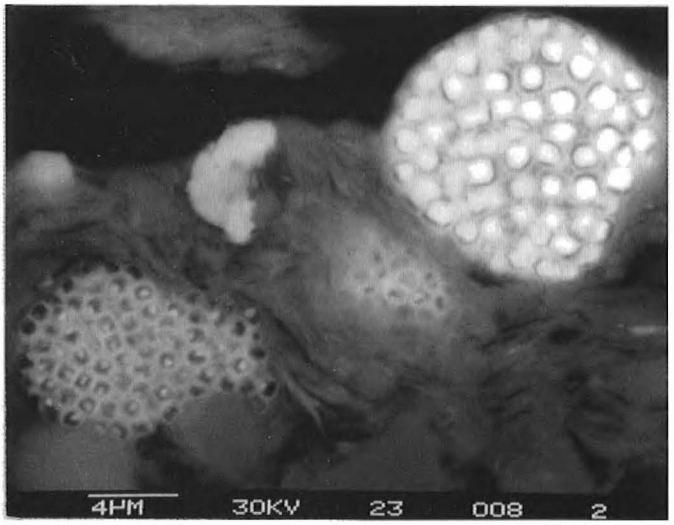
4µM 30KV 23 008 2

e

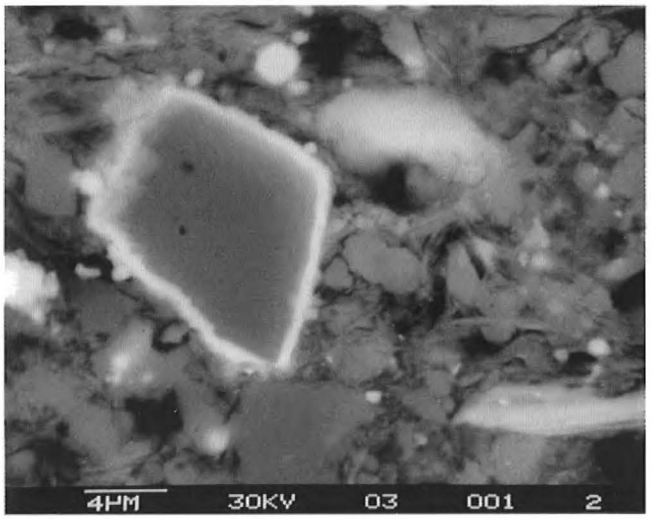
4µM 30KV 03 001 2

c

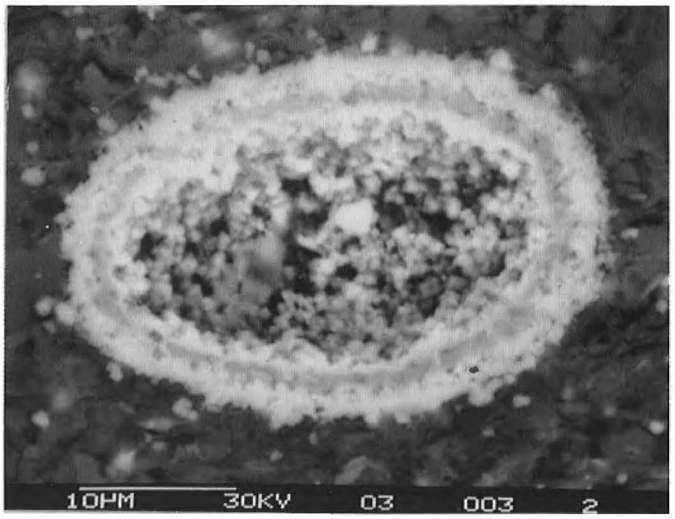
10µM 30KV 03 003 2

f

Plate 7

Fish Scales Formation. **a)** sand-sized quartz grain in an otherwise very fine-grained matrix (#103514, 443 m - GSC # 3671-21). **b)** matrix-supported, very fine silt-sized detrital grains of quartz and micas (arrows) (#103514, 443 m - GSC #3671-22). **c)** Ca-rich plagioclase (P) and authigenic, Mn-bearing siderite (arrow) (#103514, 443 m - GSC #3671-18). **d)** well-preserved K-feldspar (F) (#103514, 443 m - GSC #3671-19). **e)** fish bone fragments (lenticular light grey) lie on both sides of a fracture that is partially filled with Ca-sulphate (arrow) (#103514B, 444 m - GSC #3671-29). **f)** higher magnification of bone fragments in fine-grained matrix (#103514B, 444 m - GSC #3671-28).

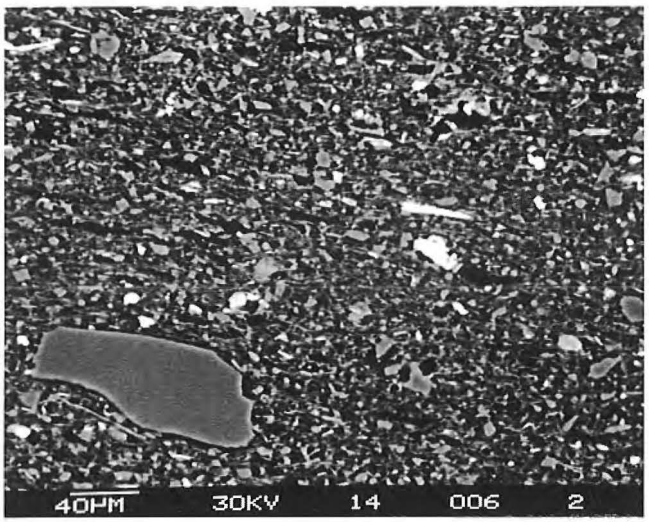
40PM 30KV 14 006 2

a

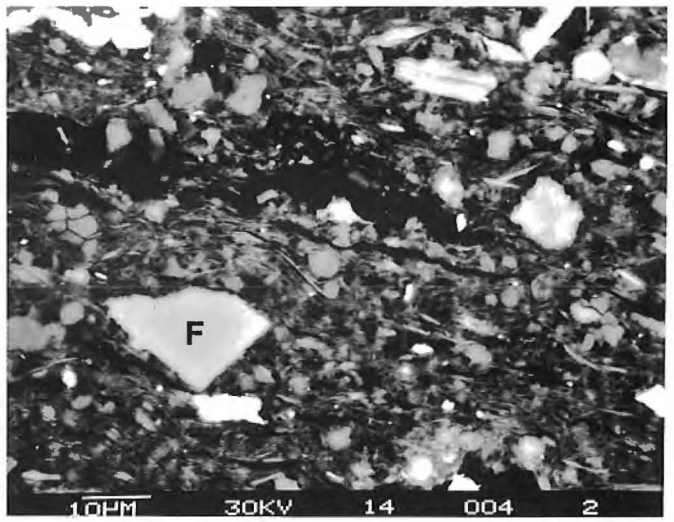
F
10PM 30KV 14 004 2

d

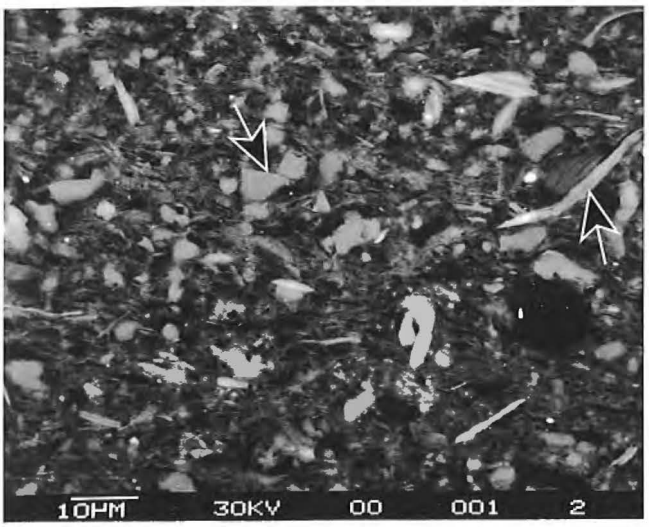
10PM 30KV 00 001 2

b

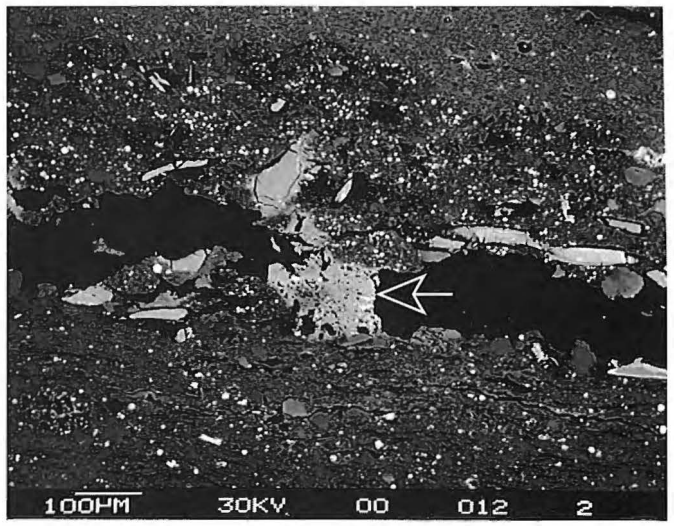
100PM 30KV 00 012 2

e

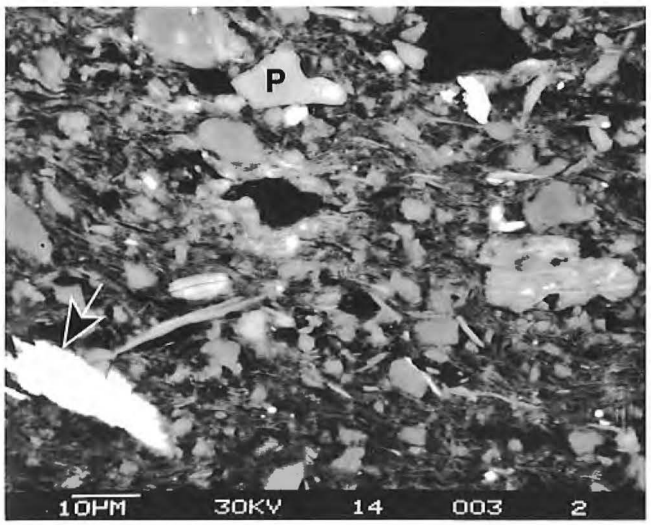
P
10PM 30KV 14 003 2

c

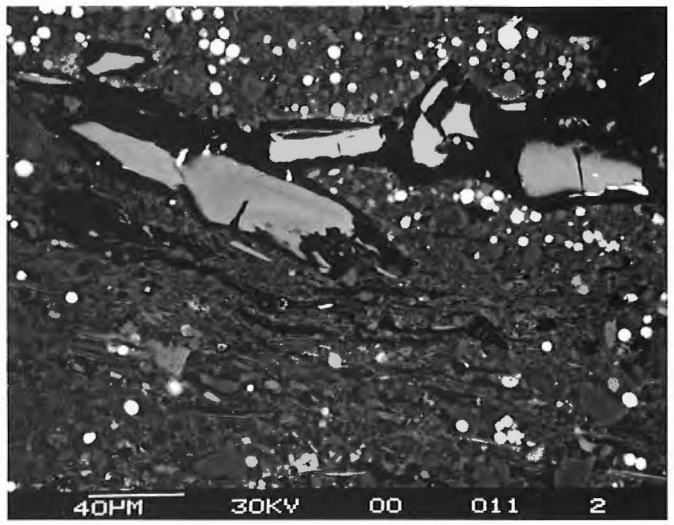
40PM 30KV 00 011 2

f

Plate 8

Belle Fourche Formation. **a)** laminated mudstone (top and bottom) and siltstone (middle). Matrix in siltstone appears black because it has been plucked during polishing. Plucking of matrix in framework-supported material is common (#050102, 384 m - GSC #3860-26). **b)** mudstone matrix showing a large, detrital muscovite (top), K-feldspars (light grey, left and right) and quartz (#050102, 384 m - GSC #3860-20). **c)** foraminifer and small ostracod (?) tests filled with authigenic kaolinite. White spheres are framboidal pyrite (#090907, 32268 m - GSC #3860-75). **d)** compactionally deformed muscovite (top) and biotite (bottom) with quartz grains and intergrown siderite. Note quartz suturing in contact with muscovite (#050102, 384 m - GSC #3860-18). **e)** detrital chamosite (bottom) with muscovite (left) and an "exploded" biotite (top) with intergrown siderite (#050102, 384 m - GSC #3860-22). **f)** sideritized fecal pellet (#050102, 384 m - GSC #3860-17).

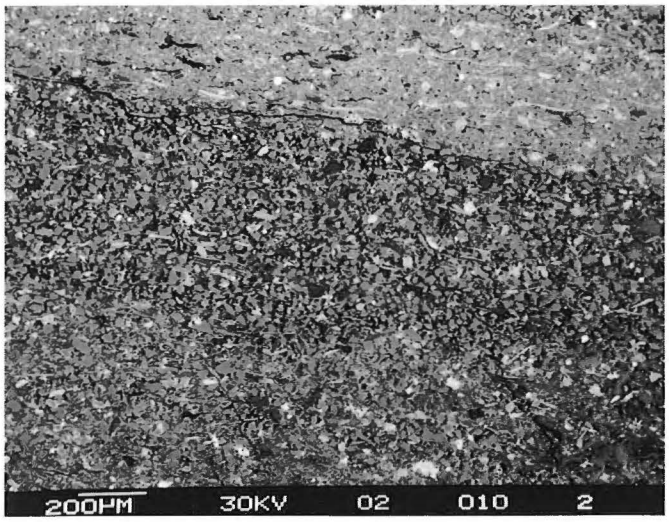
200µM 30KV 02 010 2

a

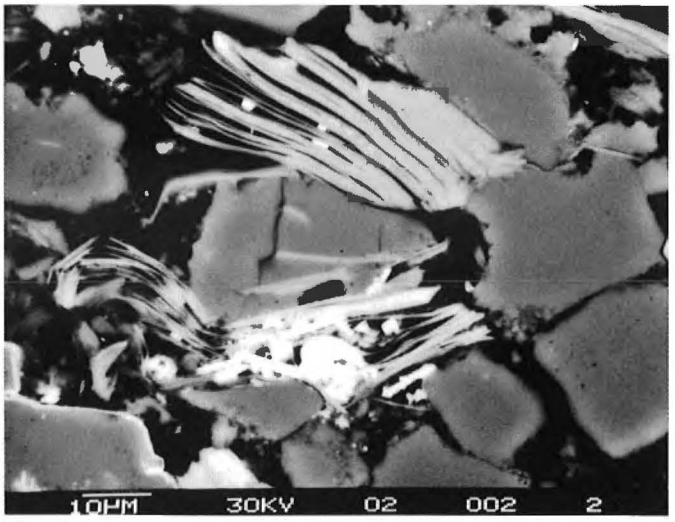
10µM 30KV 02 002 2

d

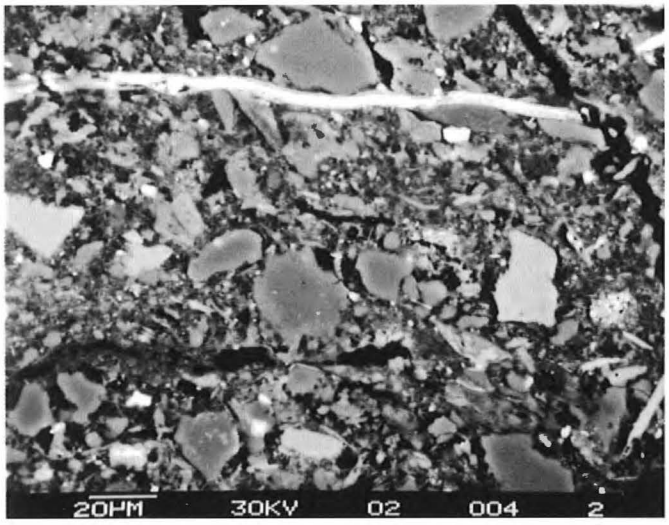
20µM 30KV 02 004 2

b

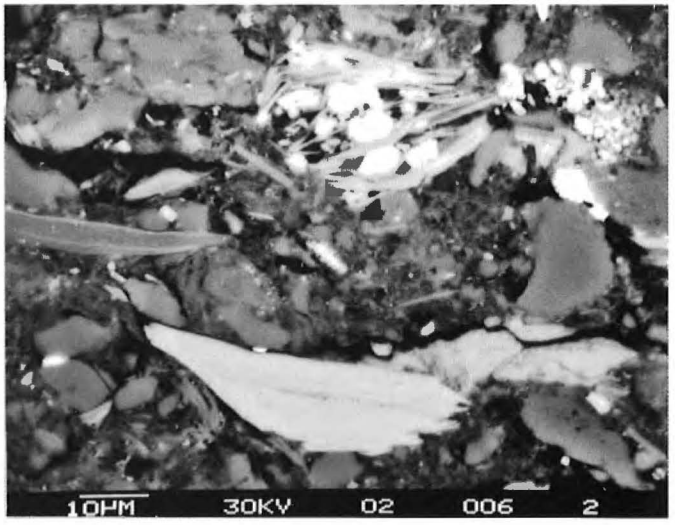
10µM 30KV 02 006 2

e

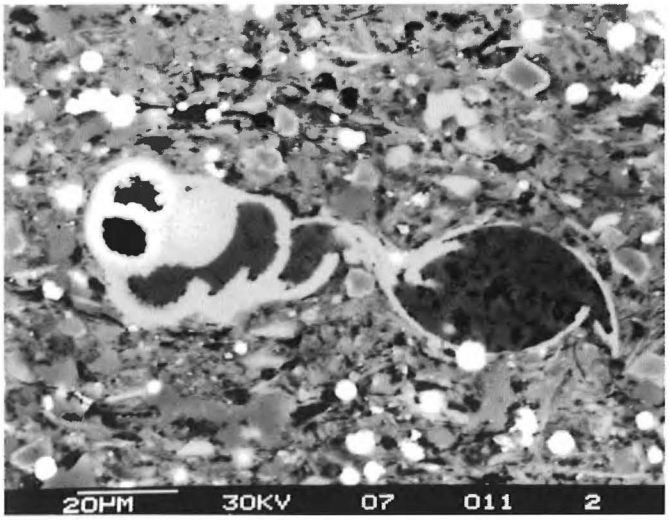
20µM 30KV 07 011 2

c

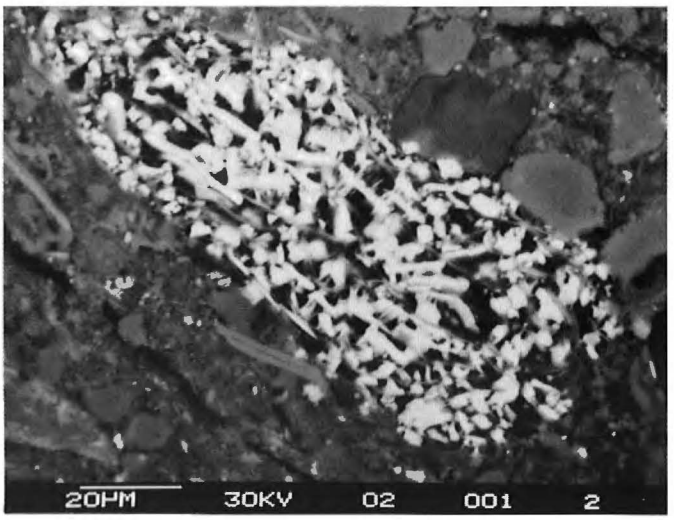
20µM 30KV 02 001 2

f

Plate 9

Second White Specks Formation. **a)** bedding-parallel fractures partly filled with Ca-sulphate (light grey), probably gypsum. Note homogeneous distribution of pyrite framboids (white spheres) (#0103506, 413 m - GSC #3671-12). **b)** flattened fecal pellets (arrows) are the "specks" in the Second White Specks Formation. Kaolinite-filled foram tests are abundant as is framboidal pyrite (#041304, 2114 m - GSC #3671-53). **c)** secondary-electron image of coccoliths and rhabdoliths (laths) that make up the fecal pellets shown in "b" (#063410, 738 m - GSC #3897-51). **d)** laminated bioclastic hash (top and bottom) with claystone. Inoceramid prism fragment is at lower left (#061801, 398 m - GSC #3680-57). **e)** Bioclasts include a fish vertabra and Inoceramid prisms (arrows). Dark areas are I/S -rich matrix. Calcite cement fills spinal cord cavity and below vertabra (#061801, 398 m - GSC #3680-64). **f)** high magnification of siliclastic matrix shows fine silt-sized quartz with muscovite (upper right) and K-feldpsar (arrow) in clay matrix (#103402, 408 m - GSC #3680-82).

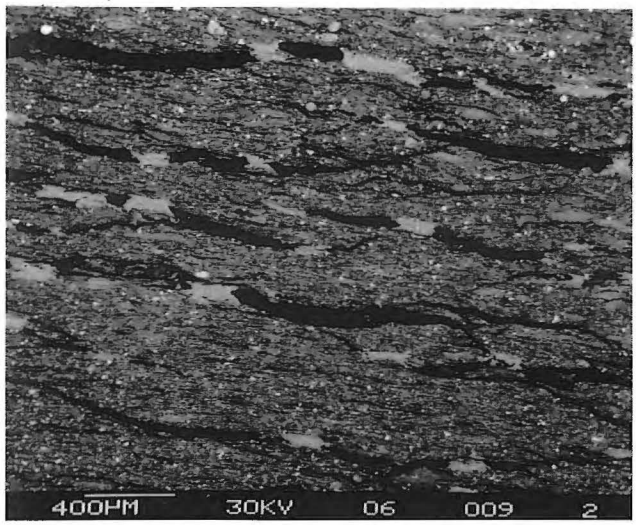
400PM 30KV 06 009 2

a

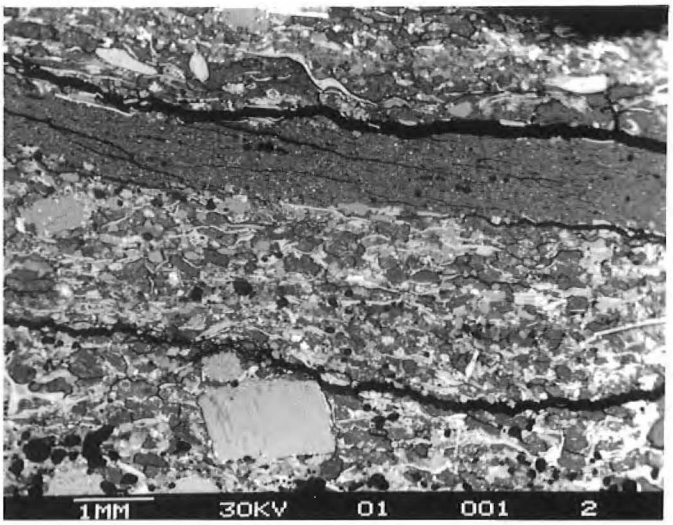
1MM 30KV 01 001 2

d

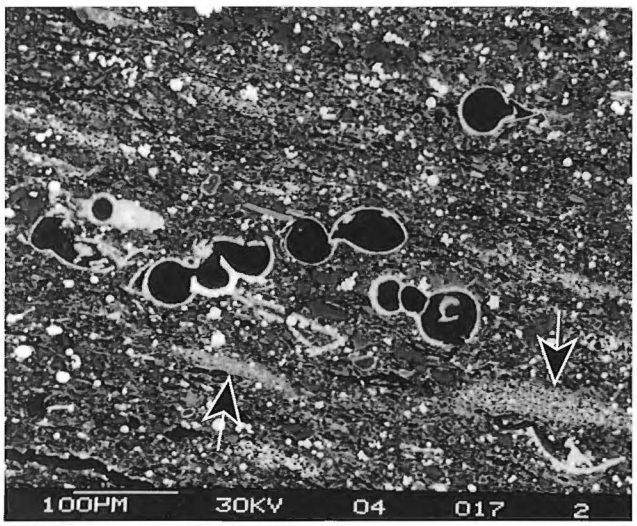
100PM 30KV 04 017 2

b

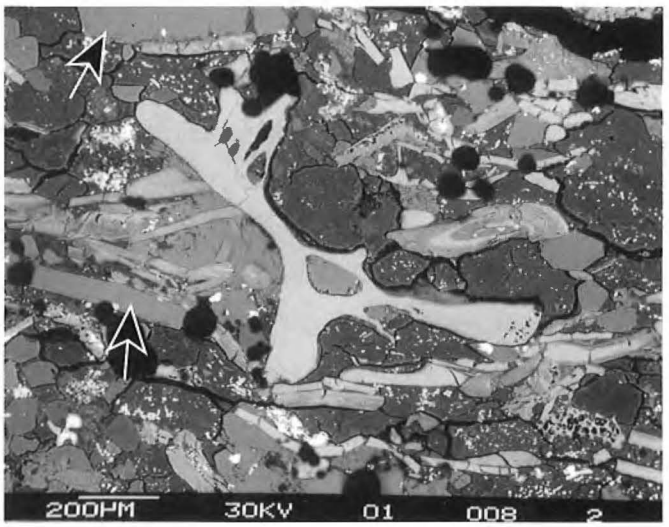
200PM 30KV 01 008 2

e

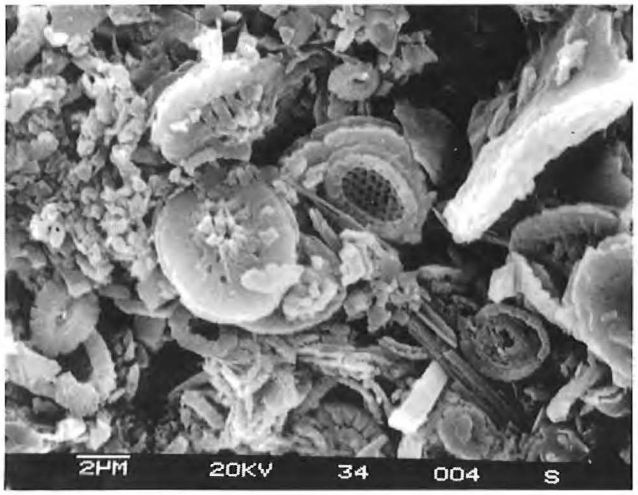
2PM 20KV 34 004 S

c

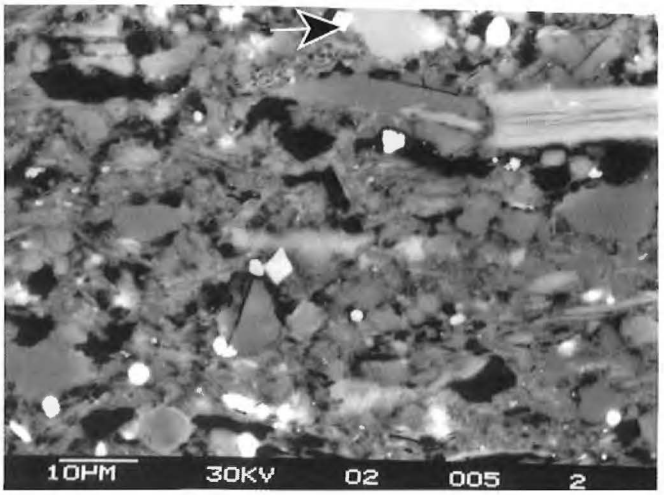
10PM 30KV 02 005 2

f

Plate 10

Selected foraminiferal species of the *Miliammina manitobensis* Zone

Figure 1. *Bathysiphon brosgei* Tappan GSC 115350, x45, from 6-34-30-8W4, 829.4 m.

Figure 2. *Saccammina alexanderi* (Loeblich and Tappan) GSC 115351, x60, from 6-34-30-8W4, 824.4 m.

Figure 3. *Placentammina* sp. GSC 115352, x150, from 6-34-30-8W4, 824.4 m.

Figure 4. *Reophax sikanniensis* Stelck GSC 115353, x50, from 6-34-30-8W4, 829.4 m.

Figure 5. *Psamminopelta browsheri* Tappan GSC 115354, x200, from 6-34-30-8W4. 794.7 m.

Figure 6. *Miliammina manitobensis* Wickenden GSC 115355, x262, from 6-34-30-8W4, 814.4 m.

Figure 7. *Ammobaculites tyrrelli* Nauss GSC 115356, x80, from 11-16-35-8W3, 5-4.6 m.

Figure 8. *Ammobaculites fragmentarius* Cushman GSC 115357, x50, from 6-34-30-8W4, 829.4 m.

Figure 9. *Verneuilinoides borealis* Tappan GSC 115358, x60, from 6-34-30-8W4, 829.4 m.

Figure 10. *Verneuilina canadensis* Cushman GSC 115359, x110, from 6-34-30-8W4, 779.7 m.

Figure 11. *Gaudryina irenensis* Stelck and Wall GSC 115360, x120, from 10-35-45-2W4, 456.4 m.

Figure 12. *Haplophragmoides linki* Nauss GSC 115361, x160, from 11-16-35-8W3, 460.8 m.

Figure 13. *Haplophragmoides topagorukensis* Tappan GSC 115362, x70, from 10-35-45-2W4, 470.4 m.

Figures 14, 15. *Haplophragmoides* sp. GSC 115363, lateral and apertural views, x110, from 11-16-35-8W3, 504.6 m.

Figure 16. *Haplophragmoides howardense* Stelck and Wall GSC 115364, x180, from 6-34-30-8W4, 794.7 m.

Figures 17, 18, 19. *Trochammina rutherfordi* Stelck and Wall GSC 115365, spiral, edge and umbilical views, x130, from 10-35-45-2W4, 460.4 m.

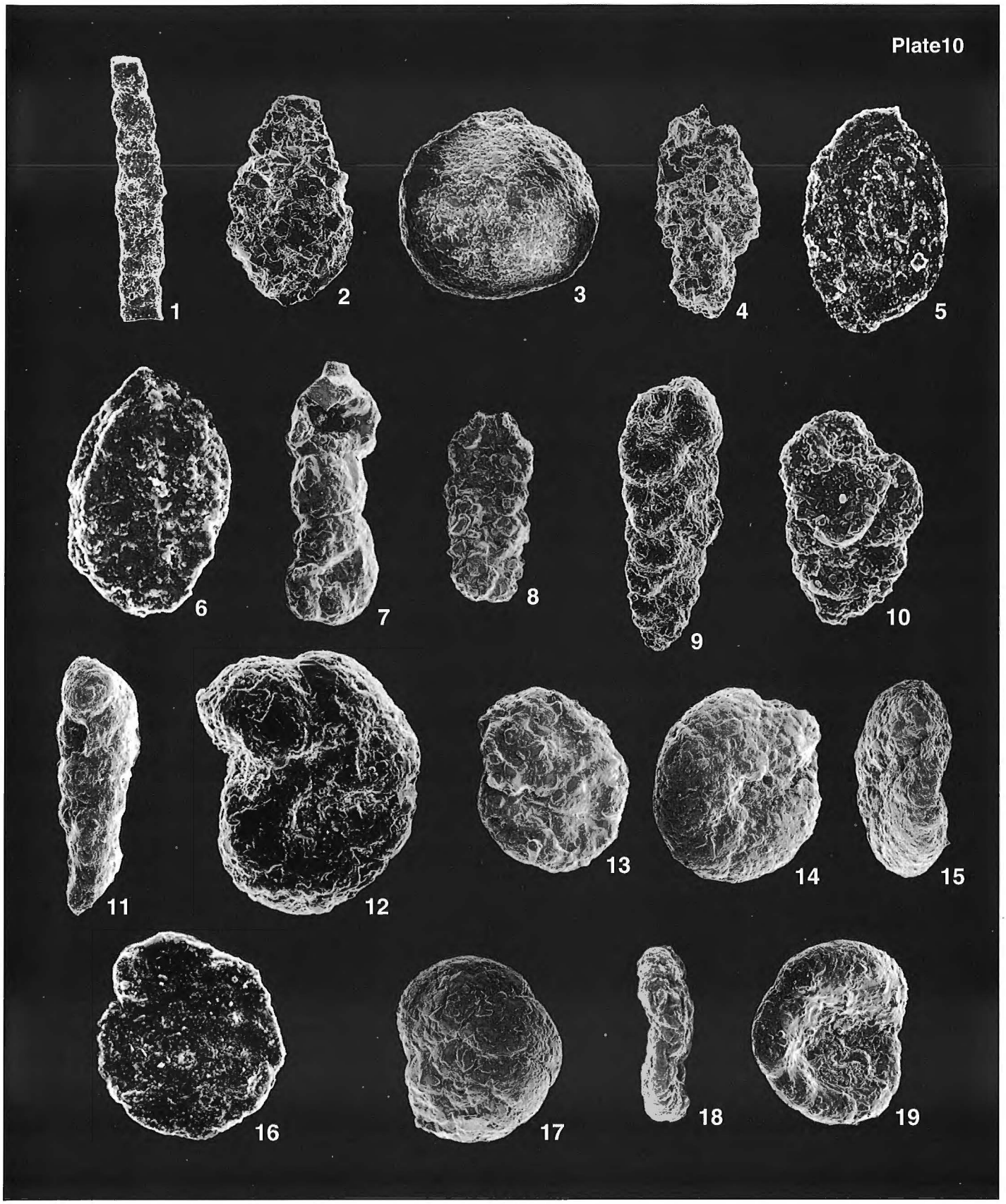
Plate10
1
2
3
4
5
6
7
8
9
10
11
12
13
14
15
16
17
18
19

Plate 11

Selected foraminiferal species of the *Verneuilinoides perplexus* Zone

Figure 1. *Hippocrepina* sp. GSC 115366, x130, from 6-34-30-8W4, 753.2 m.

Figure 2. *Psamminopelta browsheri* Tappan GSC 115367, x150, from 6-18-45-1W4, 412.52 m.

Figure 3. *Reophax incompta* Loeblich and Tappan GSC 115368, x75, from 6-34-30-8W4, 753.2 m.

Figure 4. *Verneuilinoides perplexus* (Loeblich) GSC 115369, x120, from 11-16-35-8W3, 401.7 m.

Figure 5. *Pseudobolivina rollaensis* (Stelck and Wall) GSC 115370, x100, from 11-12-6-16W4, 570.64 m.

Figures 6, 7. *Trochammina wetteri* Stelck and Wall GSC 115371, spiral and umbilical sides, x120, from 6-34-30-8W4, 753.2 m.

Figure 8. *Spiroplectammina ammovitrea* Tappan GSC 115372, x90, from 10-25-1-27W3, 848 m.

Figure 9. *Spiroplectammina* sp. GSC 115373, x90, from 11-12-6-16W4, 576.64 m.

Figures 10, 11. *Trochammina rainwateri* Cushman and Applin GSC 115374, x125, from 6-18-45-1W4, 412.52 m.

Figure 12. *Heterohelix globulosa* (Ehrenberg) GSC 115375, x110, from 11-36-22-1W2, 285.1 m.

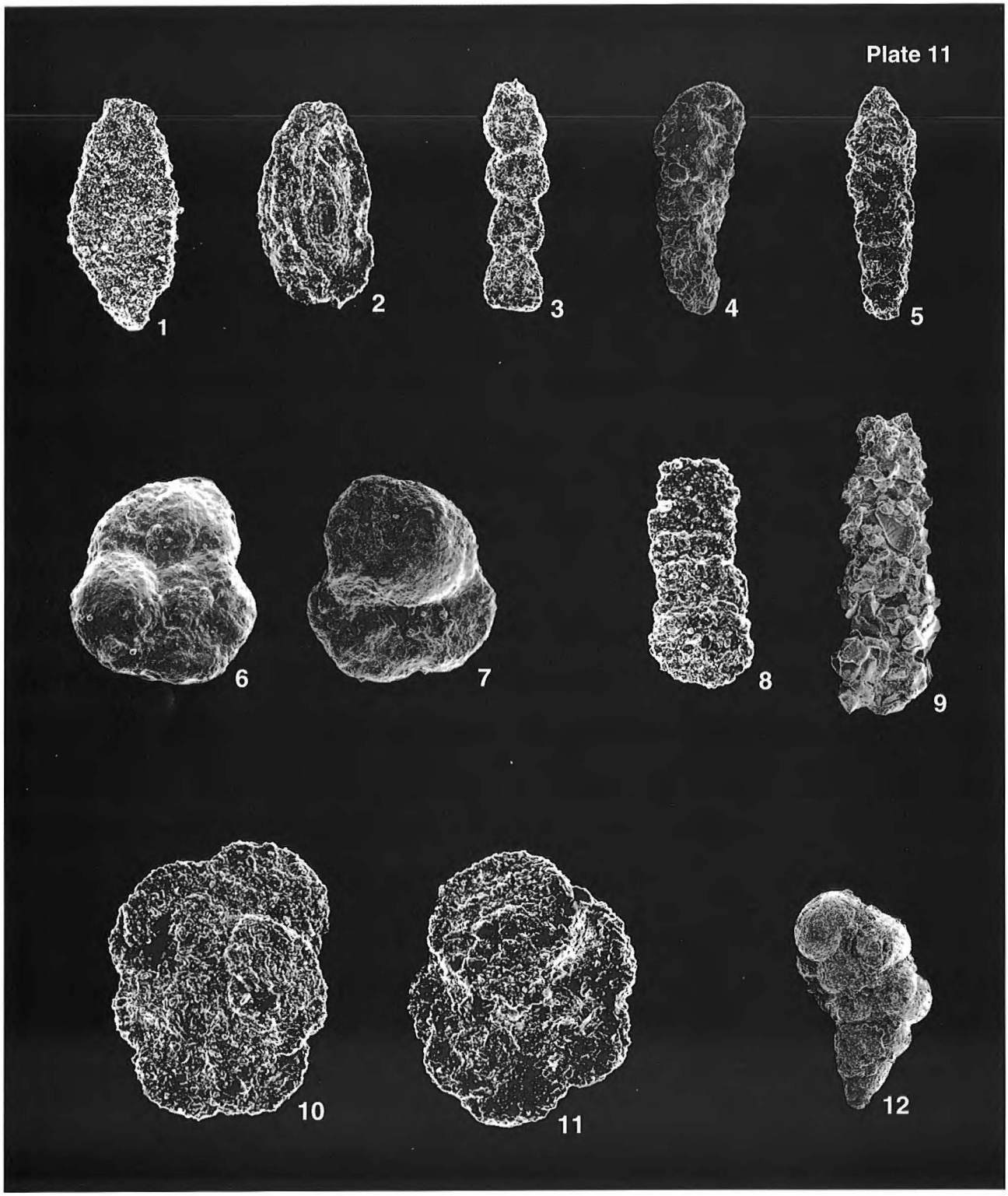
Plate 11
1
2
3
4
5
6
7
8
9
10
11
12

Plate 12

Selected foraminiferal species of the *Hedbergella loetterlei* Zone

Figure 1. *Pseudobolivina variana* (Eicher) GSC 115376, x120, from 6-34-30-8W4, 733.2 m.

Figure 2. *Neobulimina albertensis* (Stelck and Wall) GSC 115377, x200, from 6-18-45-1W4, 407.5 m.

Figure 3. *Heterohelix globulosa* (Ehrenberg) GSC 115378, x130, from 1-36-22-1W2, 281.3 m.

Figures 4, 5. *Hedbergella loetterlei* (Nauss) GSC 115379, dorsal and umbilical views, x110, from 11-36-22-1W2, 277.5 m.

Figures 6, 7, 8. *Hedbergella planispira* (Tappan) GSC 115380, dorsal, edge and umbilical views, x160, from 11-16-35-8W3, 401.0 m.

Figures 9, 10. *Hedbergella delrioensis* (Carsey) GSC 115381, dorsal and umbilical views, x120, from 11-36-22-1W2, 277.5 m.

Figures 11, 12. *Hedbergella amabilis* Loeblich and Tappan GSC 115382, dorsal and umbilical views, x175, from 10-35-45-2W4, 415.6 m.

Figures 13, 14, 15. *Whiteinella aprica* (Loeblich and Tappan) GSC 115383, dorsal, edge and umbilical views, x70, from 11-16-35-8W3, 401.0 m.

Figure 16. *Whiteinella aprica* (Loeblich and Tappan) GSC 115384, x95, from 6-34-30-8W4, 708 m.

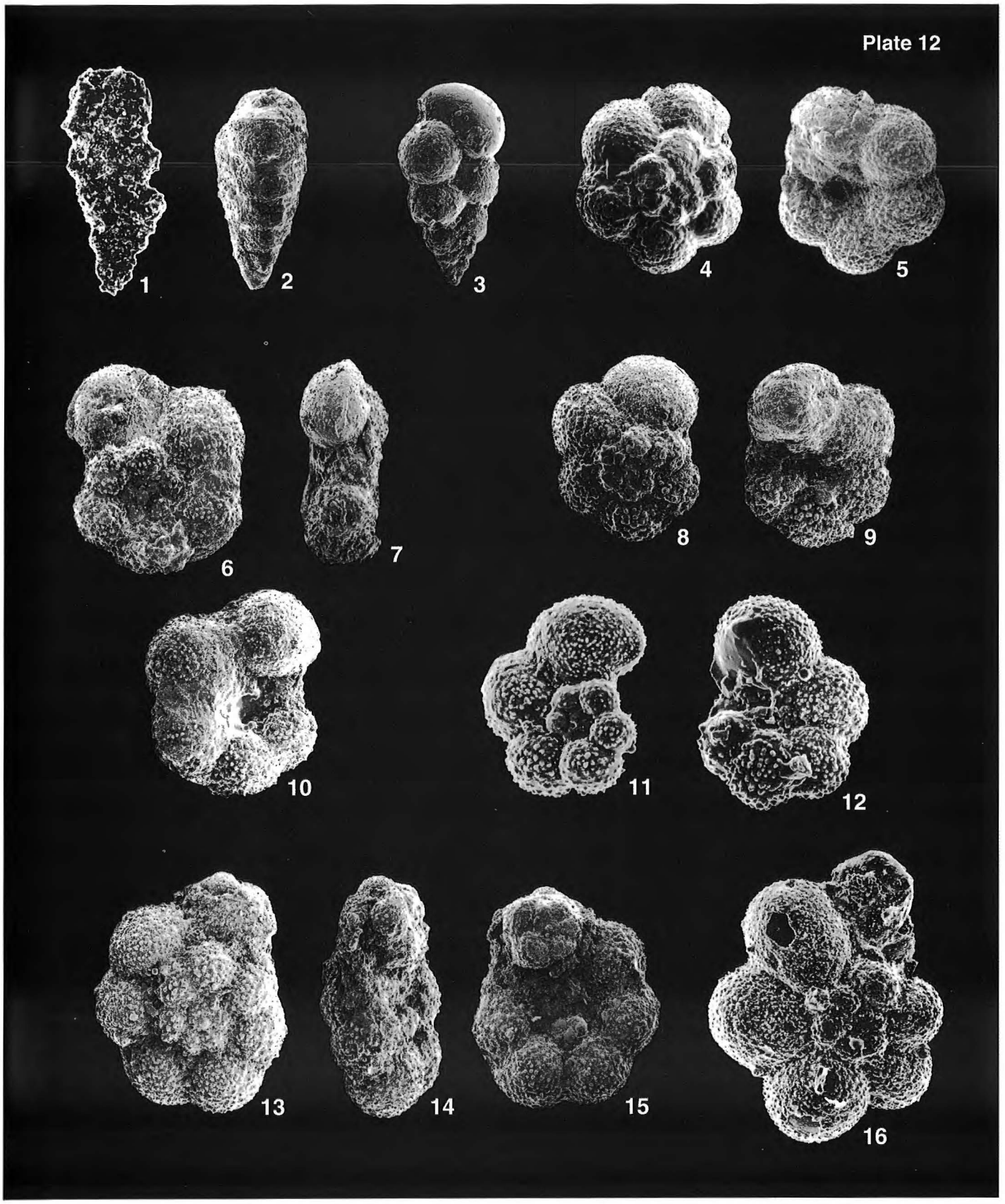
Plate 12
1
2
3
4
5
6
7
8
9
10
11
12
13
14
15
16

Plate 13

Selected coccolith species of the Second White Specks Formation. Scale bar equals 1 mm

Figure 1. *Discorhabdus ignotus* (Gorka)

Figure 2. *Parhabdolithus angustus* (Stradner)

Figure 3. *Lithastrinus floralis* Stradner

Figure 4. *Biscutum contans* (Gorka)

Figure 5. *Cretarhabdus conicus* Bramlette and Martini

Figure 6. *Predicosphaera spinosa* (Bramlette and Martini)

Figure 7. *Sollasites horticus* (Stradner, Adamiker and Maresch in Stradner and Adamiker)

Figure 8. *Cyclolithella armilla* (Black)

Plate 13

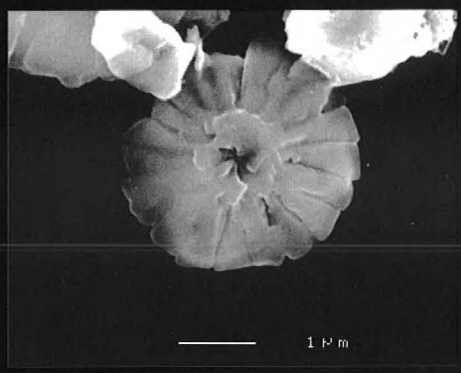

1

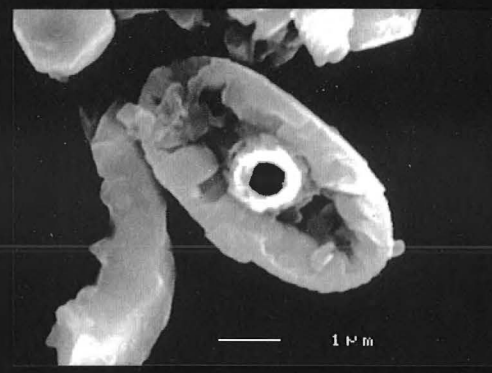

2

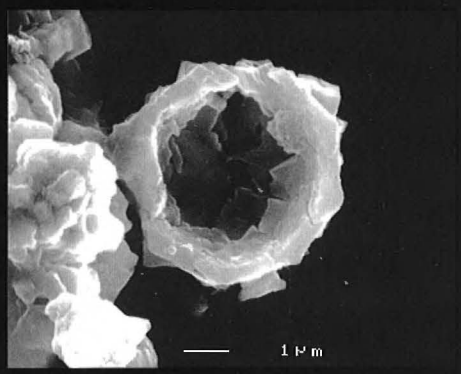

3

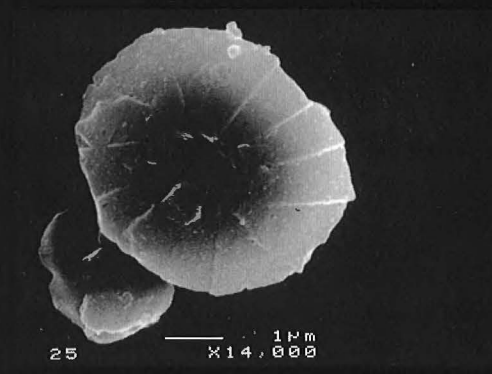

4

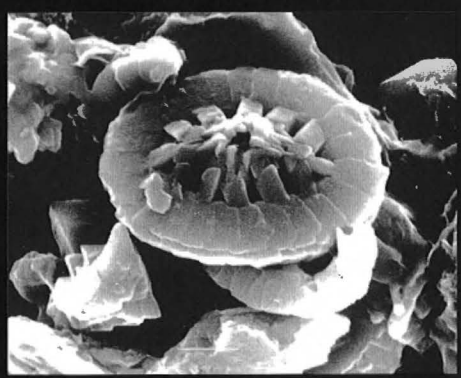

5

6

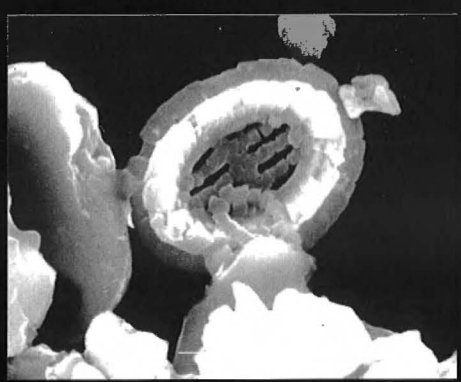

7

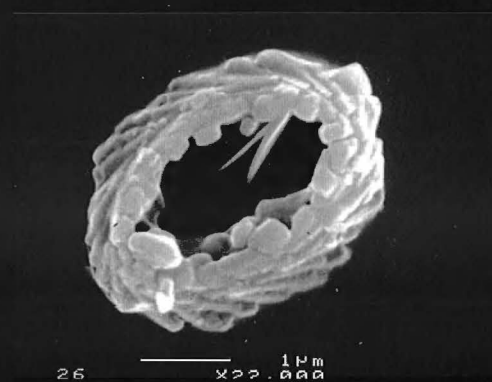

8

Plate 14

Bioturbated (3A and 6A) and laminated concretions (4, 5A and 2A). 6A and 5A are rimmed with pyrite. 4 shows remnant bedding crosscut by calcite-spar-filled septa. These concretions show no isotopic zoning (see Table 7).

9-9-56-19W5 #6A

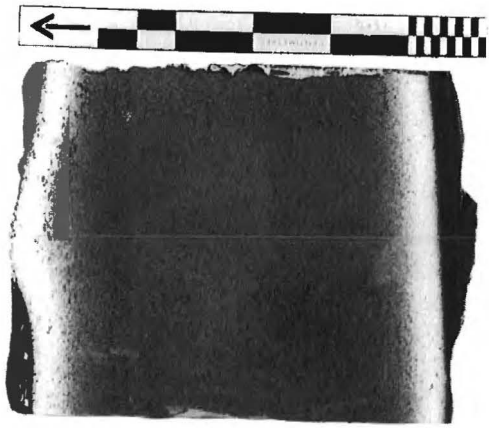

CG91-4

16-1-61-22W5 #3A

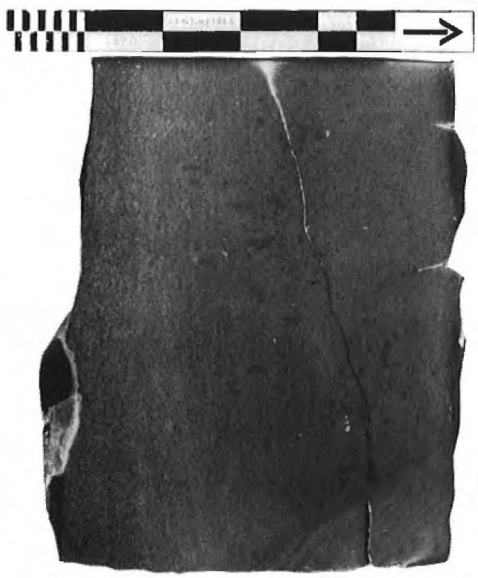

10-34-42-22W4 #5A

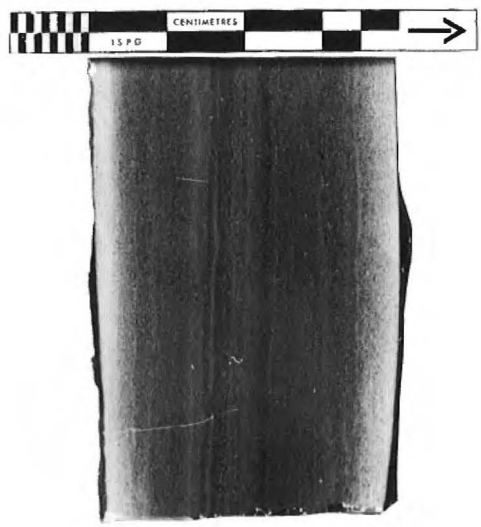

10-34-42-22W4 #2A

Plate 15

Isotopically zoned siderite concretion 2B from the Westgate Formation (10-25-65-20W5, 1325 m). This concretion also shows evidence of bioturbation, as in sample on Plate 16, but contains botryoidal pyrite throughout. Botryoidal pyrite fills uncompacted burrows indicating early cementation. Textural zoning is not evident.

10-25-65-20W5 #2B

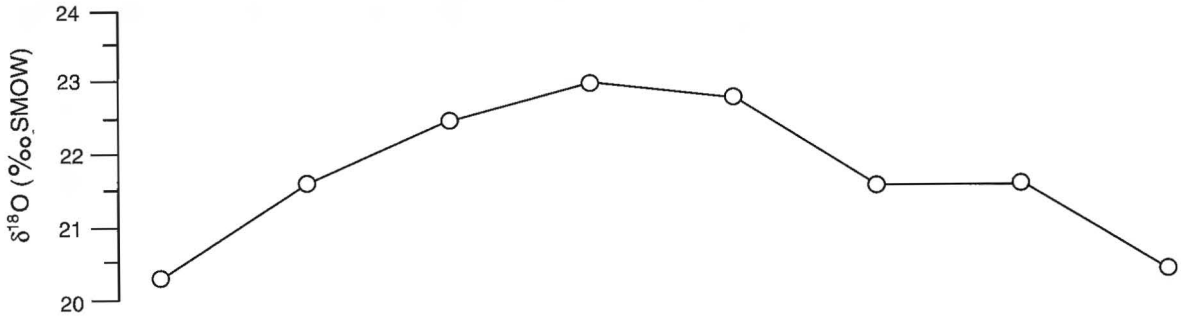

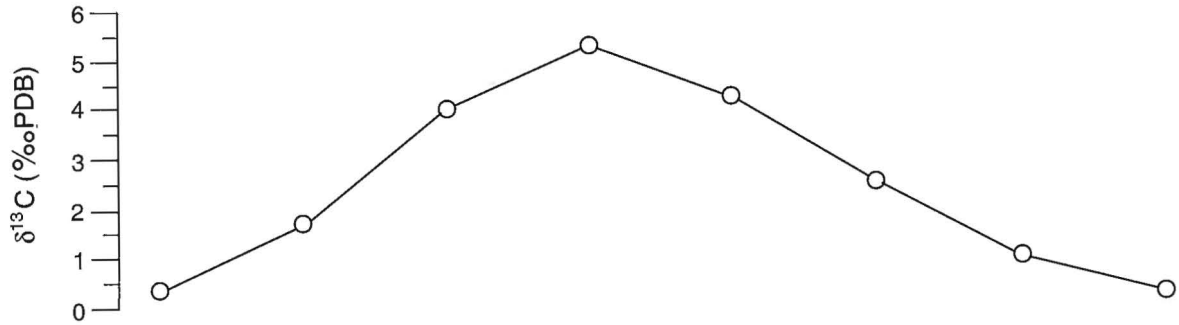

Plate 16

Texturally and isotopically zoned siderite concretion 2A from the Westgate Formation (10-25-65-20W5, 1324.7 m). Center of concretion is well-bioturbated and margins contain abundant, botryoidal pyrite. Light grey, wispy, star-shaped areas are dolomite. Partly flattened large burrow (~1.5 cm wide) is visible just below center of the concretion.

10-25-65-20W5 #2A

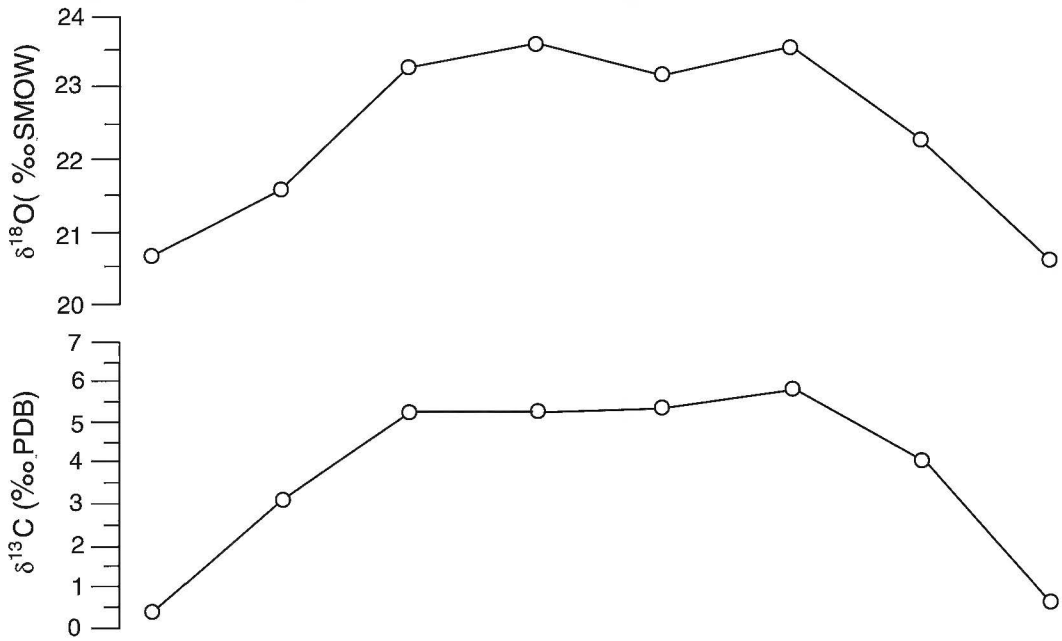

Plate 17

a) coring-induced petal-centerline fractures (terminology after Kulander et al., 1990) in the Second White Specks Formation. **b)** induced fracture surface showing slickensides (arrow), Second White Specks Formation.

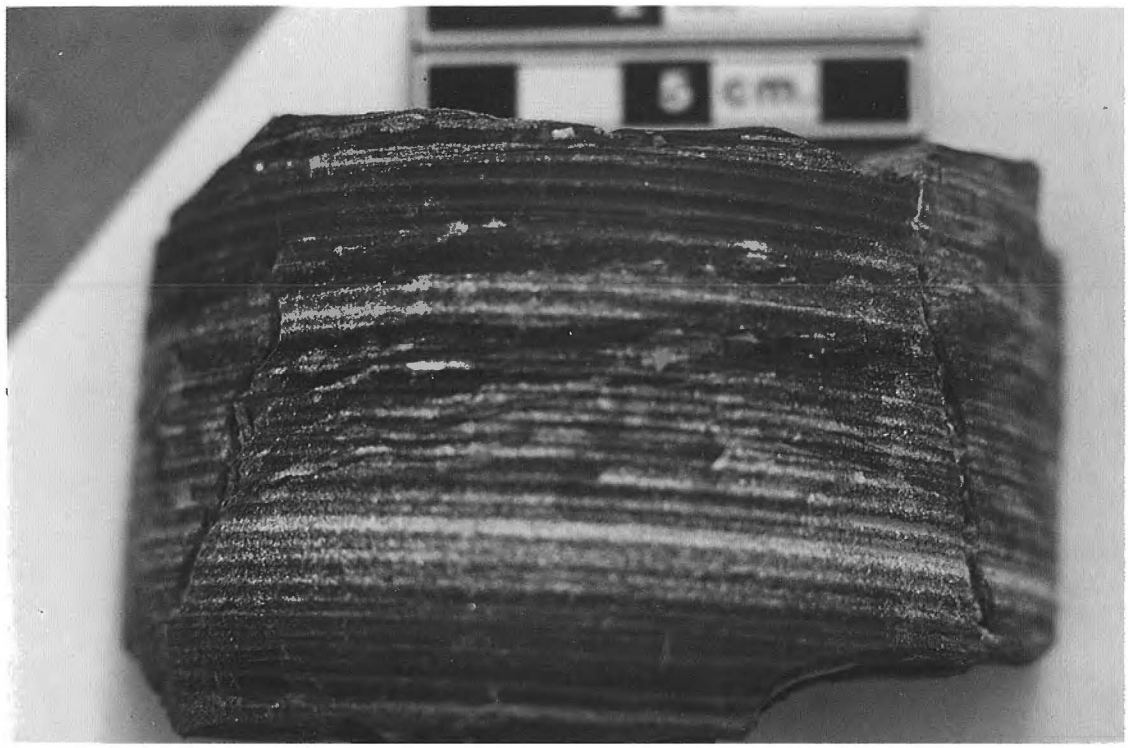

a

b

Plate 18

a) parallel fracture sets in the Jumping Pound Sandstone, which directly overlies the Second White Specks Formation, Highwood River outcrop (see Table 1 for location). **b)** close-up of **a** shows clearly that bedding-perpendicular fractures are filled with calcite. Hammer (33 cm in length) is oriented parallel to direction of thrusting.

a

b

Plate 19

a) calcite-filled, bedding-perpendicular fractures (below notebook) and bedding-parallel fractures (above notebook). Note difference in fracture set spacing. Notebook is 21 cm in length. Highwood River outcrop (see Table 1 for location). **b)** oil stains (arrow) on fresh fracture surface. Highwood River outcrop.

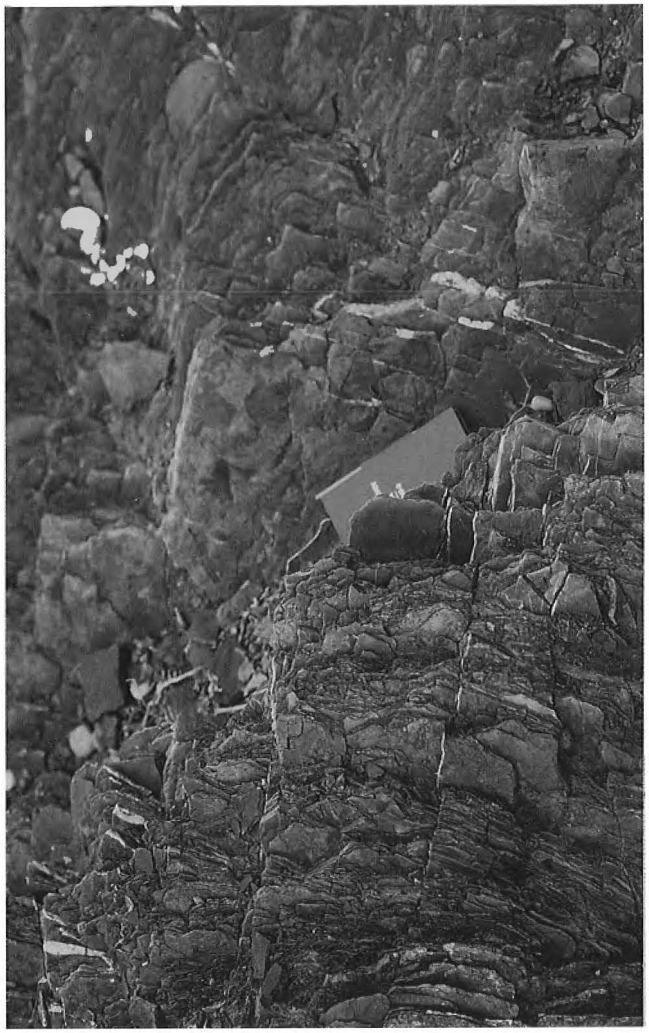

a

b

Plate 20

a) bedding-perpendicular calcite-filled fractures in the Second White Specks Formation. Strata at this location are complexly folded and these fractures result from folding-induced extension. Mill Creek Bridge outcrop (see Table 1 for location). **b)** close-up of fracture fill cement in **a**. Thin laminae give way to coarse spar suggesting successive cementation events in response to increased fracture volume. Note small Inoceramid impression (arrow).

a

b

Plate 21

a) fractured sandstone bed indicating brittle behaviour whereas mudstone reflects ductile deformation. **b)** fracture porosity is preserved in ductile mudstone. **c)** well-preserved fracture porosity. **d)** annealed fracture porosity. Note slickensides on dark core face. All samples from Dome et al Claresholm well (14-29-11-28W4; 2502-2521 m depth).


2 in.
5 cm.
a
b
c
d
2 in.
5 cm.